UNIVERSITY OF SOUTHAMPTON

FACULTY OF MEDICINE, HEALTH AND BIOLOGICAL SCIENCES

School of Medicine

Epithelial tight junction function in a co-culture model of the human bronchial epithelium and endothelium

By Ferdousi Chowdhury

Thesis for the degree of Doctor of Philosophy

December 2003

UNIVERSITY OF SOUTHAMPTON

ABSTRACT

FACULTY OF MEDICINE, HEALTH AND BIOLOGICAL SCIENCES
RESPIRATORY CELL AND MOLECULAR BIOLOGY

Doctor of Philosophy

Epithelial tight junction function in a co-culture model of the human bronchial epithelium and endothelium

By Ferdousi Chowdhury

Epithelial cells line the conducting airways of the bronchial tract, with endothelial-lined capillaries in the submucosa, forming an integrated system and acting as a barrier to the environment. When the epithelial surface is challenged, the epithelial and endothelial response is locally co-ordinated to allow infiltrating cells to cross the endothelium and target the site of challenge on the luminal surface. This thesis reports the establishment of a co-culture model reflecting this co-ordinated system, to enable epithelial-endothelial cell interactions to be investigated.

16HBE 14o-, SV40-transformed bronchial epithelial cells were grown on the underside of insert membranes, and HUVEC (human umbilical vein endothelial cells) were grown on the upper side. Immunofluorescent staining with HEA-125 (human epithelial antigen-125) provided an epithelial-surface marker and vWF (von Willebrand factor) an intracellular endothelial-specific marker. Using these markers in confocal microscopy, showed that confluent epithelial and endothelial cell layers were growing on opposite sides of the membrane. This was confirmed by scanning and transmission electron microscopy. Transepithelial electrical resistance (TER) was used as a functional measurement reflecting tight junction formation. The final model improves on existing models of the conducting airways, allowing the effects of cell-to-cell interaction on tight junction function to be investigated, better reflecting the *in vivo* situation in which epithelial and endothelial cells coexist.

The bilayer had an increased TER ($464\Omega.cm^2$, S.E. $\pm$ 18) in comparison to the epithelial monolayer ($238\Omega.cm^2$, S.D. $\pm$ 25), and this increase only occurred when 16HBE 14o- cells were grown with endothelial cells. Furthermore, this same increase was seen when HUVEC conditioned medium was added to the basolateral side of 16HBE 14o- cells, confirming that the increase in TER was occurring in the 16HBE 14o- cells. These results revealed that functional differences exist between epithelial cells grown as a monolayer and epithelial cells grown as a bilayer with endothelial cells.

Changes in TER reflect changes in tight junction function, and this change was further investigated. Cell density or cell height did not differ between 16HBE 14o- grown as a monolayer, bilayer or in conditioned medium. RT-PCR was performed to identify differences in mRNA expression of claudins, JAM and occludin. RT-PCR results showed an increase in occludin gene expression, as well as an increase in expression of an occludin isoform. Occludin was therefore identified as an important molecule regulating changes in tight junction function. This was investigated further using western blotting and immunfluorescent labelling, to

establish whether this increase in occludin was translated at the level of protein expression. The results suggest that both the amount of occludin expressed and its distribution differ in bilayers. Higher levels of occludin expression and an increase in occludin localisation at the tight junctions would explain an increase in barrier integrity.

Initial characterisation of the factor mediating the increase in TER, has shown it to be a soluble heat-stable, non-protease mediator which has an effect at least 6 hours after addition to the 16HBE 14o- cells and acts on epithelial layers only from the basolateral direction. Using an epidermal growth factor (EGF)-receptor inhibitor reduced the increase in TER seen, suggesting an EGF receptor agonist may be a possible candidate.

These results emphasise the importance of epithelial-endothelial interactions in regulating the barrier function of the bronchial epithelium. Any further understanding of tight junction proteins in barrier function, as well as identification of any mediator that can maintain barrier function, has important therapeutic implications, in disease where the barrier function is impaired.

LIST OF CONTENTS

LIST OF FIGURES

Chapter 1

Chapter 2

Chapter 3

Chapter 5

LIST OF TABLES

ACKNOWLEDGEMENTS

I wish to thank my supervisor Dr Peter Lackie for all his help, support, guidance and encouragement, throughout my PhD, as well as my ex-supervisor Dr Will Howat! Special thanks goes to Dr John Holloway and Dr Ian Yang, for help with developing primers and optimising conditions for the RT-PCR work, as well as helping with the gene sequencing. All the Biomedical Imaging Unit Team, and in particular Dr Anton Page for help and use of the microscopy imaging equipment. Thanks are also due to the Child Health Unit for the original supply of HUVEC cells. Finally I would like to thank my sponsors and my industrial supervisor Dr Gary Phillips at Dstl, Salisbury.

Everyone in the Brookes Lab deserve a mention for making it an enjoyable place to work, especially James Hughes and Liz Adams!!! And of course, my family, in particular my husband Shoab for his support and patience, especially in keeping the homefront sorted, and my children: Tazneem, Najibah, and Adil for behaving themselves (most of the time!).

ABBREVIATIONS

APC	Antigen presenting cell
ASIP	atypical-PKC-specific interacting protein
CAR	Coxsackievirus and adenovirus receptor
EGF	Epidermal growth factor
EXO I	Exonuclease I
FITC	Fluorescein isothiocyanate
GM-CSF	Granulocyte-macrophage colony stimulating factor
HBSS	Hanks buffered salt solution
HEA-125	Human epithelial antigen-125
HEV	High endothelial venules
HPAEC	Human pulmonary artery endothelial cells
HUVEC	Human umbilical vein endothelial cells
IFN-γ	Interferon-gamma
Ig	Immunoglobulin
IL	Interleukin
JAM	Junctional adhesion molecule
MAGUK	Membrane-associated guanylate kinase homologues
MDCK	Madine-Darby canine kidney epithelial cells
PAF	Platelet activating factor
PAMR	Perijunctional actinmyosin ring
PBS	Phosphate buffered saline
PCR	Polymerase chain reaction
PECAM	Platelet endothelial cell adhesion molecule
PET	Polyethylene terephthalate
PILT	Protein incorporated later into tight junctions
PKC	Protein kinase C
RT	Reverse transcription
SAP	Shrimp alkaline phosphotase
SEM	Scanning electron microscopy
TEM	Transmission electron microscopy
TER	Transcellular electrical resistance

TGF	Transforming growth factor
TJ	Tight junction
TNF	Tumor necrosis factor
vWF	Von-Willebrand factor
ZAK	ZO-1 associated kinase
ZO	Zonula occluden
ZONAB	ZO-1 associated nucleic acid-binding protein

CHAPTER 1
INTRODUCTION

Chapter 1. Introduction

1.1 Overview of lower airways of the respiratory system

The lower airways (trachea, bronchi and bronchioles) act as the conducting portion of the human respiratory system, with the most peripheral conducting airways consisting of the bronchioles, with about 20 generations of branching (Weibel, 1991). These conducting airways also provide a route of entry for external irritants and pollutants from the environment, and the respiratory epithelium lining the airway walls will be their first point of contact.

The airway walls are composed of a mucosa (surface epithelium, basement membrane and supporting elastic lamina propria), and submucosa (in which lie glands, muscle, cartilage and endothelium lined blood capillaries), and are surrounded by adventitia (Fig.1.1), (Jeffery, 1995).

As the respiratory tract progressively bifurcates, there is a gradual structural change in the airway walls, which reflect the change in function. The airways become smaller, but the total cross-sectional area increases markedly. The larger bronchioles have a lumenal diameter of approximately 1mm and the smaller bronchioles approximately 0.3mm. The cartilage diminishes and the smooth muscle layer increases, and the epithelium become progressively thinner. The walls of the bronchioles are characterised by the absence of cartilage, but with a prominent layer of smooth muscle, and are lined with ciliated, cuboidal epithelium, interspersed with mucus-secreting cells.

Cross section of Bronchiole airway (A) (not to scale)

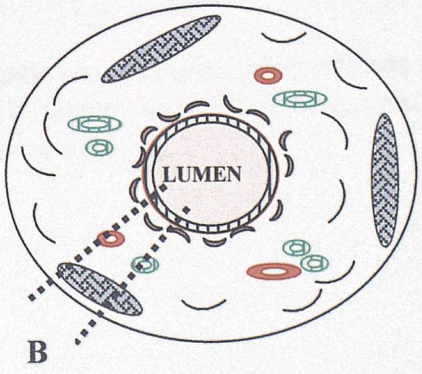

Section through airway wall (B) (not to scale)

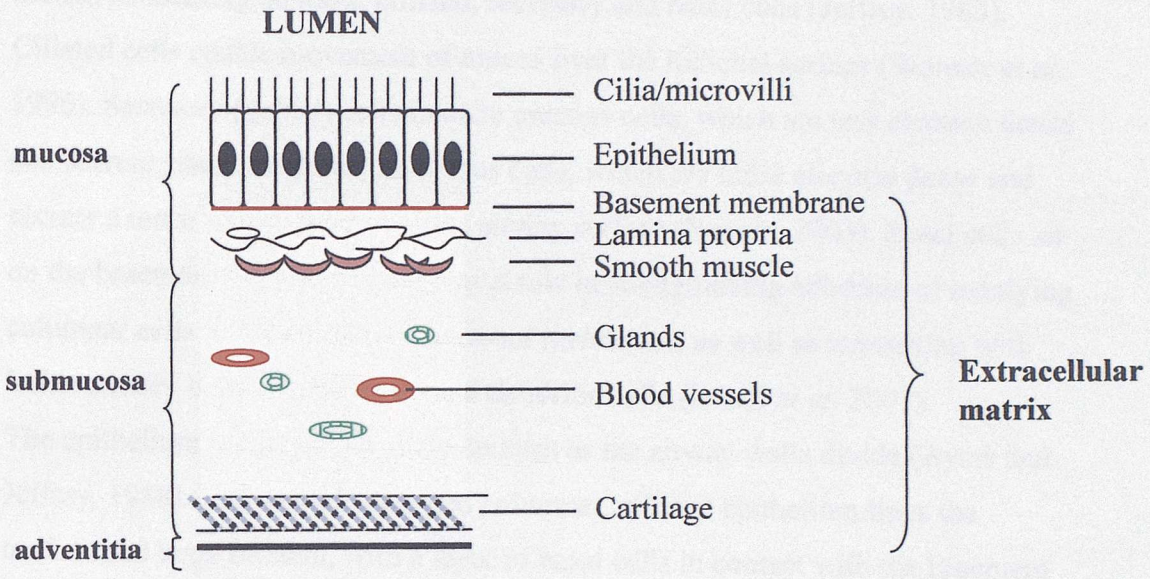

(C) TEM image (x590) of bronchiole wall:
1. Lumen, 2. Ciliated epithelium, 3. Lamina propria, 4. smooth muscle, 5. Glands, 6. submucosa, 7. perichondrium, 8. cartilage, 9. chondrocytes, 11. arterioles. (*Image from Histology, Oxford University Press*)

Fig.1.1 Schematic cross-section of bronchiole airway (**A**), and schematic representation of airway wall (**B**), in comparison to TEM picture of bronchiole airway wall (**C**).

1.2 Respiratory Epithelium

A continuous layer of epithelial cells, which sit on a basement membrane, lines the airway walls. There are at least three different surface epithelial cell types in the human conducting airways: ciliated, secretory and basal cells (Jeffrey, 1983). Ciliated cells enable movement of mucus over the lumenal surface (Wanner *et al.* 1996). Secretory (goblet) cells include mucous cells, which are less electron dense and secrete viscous mucin; and serous cells, which are more electron dense and secrete a more watery fluid onto the airway surface (Rogers, 2003). Basal cells sit on the basement membrane, and play a role in strengthening adhesion of overlying columnar cells to the epithelial basement membrane, as well as interacting with inflammatory cells, lymphocytes and dendritic cells (Evans *et al.* 2001).

The epithelium progressively differentiates as the airway walls divide (Ayers and Jeffrey, 1988). Tall, pseudostratified columnar, ciliated epithelium lines the trachea and large bronchi, with a layer of basal cells in contact with the basement membrane. The epithelium progressively decreases in height to become simple cuboidal, non-ciliated in the smallest airways, and eventually flattened thin epithelium in the alveoli walls.

Epithelial cells are connected to each other by intercellular junctions (fig. 1.2). These consist of zonula adherens (adheren junctions) and desmosomes, which are important in maintaining a strong structure by connecting the cells to each other and the cytoskeleton; hemidesmosomes and focal adhesions, which are important in anchoring the cells to the basal lamina; gap junctions which are essential for cell-to-cell communication via channels formed by the transmembrane protein connexin; and *zonula occludens* (tight junctions), which help maintain cell polarity by keeping the apical and basolateral membranes and their extracellular fluids separate, as well as forming a continuous permeability barrier across the epithelium (Cerijido *et al.* 1998).

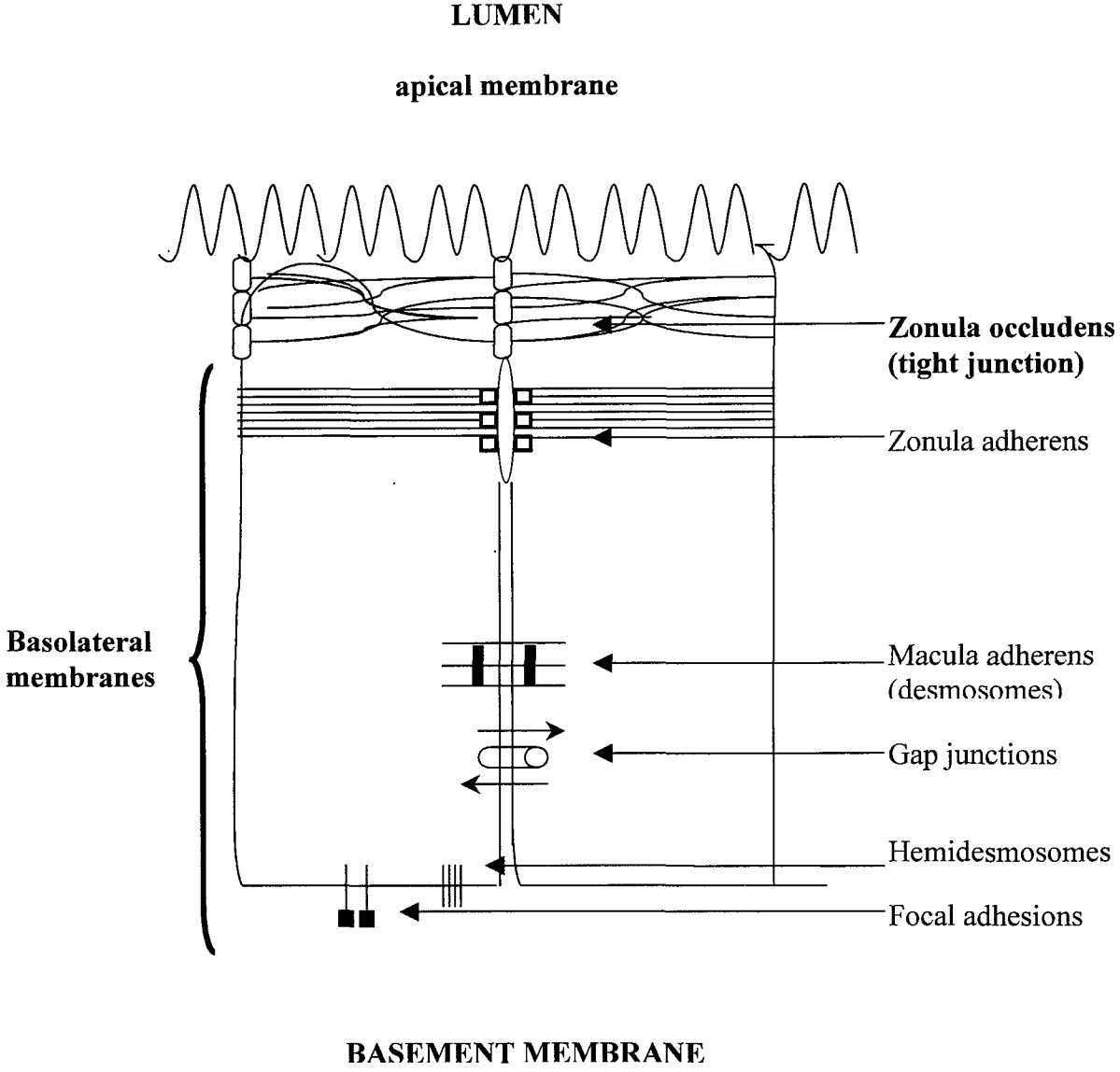

Fig 1.2 Diagram to show location of junctional complexes between epithelial cells (not to scale).
Tight junctions are the most apical of junctions, separating the apical and basolateral membranes and fusing together the plasma membrane of adjacent cells with a continuous belt of strands forming a permeability barrier between the lumen and underlying tissue.

1.3 Epithelial response to challenge

Environmental pollutants such as dust, chemicals and microorganisms will be inhaled through the respiratory tract, which must therefore have a robust defence mechanism to prevent them crossing from the airway lumen into the lung parenchyma. The first protective barrier that a contaminant meets is the epithelium. The epithelium provides non-specific immunity, such as mucocilliary clearance, and specific immunity through inflammatory cells and neutralising antibodies (Bascom *et al.* 1995). Irritants typically stimulate nonspecific immunity, allergens stimulate specific immunity, and infecting organisms and carcinogens interact with both (Bascom *et al.* 1995). However, for optimal lung defence the specific and non-specific immune responses are complimentary, such that if one defence mechanism fails the risk of infection increases but another mechanism will usually still be able to overcome any contaminants, and chronic infection is usually associated with several defects in respiratory defence (Rennard and Romberger, 2000).

1.3.1 Non-specific immunity

The larger bronchial airways, (those with non-continuous cartilage rings) are lined by ciliated epithelium, which are covered by a layer of mucus. The combination of mucus and cilia provide the first line of defence against pollutants in the respiratory airway (Boyton and Openshaw, 2002). The mucus lining is produced by goblet cells and submucosal glands and is composed of water, ions, mucins (which maintain viscosity) and anti-microbial, anti-oxidant and anti-protease macromolecules (which protect against foreign particles) (Lillehoj and Kim, 2002). The interaction between mucus and cilia, show cilia beating patterns result in the movement of mucus, which led to the understanding of mucocilliary clearance (Sleigh *et al.* 1988). Scanning electron microscopy has further enabled the understanding of ciliary motility (Satir, 1992), demonstrating cilia of a given cell have the same orientation as the surrounding cells, and bend in co-ordination with each other. The combination of beating cilia and air flow propel the mucus forward from the lower respiratory tract to the pharynx, eventually reaching the back of the throat where it is cleared by swallowing or coughing (Rubin, 2002). The cough reflex is particularly important when there is impaired mucocilliary

clearance and increased risk of infection, such as that seen in smokers, as it allows forceful expiration of particles (Foster, 2002). Other non-specific defences include mediators of the innate immune system, such as lactoferrin, lysozyme, collectins and defensins (Boyton and Openshaw, 2002). Macrophage and neutrophils, phagocytic cells of the innate immune system, play an important role in killing and degrading microorganisms by phagocytosis, which are then removed by mucocilliary clearance (Zhang *et al.* 2000; Gordon and Read, 2002). Mast cells are also present in the airway, and are activated by allergens producing immunoglobulin-E (IgE), resulting in the release of mediators which recruit eosinophils (Frew, 1996). The respiratory tract also contains immunoglobulin A (IgA), which is thought to be secreted by the epithelium itself (Salvi and Holgate, 1999) or transported by the epithelium from the lamina propria to the airway lumen (Pilette *et al.* 2001), and has an important role in binding microorganisms preventing them from attaching to the epithelium.

Certain microorganisms including viruses and bacteria have developed mechanisms to overcome these respiratory defence mechanisms and penetrate the epithelial barrier, resulting in respiratory infection and disease.

Viruses and bacteria can avoid mucocilliary clearance by attaching to the epithelium, such as rhinoviruses, which recognise ICAM-1 expressed on the surface of epithelial cells (Bella and Rossmann, 1999). Once attached the virus or bacteria could either directly enter the epithelial cells or cross the damaged epithelium by paracellular movement, which would involve transepithelial migration through disrupted epithelial tight junctions.

If microorganisms are able to overcome these non-specific defence mechanisms and penetrate the lung barrier, then inflammatory cells are recruited to the site of infection and activated by cytokines and chemokines released by the phagocytic cells (Zhang *et al.* 2000).

1.3.2 Specific Immunity and response to allergen

A vast amount of work on allergen challenge and immune responses has led to an extensive breadth of knowledge, which is outside the scope of this project, but recent reviews give a useful update (Wiedermann, 2003; Prince *et al.* 2003; Boyton and Openshaw 2002). The main points are discussed here briefly.

When antigens are inhaled and the antigen is able to penetrate the epithelium surface an adaptive or specific immune response occurs. The mechanisms by which antigen cross the epithelial barrier is unclear, but studies using the house dust-mite antigen, Der p1, suggest that both intracellular and paracellular mechanisms can occur. Der p1 has been shown to possess proteolytic activity, which is thought to disrupt tight junctions, enabling antigens to cross the epithelium paracellularly (Wan *et al.* 1999). Incubating epithelial cells with FITC-labelled Der p1 was used to show its intracellular localisation in endosomal and lysosomal compartments, indicating intracellular migration of antigens can also occur (Mori *et al.* 1995).

Once the antigen has penetrated the epithelial surface, it interacts with dendritic cells (professional antigen presenting cell) present in the airways to initiate an immune response (Holt, 1996). Although it has been shown that bronchial epithelial cells express major histocompatibilty complex class II molecules on their surface, which is required for antigen presentation (Kalb *et al.* 1991), epithelial cells are not effective at presenting antigen to T-cells (Mezzetti *et al.* 1991). It is the uptake and presentation of antigen by dendritic cells to specific T-cells, which result in T-cell activation (Lambrecht, 2001). Activated T-cells can kill directly, or produce cytokines to activate phagocytic macrophage, and B-lymphocytes that produce immunoglobulins against the foreign antigen (Moore *et el.* 2001).

Activating or 'danger' signals are released by damaged cells, for example when there is an allergen challenge on the epithelial surface, and include heat shock proteins, extracellular-matrix breakdown products and cytokines such as IFNγ (reviewed by Gallucci and Matzinger, 2001). These 'danger' signals trigger adhesion and migration of leukocytes from the blood and across the endothelium of the blood vessel (Springer 1995) (Fig.1.3).

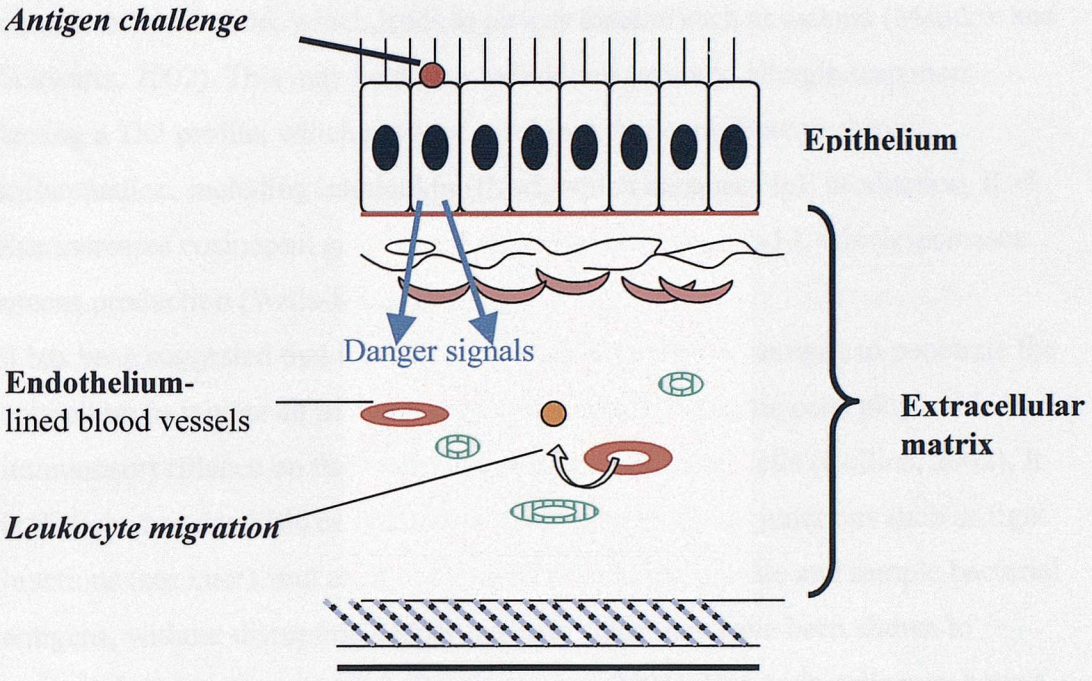

Fig. 1.3 Schematic drawing of epithelium challenge and subsequent leukocyte migration (not to scale).

When the epithelium is challenged, it releases danger signals to trigger an immune response, resulting in leukocyte migration across the endothelium-lined blood vessels. Chemattractants allow these infiltrating immune cells to target the site of challenge, enabling them to ingest, kill and degrade the offending body.

The respiratory tract has a fragile architecture, such that an excessive or inappropriate inflammatory response can lead to damage (Boyton and Openshaw, 2002). Uncontrolled leukocyte infiltration into the airway walls leads to persistent chronic inflammation, which leads to airway disease such as asthma (Maddox and Schwartz, 2002). This may be due to individuals prone to allergic responses having a Th2 profile, which produce cytokines that contribute to chronic inflammation, including interleukin (IL)-4, which enhances IgE production, IL-5 that increases eosinophil growth and differentiation, and IL-13, which increases mucus production (Wills-Karp, 1999).

It has been suggested that it is not always necessary for an antigen to penetrate the epithelium to initiate an immune response, and that dendritic cells play a role in immunosurveillance on the lumenal side of gut epithelial cells (Collins, 2002). It is thought that dendritic cells are able to open intercellular junctions such as tight junctions (see later), and extend their dendrites to the outside and sample bacterial antigens, without disrupting barrier integrity since they have been shown to express tight junction proteins (Rescigno *et al.* 2001). Dendritic cells may have a similar role in immunosurveillance of other mucosal surfaces such as the respiratory tract (Stumbles *et al.* 2003).

Receptor mediated transport or transcytosis of immunoglobulins (IgA, IgG and IgM) across the epithelial cells are also capable of neutralising pathogens and are therefore also important in immunity (Rojas and Apodaca, 2002).

1.3.3 Transepithelial migration

To leave the blood and reach the site of challenge, leukocytes need to migrate from the apical to the basolateral side of the endothelium, and for external challenges they may also need to migrate from the basolateral to apical side of the epithelium, suggesting two different mechanisms of migration occur (Liu *et al.* 1996). Transendothelial migration of leukocytes is well documented and will be discussed in section 1.5.2; transepithelial migration however, is not yet clearly understood, but it may not be necessary in situations of damage, where epithelial junctions will be disrupted and cells can cross freely.

Transepithelial migration may be triggered by epithelial cells producing their own chemoattractants (eg. interleukin (IL)-8), in response to external stimuli, such as proinflammatory cytokines (Cromwell *et al.* 1992), or respiratory viruses (Tomee

et al. 1997). Other regulators of transepithelial migration include lipid mediators such as platelet activating factor (PAF), and macrophage factors such as granulocyte-macrophage colony stimulating factor (GM-CSF), which prolongs neutrophil survival (Petterson and Adler, 2002). T-lymphocytes in the airway tend to be memory T-cells (those that have been previously exposed to antigen), and are thought to migrate across the bronchial epithelium via a G-protein signalling event (Miller and Butcher, 1998). Most studies have focussed on neutrophil transepithelial migration, and is thought to involve co-ordinated opening and closing of intercellular junctions, in particular tight junctions (see 1.6), (Huber *et al.* 2000). This is further supported by studies showing leukocyte expression of tight junction proteins, in particular occludin (see 1.9), in response to certain stimuli, suggesting a possible means of leukocyte-epithelial interaction which would maintain epithelial barrier integrity during transepithelial migration (Alexander *et al.* 2001). Once migrated, the leukocytes must remain in the airway lumen until the challenge is overcome. This may occur by the expression of Fc receptors on the epithelial apical surface, specifically binding leukocytes such as neutrophils, which has been shown for colonic epithelial cells (Reaves *et al.* 2001), thus retaining them in the airway lumen. Once the foreign body is expelled, neutrophils undergo programmed cell death (apoptosis), and are cleared by phagocytosis of macrophage (Petterson and Adler, 2002).

1.4 Endothelium

Blood vessels are lined by a single layer of squamous endothelial cells supported by a basement membrane (the *tunica intima)*. In large blood vessels, such as arteries and veins, a thick wall of connective tissue (the *tunica adventitia*) and smooth muscle (the *tunica media*) exists, supporting the endothelial layer, with the amount of connective tissue and smooth muscle varying according to the size and function of the vessel (Fig 1.4).

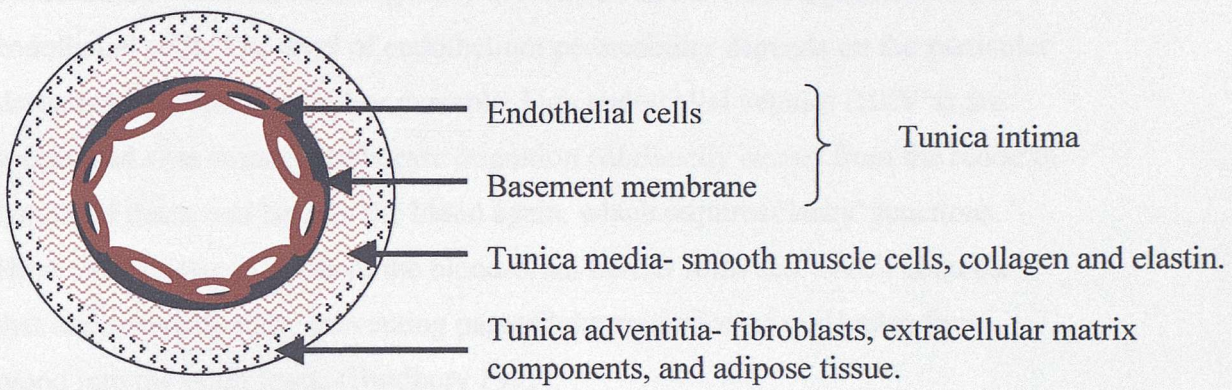

Fig. 1.4 Schematic drawing of the component layers of the blood vessels

The endothelium of the lung consists of pulmonary arteries and veins, which divide and branch in parallel with the airways, leading to smaller arterioles and veins. The pulmonary blood vessels have characteristic elastic walls rather than muscular (Burkitt *et al.* 1993), which become progressively thinner and eventually absent. Endothelial cells are polygonal, elongated multifunctional cells, which form an anti-coagulant barrier between the vessel wall and blood, as well as forming a selective permeability barrier, and are involved in growth regulation, thrombosis, vascular tone and blood flow, production of extracellular matrix components and in the immune response (Sumpio *et al.* 2002). Endothelial cells contain membrane bound storage organelles for von-Willebrand factor called Weibel-Palade bodies, and antibodies against von-Willebrand factor (also known as factor VIII-related antigen) are commonly used immunohistochemically to identify endothelial cells (Zanetta *et al.* 2000).

Endothelial cells are all derived from the mesoderm but heterogeneity exists in the interactions between the cells, depending on the tissue environment (Gerritsen 1987). There are two hypotheses on endothelial cell development and how endothelial heterogeneity arises (Stevens *et al.* 2001). First, the endothelial cells leave the mesoderm with a predetermined phenotype and then migrate to their specific tissue. And second, the endothelial cells migrate from the mesoderm all the same, and then undergo differentiation at a later stage once reaching a specific site.

Whichever hypothesis applies, it is quite clear that intercellular differences in the endothelium occur, and heterogeneity is reflected in the varying permeability of endothelial cells. The level of endothelium permeability depends on the particular tissue environment it is in. For example, high endothelial venules (HEV's) are specialised sites where lymphocyte migration continually occurs from the blood to lymphoid tissue and back to the blood again, which requires 'leaky' junctions. However, endothelial cells of the blood-brain-barrier form cell-to-cell contacts that are extremely tight, preventing paracellular migration of molecules from blood into the brain tissue (Bradbury 1993).

The endothelium acts as a barrier between the blood and the surrounding tissue, and three different mechanisms have been identified to explain transport across the endothelium. Firstly, passive diffusion of small molecules (MW less than 3000) such as gases, ions, low molecular weight metabolites and peptides, is thought to occur via intercellular clefts, and allow the molecule to diffuse through the cell cytoplasm (Bendayan, 2002); secondly transcytosis, which involves the transport of proteins and some lipids in vesicles (Tuma and Hubbard, 2003); and thirdly through the intercellular space between cells, which involves passing through junctions, and is the mechanism used for leukocyte migration (Dejana *et al.* 2001).

1.5 Endothelial response to pathogens

Endothelial cells must allow controlled leukocyte migration (extravasation) into normal or inflamed tissue, and form fairly loose junctions (5nm wide) only restricting the passage of relatively large solutes such as albumin (DeFouw *et al.* 1993). Adjacent endothelial cells form junctional complexes, similar to those of epithelial cells (fig.1.5), and it is thought leukocytes trigger signals in the endothelial cells promoting the opening of endothelial cell contacts and junctions during leukocyte migration (Vestweber, 2000).

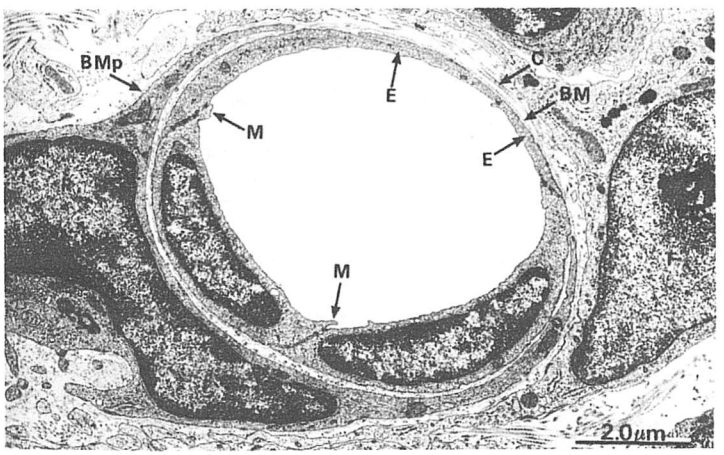

Fig.1.5 TEM (x12000) of capillary showing continuous endothelial cells (E) lining the lumen. Adjacent cells have overlapping cytoplasmic 'marginal folds' (**M**), which form junctional complexes. The endothelium is supported by a basement membrane (**BM**) and collagen fibrils (**C**).
(*Image from Wheater's Functional Histology, Churchill Livingstone*)

1.5.1 Immune response of endothelium- extravasation

It is thought chemokines released during an immune response by damaged epithelium, activates endothelial cells by binding heparan sulphate glycosaminoglycans on their surface (Gotte, 2003). The endothelial cells are thought to transcytose these chemokines, and present them to leukocytes leading to extravasation (Middleton *et al.* 2002).

During an immune response, three main steps occur during extravasation (fig.1.6), and the steps involved have been summarised here from Szekanecz and Koch (Szekanecz and Koch, 2000). Firstly, the leukocytes (neutrophils, monocytes, lymphocytes, eosinophils and basophils), roll, become activated and adhere to the endothelium. Secondly, the attached leukocytes extend pseudopods between adjacent endothelial cells and squeeze through endothelial junctions. Certain homophilic adhesion molecules present in the intercellular junction are thought to be involved in this process, such as PECAM-1 (platelet endothelial cell adhesion molecule) or CD31, which is used as an immunohistochemical marker of endothelial cells (Jackson, 2003). Leukocytes are then thought to degrade the basement membrane by secreting collagenases, allowing them to enter the surrounding tissue. The final step in the inflammation process is for the leukocytes to migrate to the site of injury by chemotaxis, where the pathogen can then be removed by phagocytosis.

All these steps must be controlled and coordinated, and the epithelium, endothelium and surrounding components must communicate to efficiently overcome the challenge. When the sequence of events are not controlled, for example, if there is a prolonged immune response, chronic inflammation can occur and activated leukocytes continue to release toxic metabolites and proteases which result in epithelium and tissue damage.

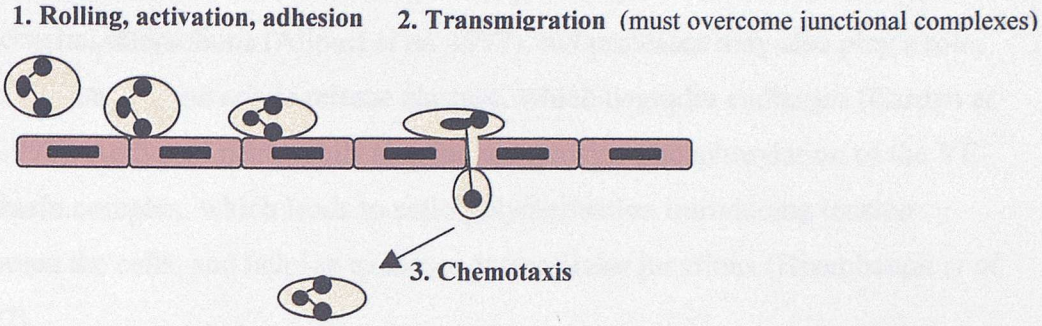

Fig 1.6 Sequence of events during leukocyte migration, from lumen of blood vessel to surrounding tissue, in inflammation.

1.5.2 Transendothelial migration

As discussed earlier, leukocyte transendothelial migration occurs when an immune response is triggered in response to danger signals during epithelial damage. Leukocyte populations found to migrate into the airways during an inflammatory response, such as in chronic bronchitis, have been determined from bronchoalveolar lavage(Balbi *et al.* 1994), and include neutrophils, eosinophils and T-lymphocytes. Neutrophils have been used to determine the steps of rolling, activation and adhesion of leukocytes (Girard and Springer, 1995), but mechanisms of transendothelial migration are not well understood. Studies suggest that interendothelial junctions are disrupted in a specific and localized manner during neutrophil migration (Allport *et al.* 2000). If this were the case, then the most apical junction to be overcome would be the tight junction. However, most studies have focussed on the adherens junction, in particular on VE-cadherin, an adheren junction protein specific to endothelial cells, which is linked to the cytoskeleton by forming complexes with catenin (Lampugnani *et al.*1992). VE-cadherin is thought to be important in vascular permeability. Since when neutrophils adhere to endothelial cells, a loss of VE-cadherin staining is seen at the cell surface in addition to an increase in permeability, suggesting the VE-cadherin-catenin complex was disrupted (Del Maschio *et al.* 1996). This was further supported by studies showing blocking VE-cadherin with an antibody resulted in an increased permeability and neutrophil transmigration, which was associated with a redistribution of VE-cadherin from being concentrated at cell-to-cell contact sites to being diffuse (Hordijk *et al.* 1999).

Disruption of the VE-cadherin-catenin complex may be initiated by leukocyte-endothelial interactions (Allport *et al.* 1997), but proteases may also play a role, since activated neutrophils release elastase, which degrades cadherins (Carden *et al.* 1998). Activated neutrophils also induce tyrosine phosphorylation of the VE-cadherin complex, which leads to actin polymerisation introducing tension between the cells, and helping to loosen intracellular junctions (Hixenbaugh *et al.* 1997).

It has been suggested that neutrophil transmigration may not involve tight junctions, since they appear to cross at areas where tight junctions are discontinuous enabling them to remain intact (Burns *et al.* 2000), but key information on how leukocytes actually cross between endothelial cells is still to be determined.

1.6 Tight junctions

Tight junctions (TJ) or *zonula occludens* are the most apical junctions on the lateral surface of epithelial and endothelial cells. They were first identified by electron microscopy (Farquhar and Palade, 1963), and freeze-fracture studies showed them as a net-like meshwork of fibrils forming a continuous barrier across the epithelium (Staehelin, 1973). TJ maintain the key functions of the epithelium and endothelium. Firstly, they maintain cell surface polarity by forming an intramembrane diffusion barrier that restricts the diffusion of lipids (Cerijido *et al.*1998). Membrane proteins and extracellular fluids of the apical and basolateral compartments of the cells are kept separated, resulting in cell polarity. TJ also form an important paracellular permeability barrier, regulating paracellular movement of water, solutes, ions and immune cells (Madara 1998). More recently, TJ have been suggested to have a role in regulating cell proliferation and cell density (Balda *et al.* 2003). Tight junctions are therefore essential in forming and maintaining cellular polarity and paracellular permeability in the epithelium and endothelium.

1.6.1 Tight junction and paracellular permeability

Tight junctions are the rate-limiting factor in paracellular permeability of cell layers and two methods are generally used to assess the extent of TJ formation (Madara *et al.* 1998). Firstly, the measurement of electrical resistance across an epithelial layer is an established method for measuring the extent of TJ formation. The total transepithelial electrical resistance (TER) is composed of the transcellular resistance, consisting of the resistance of the apical and basolateral membranes of the cells, and the paracellular resistance, consisting of the resistance of the TJ and that of intercellular space in between the cells below the TJ (fig.1.7), (Claude 1978). Since the TJ is the rate-limiting factor in paracellular movement of ions, any changes seen in electrical resistances are used as a reflection of changes in TJ function (Madara *et al.* 1998). Secondly, the movement (flux) of small neutral markers (eg. mannitol and fluorescent dextran molecules), across an epithelial layer can be measured, which will pass passively through the paracellular pathway. Studies show a non-linear relationship between mannitol flux and electrical resistance (Madara *et al.* 1992). A large mannitol flux is seen at low electrical resistances, with small increases in flux resulting in a large decrease

in electrical resistance. At high electrical resistances mannitol flux is low and a small change in flux is associated with a small change in electrical resistance. In general, permeability studies show low values of TER relate to a high paracellular flux, and vice versa.

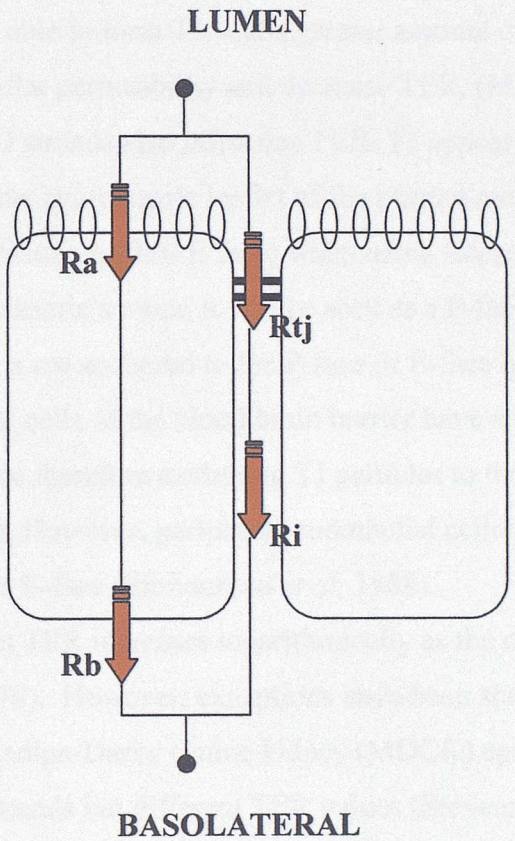

Fig.1.7 Diagram of electrical circuit of epithelium.
Transcellular electrical resistance consists of how much flow or conductance is prevented at the apical membrane (Ra) and basolateral membrane (Rb). The paracellular resistance consists of the conductance prevented at the tight junction (Rtj) and intercellular space (Ri). The total electrical resistance is a combination of all four. (Adapted from Madara *et al.* 1998).

1.6.2 Tight junctions and TER

The configuration of TJ is found to influence the TER of cells. The length of TJ represents the linear amount of paracellular passage per square centimetre. It is therefore logical, assuming continuous TJ formation at cell-to-cell boundaries, that as the length of TJ increases, the length available for paracellular permeability will increase resulting in a decrease in TER. Two factors influence the length of TJ- cell density, since a greater cell density will give a greater junctional density and lower TER; and cell periphery, since cells with interdigitated borders will have a greater cell periphery able to form TJ, and a greater amount of TJ per unit area will increase paracellular permeability and decrease TER, (Marcial *et al.* 1984).

The morphology of TJ strands also influence TER. TJ appear as a meshwork of strands or fibrils (on the cytoplasmic leaflet of the plasma membrane- P face), or grooves (on the exoplasmic leaflet- E face) when using freeze-fracture techniques. When there is a cytoplasmic anchor, it will be seen as a P-face fracture, and whether tight junctions are anchored to the P-face or E-face has been shown to be important. Endothelial cells of the blood brain barrier have a high TER and TJ's are found on the P-face therefore anchoring TJ particles to the cytoplasm (Wolberg *et al.* 1994). However, peripheral endothelial cells with a low TER have TJ associated with the E-face (Simionescu *et al.* 1988).

Studies also show that TER increases logarithmically as the number of TJ strands increases (Claude 1978). However, exceptions have been shown, in which two different strains of Madine-Darby canine kidney (MDCK) epithelial cells had the same number of TJ strands but different TER values (Stevenson *et al.* 1988). MDCK Type I cells reached electrical resistances of more than 30-fold greater than MDCK Type II cells, despite having the same number and density of junctional strands.

TJ strands of adjacent cells associate with each other to form a tight seal, but these seals have been postulated to contain pores or channels, which fluctuate between open and closed states regulating permeability (Claude, 1978). It is unclear how these channels are formed or regulated, but it may be due to differences in the combination of proteins assembled at the TJ, in particular, claudins (Furuse *et al.* 1999).

1.6.3 Tight junctions and endothelial cells

Tight junctions have also been described in endothelial cells (Staehelin, 1973). The main difference in TJ formation between endothelial and epithelial cells is that endothelium form discontinuous strands (Simionescu *et al.* 1976), as opposed to a continuous seal found in epithelial cells. (The exception being blood vessels of the brain, in which tight junctions are continuous (Rubin and Staddon, 1999)). However, as mentioned earlier, heterogeneity exists between endothelia. The development and formation of TJ varies between endothelial cells depending on the tissue it surrounds (Edens and Parkos, 2000). For example, the endothelium of the blood-brain barrier forms impermeable TJ with high electrical resistances (1-2000Ω), whereas vascular endothelial cells form permeable monolayers, (human umbilical vein endothelial cells (HUVEC) monolayers show a resistance 6-40Ω). However, HUVEC are the most commonly used endothelial cells for *in vitro* studies, due to their availability and relative ease of growth. *In vitro* studies show that HUVEC and human pulmonary artery endothelial cells (HPAEC) are similar in appearance and in their growth (Mackarel *et al.* 1999). Therefore, HUVEC are useful for studies involving the endothelium system.

Most studies in endothelial cells have focused on the role of adherens junctions (Dejana *et al.* 1995; Moll *et al.* 1998), even though TJ are still the most apical junction and form circumferential belt-like structures between adjacent endothelial cells (Anderson and Van Itallie 1995). This is mainly due to *in vitro* data using HUVEC as a TJ negative cell type. Recent studies (Burns *et al.* 1997) have overcome this problem by growing HUVEC in astrocyte-conditioned medium to enhance TJ expression. These studies focused on transendothelial migration, an important feature of most vascular endothelial cells. They suggest that neutrophils preferentially migrate across tricellular corners, preventing TJ disruption and maintaining the endothelial barrier. Tricellular corners occur at the borders of three intersecting endothelial cells, where discontinuities are found in the border staining of occludin, ZO-1, cadherin and β-catenin (Burns *et al.* 1997). However, the involvement of tricellular corners still remains controversial and more physiological models need to be established to study them.

1.7 Tight junction proteins

In recent years, knowledge of tight junctions has dramatically expanded, and this is mainly due to the identification of TJ proteins, to date over 40 have been discovered.

TJ are composed of a complex arrangement of proteins, consisting of transmembrane proteins and peripheral proteins. TJ transmembrane proteins include occludin, the claudins and the JAM family proteins, and are directly involved in creating the TJ seal between adjacent cell membranes. The TJ seal can be viewed in TEM micrographs where the membranes of two adjacent cells fuse together termed as kissing points (Farquhar and Palade 1963).

The peripheral proteins (or TJ associated proteins) are located in the plaque region, in the cytoplasm immediately below the TJ strands, which can be seen as a darker electron dense area in TEM micrographs (Farquhar and Palade, 1963). These proteins have a structural role cross-linking TJ proteins to each other and to the cytoskeleton, and a role in cell signalling regulating cell differentiation and proliferation.

All the transmembrane protein and peripheral protein interactions and roles are still not understood, but a complex arrangement is emerging (fig.1.8), which is essential to the overall function of the cell.

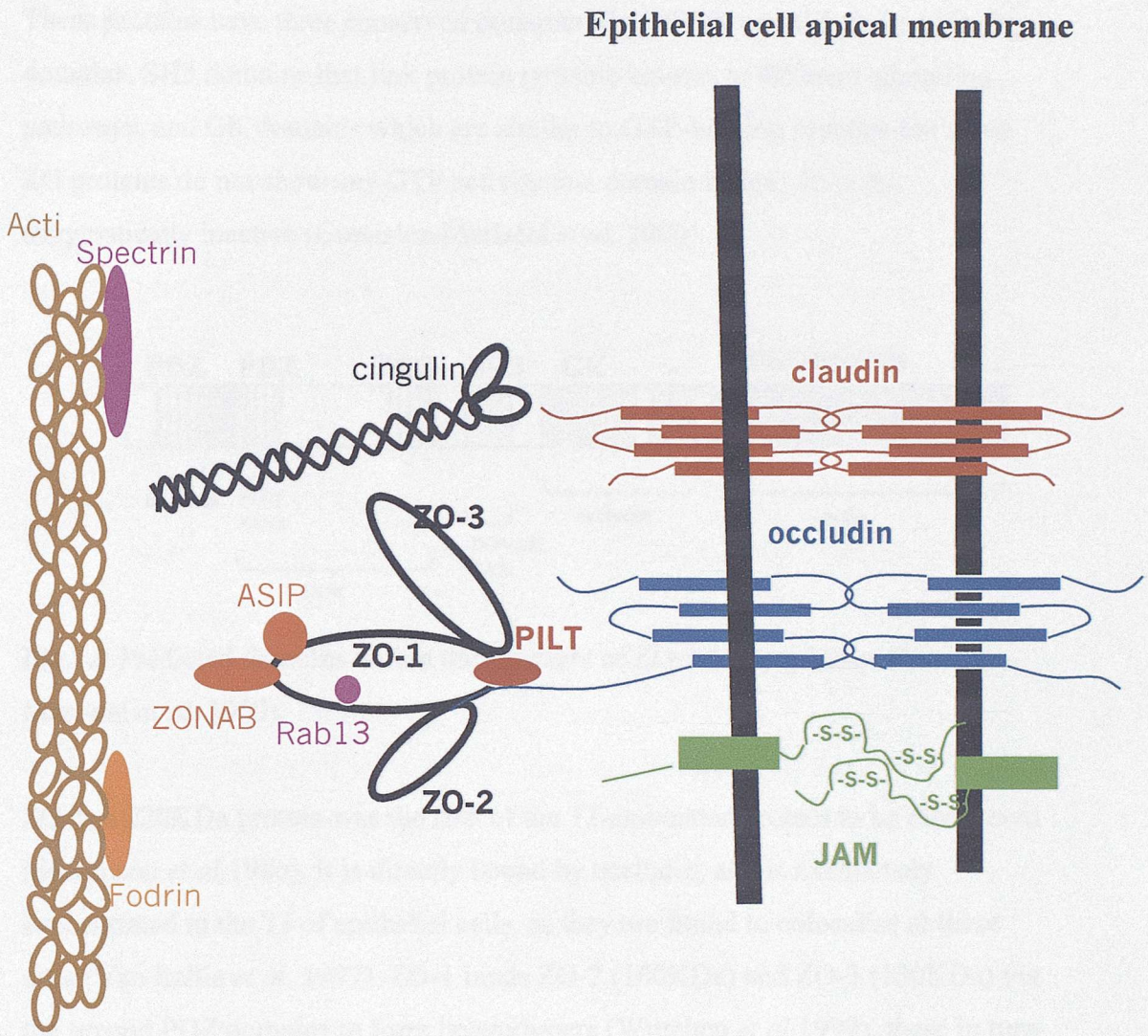

Fig. 1.8 Hypothetical assembly of TJ proteins (not to scale)

1.8 TJ-associated proteins

The first group of TJ-associated proteins, ZO-1, ZO-2 and ZO-3, are members of the membrane-associated guanylate kinase homologues (MAGUK) protein family. These proteins have three conserved domains (fig.1.9): three PDZ protein binding domains, SH3 domains that link protein tyrosine kinases to different signalling pathways, and GK domains which are similar to GTP-binding proteins but since ZO proteins do not show any GTP activity this domain is thought to be enzymatically inactive (Gonzalez-Mariscal *et al.* 2000).

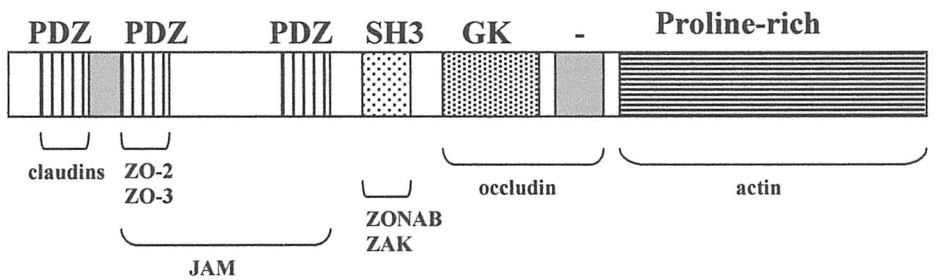

Fig.1.9 Predicted domains within the structure of ZO-1 (adapted from Gonzalez-Mariscal *et al.* 2000).

ZO-1, a 220KDa protein was the first of the TJ-associated protein to be discovered (Stevenson *et al.*1986). It is directly bound by occludin, and is exclusively concentrated at the TJ of epithelial cells, as they are found to colocalise at these sites (Van Itallie *et al.* 1997). ZO-1 binds ZO-2 (160KDa) and ZO-3 (130KDa) via the second PDZ domains to form heterodimers (Wittchen *et al.*1999), these in turn bind occludin and claudins. The interaction of occludin with ZO-1 is not via a PDZ domain but through the GK and acidic domains, which associate with the cytoplasmic carboxyl terminal of occludin, and the proline-rich carboxy-terminal of ZO-1 and ZO-2 bind F-actin filaments, cross-linking the cytoskeleton to occludins at tight junctions (Fanning *et al.* 1998; Itoh *et al.* 1999). The first PDZ domain of occludin binds the carboxyl terminal of claudins (Itoh *et al.* 1999), and the second and third PDZ domains bind JAM (Ebnet *et al.* 2000). The amino terminal of ZO-2 and full length ZO-3 directly bind the carboxyl terminal of occludin (Itoh *et al.* 1999; Haskins *et al.* 1998). In addition to their importance as scaffolding proteins in cell-to-cell junctional contacts, the ZO proteins play an important role in signalling pathways, since they interact with kinases such as

ZAK (ZO-1 associated kinase) and aPKC (atypical protein kinases) and GTP-binding proteins such as RAB13 (Balda *et al.*1996; Dodane *et al.* 1996; Zahraoui *et al.* 1994). More recently ZO-1has been shown to interact with the transcription factor, ZONAB, regulating paracellular permeability and gene expression (Balda and Matter 2000). Furthermore, tyrosine phosphorylation of ZO-1 can lead to either an increase in tight junction formation (Van Itallie *et al.* 1995), or a disruption of TJ (Staddon *et al.* 1995), and hence, has a role in modulating TJ permeability. It is not known whether this is due to different sites being phosphorylated or some other parameter, but these studies suggest changes in the quaternary structure of TJ proteins have an influence on TJ function.

There are many other plaque proteins still being discovered which are not as well understood as the ZO-proteins, some of which have PDZ domains and some without (see table 1.1), a summary of a few follows.

Other plaque proteins containing PDZ domains include MAGI-1 (membrane associated guanylate kinase) which colocalises with ZO-1 but its role is unknown (Ide *et al.* 1999), ASIP (atypical-PKC-specific interacting protein)/PAR-3 and PAR-6 proteins which form a complex with aPKC and Cdc42 which is thought to have a role in establishing epithelial cell polarity (Wodarz *et al.* 2000), MUPP1 which contains 13 PDZ domains and is thought to be an important scaffolding protein interacting with claudins and JAM molecules (Hamazaki *et al.* 2002), and PATJ which also has multiple PDZ domains and is thought to have a role in maintaining TJ integrity since overexpression results in the disruption of ZO-1 and ZO-3 localisation (Roh *et al.* 2002).

Plaque proteins without PDZ domains include cingulin which cross-links TJ proteins with the actomyosin cytoskeleton (Bazzoni *et al.* 2000), spectrin and fodrin, which link transmembrane proteins to the cytoskeleton (Bennett and Gilligan, 1993), and PILT (protein incorporated later into tight junctions) named due to its incorporation into tight junctions after claudin-based junctional strands were formed (Kawabe *et al.* 2001).

NAME		ROLE	Reference
ZO-1	**Contain PDZ domains**	Scaffolding and signalling	Stevenson *et al.* 1986
ZO-2		Scaffolding and signalling	Gumbiner *et al.* 1991
ZO-3		Scaffolding and signalling	Balda *et al.*1993
MAG-1		Unknown	Ide *et al.*1999
ASIP/PAR3		Establish cell polarity	Joberty *et al.*2000
PAR-6		Establish cell polarity	Johansson *et al.*2000
AF-6		Neuroepithelial development	Prasad *et al.* 1993
Cingulin	**No PDZ domains**	Cross links TJ proteins to cytoskeleton	Citi *et al.* 2000
symplekin		Possible role in scaffolding/assembly	Keon *et al.* 1996
ZONAB		Regulates paracellular permeability and gene expression	Balda and Matter, 2000
Ash-1		Colocalises with ZO-1 and cingulin	Nakamura *et al.* 2000
4.1R		Binds ZO-2	Mattagajasingh *et al.* 2000
spectrin		Cytoskeletal linker protein	Bennett and Gilligan, 1993
fodrin		Cytoskeletal linker protein	Bennett and Gilligan, 1993
RAB-13		Signalling	Zahraoui *et al.* 1994
aPKC		Signalling	Izumi *et al.* 1998
ZAK		Signalling	Balda *et al.* 1996

Table 1.1 List of tight junction plaque proteins (modified from Cereijido and Anderson 2001).

1.9 Transmembrane proteins

Tight junction-associated proteins may be involved in the recruitment of different transmembrane proteins, but it is ultimately changes in the expression or configuration of transmembrane proteins forming the cell-to-cell contacts that will contribute to changes in TJ barrier function. A detailed discussion of each type of transmembrane protein follows.

1.9.1 Occludin

Occludin, with a molecular mass of approx. 60KDa, was the first integral tight junction protein identified (Furuse *et al.* 1993). It has four transmembrane domains, a long carboxyl-terminal cytoplasmic domain, short amino-terminal cytoplasmic domain and two similar length extracellular loops that are rich in tyrosine residues (fig.1.10). It has also been found expressed at cell borders of HUVEC monolayers (Burns *et al.* 2000).

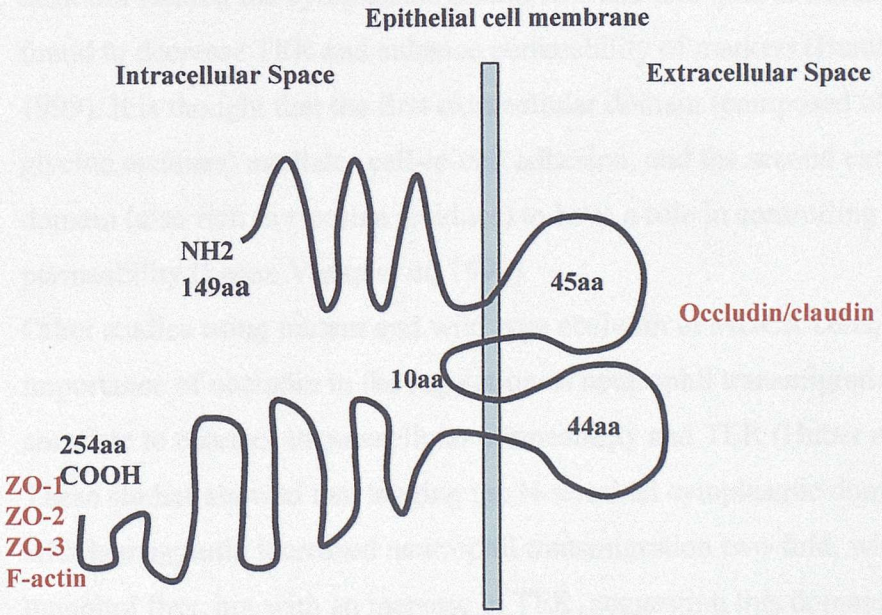

Fig.1.10 Schematic diagram of occludin, showing binding regions (in red). (adapted from Gonzalez-Mariscal *et al.* 2003).

Occludin is a calcium-independent intercellular adhesion molecule (Van Itallie and Anderson, 1997) and forms oligomers laterally in the membrane (Chen *et al.* 1997). Immunofluorescent labelling shows occludin is localised at the TJ's of epithelial and endothelial cells (Furuse *et al.* 1993). McCarthy *et al.* (1996), have shown that overexpression of occludin in MDCK cells leads to an increase in transepithelial electrical resistance, indicating a direct correlation between expression of occludin and electrical resistance (McCarthy *et al.* 1996).

The level of occludin phosphorylation is also important. Studies with epithelial cells suggest an increase in occludin phosphorylation is related to an increase in tight junction assembly, as highly phosphorylated occludin is found to be concentrated at TJ but less phosphorylated occludin is found in the cytoplasm (Andreeva *et al.* 2001). This suggests the level of phosphorylation determines the location of occludin, and may be important in TJ assembly.

Various studies suggest different structural domains of occludin are important for different functions. Firstly, mutant occludin expressing a truncated COOH-terminal had an increased permeability to small molecular weight markers, suggesting its importance in TJ barrier function (Chen *et al.* 1997). Mutant occludin lacking the cytoplasmic amino terminal and both extracellular loops was found to decrease TER and enhance permeability of markers (Bamforth *et al.* 1999). It is thought that the first extracellular domain (composed of tyrosine and glycine residues) mediates cell-to-cell adhesion, and the second extracellular domain (also rich in tyrosine residues) to have a role in controlling paracellular permeability (Lacaz-Vieira *et al.* 1999).

Other studies using mutant and wild type occludin in MDCK cells, show the importance of occludin in the regulation of neutrophil transmigration, but do not correlate to changes in paracellular permeability and TER (Huber *et al.* 2000). These studies showed that tagging the N-terminal cytoplasmic domain of occludin with hemagglutin increased neutrophil transmigration two-fold, without effecting mannitol flux, but with an increase in TER, suggesting this domain is important in specifically regulating transepithelial migration, but with no correlation to paracellular permeability and TER.

Recent studies utilising occludin-deficient embryonic stem cells differentiated into epithelial cells could still form well-developed TJ structures (Saitou *et al.* 1998).

Therefore, occludin is not required for morphologically normal TJ formation, but is involved in selective permeability and fence function (Matter and Balda 1999). Recently, two occludin isoforms have been identified. Firstly, the occludin 1B alternative spliced variant was discovered in MDCK cells, which was longer than occludin due to a 193-base pair insertion, and also differs in its amino terminal sequence (Muresan *et al.* 2000). This study used immunolabelling with an antibody specific for the amino-terminal to show occludin 1B colocalised with occludin at cell to cell contact points, suggesting it may have a role in TJ formation.

The second alternatively spliced isoform, TM4-, was found to be shorter than occludin, having a 162 base pair deletion at the fourth transmembrane domain (TM4) and immediate 3'-flanking sequence (Ghassemifar *et al.* 2002). This would result in the cytoplasmic C-terminal of occludin becoming extracellular. Since, the C-terminal is important in interacting with tight junction plaque proteins, it is suggested that TM4- may have a role in negatively regulating TJ integrity.

The presence of occludin does not always reflect the extent of TJ formation, since targeted disruption of the occludin gene from embryonic stem cells still resulted in normal TJ expression (Saitou *et al.*1998).

Occludin is therefore an important protein in TJ structure and function, but its actual role is still to be determined. However, since cells lacking occludin could still form TJ it was predicted that other proteins must be involved in TJ formation.

1.9.2 Claudins

Studies by Furuse *et al.*, led to the identification of claudins from isolated junctional fractions of mouse membrane. Two novel tight junction-transmembrane proteins with no sequence similarity to occludin were copartitioned with occludin in the TJ-enriched fraction (Furuse *et al.* 1998). To date approximately 24 claudins have been identified and sequenced, which display a level of homology in their primary structure, although not all are well characterized (Tsukita *et al.* 2001). Claudins have a molecular weight of approximately 20-27kDa, with four transmembrane domains, two extracellular loops (one longer and more hydrophobic than the other) and a short amino terminal (fig.1.11). Sequences of the first and fourth transmembrane region and the two extracellular loops are highly conserved, but differences occur in the second and third transmembrane regions and in the cytoplasmic carboxyl terminal (Heiskala *et al.* 2000).

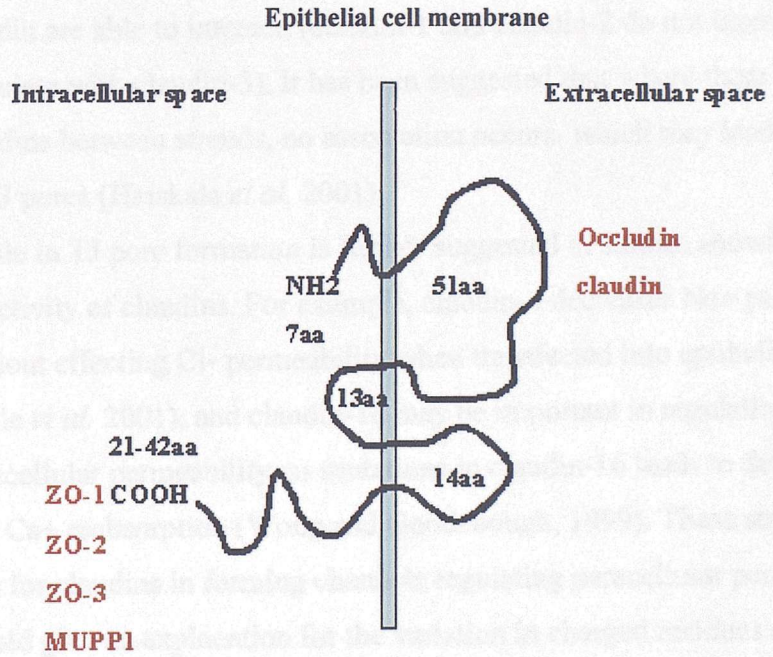

Fig.1.11 Schematic drawing representing general structure of claudins, showing binding regions in red, (adapted from Heiskala *et al.* 2001).

Claudin-1 and Claudin-2, approx. 23Kda, have four transmembrane domains with a 38% amino acid sequence homology. When claudin-1 (Furuse *et al.* 1998) or claudin 3 (Sonoda *et al.* 1999) were transfected into mouse L-fibroblasts lacking tight junctions, freeze-fracture images showed continuous TJ strands were formed, whereas occludin alone formed short strands. However, these same studies showed that claudin-2 and claudin-11 form discontinuous strands, suggesting different claudins impart different characteristics to the TJ.

Studies into the expression and function of claudin within TJ, showed more than one type, coexpressed in cells of various tissues (Furuse *et al.* 1998). The expression of claudin does not appear to correlate to the number of TJ. Rather, the distribution of claudins within the tissue reflects TJ function. This suggests that multiple claudins are involved in the formation of TJ in a tissue-dependent manner (Morita *et al.* 1999).

Claudins copolymerise, either via homophilic or heterophilic interactions, to form the backbone of TJ strands and occludin is copolymerised into these strands, which then laterally associate with the TJ strands of the adjacent cell, sealing the membranes together (Furuse *et al.* 1999). However, only distinct species of claudin are able to interact, (claudin-1 and claudin-2 do not interact but either can associate with claudin-3). It has been suggested that where there is a mismatch of claudins between strands, no association occurs, which may lead to the formation of TJ pores (Heiskala *et al.* 2001).

A role in TJ pore formation is further suggested in studies showing ionic selectivity of claudins. For example, claudin-4 decreases Na+ permeability without effecting Cl- permeability when transfected into epithelial cells (Van Itallie *et al.* 2001), and claudin-16 may be important in regulating Mg+ and Ca+ paracellular permeability, as mutations in claudin-16 leads to defects in renal Mg+ and Ca+ reabsorption (Wong and Goodenough, 1999). These studies suggest a role for claudins in forming channels regulating paracellular permeability, which would give an explanation for the variation in charged residues seen in the extracellular loops of claudins.

TJ tightness is possibly determined by the combination and ratio of claudin species (Tsukita and Furuse 2000). Comparison of two MDCK strains, showed claudin-2 expression in one type (MDCK II) but not the other (MDCK I). When claudin-2 was introduced into MDCK I cells, its TJ became more leaky to ions,

and were functionally and morphologically similar to those in MDCK II cells, as determined by TER measurements and number of TJ strand formation. This suggested that the combination of claudins play a role in the tightness of TJ strands (Furuse *et al.*2001). Overexpression of claudin-1 in MDCK cells increases electrical resistance several fold (Inai *et al.* 1999).

More recently it has been suggested that the combination of occludin and claudin-1 is essential for paracellular barrier function, since mice with occludin but lacking claudin-1 allow permeability across mouse skin layers (Furuse *et al.* 2002).

Claudins are expressed in different cell types and differ in distribution, suggesting tissue specific functions (Rahner *et al.* 2001), for example Claudin-5 is associated with endothelial tight junctions (Morita *et al.*1999). Claudins have also been found to be distributed on the lateral surface of cell membranes and not just at the TJ, suggesting either an excess pool of claudins that can be recruited when required, or another role for claudins separate from TJ's (Rahner *et al.* 2001).

The full role of claudins and their interaction with other TJ proteins is still unclear, and as more claudins are identified, the task of determining their function is becoming more complex.

1.9.3 JAM (Junction associated Molecule)

This is a recently identified family of proteins, three of which have been discovered to date, that are located at the TJ of epithelial and endothelial cells. JAM-1 a 43kDa protein, found to localise at TJ of epithelial and endothelial cells (Martin-Padura *et al.* 1998). JAM is a member of the immunoglobulin superfamily, with a single transmembrane domain, a short intracellular tail and an extracellular region consisting of two Ig domains (fig.1.12). JAM interacts with other proteins via its carboxyl terminal, including ZO-1 (Bazzoni *et al.* 2000), and ASIP/PAR-3 (Itoh *et al.* 2001). JAM also associates with cingulin, linking it to the cytoskeleton (Bazzoni *et al.* 2000). Recently, it has been shown that JAM interacts homophilically to form U-shaped dimers at the tight junction, and the amino terminal of dimers of adjacent cells interact (Kostrewa *et al.*2001).

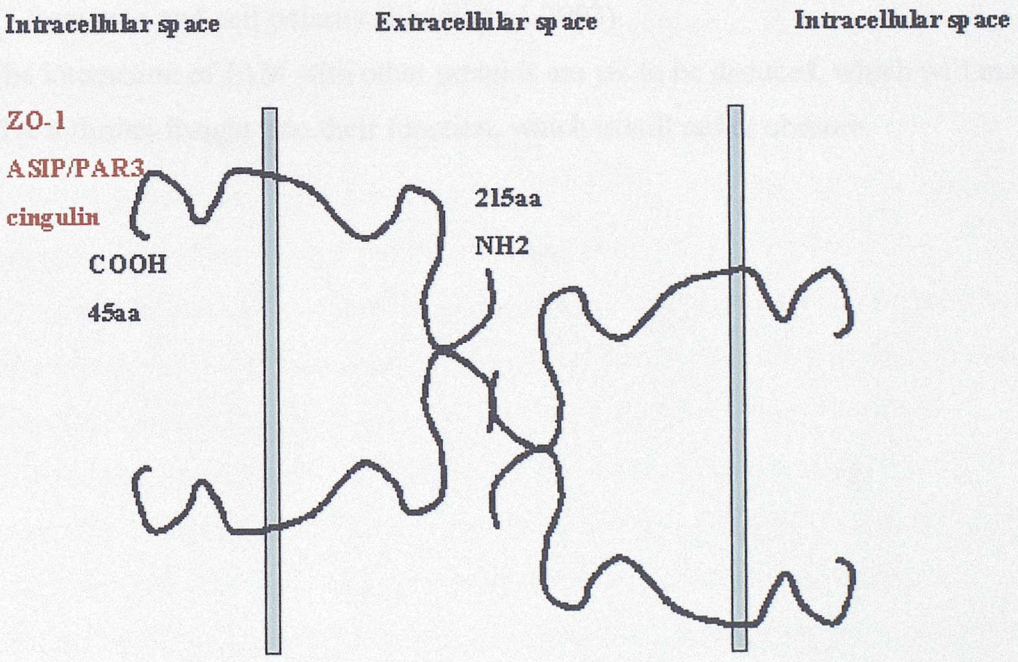

Fig.1.12 Schematic drawing representing general structure of JAM molecules forming dimers, showing dimmers of adjacent cells interacting, other binding regions in red, (adapted from Gonzalez-Mariscal *et al.* 2003).

Unlike claudins and occludin, transfecting JAM-1 into L-fibroblasts does not lead to the formation of TJ strands (Itoh *et al.* 2001), suggesting JAM does not form tight junctions directly.

JAM-1 appears to play a role in monocyte transmigration across endothelial monolayers, by transducing a signal within the endothelial cell to open the junctional space, which can be inhibited with a monoclonal antibody (Martin-Padura *et al.*1998).

It is thought JAM-1 is important for TJ formation, since it colocalises with E-cadherin and ZO-1 at cell-to-cell contacts during junction formation (Ebnet *et al.* 2001). If JAM-1 is one of the first TJ proteins to be expressed at cell-to-cell adhesion sites it can be speculated that it is involved in signalling and recruiting other proteins involved in TJ formation.

JAM-2 and JAM-3 are expressed in endothelial cells (Aurrand-Lions *et al.* 2001) and have a similar structure to JAM-1. Both of these proteins associate with PAR-3 and ZO-1, and are therefore thought to have a possible role in the regulation of TJ formation and cell polarity (Ebnet *et al.* 2003).

The interaction of JAM with other proteins are yet to be deduced, which will may give a further insight into their function, which is still rather obscure.

1.10 Interaction of tight junction proteins

Although the binding of occludin with ZO is important in its recruitment and assembly at TJ, occludin can still be incorporated into the junctions by polymerisation with other occludin or claudin molecules (Furuse *et al.* 1998). Claudins directly interact with both occludin and ZOs (Itoh *et al.* 1999). Polymerisation of claudins, either homophillic or heterophillic, form the structural backbone of TJ strands. Each claudin polymer will interact with a claudin polymer on an adjacent cell, leading to TJ formation (Furuse *et al.* 1999). It can be speculated that the strength of TJ depends on the claudins involved and their combination in forming these polymers.

JAM-1 has also been show to colocalise with ZO-1 and occludin, as well as cingulin at TJ (Bazzoni *et al.* 2000). JAM-1 is thought to stabilise occludin at TJ strands, and links the TJ to the actomyosin cytoskeleton via its interactions with ZO-1 and cingulin.

The TJ structure can now be pictured (fig.1.13) with the three transmembrane proteins, occludin, claudins and JAM, forming a polymerised structure across the cell membrane, which associates with a similar structure on the membrane of the adjacent cell forming a tight seal. The transmembrane proteins are then linked to the cytoskeleton either directly or indirectly via plaque proteins.

It should also be noted that assembly of TJ first requires establishment of cell-to-cell adhesion, which is mediated by adherens junctions. Extracellular Ca+ initiates cell adhesion via E-cadherin molecules, initially forming weak complexes, which then become progressively stronger as more cadherin is recruited to the adherens junction, forming links to the cytoskeleton via cadherin-catenin complexes (Adams and Nelson, 1998). During this initial stage of cell adhesion, ZO-1 colocalises with cadherin, forming spot-like junctions at the tips of extending cells (Asakura *et al.* 1999). As cell polarization continues, claudin and occludin accumulates at these spot-like junctions eventually forming continuous belt-like structures of the TJ, while cadherin appears to move away and accumulate at the adherens junction (Ando-Akatsuka *et al.* 1999). The full mechanism of TJ assembly is still to be deduced.

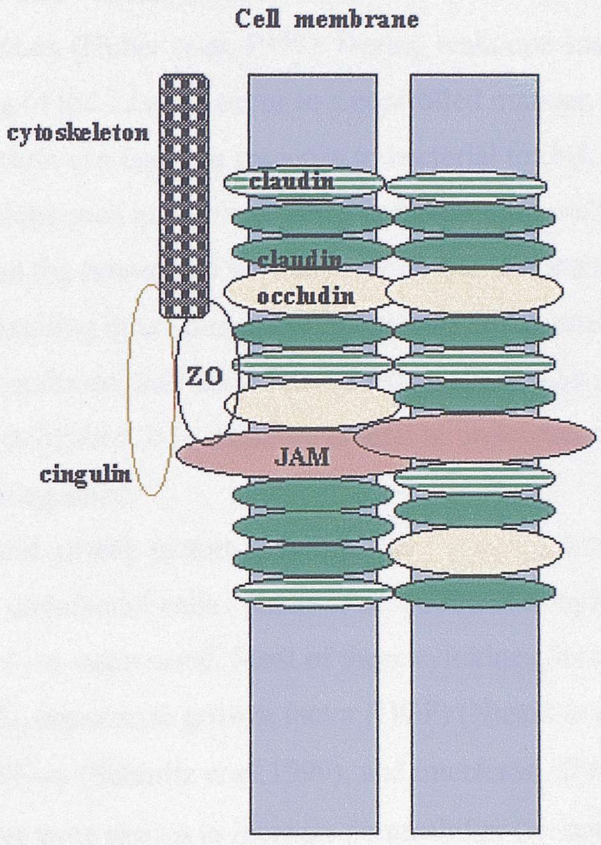

Fig.1.13 Schematic representation showing arrangement of tight junction transmembrane proteins of two apposing cell membranes. The backbone consists of at least two types of claudin copolymerising with occludin. The transmembrane proteins will interact with plaque proteins, such as cingulin and ZO proteins, linking them to the cytoskeleton.

1.11 Modification of tight junction barrier function

Tight junctions regulate paracellular permeability of the epithelium. When the lumenal surface of the epithelium is challenged by an external allergen, leukocytes from the blood cross the endothelium, in response to chemoattractants, to reach the inflamed epithelium (Huber *et al.* 1999). During leukocyte transmigration, the opening and closing of the TJ must occur in a controlled manner.

Loss of barrier function can occur in response to bacterial toxins, or in pathological conditions such as asthma, which is thought to result in uncontrolled flux of allergen from the lumen into the submucosa, and uncontrolled immune cells responding, resulting in inflammation in the lung. Inflammation and epithelial damage continues until the barrier function is restored and junctional complexes are re-established. It is therefore crucial to understand how the epithelial barrier is regulated.

Several cytokines and growth factors have been shown to regulate TJ function in both epithelial and endothelial cells (Walsh *et al.* 2000), although their mechanisms are not yet understood. Most of these cytokines, interleukin (IL)-4 (Colgan *et al.* 1994), hepatocyte growth factor (HGF) (Nusrat *et al.* 1994), tumor necrosis factor (TNF)-α (Schmitz *et al.*1999), and interferon (IFN)-γ (Madara and Stafford 1989), have been shown to increase permeability (ie. decrease TJ barrier function). Epidermal growth factor (EGF), (Soler *et al.* 1993) and transforming growth factor (TGF)-β1 (Planchon *et al.*1999) appear to increase barrier function. The majority of these studies have used intestinal epithelial cells and there appears to be a lack of studies on respiratory epithelium. In fact, it may be that different cytokines exert different effects on the tight junctions of different epithelium. It has already been shown that IFN-γ actually enhances lung epithelial barrier function (Ahdieh *et al.* 2001), and TNF-α is not always reported to have an effect on epithelial barrier function (Madara and Stafford 1989)

Increased understanding of the effects and mechanisms of cytokine action on TJ may help in maintaining barrier integrity during pathological conditions.

1.12 Models of respiratory epithelial/endothelial systems

In order to study TJ function *in vitro*, it is important to establish and characterise models that will reflect the physiological situation and also enable relevant investigations to be made. A model designed to look at TJ function in the epithelial and endothelial barriers of the human bronchial tract would be relatively unique and individual, and help in the understanding of cell barrier interaction as a whole rather than as separate entities.

There have been several studies looking at either respiratory epithelial (Casale *et al.* 1998; Liu *et al.* 1996) or endothelial cell barriers (Yamamoto *et al.* 2000) using single monolayer systems. Models have been further modified by growing bronchial epithelial cells at an air-liquid interface (Kidney and Proud, 2000), to study the relationship between resistance and neutrophil transmigration in an airway epithelial cell line. These are all monolayer models, but more recent studies have involved models of both an endothelial and an epithelial barrier to reflect a more physiological system, for example, the effect of environmental toxins (ozone) on airway tissue has been studied using a co-culture system involving bronchial epithelial and endothelial cells (Mogel *et al.* 1998). A co-culture system of the air-liquid interface has also been established using rat pneumocytes and bovine endothelial cells (Gueven *et al.* 1996). However, this has the obvious drawback of using cells derived from two different species other than human. Co-culture models using human cells have been established to study neutrophil migration, for example, through human type II alveolar epithelial cell line and endothelial cells (Casale and Carolan, 1999). A similar model showed neutrophil migration across the bilayer was more efficient than single epithelial monolayers, and that epithelial and endothelial cells do exert an effect on each other (Mul *et al.*2000).

These studies show the need to study both epithelial and endothelial systems together, as individual monolayers differ in their results from bilayer models, and do not fully reflect the *in vivo* situation. These studies have also focussed on cell migration, and not directly on TJ function. Models that have been developed to study TJ function either use monolayers or co-culture models relating to other physiological systems such as the blood-brain-barrier (Gaillard *et al.* 2001).

There is a need for models that would better reflect the human respiratory airways, to enable the study of barrier function. Models are essential tools to further our knowledge of biological systems. The *in vivo* situation is very complex with many components interacting, and it would be difficult to reflect the full complexity in an *in vitro* model. Also, a model consisting of many components would make it difficult to interpret results, as there would be too many interactions occurring, that could be producing an effect. It is therefore ideal for model systems to be simple, so a particular result can be related to a particular interaction. A well characterised bilayer model reflecting the two barriers of the human bronchial airway- the epithelium and endothelium would be simplistic but also allow cell-to-cell interaction of these two components to be investigated, giving a more physiological reflection of the *in vivo* conditions in the bronchial system. Such a model would also allow the effects of epithelial-endothelial interactions on barrier function to be investigated.

1.13 Final synopsis

The airway wall of the bronchial system consists of epithelial mucosal surfaces with endothelial-lined capillaries in the underlying lamina propria. The airway wall functions as an integrated unit, acting as a barrier between the internal and external environments of the lung. The possibility of cell-to-cell interactions and the production of soluble factors (eg. cytokines) must be considered as they may regulate cell responses. Therefore, when studying the respiratory epithelium, it is important to also understand how the whole system interacts ie. epithelium, endothelium and extracellular matrix.

The two barriers, the epithelium and endothelium, must be communicating with each other in order to enable them to co-ordinate their activities. For example, when the epithelium is challenged, it must communicate with the immune system to trigger a response. Immune cells must then cross the endothelium into the surrounding tissue and target the site of challenge. The epithelium and endothelium activity is locally coordinated, facilitating an effective immune response.

Both epithelial and endothelial-cell tight junctions form an important permeability barrier. The barriers serve different functions, such that epithelial cells require a tight barrier to prevent external irritants in the lumen entering the underlying tissue but must allow leukocyte migration in the opposite direction; whereas the endothelium tends to form looser junctions that allow the migration of solutes, ions and leukocytes from the blood into the surrounding tissue. As a consequence, even though the tight junction is structurally similar, they differ in the protein composition at the tight junction.

Mechanisms of transepithelial migration are unclear, but it is thought that barrier integrity is maintained during leukocyte migration, whereas during infection tight junctions are disrupted resulting in barrier function being diminished. Damage to the epithelium will result in the release of danger signals, which will activate and maintain the stimulation of immune cells, and allow their migration across the endothelium, through the tissue and basement membrane and across the epithelium into the lumen.

A model to study the integrity of bronchial epithelial barrier function, and the effect of endothelial cells on this function, would be invaluable in furthering our knowledge in tight junction function.

1.14 AIMS

1. To establish an *in vitro* bilayer model reflecting the *in vivo* situation of the two barriers of the human bronchial airway- the epithelium and the endothelium.
2. To fully characterise and optimise conditions so that the model is consistent and reproducible and easily manipulated for various studies, such as permeability and cell migration.
3. Use the model to identify and further examine changes in epithelial barrier function induced by endothelial cells.

1.15 HYPOTHESES

1. An *in vitro* epithelial-endothelial model will provide a better reflection of the *in vivo* situation, in comparison to monolayer systems.
2. Epithelial-endothelial interactions occur in vivo, as they are components of an integrated biological unit, and these interactions will be of particular importance in maintaining barrier function.
3. Endothelial cells will influence barrier function by modulating epithelial tight junction function.

CHAPTER 2
MATERIALS AND METHOD

Chapter 2: Materials and Methods

2.1 Cell culture

2.1.1 General cell culture

All cell culture and experiments involving live cells were undertaken in a sterile laminar flow hood (Holten LaminAir class 2 hood). Cells were grown in medium (see Table 1), at 37°C in a humidified incubator with 5% CO_2. 16HBE 14o- and H292 cells were grown in 75cm^2 flasks (Falcon) containing 10ml growth medium, and all endothelial cells were grown in 25cm^2 (Falcon) flasks containing 5ml growth medium. Medium was changed every two days. Once confluent, cells were passaged into new flasks, every 6-7 days. All culture reagents were from Life Technologies, Invitrogen Ltd unless otherwise stated.

2.1.2 Handling and establishing frozen cell stocks

To establish cell stocks, each cell type was frozen in liquid nitrogen as follows. Confluent flasks of cells were trypsinised as described above. The cell pellet obtained was resuspended in 1ml growth medium supplemented with 5% DMSO (Sigma), and put into a cryogenic vial. The vials were stored at –80°C for 24 hours, and then transferred to liquid nitrogen vapour until required.

Cell cultures were started from frozen stocks as follows.
Frozen vial of cells were gently but rapidly thawed at 37°C. As soon as the contents were thawed, the vial was sprayed with 70% ethanol and the contents transferred to a tube containing 10ml of the relevant growth medium. The cell suspension was centrifuged at 1500rpm for 5 minutes, 800rpm for endothelial cells. The supernatant was discarded and the cell pellet resuspended with fresh growth medium at the relevant seeding density (see above) and added to culture flasks.

Cell name	Cell type	Growth medium	Origin
16HBE 14o-	SV40-transformed bronchial epithelial cell line	MEM, 10% FCS, L-glutamine, antibiotics (penicillin (100U/ml), streptomycin (100U/ml))	Dr D C Gruenert Univ of California
H292	Carcinoma derived tracheal epithelial cell line	RPMI, 10% FCS, antibiotics	ATCC
HUVEC	Primary human umbilical vein endothelial cells	M199, 20% FCS, heparin (5U/ml), EGF (5ng/ml), antibiotics	Human umbilical cord
HUVEC	Primary human umbilical vein endothelial cells	EBM-2 medium (Clonetics)	Clonetics – derived from human umbilical cord
HUV-EC-C	Human umbilical vein endothelial cell line	Kaighns modified F12K, 10% FCS, ECGS (0.03mg/ml), heparin (5U/ml), antibiotics	ATCC
HUVE-12	Human umbilical vein endothelial cell line	Same as HUV-EC-C	ATCC
HUVS-112D	Fibroblast-like endothelial cell line	Same as HUV-EC-C	ATCC

Table 2.1. *Growth conditions of cells*

2.1.3 Extraction of primary HUVEC from human umbilical cord

Primary human umbilical vein endothelial cells (HUVEC) were extracted from fresh human umbilical cords (obtained from Child Health, SGH). All equipment was autoclaved prior to use.

1. Small cell culture petri dishes (Falcon) were coated with 1ml of 0.5% gelatin (in sterile distilled water) for 2-3 hours, and air dried in sterile culture hood.
2. The cord was cut to approximately 10cm in length and washed well in sterile PBS. The umbilical vein was washed several times using a 5ml syringe to push through PBS.
3. One end of the cord was clamped and 5mls of 1mg/ml collagenase (Life Technologies) in HBSS was syringed into the vein. The vein expands under the pressure. The other end was carefully clamped.
4. The cord was placed in a sterile basin and incubated for 15 minutes at 37°C. Every 2-3 minutes the vein was pressed well to ensure the enzyme covered the whole of the vein.
5. The ends of the cord were washed well in PBS. One clamp was removed carefully and the contents of the vein collected carefully into a 50ml tube.
6. The other clamp was removed, and 10-20 ml HBSS with 10% FCS was syringed through the vein and collected, to wash out the rest of the enzyme from the vein.
7. The fluid collected was centrifuged at low speed (800 rpm) for 5 minutes.
8. Supernatant was discarded and the pellet was gently resuspended in 2ml growth medium (see table 1). Cells were seeded as clumps, at a density of $1x10^6$ cells/small petri dish.
9. The next day the cells had attached and were washed well with PBS and 2ml of fresh medium added.
10. The cells were continued to be grown and once confluent were trypsinised (as above), and transferred to $25cm^2$ flasks.

2.1.4 Cell culture for immunostaining

Immunostaining was performed on glass coverslips to establish specific markers for each cell type. Glass coverslips (13mm diameter) were sterilised with 70% ethanol for 15 minutes and then air-dried in a sterile culture hood. Six coverslips were placed into small petri dishes and cells were seeded at a density of $5x10^4$ in 100µl of growth medium per coverslip, and placed in an incubator for 2 hours. Once the cells had attached, 2mls of growth medium was added to the petri dish and placed in an incubator. The cells were grown to 70-80% confluence, with the medium being changed every two days.

2.1.5 Cell culture on inserts

Cells were seeded at different concentrations (0, $1x10^4$, $5x10^4$, $1x10^5$ and $5x10^5$) in a volume of 500µl in 0.4µm pore size PET inserts (Falcon) in a 24-well plate. Each well also contained 500µl of medium. The culture medium in the insert and well was changed daily. After each medium change electrical resistance was measured with an Endohm-6 electrode measurement system and resistance meter from World Precision Instruments (see section 2.3).

16HBE 14o- cells were also seeded on the underside of 0.4µm inserts at different densities (0, 10^4, $5x10^4$, 10^5 and $5x10^5$ cells/insert). After 4 hours incubation at 37°C, the inserts were reinverted into 24 well plates containing 500µl medium/well. The following day 500µl of medium was added to the insert. The medium was changed on a daily basis and the electrical resistance measured. The optimal seeding density at which cells attached the quickest to the underside of the insert was established.

16HBE 14o- and HUVEC were seeded on inserts at $1x10^5$ cells/insert with different pore sizes (3µm, 1µm and 0.4µm). Day 1 and day 2 after reaching confluence, the cells were fixed and processed for SEM (section 2.5), and each side of the membrane examined for evidence of cell migration through the pores. Cell density counting was also performed on cells grown on inserts. After TER was measured, insert membranes were removed, washed 3 times with PBS and nuclei stained with Hoechst. After a further 3 washes, the membrane was mounted on a glass slide with mowiol/citifluor. Consecutive images were taken across the middle of the membrane, and analysed using ImageJ software to count cell nuclei.

2.1.6 Final set-up of bilayer model

16HBE 14o- cells were seeded at the optimal density ($2x10^4$/50µl) on the underside of 0.4µm pore-sized PET inserts, inverted in a sterile dish. After 4 hours incubation, the filters were placed, in their correct orientation, into 24 well plates containing 500µl medium/well. The following day 500µl of medium was added to the insert. The medium was changed on a daily basis and the electrical resistance measured. On reaching confluence, when TER was greater than 78Ω.cm^2, HUVEC were added at high density ($2x10^5$/200µl) to the upper side of the insert. Both cell layers were then grown to confluence, TER measured and on day1 and 2 the inserts were fixed for confocal microscopy, SEM and TEM.

2.1.7 16HBE 14o- monolayer grown in presence of HUVEC medium

16HBE 14o- cells were grown in three different conditions. First as a monolayer, second as a bilayer, and third as a monolyer but in the presence of HUVEC conditioned medium taken from flasks with confluent HUVEC growing. The medium was first sterile filtered through a 0.2µm filter, and then 200µl added to the inside of the insert.

2.1.8 Cell permeability assay

16HBE 14o- cells were grown in the three conditions as above (2.1.7) and were assessed for permeability using FITC-dextran with a molecular weight of 4KD (Sigma). On day 1 after addition of HUVEC/conditioned medium, 110µl of medium was removed from each insert and 10µl of FITC-dextran added (stock concentration 5mg/ml). After 30 minutes incubation at 37°C to equilibriate, the inserts were transferred to fresh plates containing 700µl of pre-warmed growth medium. On day 2 (24 hours after addition of FITC-dextran), the amount of FITC-dextran migrated from the insert into the well was assessed by measuring the absorbance of the 700µl medium in the well using a cytofluor. The amount of FITC-dextran was calculated from a standard curve generated from the absorbance measurements of titrated amounts of FITC-dextran.

2.1.9 Conditioned medium treatments

Medium removed from confluent HUVEC cell cultures was sterile filtered through a 0.2μm filter and treated as follows before being added to the inside of inserts with 16HBE 14o- cells growing on the bottom of the insert. TER was measured prior to medium being added, and 24 hours later.

- Heat-inactivation- 200μl of medium put into sterile tubes and heated on heat block at 65°C for 1 hour.

- Protease inhibitors- cocktail of protease inhibitors (Sigma) containing:
  AEBSF inhibits serine proteases
  EDTA inhibits metalloproteases
  Bestatin inhibits aminopeptidases
  E-64 inhibits cysteine proteases
  Leupeptin inhibits serine and cysteine proteases
  Aprotinin inhibits serine proteases

This cocktail of protease inhibitors was added to the medium to give a final concentration of 20 and 40μl/ml. 200μl was added to the inserts.

- Activation of epidermal growth factor (EGF) receptor has been shown to increase TER (Singh and Harris, 2003) and for this reason was chosen as a possible candidate for inducing the changes seen in my model. The EGF receptor inhibitor- AG1478 (gift from Nveed Chaudhary) is a selective inhibitor of the EGF receptor by inhibiting tyrosine kinase phosphorylation. AG1478 (stock concentration 4.2mg/ml) was added to the medium to give a final concentration of 50, 100, 200μg/ml.

AG1478 has been shown to specifically block tyrosine kinase phosphorylation of the EGFR. In mitogenesis assays, the drug blocked EGF-induced DNA synthesis in H292 cell line and NR6/HER fibroblasts but was without effect on that induced by aFGF (acidic fibroblast growth factor), KGF (keratinocyte growth factor), or bFGF (basic fibroblast growth factor), (Puddicombe *et al.* 2000).

2.2 Immunofluorescence staining

2.2.1 Fixing of cells

Culture medium was removed from cells grown on coverslips to 70-80% confluence. The cells were washed three times with sterile PBS, and then fixed for 15 minutes using ice-cold methanol (stored at –20°C). The cells were then washed in PBS three times and could either be used immediately for immunostaining or stored in sterile PBS at 4°C for later use.

2.2.2 Immunostaining

1. Cells on coverslips were blocked using 1% BSA/PBS, or serum for 10 min (except for occludin antibody-no blocking required).
2. 50µl of primary antibody (diluted in 0.1% BSA/PBS or serum, was placed on a piece of flat parafilm), (see Table 2 for concentration). The coverslip with cells was gently inverted over the drop, covered in a damp box, and left for 45 minutes. (Optimal concentration was determined by titrating the antibody at different concentrations to see which concentration gave the strongest staining with the lowest background staining.)
3. The cells were washed three times in PBS. (Washes were carried out by placing a drop of 100µl PBS on the parafilm, and gently floating the coverslip on the drop for 3 minutes. Excess fluid was drained using a tissue).
4. 50µl of relevant secondary antibody (see table 2), diluted in 0.1% BSA/PBS was placed on parafilm, the coverslip was inverted over the drop and incubated for 30 minutes in the dark.
5. After washing, the coverslip was placed over 10µl of propidium iodide (2.5µg/ml in PBS) on the parafilm for 5 minutes, to counterstain the cell nuclei.
6. The cells were washed a final three times and the coverslip (cells facing down) was mounted on a microscope slide using a small drop of anti-fading mounting solution - Mowiol with citifluor (20g Mowiol powder was dissolved in 80ml PBS at 60°C, stirring. 40ml glycerol was added and mixed for 8 hours. After centrifuging for 15 minutes at 12,000 rpm, one citifluor tablet dissolved in 300µl PBS was added. The mounting solution was then stored at 4°C).
7. When the mounting solution on the slides was dry, images were taken with an upright-fluorescent microscope (Leica DME).

Primary antibody	Concentration	Secondary antibody	Concentration
Mouse anti-human cytokeratin 18 (Sigma-purified ascites)	1:500	Rabbit anti-mouse FITC (DAKO)	1:100
Mouse anti-human cytokeratin 13 (Sigma-purified ascites)	1:500	Rabbit anti-mouse FITC	1:100
Mouse IgG1 (isotype control) (DAKO)	1:100	Rabbit anti-mouse FITC	1:100
Mouse anti-human von-Willebrand factor (vWF) (Serotec-purified ascites)	1:100	Rabbit anti-mouse FITC	1:100
Mouse anti-human CD31 (PECAM-1) (Serotec-tissue culture supernatant)	1:100	Rabbit anti-mouse FITC	1:100
Mouse anti-human HEA-125 (Serotec-purified ascites)	neat	Rabbit anti-mouse FITC or goat anti-mouse rhodamine red (Jackson Immunoresearch)	1:100 1:100
Sheep anti-human vWF (Serotec-antisera)	1:100	Rabbit anti-sheep FITC (Jackson Immunoresearch)	1:100
Sheep IgG (isotype control) (Sigma-antisera)	1:100	Rabbit anti-sheep FITC	1:100
Rabbit anti-mouse occludin (Zymed-antisera)	1: 50	Swine anti-rabbit FITC (DAKO)	1: 80

Table 2 .2 Antibody concentrations

2.3 Measurement of electrical resistance

Two different types of resistance measuring electrodes were used with the EVOM resistance meter, all from World Precision Instruments.

2.3.1 STX-2 or 'chopstick' electrodes

The STX-2 or 'chopstick' electrodes were used to measure electrical resistance across cell layers grown on inserts, with the insert still in the well. The electrodes were sterilised prior to use with 70% ethanol and air-dried. One electrode was positioned between the well and the insert, and the other was positioned within the insert (see figure 2.1). These electrodes, however, gave variable readings, depending on where the electrodes were placed, and gave a background resistance of a blank insert as 150Ω.

2.3.2 Endohm-6 resistance measurement chamber

The Endohm-6 resistance measurement chamber consists of two opposing circular electrodes, positioned in exactly the same position each time above and below the insert (see figure 2.2). The chamber and top electrode were sterilised with 70% ethanol and air-dried prior to use. The top electrode and insert membrane must have a gap of 1-2mm minimum, and the medium in the chamber and insert must be the same level. These electrodes gave less variation between measurements compared to the STX-2 electrodes and also reduced the background resistance to 35Ω. These electrodes were useful for measuring small changes in electrical resistance (especially for endothelial cells).

2.3.3 Calculation of TER

TER of cells grown on inserts were measured on a daily basis after the medium was changed. The actual TER values were calculated by subtracting the background TER, (inserts with no cells), and multiplying the result by the surface area of the insert ($0.3cm^2$). The best density to seed cells to give an optimal TER was determined. (The optimal density reached the highest TER the fastest).

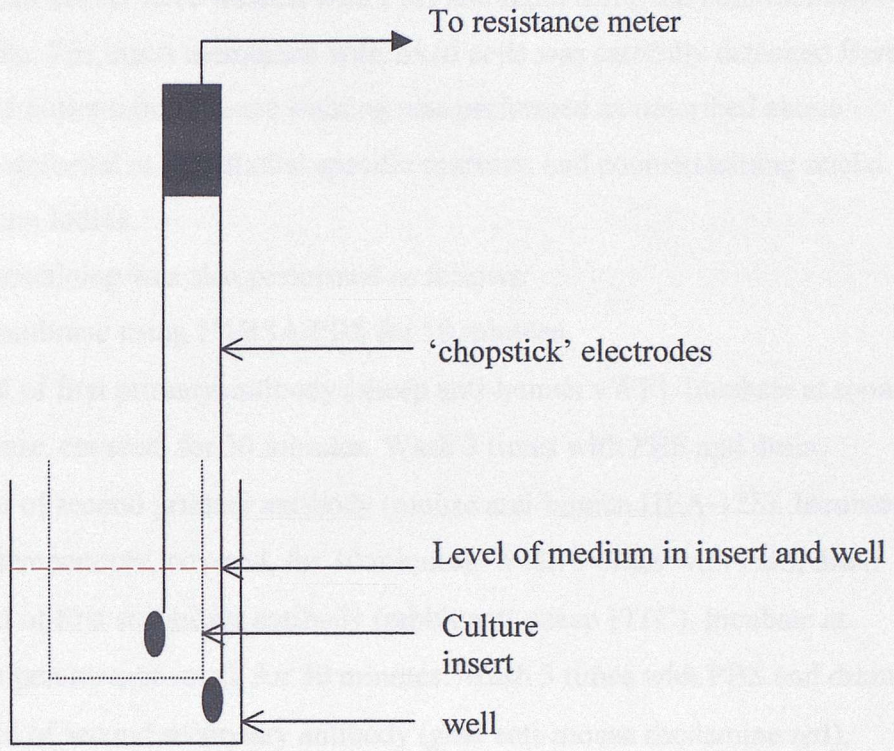

Figure 2.1 *STX-2 electrodes*

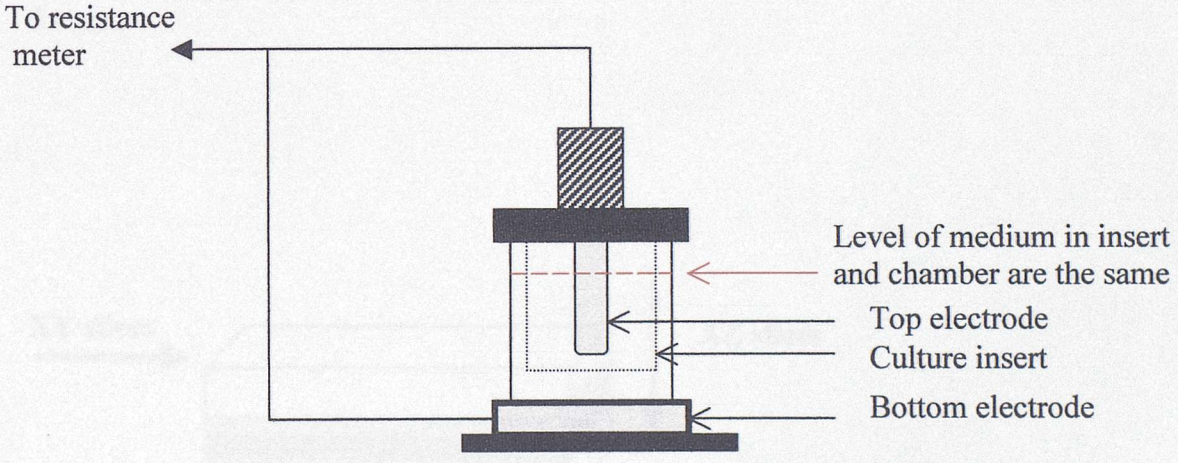

Figure 2.2 *Endohm-6 resistance measurement chamber*

2.4 Confocal microscopy

Cells grown on inserts were washed with PBS and fixed using ice-cold methanol for 15 minutes. The insert membrane with fixed cells was carefully detached from the insert and immunofluoresence staining was performed as described above using either epithelial or endothelial specific markers, and counterstaining nuclei with propidium iodide.

Dual immunostaining was also performed as follows:

1. Block membrane using 1%BSA/PBS for 10 minutes
2. Add 50µl of first primary antibody (sheep anti-human vWF). Incubate at room temperature, covered, for 30 minutes. Wash 3 times with PBS and drain.
3. Add 50µl of second primary antibody (mouse anti-human HEA-125). Incubate at room temperature, covered, for 30 minutes. Wash 3 times with PBS, drain.
4. Add 50µl of first secondary antibody (rabbit anti-sheep FITC). Incubate at room temperature, covered, for 30 minutes. Wash 3 times with PBS and drain.
5. Add 50µl of second secondary antibody (goat anti-mouse rhodamine red). Incubate at room temperature, covered, for 45 minutes. Wash 3 times with PBS and drain.
6. Mount membrane onto a coverslip with mowiol and citifluor (see 2.2.2).
7. Images were taken in the XY and XZ plane (see below) using a Leica SP2 confocal laser-scanning microscope, and stored as digital images in TIF format.

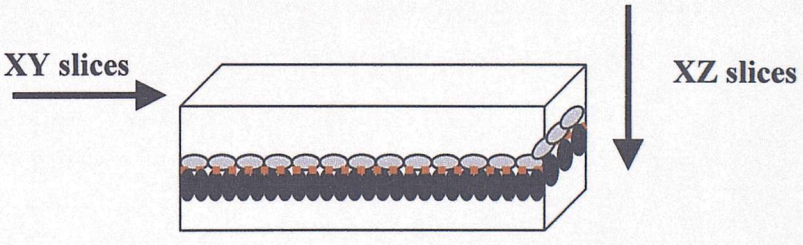

2.5 Scanning electron microscopy

The membranes of cell culture inserts were carefully detached from the insert and processed for SEM:

1. Cells were incubated for at least 1 hour in main fixative (3% glutaraldehyde, 4% formaldehyde in 0.1M PIPES buffer at pH7.2).
2. Wash for 10 minutes in buffer rinse (0.1M PIPES pH7.2) on a rotator x2.
3. Incubate for 1hour in post fixative (1% osmium tetroxide in 0.1M PIPES pH7.2).
4. Samples were dehydrated by incubating in increasing concentrations of ethanol as follows

30% ethanol 10 minutes
50% ethanol 10 minutes
70% ethanol 10minutes
95% ethanol 10 minutes
absolute ethanol 20 minutes
absolute ethanol 20 minutes

5. Samples were then critical point dried and mounted on stubs, and sputter coated with gold palladium.
6. Images were taken of both sides of the membrane using a Hitachi S800 scanning electron microscope.

2.6 Transmission electron microscopy

2.6.1 Processing samples into blocks for TEM

The membranes of cell culture inserts were carefully detached from the insert and processed from TEM.

1. Cells were incubated (in fume cupboard), for at least 1 hour in main fixative (3% glutaraldehyde, 4% formaldehyde in 0.1M PIPES buffer at pH7.2).
2. Wash for 10 minutes in buffer rinse (0.1M PIPES pH7.2) on a rotator x2.
3. Incubate (in fume cupboard), for 1hour in post fixative (1% osmium tetroxide in 0.1M PIPES pH7.2).
4. Samples were dehydrated by incubating in increasing concentrations of ethanol as follows

30% ethanol 10 minutes
50% ethanol 10 minutes
70% ethanol 10minutes
95% ethanol 10 minutes
absolute ethanol 20 minutes
absolute ethanol 20 minutes

5. Incubate for 10 minutes in acetonitrile (in fume cupboard).
6. Incubate overnight with 50:50 acetonitrile:Spurr resin (in fume cupboard on rotator). Resin needs to be warmed to room temperature.
7. Incubate for at least 6 hours in spurr resin, in fume cupboard.
8. Place sample into vials and embed in fresh resin. Polymerise at 60°C for 20-24 hours.
9. Blocks were removed from vials, and the portion containing the membrane was cut, and using araldite adhesive, was fixed to position the membrane transversely, as below. This would allow sections to be cut transversely across the cell layers and insert membrane.

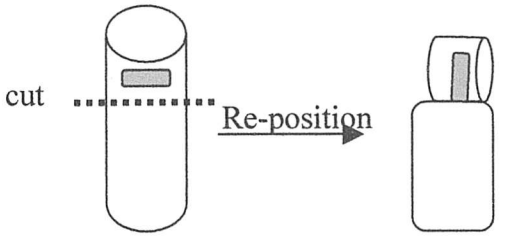

2.6.2 Staining sections for TEM

Sections were cut using an ultra microtome. 'Thick' sections were cut at 0.5μm thick and stained with toludine blue, and checked under a light microscope, to ensure good sections had been cut across the insert membrane. Thick sections were also used to measure epithelial cell height. Images of thick sections from monolayer and bilayer inserts were taken and analysed using ImageJ software. Epithelial cell height was measured at equal intervals, from the top of the membrane to the top of the epithelial layer. Areas of cell detachment were not used. The average epithelial height was calculated from images of sections from two blocks for each condition.

Ultra thin sections were cut between 80-90nm thick, and stained as below:

1. Sections were collected onto copper grids and allowed to dry.
2. Uranyl acetate solution and lead citrate solution were centrifuged at full speed in a microcentrifuge for 5 minutes.
3. One drop/grid was placed on a piece of wax in a Petri dish.
4. Each grid was inverted onto the droplet, so section face down, and incubated for 15 minutes at room temperature in the dark. (Uranyl acetate is very toxic, radioactive and sensitive to light).
5. Holding the grid with forceps, the grids were carefully washed in a gentle stream of distilled water.
6. Excess fluid was drained off using filter paper.
7. Each grid was placed on a drop of lead citrate stain, on wax in a Petri dish, containing sodium hydroxide pellets. (Lead citrate reacts with carbon dioxide).
8. After 5 minutes the grids washed again and dried.
9. The sections were then viewed using a Hitachi H7000 transmission electron microscope.

2.7 Reverse-Transcription Polymerase Chain Reaction (RT-PCR)

2.7.1 RNA extraction

Cells were grown as monolayers or as a bilayer as above. RNA was extracted from the different growth conditions:

16HBE 14o- monolayer;

HUVEC monolayer;

16HBE 14o- from bilayer;

HUVEC from bilayer;

16HBE 14o- grown in HUVEC conditioned medium.

Cells were scraped off the inserts using a cell scraper, and collected into a tube as a suspension. Cells were pelleted by centrifugation (5 minutes at 1500rpm). After completely aspirating the supernatant, the pellet was loosened by flicking the tube. The RNA was then extracted using the RNeasy Mini Kit (Qiagen):

1. 350µl of buffer RLT was added, and the cells homogenised by passing the lysate through a 0.6mm diameter RNase free syringe, 5-10 times. RLT buffer contains guanidine thiocyanate, which is highly denaturing and immediately inactivates RNases, to ensure isolation of intact RNA.
2. 350µl of 70% ethanol was added and mixed well by pipetting. Ethanol provides appropriate binding conditions, so that total RNA binds silica-membrane of mini-column.
3. 700µl of sample was added to an RNeasy mini column in a 2ml collection tube and centrifuged for 15 seconds at 10,000rpm. The flow-though containing any contaminants was discarded.
4. 350µl of wash buffer RWI was added to the column, which was centrifuged (15 secs, 10,000rpm), and the flow through discarded.
5. DNase digestion step was performed using RNase-free DNase set, for efficient on-column digestion of DNA during RNA purification. 10µl of DNase I solution was added to 70µl buffer RDD and added to the column, which was left on the bench (20-30°C) for 15mins.
6. 350µl buffer RWI was added and the column centrifuged (15 secs, 10,000rpm), for efficient removal of DNase. The column was transferred to a new collection tube.

7. 500µl of buffer RPE was added to the column, which was centrifuged (15 secs, 10,000rpm), and the flow through discarded.
8. A further 500µl of buffer RPE was added, the column centrifuged for 2 mins at 10,000 rpm to dry the silica-membrane, and remove any residual ethanol that may effect downstream reactions.
9. The column was transferred to a 1.5ml collection tube.
10. To elute the RNA, 50µl RNase-free water was added directly onto the column membrane, and the column centrifuged for 1 min at 10,000rpm.
11. The eluate was re-pipetted into the column and centrifuged for a further minute at 10,000rpm.
12. The collected RNA was then stored at –20°C until required.

2.7.2 RNA quantitation

The RNA extracted was then quantitated using the ribogreen RNA quantitation kit (Qiagen).

The kit uses TE buffer as an assay buffer (10mM Tris-HCl, 1mM EDTA, pH7.5), which is diluted to a 1X concentration using DEPC water (nuclease-free water: distilled, deionised water treated with 0.1% diethyl pyrocarbonate (DEPC) and incubated for several hours at 37°C, then autoclaved for at least 15 mins to sterilise).

The ribogreen reagent is used at a 200-fold dilution.

The stock RNA standard (100µg/ml) is diluted to working concentration of 2µg/ml in TE and then diluted as follows to establish standard curve values:

TE volume (µl)	**2µg/ml RNA volume (µl)**	**Ribogreen (µl)**	**Final RNA concentration (ng/ml)**
0	100	100	1000
50	50	100	500
90	10	100	100
98	2	100	20
100	0	100	blank

1. Using a 96-well flat-bottomed plate, standard RNA (as above) and 100µl of sample RNA (as a series dilution from 1/50 to 1/6400 dilution), was added to the wells in duplicate.
2. 100µl of Ribogreen reagent (diluted 200-fold in TE buffer) was added to each of the wells, and the plate incubated for 2-5 mins at room temperature in the dark.
3. The fluorescence was measured at excitation 400nm, and emission 520nm.
4. The fluorescence value of the blank was substracted from each sample.
5. An RNA standard curve was generated from which the RNA concentration of samples was determined.

2.7.3 Reverse-Transcription (RT)

Reverse transcription was performed on RNA extracted using the Omniscript RT kit (Qiagen).

1. RNA samples extracted from cells were thawed.
2. All reagents were thawed, vortexed for 5 seconds and kept on ice.
3. Master mix was prepared in autoclaved tubes as follows (per sample tube):

   2µl 10x buffer RT

   2µl dNTPs

   2µl oligo dT primers (10µM)

   1µl RNase I (10units/20µl)

   1µl omniscript RT

4. 8µl of master mix was added per tube, then template RNA (<2µg) added, and then RNase free water added to make a total volume of 20µl/tube.
5. The tubes were placed into a thermal cycler with the following cycle:

   60 minutes 37°C

   5 minutes 93°C

   60 minutes 4°C

6. The final cDNA products were then stored at –20°C until required.

2.7.4 Polymerase Chain Reaction (PCR)

PCR was performed on cDNA samples using primers designed for tight junction proteins mRNA (Table 2.3). β-actin primers (Promega) were used as a positive control, and a tube containing no cDNA sample was used as a negative control. (All primers synthesized by MWG-Biotech AG, UK).

1. All reagents (Sigma) were thawed and kept on ice.
2. Master mix was prepared using the following volumes per reaction tube:
   2.75μl PCR buffer II (x10)
   1.65μl 25mM Mg (final conc. 1.5mM)
   0.55μl 10mM dNTP (final conc. 200μM)
   0.07μl 10U/μl Taq polymerase (final conc. 0.025U/μl)
   +RNase free water to make a total volume of 23μl/tube.
3. 23μl of master mix was added to each reaction tube.
4. 0.5μl of each primer (upper and lower) was added, followed by 1μl of cDNA sample.
5. With the thermal cycler prewarmed to 94°C, the PCR tubes were incubated as follows:

94°C	2mins	
94°C	20 sec	} x35 cycles
60°C	30 sec	
72°C	10sec	
10°C	soak	

6. The final PCR products were then be stored at –20°C until ready to run on agarose gels.

Tight junction protein	Primer sequence	Predicted Product size
β-actin	*Upper:*5'-TCA TGA AGT GTG ACG TTG ACA TCC GT-3' *Lower:*5'-CTT AGA AGC ATT TGC GGT GCA CGA TG-3'	285bp
Occludin	*Upper*: 5'–TGG GCA TCA TGG TGT TTA TTG-3' *Lower*: 5'-CGC CGC CAG TTG TGT AGT CT-3'	655bp
Claudin-1	*Upper*: 5'-CAC CTG CCA CCC CTG AGC-3' *Lower*: 5'-AGC AGC CCA GCC AGT GAA GAG-3'	533bp
Claudin-2	Upper: *5'*-TCC CTG CCC TGC TCT GCT TC-3' *Lower*: 5'-CCA CCT GCT ACC GCC ACT CTG-3'	653bp
Claudin-3	Upper: *5'*-TCA TCG GCA GCA ACA TCA TC-3' *Lower*: 5'-GTC TCC CTG CGT CTG TCC C-3'	563bp
Claudin-4	Upper: *5'*-GGC AGC AAC ATT GTC ACC-3' *Lower*: 5'-CCA GCG GAT TGT AGA AGT CTT-3'	325bp
Claudin-5	Upper: *5'*-GCG TGC TCT ACC TGT TTT G-3' *Lower*: 5'-GAA GCG AAT CCT CAG TCT G-3'	568bp
JAM-1	Upper: *5'*-CAC GGG AAG ACA CTG GGA CAT-3' *Lower*: 5'-CGG CTG CCA CGA TGA CC-3'	412bp
JAM-2	Upper: *5'*-CCC GAC TCT CTG CTC CTT TCC-3' *Lower*: 5'-ATT TCC CCG CAT CAC TTC TTG-3'	410bp
JAM-3	Upper: *5'*-TGT CTG TAG AGT GCC GAA GG-3' *Lower*: 5'-CCG CCA ATG TTC AGG TC-3'	289bp
PILT	Upper: *5'*-CCG TCA CCT CCC AGA ATG-3' *Lower*: 5'-TCT CTA ACA CTC GGG CAA TGA-3'	676bp

Table 2.3 Primer sequences for tight junction proteins

2.7.5 Detection of PCR products on agarose gels

1. 1% agarose gels were prepared by heating 1g agarose/100ml TBE buffer in a microwave, until dissolved.
2. Once slightly cooled, 5µl ethidium bromide was added per 100ml of gel, which was then poured into the gel plates, combs were placed into position and the gel allowed to set.
3. Once set the combs were removed and the gels placed into the gel tank, which was then filled with TBE buffer so the gel was just covered.
4. Samples were mixed with loading buffer and 10ml/well was added.
5. 10ml of a DNA molecular weight ladder was also added to one well.
6. The gel was run at a constant current of 82A for 30-40 minutes.
7. The gel was viewed in a UV light box to detect any bands at the predicted molecular weight of the expected PCR products.

2.8 DNA sequencing

PCR products were analysed using automated DNA sequencing, and the resulting sequences were aligned with that of the expected product.

2.8.1 SAP/Exo 1 purification

The products had to first be purified using shrimp alkaline phosphotase (SAP) to dephosphorylate the dNTP's, and exonuclease I (Exo 1), to remove excess primers.

The following volumes were used per reaction tube:

5µl PCR product

0.9µl SAP dilution buffer

1.0µl SAP (AP Biotech)

0.1µl Exo 1 (AP Biotech)

The reaction tubes were incubated on a thermal cycler as follows:

37°C 30mins

80°C 15mins

Two sequence reactions were performed on each purified DNA template obtained, one with the forward primer and one with the reverse primer.

2.8.2 Sequence reaction

Master mix was prepared using the following volumes per reaction tube:

4µl Big Dye terminator ready mix (ABI)

4µl Half sequence buffer

5.3µl dH_2O

13.3µl of MM was added per reaction tube, followed by 3.2µl 1µM primer and 3.5µl of DNA template.

The reaction tubes were incubated on a thermal cycler as follows:

96°C 10sec
50°C 5sec
60°C 4mins
} 25 cycles

4°C soak

The reaction tubes were covered in foil and kept at 4°C.

2.8.3 Ethanol precipitation

Ethanol precipitation was then performed on each reaction to remove excess dye terminators and to concentrate the product of the sequencing reaction.

The whole of each sequence reaction was added to 1.5ml tubes each containing, 16µl dH_2O and 64µl absolute ethanol. The reaction tube was vortexed and left on the bench (room temperature) for 15 minutes covered in foil.

After centrifuging for 20 minutes at top speed (13000rpm) in a microcentrifuge, the supernatant was discarded carefully by inverting the tubes on tissue paper since the pellet was transparent.

The DNA pellet was washed by adding 250µl 70% ethanol (without mixing so as not to disturb the pellet).

The tubes were centrifuged for 10 minutes at 13000rpm, and the supernatant removed as before. The DNA pellet was dried by placing on a heat block heated to 90°C for 1 minute with the lids open.

The tubes were then stored at –20°C covered in foil until ready to sequence on ABI Prism 377 automated DNA sequencer machine.

2.8.4 Electrophoresis on ABI Prism 377

The gel used consisted of 30ml genepage plus (polyacrylamide):5% 6M Urea (Amresco), 300µl ammonium persulphate and 30µl TEMED (Sigma). Once set, the gel was placed in an ABI Prism 377, filled with buffer and pre-run for 20minutes.

Samples were prepared for loading:

1ml loading buffer and 5ml formamide was added to each sample.

Heated at 95°C for 2 minutes, then transferred to ice until ready to load.

Each sample was loaded into a separate lane of the gel, and run for 7 hours.

Sequence data was transferred to a computer and analysed and aligned using Blast 2 sequences on the website (www.ncbi.nlm.nih.gov). The percentage match confirms whether correct product has been generated from RT-PCR.

2.9 Western blotting

2.9.1 Protein extraction

Cells that had been grown in the three conditions: monolayer, bilayer and conditioned medium, were washed twice in PBS. 1ml of boiling PBS/1% SDS was added to the underside of the insert (ie. onto 16HBE 14o- cells). The cells were scraped off using the tip of a pipette and each sample collected into a 1ml epindorff. The epindorff was heated at 100°C for 15-20 minutes and then centrifuged at 10,000g for 10 minutes. The supernatant contained the protein extract and was stored at –20°C.

2.9.2 Protein quantification

The Bio-rad DC protein assay was used to quantify the protein extracted. The Bio-rad protein standard was BSA (stock concentration 1.4mg/ml), and was diluted to different concentrations (1.4, 0.93, 0.7, 0.56, and 0.47 mg/ml) with distilled water and 1%SDS (since the sample protein extracts contained 1% SDS). Protein quantification was performed using the Biorad assay, on the standards (to generate a standard curve), a PBS control (for background measurement), and on the 16HBE 14o- samples. The spectrophotometer was calibrated with the control (PBS) and absorbance measured at 750nm. The amount of protein in my samples could then be calculated from the standard curve.

2.9.3 SDS PAGE

SDS PAGE (polyacrylamide gel electrophoresis) was performed on protein extracts of 16HBE 14o- samples. Running gel was prepared as follows (all reagents Sigma):

4.9ml H_2O

2.5ml 1.5M Tris buffer pH8.8

2.5ml 40% acrylamide

100µl 10% SDS

50µl 10% ammonium persulphate (freshly made: 0.1g in 1ml H_2O)

10µl Temed

The gel mixture was poured into plates and a layer of isopropanol added at the top. After approx. 45 minutes at room temperature the gel should set.

Stacking gel was prepared as follows:

3.2ml H_2O

1.25ml 0.5M Tris buffer pH 6.8

0.5ml 40% acrylamide

50µl 10%SDS

25µl ammonium persulphate

5µl Temed

After removing the isopropanol from the set gel, the stacking gel was quickly layered over the top and a 0.75mm comb carefully slotted in, and left to set for 30 minutes at room temperature. Once set the gel was placed in the tank apparatus, which was filled with running buffer and the comb removed. 10µl of standard and 25µl of each sample (12.5 µl sample+25µl loading buffer) were loaded into separate lanes, and run at a constant 150V for one hour (or until dye front reaches the bottom).

2.9.4 Semi-dry western blotting

Two Bio-Rad filter papers and nitrocellulose membrane (cut to the size of the gel) were soaked in transfer buffer for 15 minutes. The nitrocellulose membrane was placed on top of a filter paper, followed by the gel and then the other filter, with the air being removed at each stage by rolling with a 10ml pipette. The whole sandwich was placed on the semi-dry cell, and run at 15V and 0.3A for 50 minutes.

The nitrocellulose membrane was removed and stained with Ponceau S for 30 seconds to check the transfer was successful. For each of the following steps the membrane was placed in a container on a rocking platform at room temperature (unless otherwise stated):

1. Wash in PBS for 10 minutes x2
2. Block in 5% milk powder in 0.1%Tween 20/PBS for 1 hour.
3. Wash in 0.1%Tween 20/PBS for 10 minutes x3.
4. The membrane was placed in a bag with primary antibody, rabbit anti-human occludin at 1:1000 concentration, and left overnight on a rotator at 4°C.
5. Remove membrane from bag and wash in 0.1%Tween 20/PBS for 10 minutes x3.

6. Incubate in secondary antibody, anti-rabbit HRP at 1μl in 10ml, for 1 hour.
7. Wash in 0.1%Tween 20/PBS for 10 minutes x3.
8. Visualize bands using BioRad Opti-4CN substrate kit:

Incubate in 9ml H_2O, 1ml Opti-4CN diluent, 0.2ml substrate for 30 minutes.

2.10 Statistical Analysis of data

All error bars show standard error of the mean. When comparing different growth conditions, statistical analysis was performed using the non-parametric Mann-Whitney test. Values of $p>0.05$ were considered not significant, and values<0.05 were considered significant. Correlation coefficients and their p-values have been calculated when comparing two variables in relation to each other.

CHAPTER 3

DEVELOPMENT OF AN EPITHELIAL/ENDOTHELIAL CO-CULTURE MODEL

Chapter 3: Development of an epithelial/endothelial model

3.1 Selection of cells for model

In vivo, respiratory epithelial cells and endothelial cells act as part of an integrated unit, in which cross talk must occur between cells to coordinate their activity, and to modify their barrier function when required. A bilayer model reflecting the epithelial and endothelial barriers of the human bronchial tract was designed and established. As the first stage, a range of cell lines were characterised to select the best for the planned model. Cells were morphologically characterised using light microscopy, immunofluorescent microscopy, and confocal microscopy, scanning electron microscopy and transmission microscopy. Transcellular electrical resistance was used as a functional measurement to reflect the extent of tight junction formation.

3.1.1 Phase contrast images

Phase contrast images gave an indication of the general morphology of each cell type and growth patterns.

Both the primary HUVEC isolated from the human cord (Fig.3.1A), and the commercial primary HUVEC from Clonetics (Fig.3.1B), showed the same phenotype, individual cells were round and flattened with a bulging centre representing the nucleus, giving a 'fried egg' appearance. The cells formed a confluent layer of uniform cells with an overall cobblestone appearance. This is typical of an endothelial phenotype. Primary HUVEC cells and cell lines differed in morphology. HUVS-112D endothelial cell line (Fig.3.1C), formed confluent layers (ie. each cell was in contact with its surrounding cells so that all borders were in contact and no gaps were visible between cells). They displayed a fibroblast-like morphology, being elongated spindle-shaped cells growing uniformly aligned and all in contact with each other. HUVE-12 cells (Fig.3.1E) also had the 'fried egg' appearance of a typical endothelial phenotype, but these cells did not grow to confluence (ie. spaces remained between cells). HUV-EC-C (Fig.3.1D) initially had endothelial morphology and grew to confluence for the first 3-4 passages, but then their growth slowed down as it took longer for the cells

to form confluent layers, and their morphology changed such that they formed thin extended processes and many cytoplasmic vacuoles.

Two epithelial cell lines were considered for the model, 16HBE 14o- cells (a bronchial epithelial cell line) and H292 cells (a tracheal epithelial cell line). Both of these cell types grew rapidly to form confluent monolayers. Cells were uniform and tightly packed having no gaps between cells, and the cell nuclei appear as dark spherical centres in the phase contrast images (Fig.3.1F). Morphologically these two cell types were similar, suggesting either would be suitable for the final model.

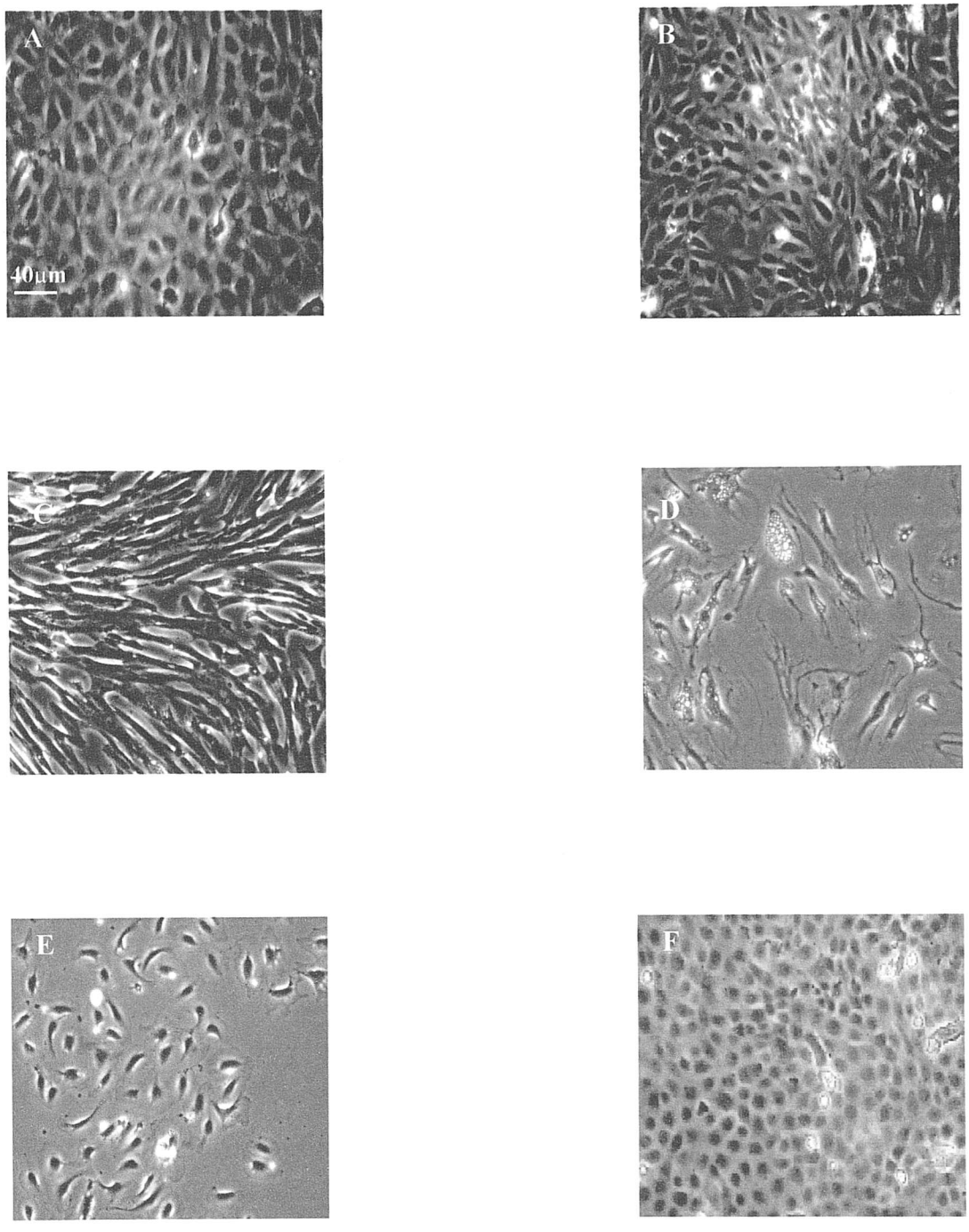

Fig.3.1 Phase contrast images of primary endothelial cells and endothelial cell lines (x10 magnification).
A: HUVEC (isolated from cord) p1
B: HUVEC (clonetics) p1
C: HUVS-112D p1
D: HUV-EC-C p4
E: HUVE-12 p1
F: 16HBE 14o- p36

3.1.2 Immunostaining

Immunostaining was performed on the HUVEC and 16HBE 14o- cells to identify cell-specific markers. This is important so that in the final model the two different cell types can be distinguished.

	% 16HBE 14o- labelled	**% HUVEC labelled**
Cytokeratin 18	100	100
HEA-125	100	0
VWF	0	100
CD31	0	100 (when confluent)

Table 3.1 *% of cells immunolabelled with the above antibodies.*

HEA-125 stained 16HBE 14o- in a pattern consistent with cell surface expression (Fig.3.2A). CK18 displayed a filamentous staining pattern surrounding the nucleus (Fig.3.2B). No fluorescence staining was seen with vWF (Fig.3.2C) or CD31 (Fig.3.2D). All cell nuclei were counterstained with propidium iodide.
With vWF, cytoplasmic staining of HUVEC displayed a punctate distribution pattern (Fig.3.3C). CD31 staining reflected the expression of CD31 at cell-to-cell borders (Fig.3.3D). HEA-125 was negative (Fig.3.3A) and CK18 displayed cytoplasmic staining (Fig.3.3B).
Therefore, HEA-125 antibody was established as a specific epithelial surface marker and vWF antibody was established as a specific endothelial marker. These antibodies were later used to detect each cell type in the bilayer model.

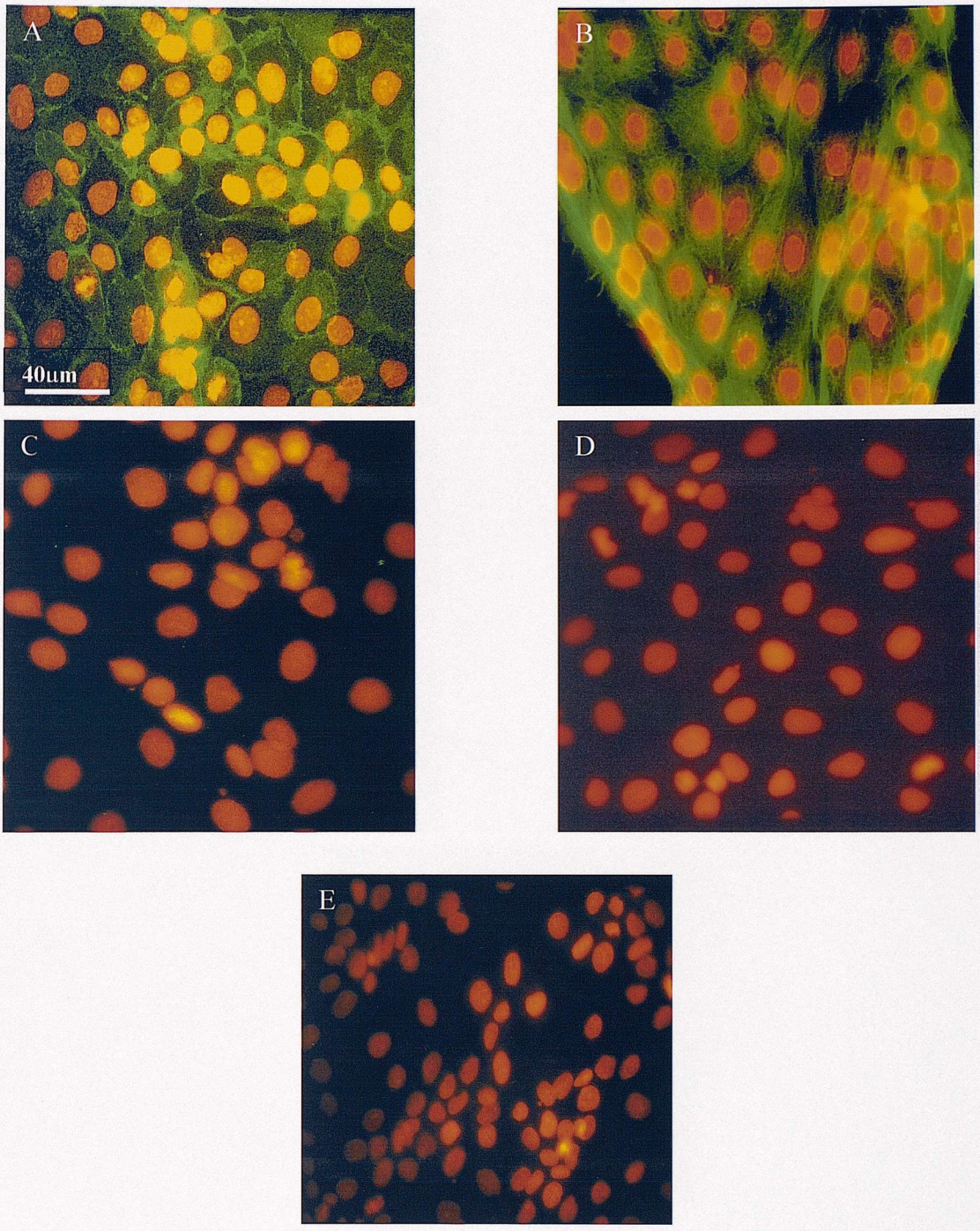

Fig.3.2 Immunostaining of 16HBE 14o- with the following primary antibodies and FITC conjugated secondary antibody. (Cell nuclei counterstained with propidium iodide). A)HEA-125; B) Cytokeratin 18; C) vWF; D) CD31; E) IgG1 negative control. All images x40 magnification.

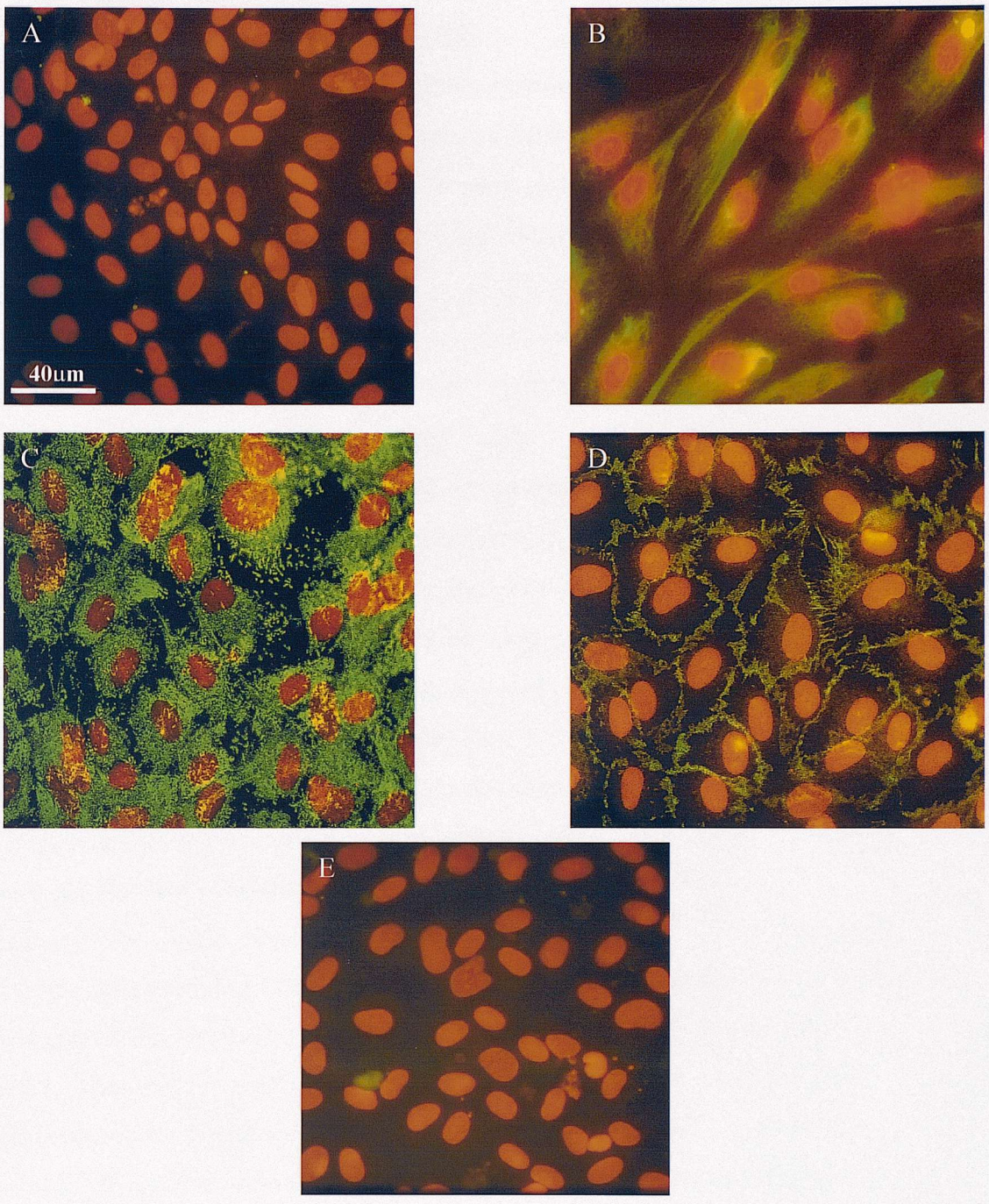

Fig.3.3 Immunostaining of primary HUVEC with the following primary antibodies and FITC conjugated secondary antibody. (Cell nuclei counterstained with propidium iodide).
A)HEA-125; B) Cytokeratin 18; C) vWF; D) CD31; E) IgG1 negative control. All images x40 magnification.

3.1.3 Transcellular electrical resistance (TER)

TER measurements were made of cells grown on inserts on a daily basis (Fig.3.4). 16HBE 14o- reached high electrical resistances, up to a mean value of 80Ω.cm^2 (SE ± 6), at confluence and continued to increase post-confluence, reaching mean values of 238Ω.cm^2 (SE ± 25) by day 2. After reaching this peak the TER dropped at day 4 to a mean value of 136Ω.cm^2 (SE ± 27.3) and then began to rise again. The H292 epithelial cell line reached significantly lower electrical resistances ($p<0.00001$) in comparison to the 16HBE 14o- cell line (Fig.3.4a), reaching a maximum value of 22Ω.cm^2 (SE ± 2.4).

In comparison HUVEC showed relatively consistent electrical resistances, between 1-6Ω.cm^2 (SE ± 0.3). TER of endothelial cell lines, HUV-EC-C and HUVE-12 showed slightly higher and similar resistances as the primary HUVEC, reaching a maximum value of 18 and 6Ω.cm^2 respectively, (Fig. 3.4b). Since the TER of HUVEC were lower than 16HBE 14o- cells, measurements were made using the Endohm high sensitive electrodes (see 2.3).

Since the H292 cell line did not reach high electrical resistances, and in combination with the immunostaining results the 16HBE 14o- and HUVEC were chosen for the final bilayer model.

When growing 16HBE 14o- long term, the TER values begin to fluctuate after day 3-4 post-confluence (Fig.3.4c). Whether or not this is a phenomenon seen *in-vivo* is not known, but the fluctuating TER may also be due to some experimental artefact. This could be due to cells being limited in growth space and changing their architecture, or perhaps following a cycle of forming multilayers, cells shedding off and then reforming again. Since the model will be used to look specifically at barrier function, it will be limited to use for only two days post-confluence (i.e. before any fluctuations occur in the TER values).

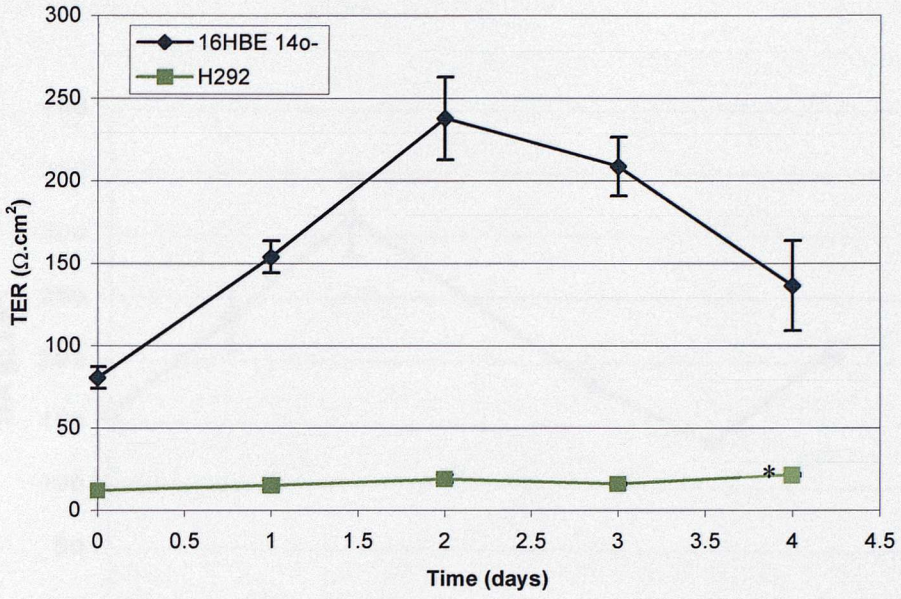

Fig. 3.4a Comparison of TER of 16HBE 14o- and H292 over time. (* Error bars for H292 < +/- 9, n=84 consisting of 7 experiments with 12 inserts per experiment).

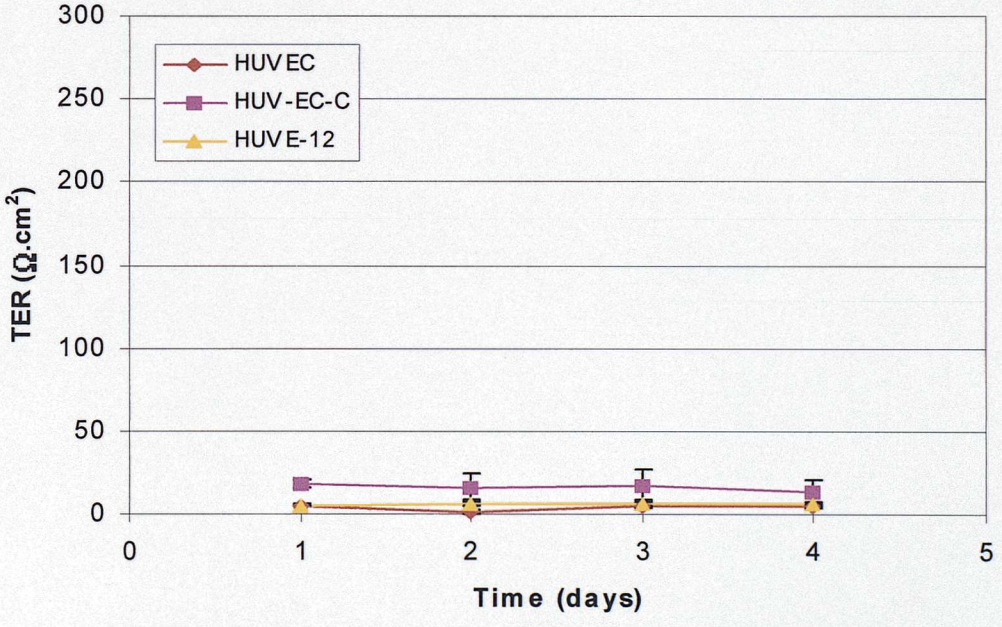

Fig. 3.4b Comparison of TER of primary HUVEC and endothelial cell lines. (Error bars < +/- 4 for HUVEC and HUVE-12, n=48 consisting of 6 experiments with 8 inserts per experiment).

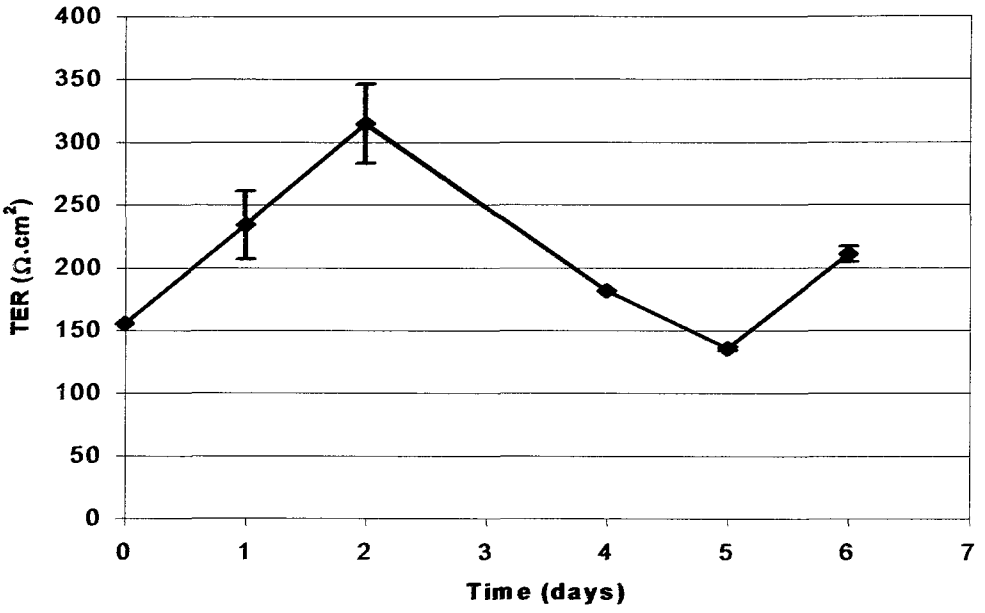

Fig. 3.4c Fluctuation of 16HBE 14o- TER values over time. (n=4, one experiment with 4 inserts)

3.1.4 Scanning electron microscopy (SEM)

SEM images of 16HBE 14o- grown on 1μm pore-size inserts (Fig. 3.5) illustrated that confluent layers were formed (Fig.3.5a), as all cells were in contact with each other, and in places contiguous borders can be seen (Fig.3.5b). Microvilli are protruding from the surface of some cells (Fig.3.5c), and on the underside of the insert, cells have migrated through (Fig.3.5d).

SEM images of 16HBE 14o- grown on 0.4μm inserts illustrated that confluent layers of cells that were indistinguishable from those formed by cells on 1μm inserts were formed, (Fig.3.5e) but they did not migrate through to the underside of the insert (Fig.3.5f). The control insert with no cells showed uniform pore sizes evenly distributed (Fig.3.5g), although the total pore area was less, since the pore density was the same for both the 1μm and 0.4μm pore size ($1.6x10^6$ pores/cm^2).

SEM images of HUVEC grown on 1μm pore-size inserts (Fig 3.6), illustrated that a thin layer of confluent cells were formed, however, cell borders were difficult to distinguish. Cell borders were not adjoining but appeared to form extended processes (Fig.3.6a). HUVEC also appeared to have migrated through to the underside of the insert (Fig.3.6b). When grown on 0.4μm pore size filters no cells were seen on the underside, indicating the cells did not migrate through.

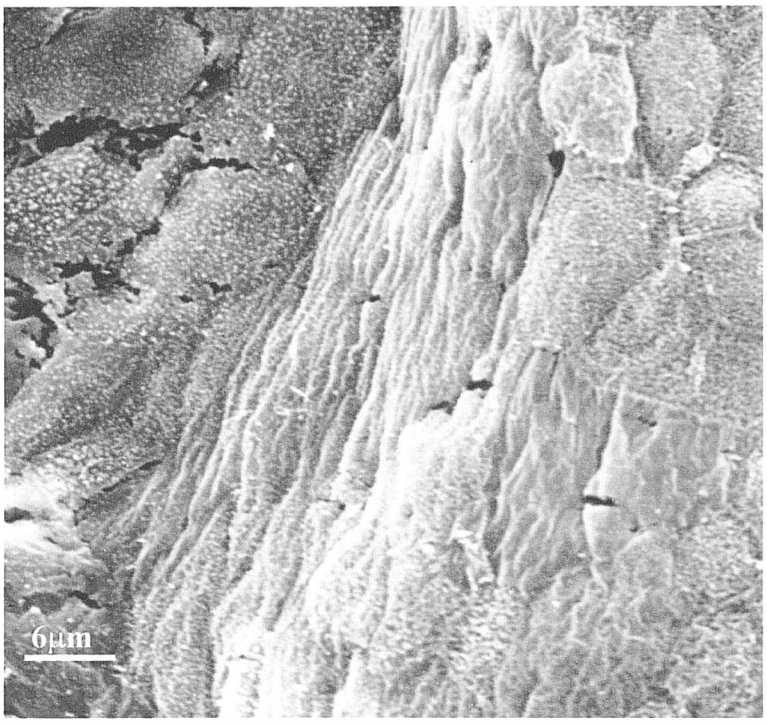

Fig 3.5a: Confluent 16HBE 14o- grown on 1µm pore size filters.

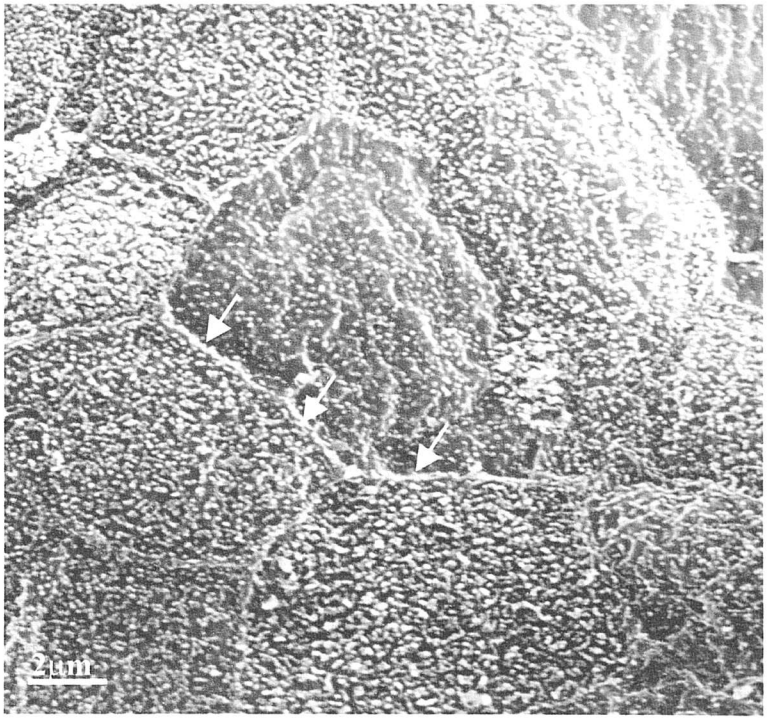

Fig 3.5b: Contiguous borders can be seen between confluent 16HBE. (arrows).

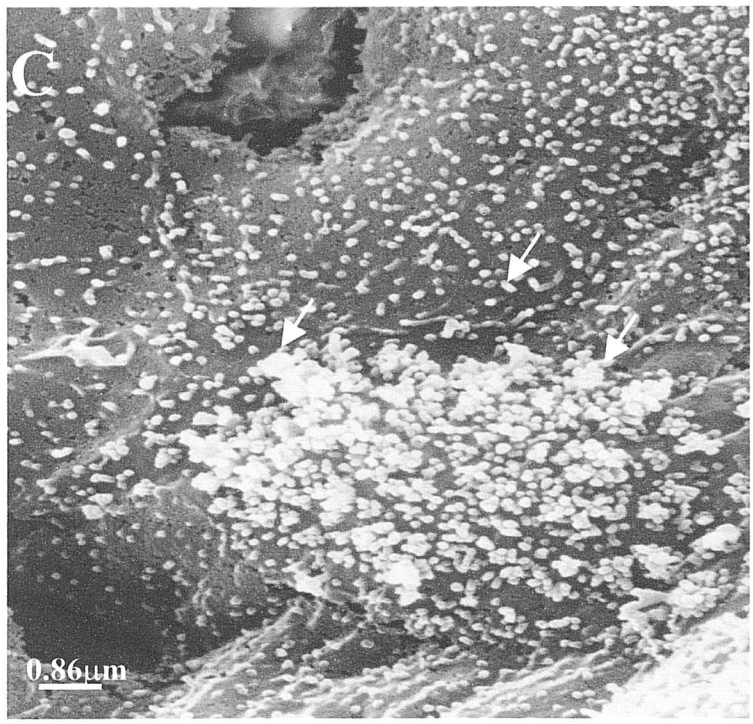

Fig 3.5c: At higher magnification, microvilli can be seen protruding from the surface of some cells (arrows).

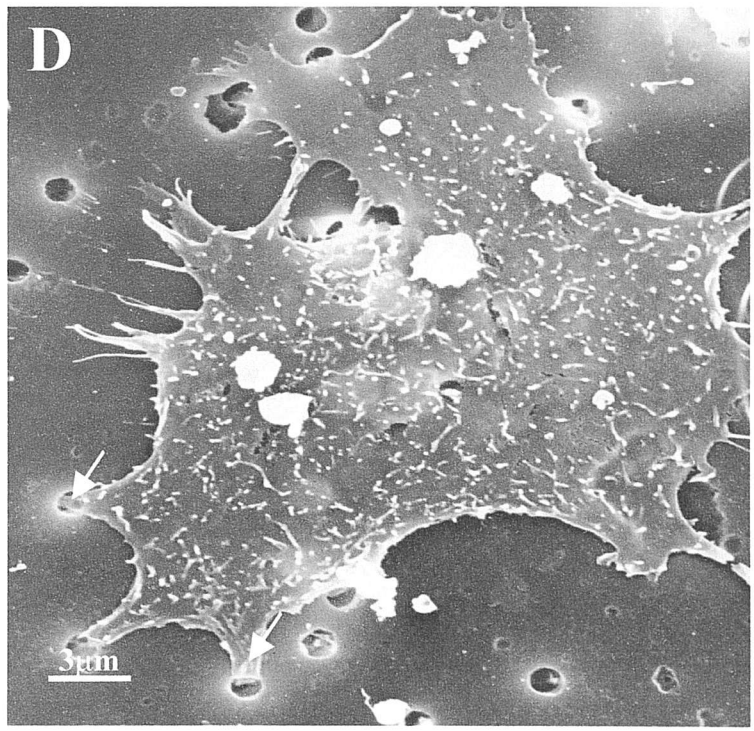

Fig 3.5d: On the underside of 1μm pore size filters, 16HBE 14o- have migrated through the pores (arrows).

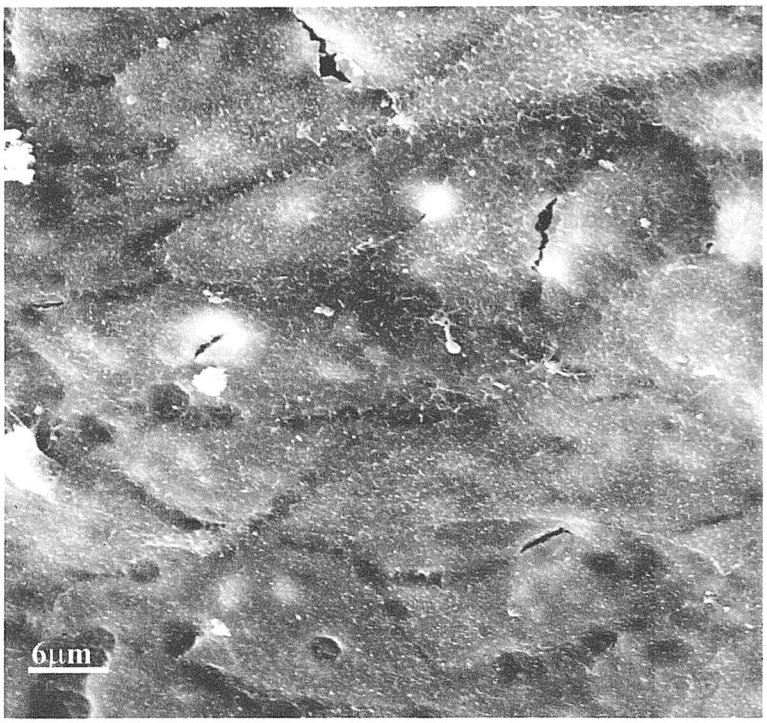

Fig 3.5e: Confluent 16HBE 14o- grown on 0.4µm pore size

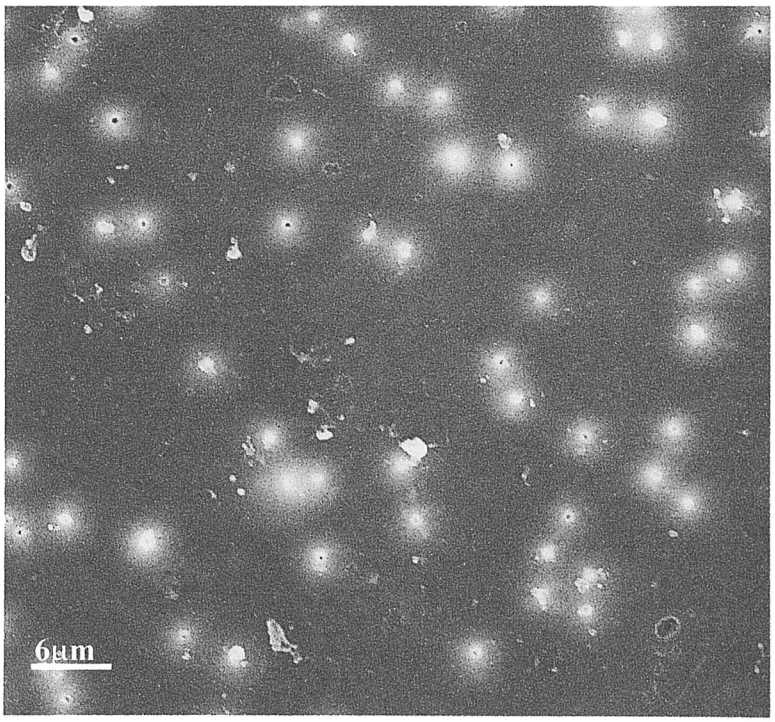

Fig 3.5f: Underside of 0.4µm pore size filter, no 16HBE 14o- have migrated through.

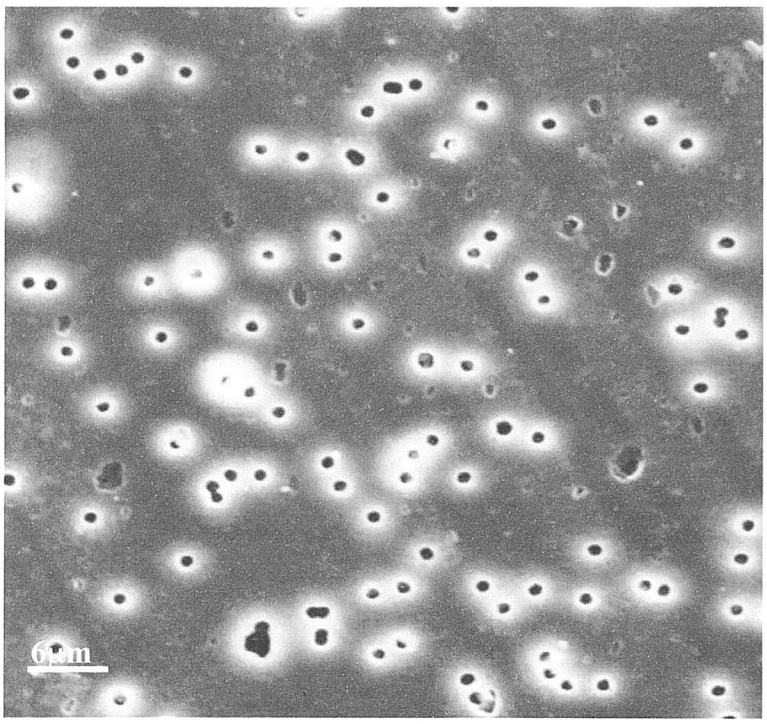

Fig 3.5g: Control 1μm pore size filter with no cells, show uniform pore sizes randomly distributed.

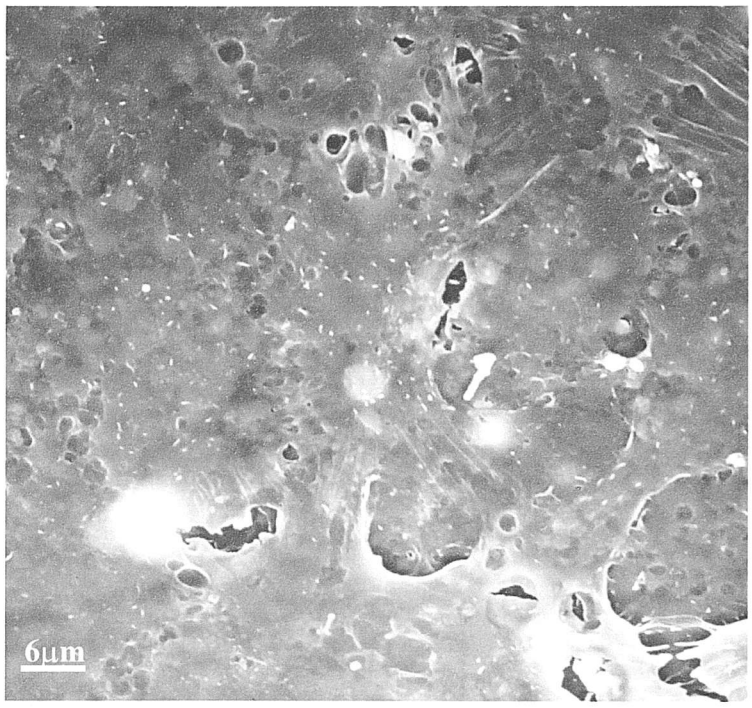

Fig.3.6a: Confluent monolayer of HUVEC grown on 1μm pore size filter.

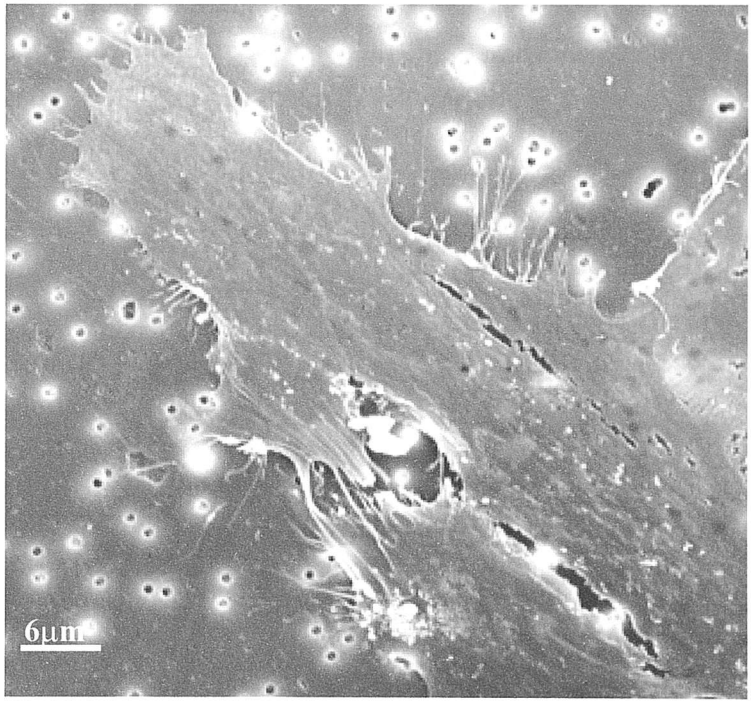

Fig.3.6b: HUVEC have migrated through to the underside of 1μm pore size filter.

3.2 Establishment of Bilayer Model:

16HBE 14o- cells were plated on the underside of 0.4μm PET (polyethylene terephthalate) inserts at different densities (0, 10^4, $5x10^4$, 10^5 and $5x10^5$ cells/50μl/insert). After 4 hours incubation, the inserts were reinverted into 24 well plates containing 500μl medium/well. The electrical resistance was measured on a daily basis (Fig.3.7), using the endohm-6 resistance measurement chamber from WPI.

It was found that neither the low density (10^4) nor the high density ($5x10^5$) gave the best electrical resistances. The cell density reaching the highest electrical resistance the fastest was 10^5 cells/50μl/insert. This was therefore established as the optimal density at which to plate down the cells.

For the bilayer model, once the 16HBE 14o- reached confluence, when TER was greater than 78Ω.cm^2, HUVEC were added at high density ($2x10^5$/200μl/insert) to the inside of the insert (Fig. 3.8). This was the optimal density to seed HUVEC to reach confluence in the shortest time. TER was then measured on a daily basis and the inserts were fixed for confocal, scanning and transmission electron microscopy.

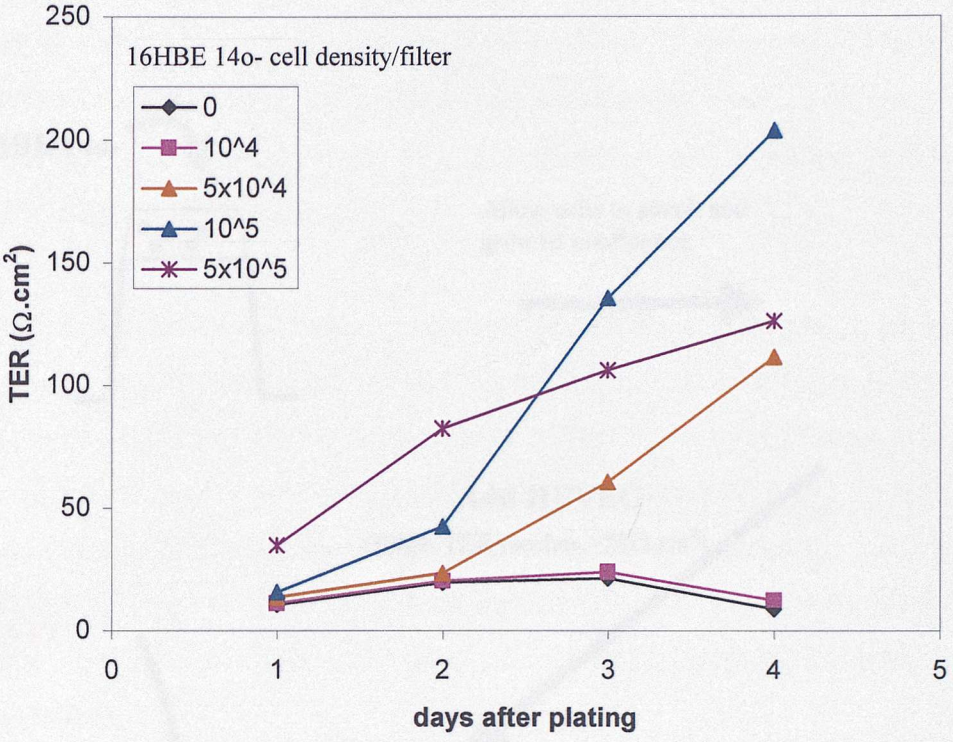

Fig.3.7 Measurement of TER with time in days, when 16HBE 14o- are plated down at different densities to the underside of filter inserts (1 insert for each cell density).

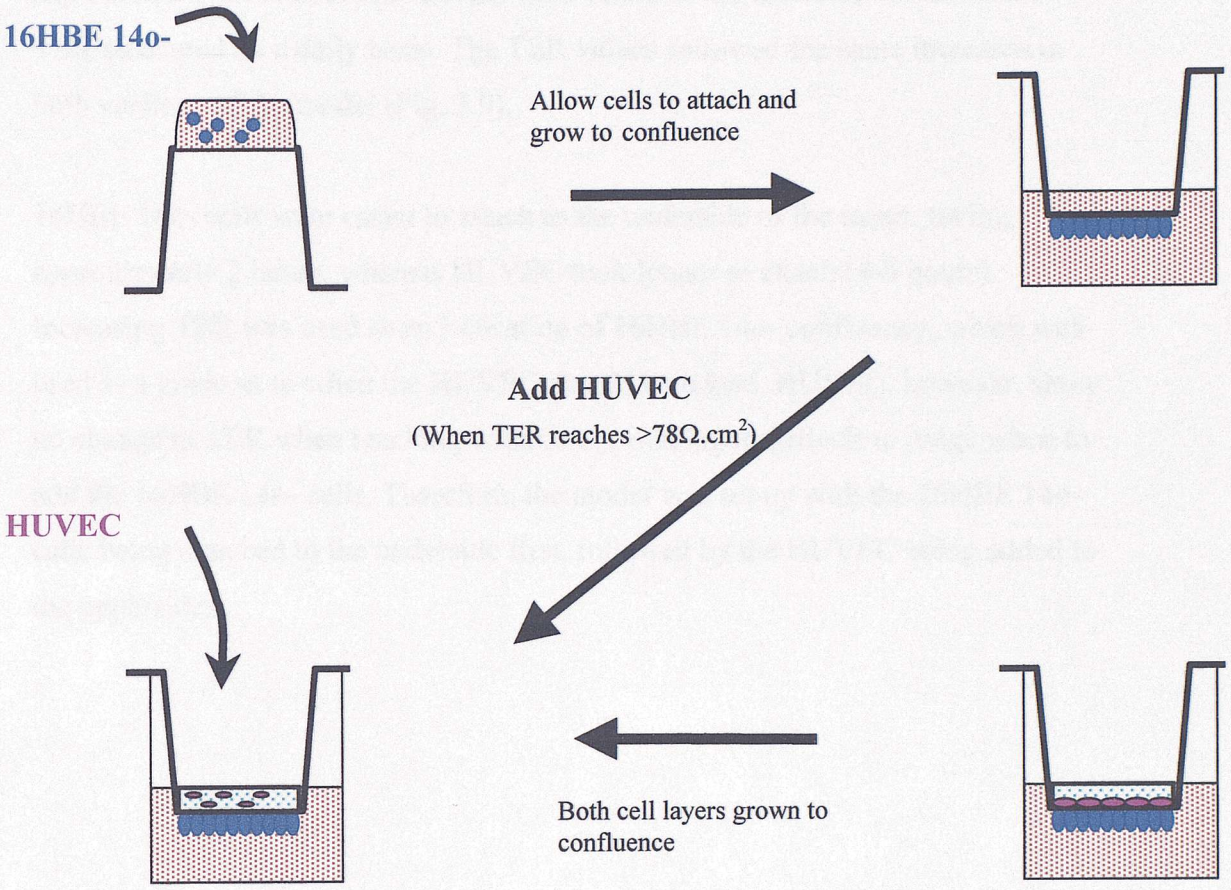

Fig. 3.8 Establishment of bilayer model

The bilayer model was also reversible, and in this case the HUVEC were seeded to the underside of the inserts first ($2x10^5$ cells/50µl/insert). Once attached the inserts were reinverted into wells with 500µl EBM-2 medium/well. The following day 16HBE 14o- cells ($2x10^5$/200µl) were added to the inside of the insert and TER measured on a daily basis. The TER values followed the same increases in both versions of the model (Fig. 3.9).

16HBE 14o- cells were easier to attach to the underside of the insert, taking approximately 2 hours, whereas HUVEC took longer to attach (4-6 hours). Increasing TER was used as an indication of 16HBE 14o- confluency, which was used as a guide as to when the HUVEC should be added. HUVEC, however, show no change in TER when reaching confluency, making it difficult to judge when to add the 16HBE 14o- cells. Therefore, the model was set up with the 16HBE 14o- cells being attached to the underside first, followed by the HUVEC being added to the upperside.

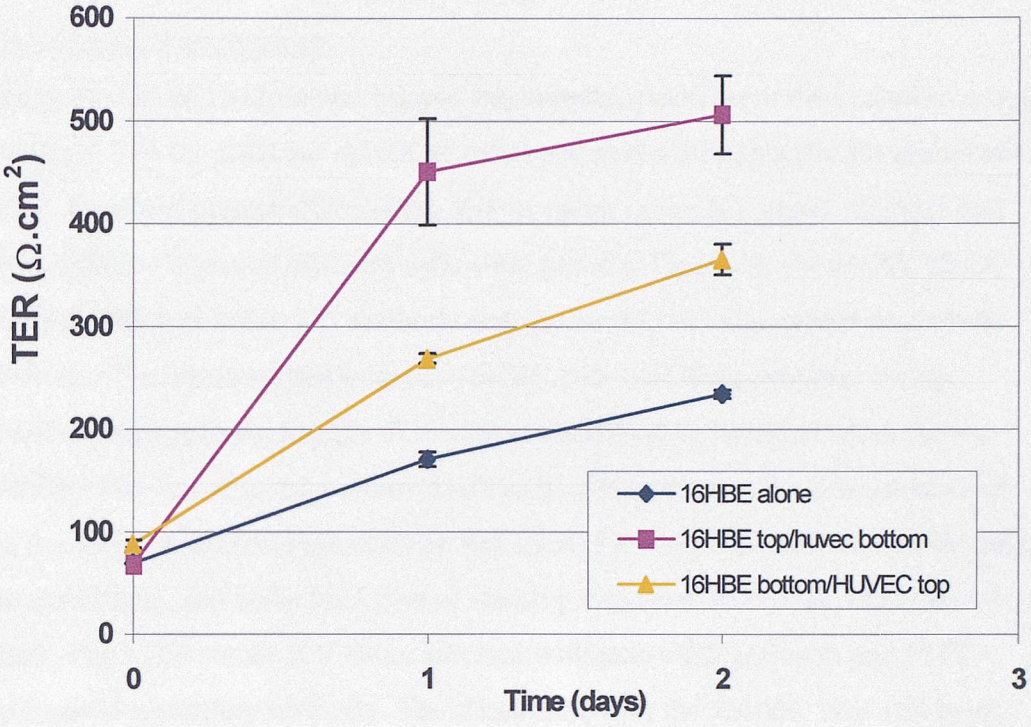

Fig.3.9 Comparison of TER measurements of 16HBE 14o- monolayer, bilayer with 16HBE 14o- on bottom/HUVEC on top and bilayer with 16HBE 14o- on top/HUVEC on bottom (n=4).

3.3 Characterisation of bilayer model

3.3.1 Confocal microscopy

The epithelial and endothelial bilayer was immunofluorescent dual labelled using anti-HEA 125 (specific for epithelial cells) and anti-vWF (specific for endothelial cells). Confocal optical slices of the bilayer taken in the XY plane, showed that two confluent layers of different cells were present. Fig.3.10a shows XY slices labelled with anti-HEA-125 antibody and rhodamine red conjugated secondary antibody. The slices started with the 16HBE 14o- cell layer showing strong positive staining (red). Images of the slices continued to be taken, from the top (16HBE 14o- cells) to the bottom (HUVEC) of the bilayer, which is invert from the model as an inverted microscope was used. Staining was reduced on reaching the membrane, and some background staining was seen on the HUVEC side of the insert. Fig.3.10b shows XY slices labelled with anti-vWF antibody and FITC-conjugated secondary antibody. The slices start with the 16HBE 14o- cell layer and no FITC labelling (green) was seen, until the HUVEC layer was reached (image 15) after which the FITC labelling became stronger. In both Fig.3.10a and Fig.3.10b, images 12-14 were negative, which is due to these images being taken through the insert membrane. The specific labelling of HUVEC for vWF illustrated that a confluent layer of HUVEC was present on one side of the insert. Images in the XZ plane showed that two separate layers of cells were present on either side of the insert membrane (Fig.3.10c). 16HBE 14o- cells were labelled on one side with HEA-125 (red), and HUVEC on the other side with vWF (green), with the insert membrane in the middle, shown as a confocal reflection image in blue.

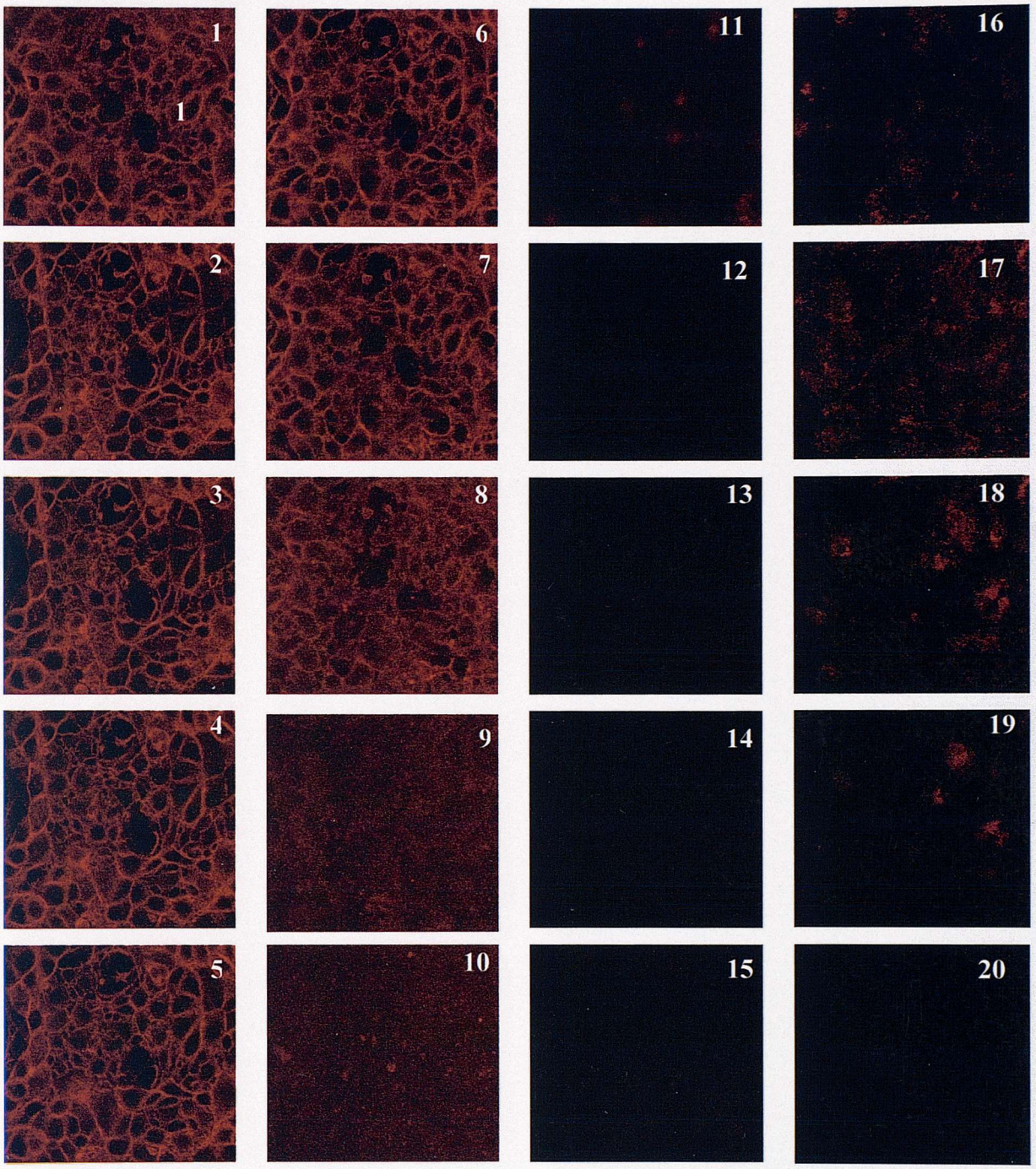

Fig.3.10a XY slices of 16HBE 14o- and HUVEC bilayer. 16HBE 14o- are labelled with HEA-125 primary antibody and rhodamine red conjugated secondary antibody. The confocal slices start from the 16HBE 14o- layer, hence strong positive staining, and finish with the HUVEC layer, where some background is seen. Specifically stained HUVEC are shown in fig.3.10b.

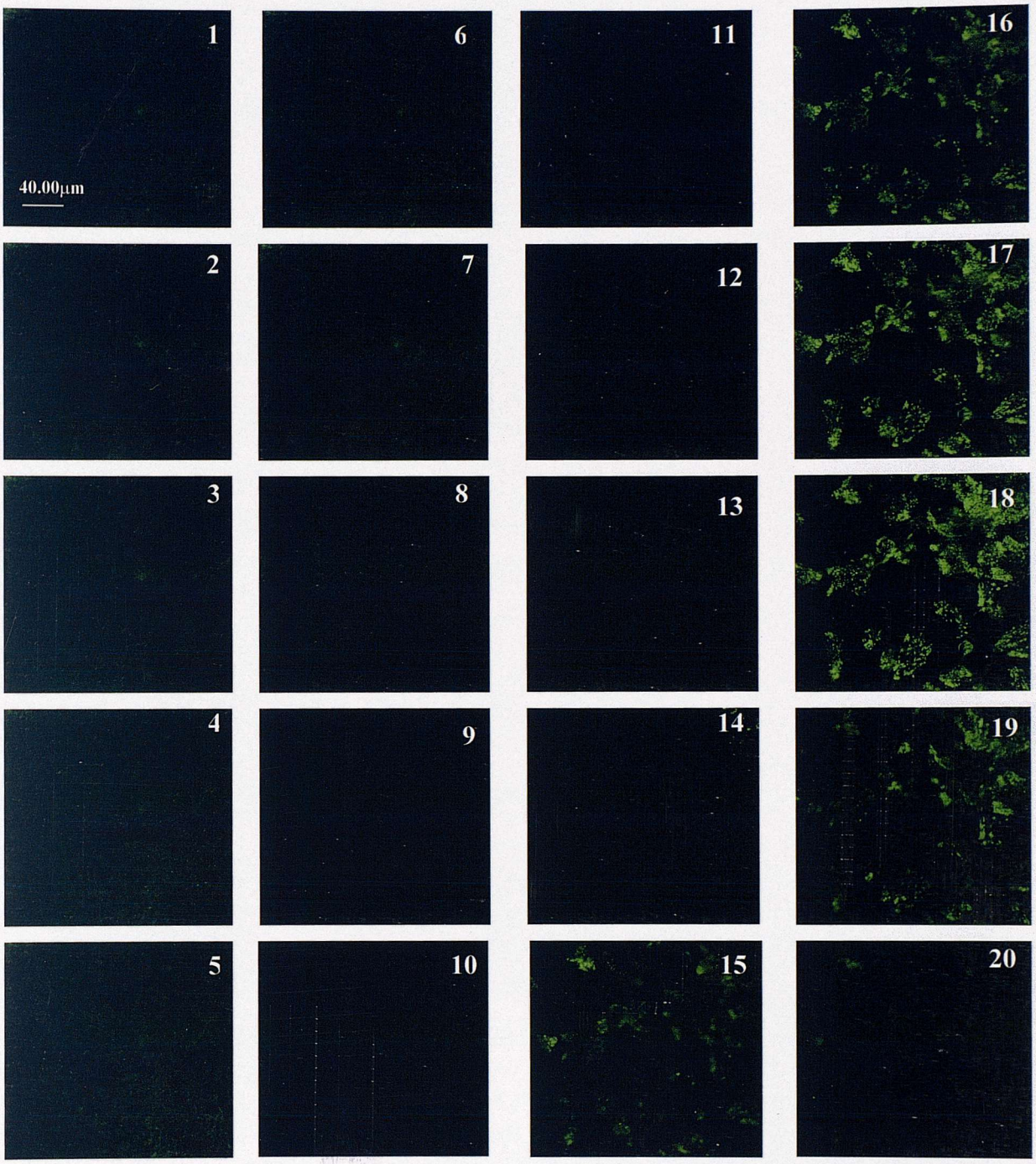

Fig.3.10b XY slices of 16HBE 14o- and HUVEC bilayer. HUVEC are specifically labelled with vWF primary antibody and FITC conjugated secondary antibody. The confocal slices start with the 16HBE 14o- layer, where some background staining occurs, and finish with the HUVEC layer, where the FITC staining becomes progressively stronger. Specifically stained 16HBE 14o- are shown in fig.3.10a.

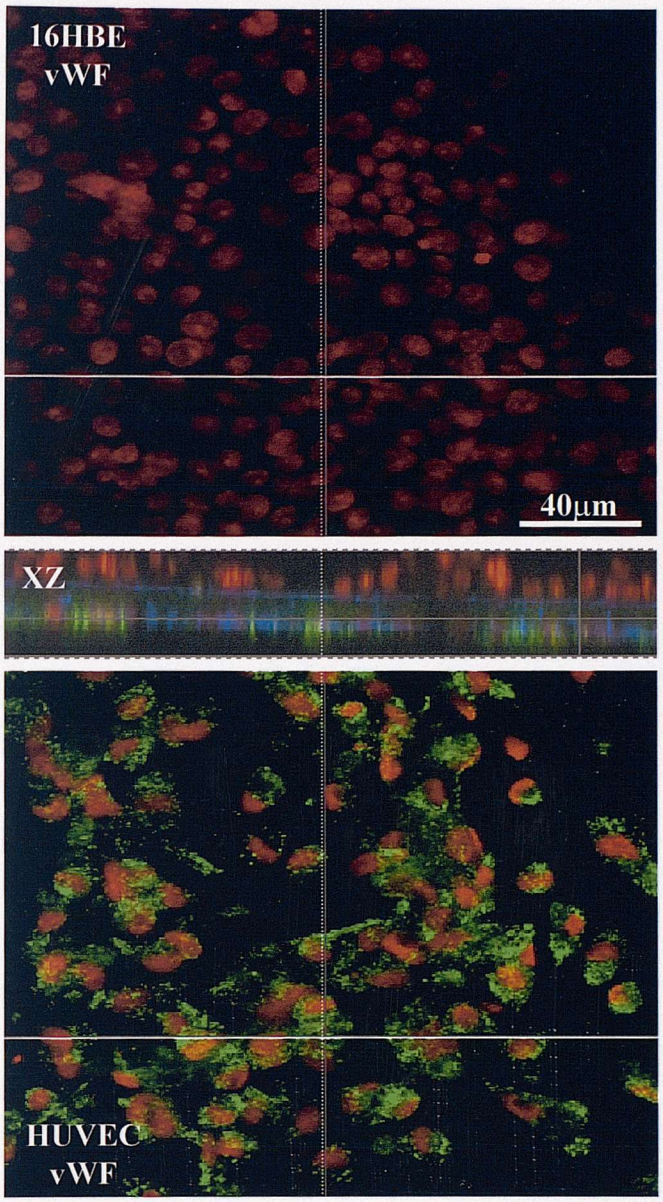

Fig.3.10c Cells on inserts stained with anti-vWF antibody and FITC conjugated secondary antibody. Nuclei were counterstained with propidium iodide. XY confocal slices (of the same area) show that vWF stained HUVEC's but not 16HBE 14o- on the opposite side of the insert. The image in the XZ plane (corresponding to the bold line in the XY images) illustrates that there were two separate layers of cells present on either side of the insert (shown as a refection in blue).

3.3.2 Scanning electron microscopy

SEM images of each side of the bilayer insert taken at day 1 and day 2 after addition of HUVEC, further confirmed the presence of two different cell types forming confluent layers on each side. 16HBE 14o- formed confluent layers by day 1 (Fig. 3.11Ai). Cell borders of adjoining cells could be seen and microvilli had formed (Fig.3.11Aii). HUVEC, however, formed thinner and flatter layers with the cells spreading out (Fig.3.11Ci). Cell borders could be seen but were uneven due to extending processes, which appeared to overlap one another (Fig. 3.11Cii).

By day 2, 16HBE 14o- appeared clearer (Fig. 3.11Bi) but similar features, such as microvilli and cell borders, were seen (Fig. 3.11Bii). HUVEC did not show much change compared to day 1 (Fig. 3.11Di). Cell borders could be seen as extended processes and appeared featureless due to their flatness (Fig. 3.11Dii).

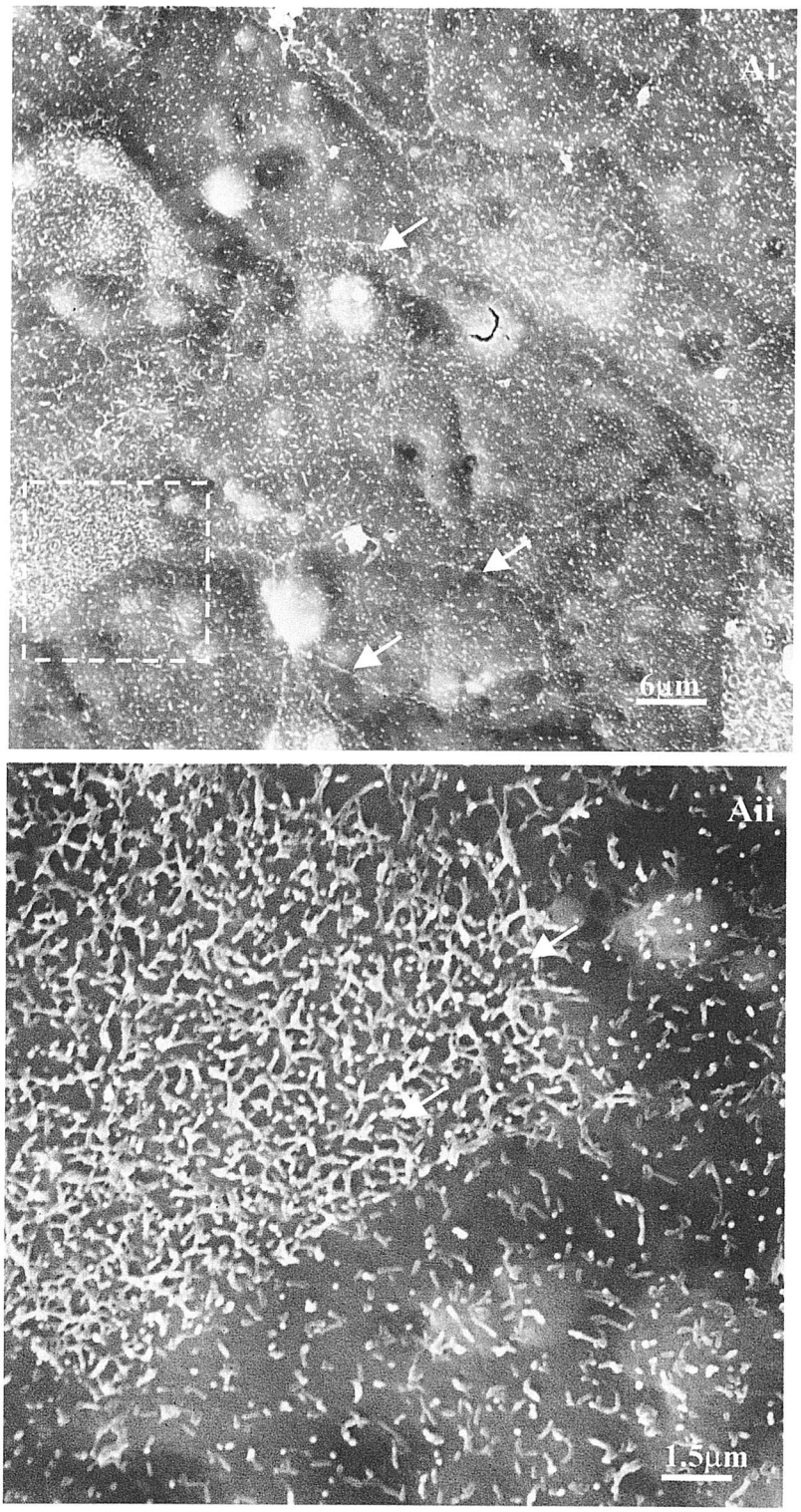

Fig. 3.11 Ai: At day 1, 16HBE 14o- cells have formed confluent layers and cell borders can be seen (arrows). Boxed area enlarged in Aii. **Aii**: Contiguous cell borders are formed and processes are protruding from cell surface (arrows).

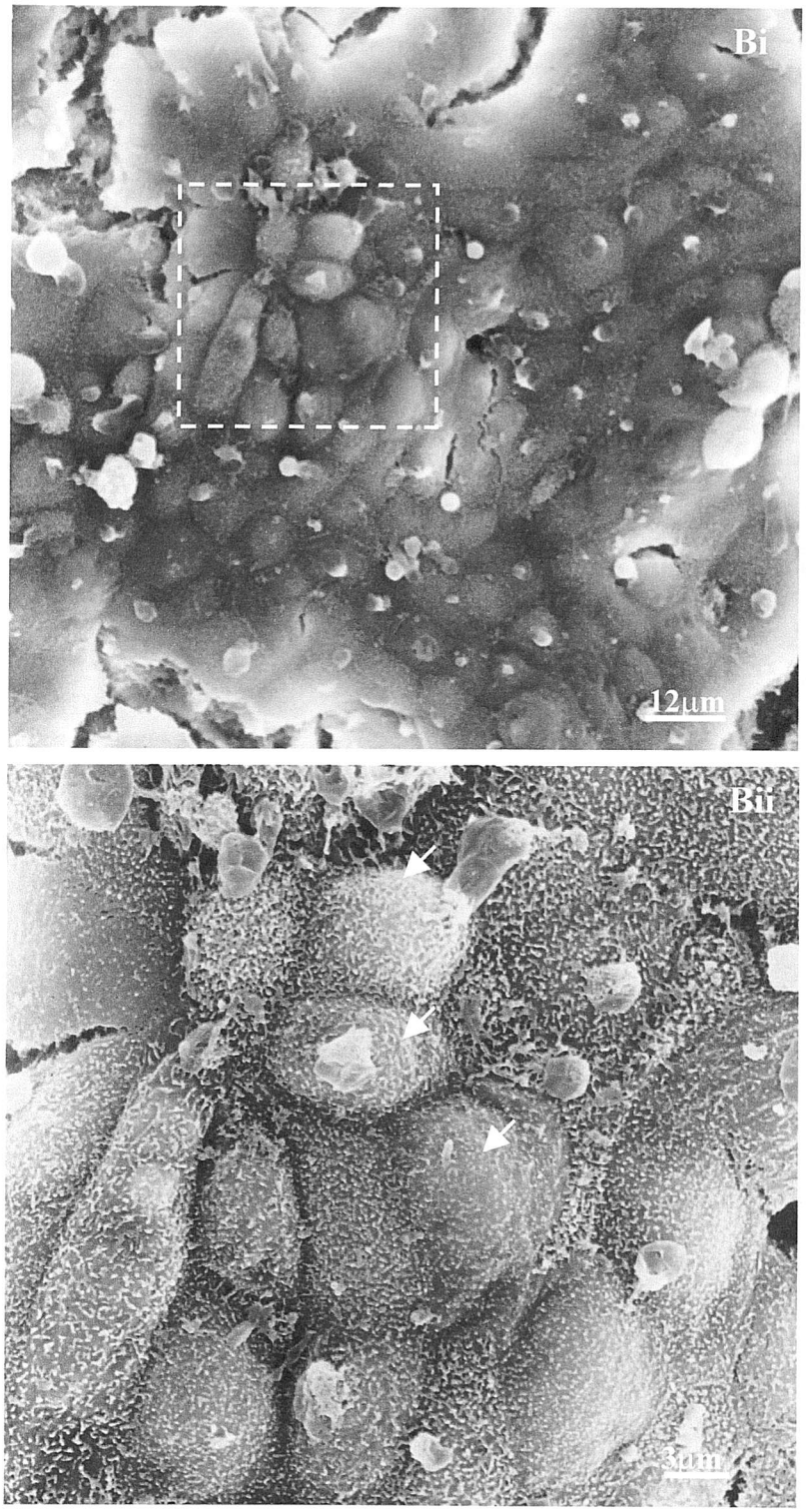

Fig. 3.11 Bi: At day 2, 16HBE 14o- appear denser and more prominent than at day 1.Boxed area enlarged in Bii.
Bii: Cell nuclei are prominent (arrows).

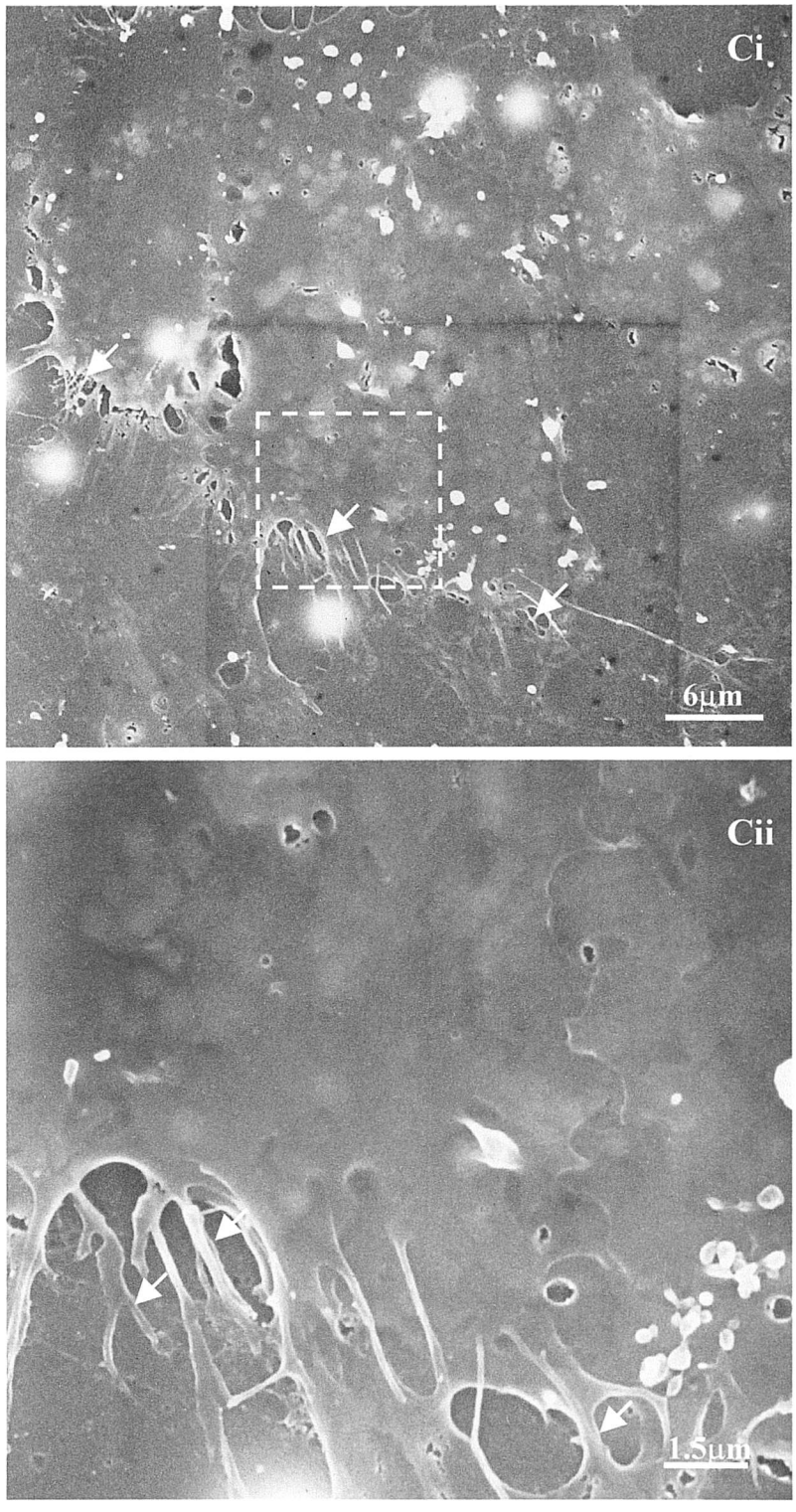

Fig. 3.11 Ci: At day 1, HUVEC have formed thinner, less prominent confluent layers, and cell borders form jagged edges (arrows).Boxed area enlarged in Cii.
Cii: Cell borders of the HUVEC can be seen to be uneven due to extended processes (arrows). Processes of adjacent cells overlap.

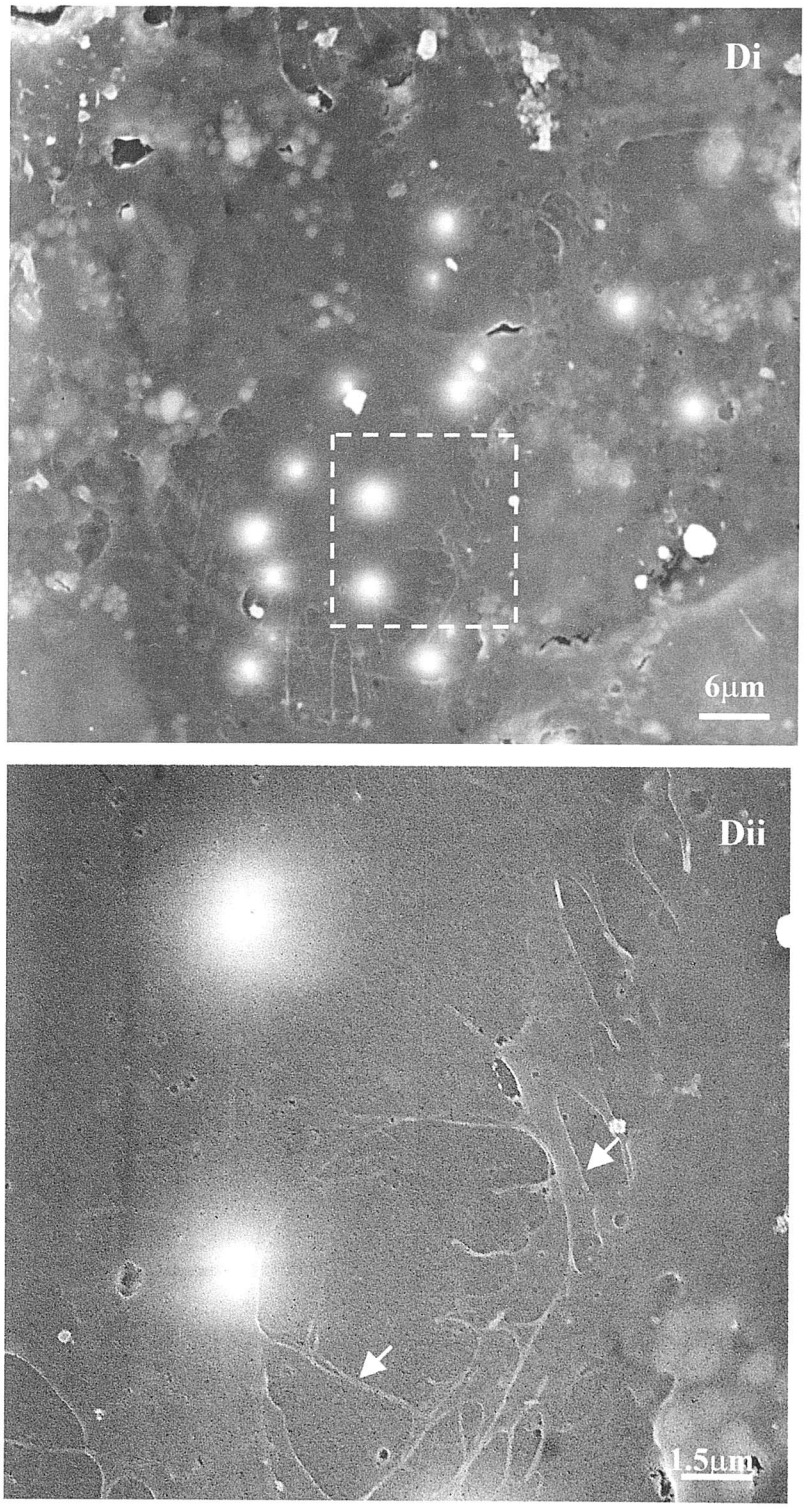

Fig. 3.11 Di: At day 2, HUVEC do not show much change compared to day 1. Cells appear featureless due to their flatness. Boxed area enlarged in Dii.
Dii: Cell borders of the HUVEC can be seen forming extended processes (arrows).

3.3.3 Transmission electron microscopy

Inserts fixed and processed for TEM showed that 16HBE 14o- and HUVEC were present on both sides of the insert (Fig.3.12a). 16HBE 14o- epithelial cells were rounder, more prominent and were two-cells deep in places. Cell borders could be visualised, and junctional complexes had been formed. HUVEC formed thinner layers and individual cells had flattened and spread out extensively. Cell borders and junctions were difficult to distinguish between HUVECs.

Tight junctions could be seen close to the apical surface of 16HBE 14o- (Fig. 3.12b), where microvilli had also formed. Further down the same membranes, desmosomes could be seen. Desmosomes could be distinguished from tight junctions by being wider and forming electron-dense plaques which extend into the cytoskeleton of the cells (Fig.3.12c). Tight junctions were close to the apical surface and the two adjacent membranes fuse together (Fig.3.12d).

Endothelial cells elongated and formed a flatter layer (Fig. 3.12e), and do not appear directly attached to the insert, but form a layer of extracellular matrix over the insert membrane. The extending cell processes of adjacent cells overlap (Fig. 3.12f) and apposing membranes form junctional complexes (Fig.3.12g).

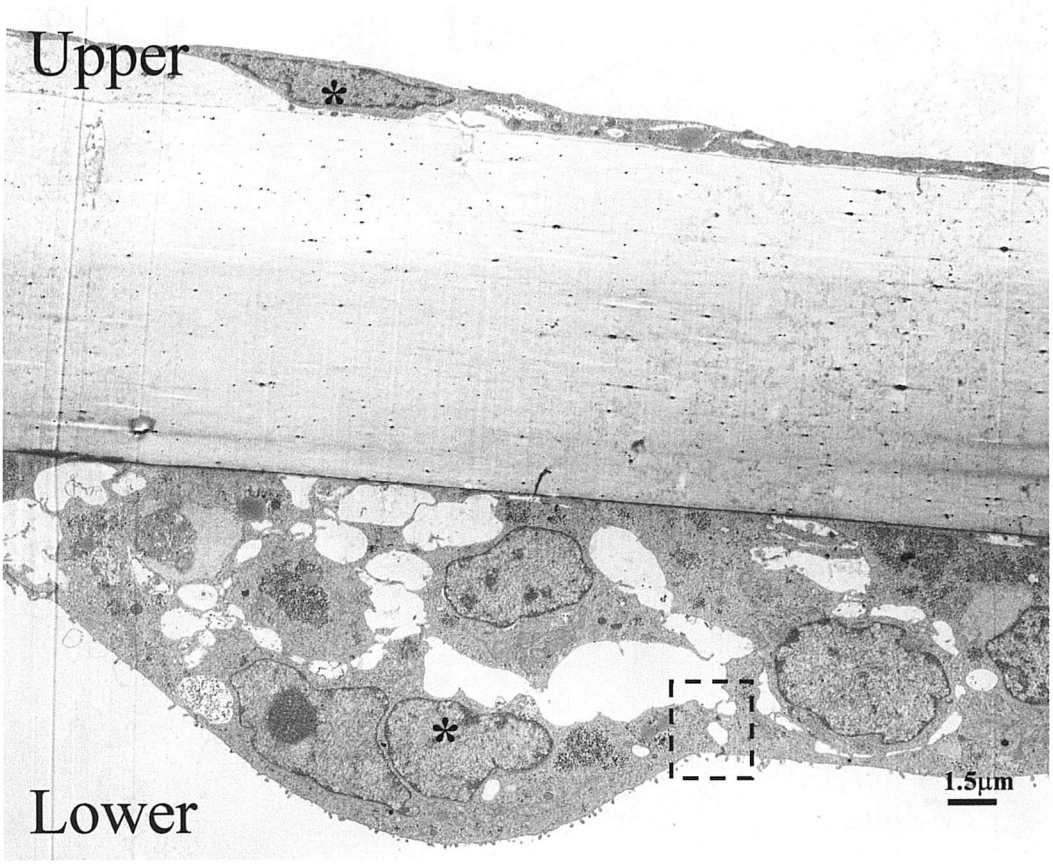

Fig.3.12a Transmission electron micrograph of 0.4µm tissue culture insert from bilayer model. Endothelial cells (HUVEC) can be seen on the upper surface and epithelial cells (16HBE 14o-) on the lower surface of the insert. Cell nuclei can be seen on both cell types (*). Boxed area indicates junctional complexes between the epithelial cells (enlarged in Fig. 3.12b). Endothelial cell borders are not present in this micrograph, but can also be seen (enlarged in Figs. 3.12c-e).

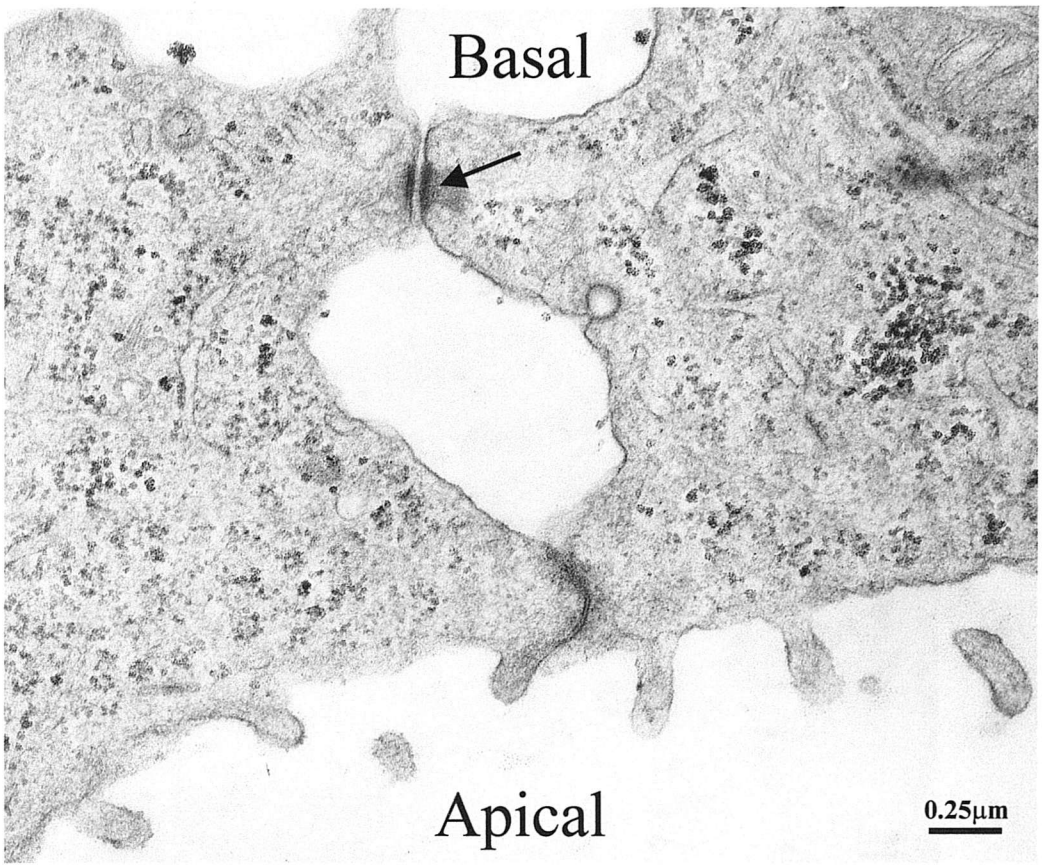

Fig. 3.12b Enlarged TEM of boxed area in Fig. 3.12a, illustrating junctional complexes between 16HBE 14o- cells. Tight junction complexes are seen close to the apical surface (*), and desmosomes are formed further down (arrow). Microvilli can be seen on the apical surface.

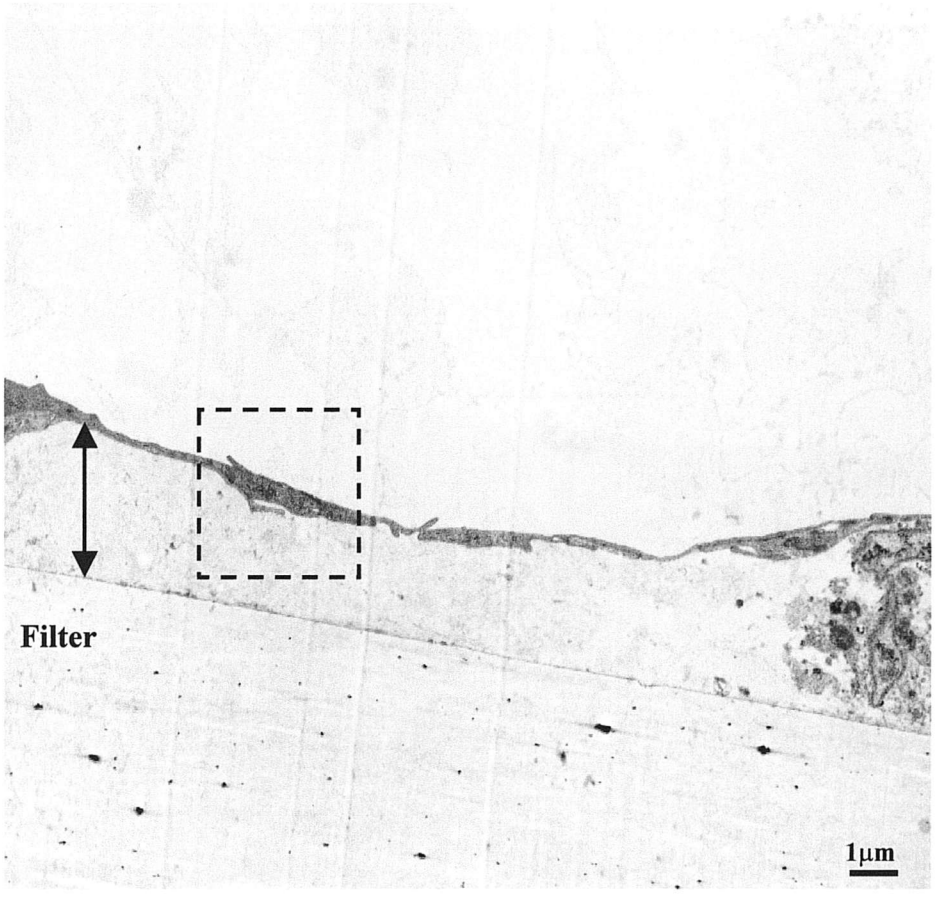

Fig.3.12c TEM of HUVEC on upper surface of insert. Extended processes of adjacent cells overlap each other (boxed area) where cell borders and junctional complexes have formed (enlarged in Figs. 3.12d-e). The cells are also separated from the insert by what appears to be extracellular matrix (**arrow**).

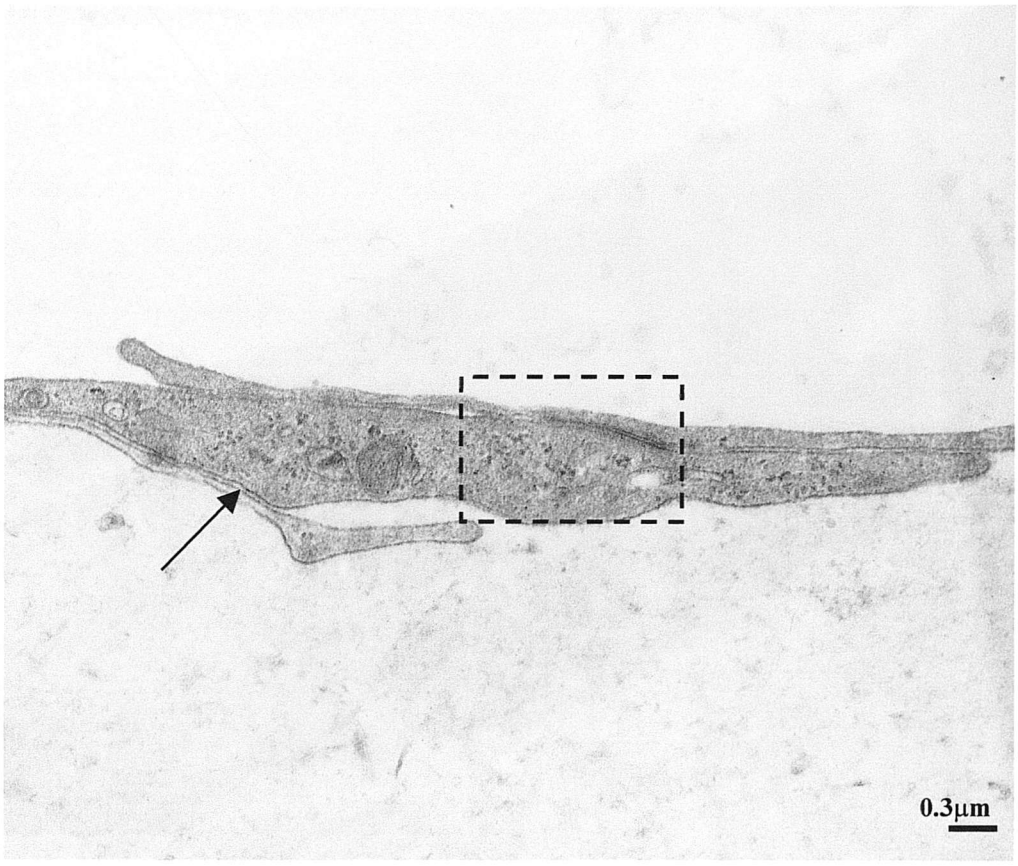

Fig. 3.12d Enlarged TEM of boxed area in Fig. 3.12c. Cell borders can be seen where the elongated processes overlap (**arrow**). Boxed area indicates junctional complexes formed, enlarged in Fig. 3.12e.

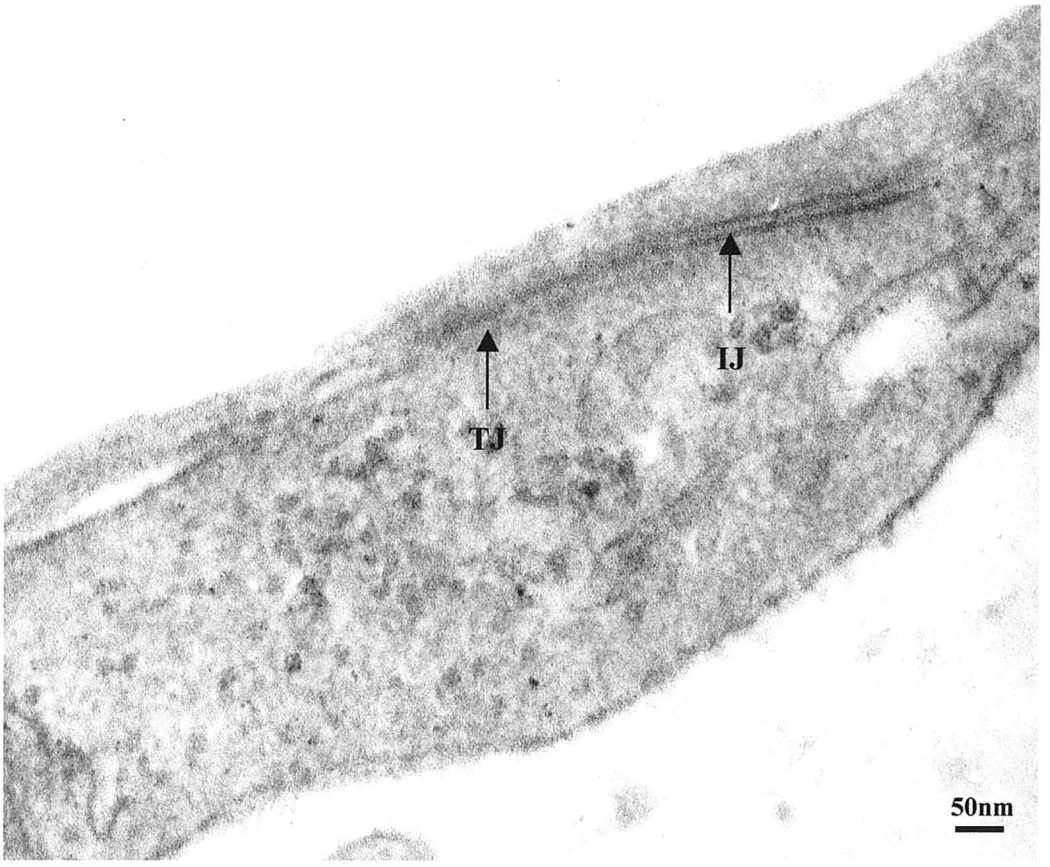

Fig. 3.12e Enlarged TEM of boxed area in Fig.3.12f, illustrating apposing membranes forming junctional complexes (**arrows**). TJ, tight junction membranes appear fused together and IJ, intermediate junction, membranes are slightly apart.

3.3.4 Transcellular electrical resistance

TER of the bilayer increased to a maximum mean of 464$\Omega.cm^2$ (S.E. $\pm$ 18) three days after addition of HUVEC's (Fig.3.13). This was significantly higher ($p<0.00001$) than the summation of the TER of individual monolayers. In comparison, 16HBE 14o- at confluence exceeded a mean value of 78$\Omega.cm^2$, and continued to increase to a mean value of 238$\Omega.cm^2$ (S.D. $\pm$ 25) at day 2. HUVEC's alone reached a maximum of 5$\Omega.cm^2$ (S.D. $\pm$ 0.1).

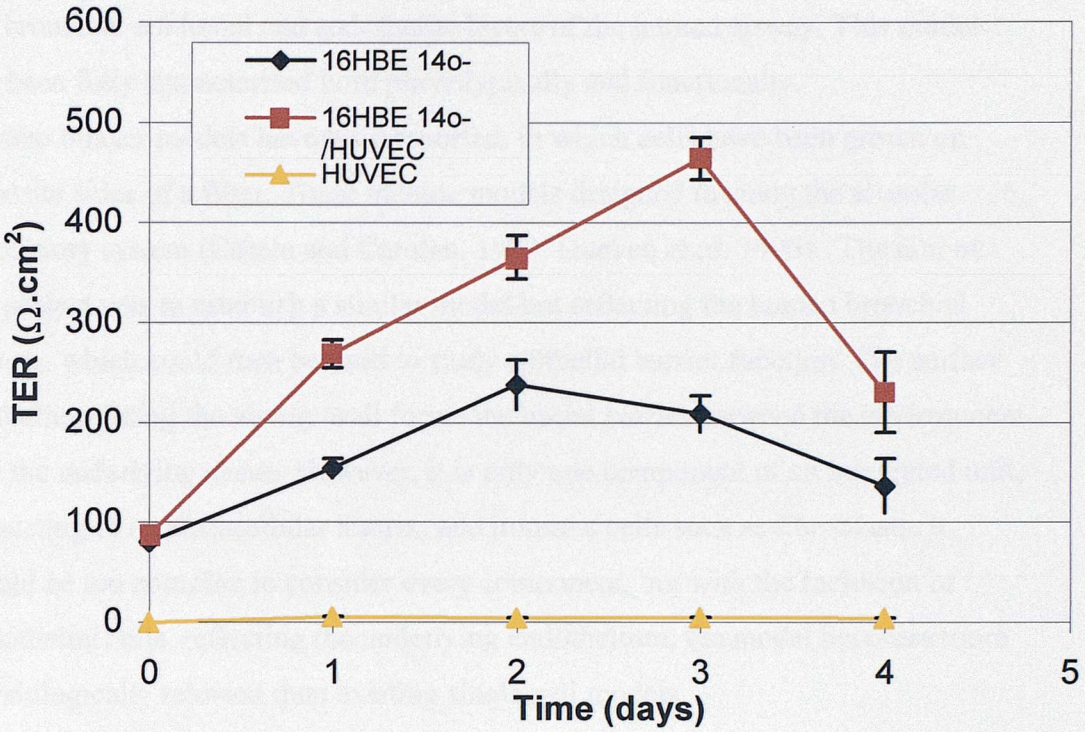

Fig. 3.13 Comparison of TER, with time, between 16HBE 14o-/HUVEC bilayer, and 16HBE 14o- and HUVEC monolayers. (Error bars show standard error of the mean, n=56 consisting of six experiments with 8 inserts per experiment).

3.4 Discussion of final model established

An *in vitro* bilayer model has been established and fully characterised, reflecting the bronchial epithelial and endothelial layers of the human airway. This model has been fully characterised both phenotypically and functionally.

In vitro bilayer models have been reported, in which cells have been grown on opposite sides of a filter. These include models designed to study the alveolar respiratory system (Casale and Carolan, 1999; Gueven *et al.* 1996). The aim of the project was to establish a similar model but reflecting the human bronchial system, which could then be used to study epithelial barrier function. The surface epithelium lining the airway wall forms the initial barrier between the environment and the underlying tissue. However, it is only one component of an integrated unit, consisting of an extracellular matrix, and immune cells such as fibroblasts. It would be too complex to consider every component, but with the inclusion of endothelial cells, reflecting the underlying endothelium, the model becomes more physiologically relevant than existing single cell models.

The different cell types have been specifically characterised, and the 16HBE 14o- epithelial cell line and the primary HUVEC were used in the final model. Epithelial cells are known to form tight junctions, and TER was used to measure the extent of tight junction formation. 16HBE 14o- were chosen to represent the bronchial epithelium rather than the H292 cell line, since 16HBE 14o- reached high electrical resistances ($790\Omega.cm^2$) in comparison to relatively low resistances reached by H292 ($72\Omega.cm^2$). TEM images also showed tight junctions had formed in confluent 16HBE 14o- layers. They also display typical epithelial immunostaining patterns, being positive for cytokeratins as well as the epithelial specific surface marker HEA-125. Primary HUVEC were used for the final bilayer model as the endothelial cell lines differed in their morphology. Primary HUVEC displayed the typical endothelial phenotype of being round and flattened with the bulging nucleus in the centre, and having a cobblestone appearance when confluent. They were consistent in their morphology with each passage and also grew to confluence, which not only was necessary for the final model but also enabled enough cells to be grown. Endothelial cell lines however, formed less confluent layers and became more elongated with extended processes with each one passage.

HEA-125 was identified as an epithelial specific marker, staining 100% of 16HBE 14o- but 0% of HUVEC, and vWF was identified as an endothelial specific marker, staining 100% of HUVEC but 0% of 16HBE 14o-. The identification of cell-specific-markers was essential to enable the two different cell types to be distinguished in the final model.

The final model consists of a layer of 16HBE 14o- epithelial cells on the underside of a 0.4 μm pore-size insert, and a layer of HUVEC on the upper side. Two separate cell layers were required, since *in vivo* the bronchial epithelium would be in close proximity (20-200μm), but not in direct contact with the endothelium. Mackarel *et al.* have shown that cells can migrate through pores, and previous models do not appear to have taken this into consideration when setting up monolayer or bilayer models (Mackarel *et al.* 1999). Any possible migration of cells will affect consequent results; hence any possible migration of cells was looked at using scanning electron microscopy of each side of the inserts. Cells were shown to migrate through the 1μm pore size inserts, but not through the 0.4μm pore size inserts, which were subsequently used in the final model. 16HBE 14o- cells were grown on the bottom of insert membranes, as they attached more quickly than HUVEC. The level of confluency could also be measured using transepithelial resistance, therefore ensuring the HUVEC were added under the same conditions for each experiment.

Confocal immunostaining showed positive HEA-125 staining on the epithelial side of the membrane and positive vWF staining for the endothelial side, confirming the presence of two separate cell layers. Transmission electrical microscopy of sections cut across the bilayer, also showed a layer of 16HBE 14o- on one side of the filter and endothelial cells on the other.

The resistance of the bilayer, reaching a maximum of 1550 $\Omega.cm^2$, exceeded that of the individual monolayers, and was significantly ($p<0.00001$), higher than the sum of the TER of the individual monolayers, (16HBE 14o- reaching 790$\Omega.cm^2$ and HUVEC reaching 20$\Omega.cm^2$). It should also be noted that the TER of the HUVEC is also significantly ($p<0.00001$), lower than that of the 16HBE 14o-, suggesting that although HUVEC form tight junctions, they do not have the same functional characteristics as the epithelial cells.

The results suggest that the increase in TER seen in the bilayer is due to a change in tight junction properties and not merely due to the combined TER of the two cell layers. This could be caused by cell-to-cell interaction or some secreted factor, which will be further investigated. These results show that when studying the epithelium of the respiratory system, it is also important to consider the underlying endothelial cells, as the results may differ in comparison to single cell studies.
The model that has been established in this study therefore has several advantages. Firstly, as a bilayer system, the cells can interact either directly or indirectly, better reflecting the *in vivo* situation in which epithelial and endothelial cells coexist. Secondly, the model uses human cell lines and primary human cell cultures, making a better human comparison, and moving away from the need for animal models. Finally, the model has been fully characterised and optimised such that it could easily and consistently be reproduced, and easily manipulated for various studies including cell migration, damage and repair, and effect of toxins. Changes in both the epithelial and endothelial cells can be examined, and the extent of cell-to-cell interactions can be assessed in comparison to monolayer systems.
The results from characterising the bilayer model provide an initial indication that my hypothesis that the bilayer model functions differently in comparison to the separate monolayers is correct. What these changes are and how they are mediated will be investigated.

CHAPTER 4

ENDOTHELIAL EFFECTS ON EPITHELIAL CELLS:

What is changing to cause an increased TER?

Chapter 4: Endothelial effects on epithelial cells: What is changing to cause an increased TER?

4.1 Introduction

The final bilayer model established has revealed that functional differences exist between epithelial cells grown as a monolayer and epithelial cells grown as a bilayer with endothelial cells. The main difference seen is an increase in TER in the bilayer, reflecting changes in tight junction function. Consequently, two questions arise:

- What is changing to cause this increased TER?
- What is mediating the change in TER?

The first question has been addressed in this section. The second will be addressed in chapter 5.

There are several possibilities that may be contributing to an increased TER. Firstly, it may simply be due to having two cell layers grown in parallel, each having an electrical resistance, the combination of which may have an additive or multiplied effect. This was investigated using 16HBE 14o- cells grown as a bilayer with cells other than HUVEC (ie. 16HBE 14o- and endothelial cell line). This would also answer whether the increase in TER was an epithelial-endothelial effect. However, it would not determine if the increase was occurring in the 16HBE 14o- cells, the HUVEC or both. Growing 16HBE 14o- cells in the presence of HUVEC-conditioned medium, and HUVEC in 16HBE 14o- conditioned medium would confirm in which cell type TER was changing as well as determining whether the change in TER could be attributed to a soluble factor. Another possibility is an increase in cell proliferation, resulting in an increased cell density or cell layers. If each cell forms the same number of tight junctions with adjacent cells, then an increase in cells per unit area would, in theory, result in an increase in tight junctions per unit area, which in turn would result in an increased TER. Differences in cell density would be determined using nuclei staining and cell counting. An increase in cell layers may also cause an increase in TER, since tight junctions would be formed between cells in each layer, so multiple layers of resistance would physically add to the overall resistance. Any

changes in cell layers would be investigated by measuring epithelial cell height from images of thick sections of the bilayer and monolayer.

Finally, changes may be occurring in protein expression, especially of tight junction proteins, which form the tight junctions. It is possible that different proteins are being expressed or upregulated, contributing to a change in TER. This would initially be investigated using RT-PCR, to deduce if there are any differences at the messenger RNA (mRNA) level. Although differences seen at the mRNA level may not necessarily be translated into protein itself, it will help give an indication of possible changes. In particular, it would pinpoint any genes no longer being expressed, or newly expressed, or genes that have been upregulated. Differences in tight junction protein expression would contribute to changes in TER, and to establish whether any changes discovered from RT-PCR were translated at the level of protein expression, western blotting and immunofluorescent staining would be used. Western blotting would give an indication of whether a protein was no longer being expressed, newly expressed or being upregulated, any of which may modify tight junction function which would be reflected in a change in TER. Differences in protein expression may not be the only reason for an increase in TER. In fact, there may not be any change in the amount of protein expressed but differences may lie in the distribution of tight junction proteins. Immunofluorescent staining would not only give an indication of differences in protein expression, but would also give an indication of possible differences in protein distribution, for example a protein distribution changing from intracellular to the cell membrane, may be causing changes in the structure of the tight junction resulting in an altered TER.

4.2 Effect of different cell types in the bilayer model

16HBE 14o- cells were grown to confluence on the underside of inserts and then the four following conditions applied:

1. 16HBE 14o- grown as a monolayer;
2. 16HBE 14o- grown as a bilayer with 16HBE 14o- (Fig.4.1);
3. 16HBE 14o- grown as a bilayer with HUVEC;
4. 16HBE 14o- grown as a bilayer with HUVE-12 (Fig.4.2).

TER was measured daily.

When 16HBE 14o- were grown, as a bilayer with 16HBE 14o- on both sides of the membrane, there was no significant increase in TER ($p=0.21$). The TER values of 16HBE 14o- grown in parallel, as a bilayer with HUVEC, still showed an increase. It could therefore, be deduced that the increased TER in the 16HBE 14o-/HUVEC bilayer was not an additive effect, since the 16HBE 14o-/16HBE 14o- bilayer did not reach a TER double that of the monolayer. There must be some other factor contributing to the change.

When 16HBE 14o- was grown as a bilayer, with HUVE-12, an endothelial cell line, there was a significant increase in TER ($p=0.009$), in comparison to that of the 16HBE 14o- monolayer ($513\Omega.cm^2$). However, the maximum reached ($670\Omega.cm^2$) was lower than that of the 16HBE 14o-/HUVEC bilayer ($896\Omega.cm^2$) grown in parallel. Both primary endothelial cells and the endothelial cell line have a low TER when grown alone as a monolayer. However, when grown as a bilayer with 16HBE 14o- cells, TER significantly increases ($p<0.01$), to a value greater than the summation of the TER of the individual monolayers. These results are consistent with those of the 16HBE 14o-/HUVEC bilayer in chapter 3 (3.3.4). This suggests that the TER increase seen in our bilayer model is an epithelial-endothelial effect.

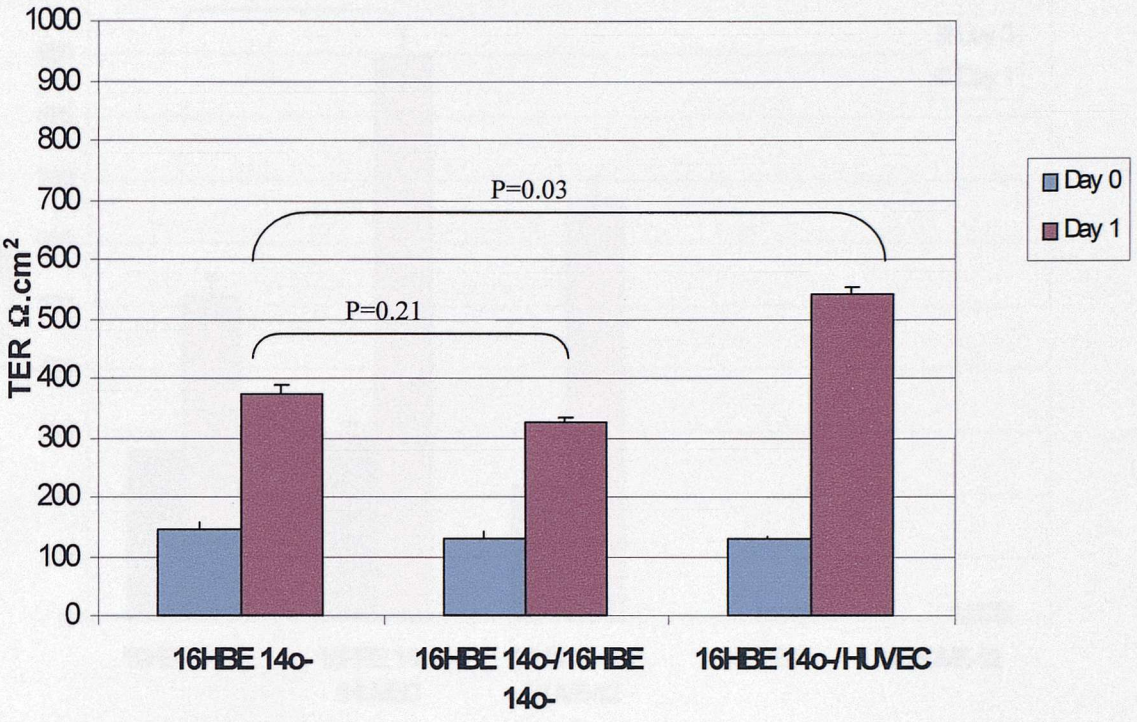

Fig.4.1 Comparison of TER: 16HBE 14o- monolayer, 16HBE 14o-/16HBE 14o- bilayer and 16HBE 14o-/HUVEC bilayer. There was no difference in TER when 16HBE 14o- were grown as a bilayer with 16HBE 14o- in comparison to 16HBE 14o- monolayer ($p=0.21$; $n=4$).

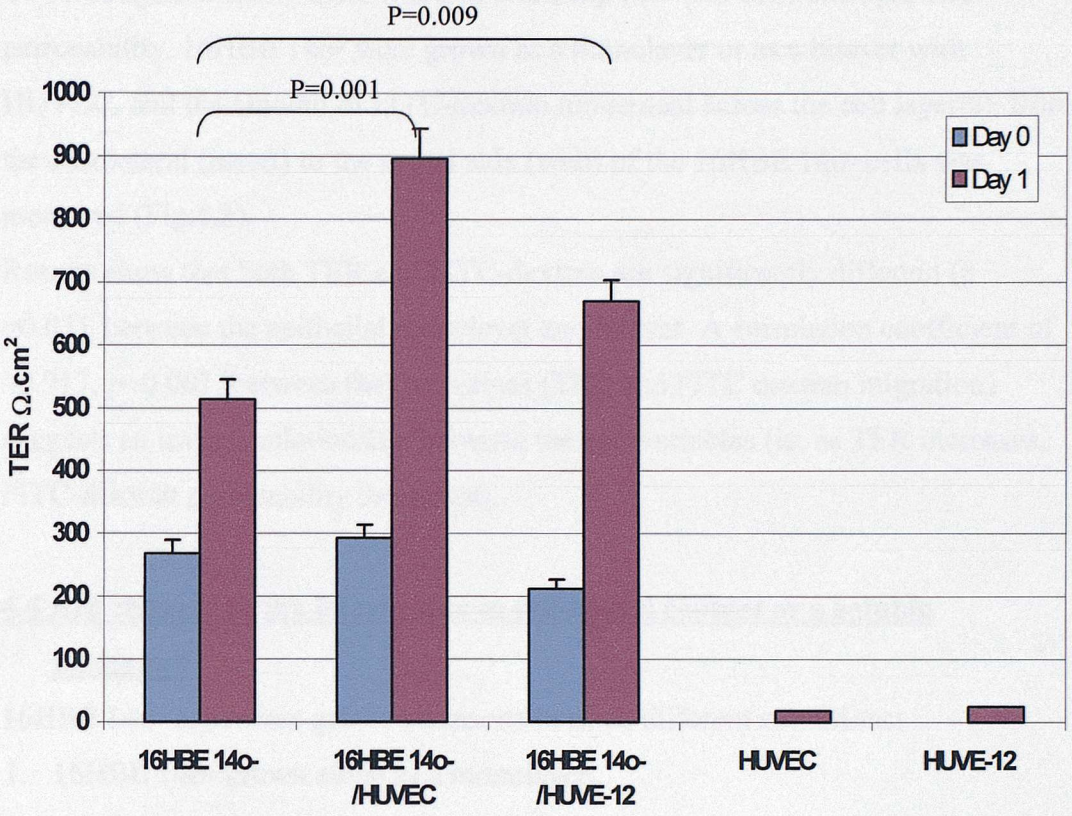

Fig.4.2 Comparison of TER: 16HBE 14o- monolayer, 16HBE 14o-/HUVEC bilayer, 16HBE 14o-/HUVE-12 bilayer, HUVEC monolayer, HUVE-12 monolayer. 16HBE 14o- grown as a bilayer with HUVEC (p=0.001) or HUVE-12 (p=0.009) induced a significant increase in TER in comparison to 16HBE 14o- monolayer (n=8).

4.3 Do changes in TER reflect a change in epithelial permeability?

To investigate whether there was a relationship between TER and epithelial permeability, 16HBE 14o- were grown as a monolayer or as a bilayer with HUVEC, and the amount of FITC-dextran movement across the cell layer(s), from the basolateral (insert) to the apical side (well) of the 16HBE 14o- cells was measured (Fig.4.3).

Results show that both TER and FITC-dextran are significantly different ($p = 0.03$), between the epithelial monolayer and bilayer. A correlation coefficient of -0.917, $p=0.001$, between the two values (TER and FITC dextran migration) suggests an inverse relationship between the two variables (ie. as TER increases, FITC-dextran permeability decreases).

4.4 Are changes in the bilayer due to cell-to-cell contact or a soluble mediator?

16HBE 14o- cells were grown on inserts in three different conditions:

1. 16HBE 14o- grown alone as a monolayer;
2. 16HBE 14o- grown as a bilayer with HUVEC;
3. 16HBE 14o- grown as a monolayer in the presence of conditioned medium taken from confluent HUVEC cell cultures.
4. HUVEC grown as a monolayer in the presence of conditioned medium taken from 16HBE 14o- cell cultures.

TER was measured daily (Fig. 4.4). 16HBE 14o- grown in the presence of HUVEC conditioned medium followed the same significant increase ($p<0.01$) in TER as the bilayer reaching a maximum of $2250\Omega.cm^2$, which was significantly greater ($p=0.0034$), than that of the monolayer (reaching a maximum of $1400\Omega.cm^2$). HUVEC grown in the presence of 16HBE 14o- conditioned medium showed no increase in TER in comparison to the HUVEC monolayer ($p=1.00$), both staying at approximately $80\Omega.cm^2$. Results show that 16HBE 14o-conditioned-medium does not have an effect on the TER of HUVEC ($p=1$). However, growing 16HBE 14o- in the presence of HUVEC-conditioned-medium results in the same increase in TER as that of the bilayer. It can be concluded that the increased TER seen in the bilayer, is due to an increased TER occurring in 16HBE 14o- cells, induced by some endothelial secreted factor.

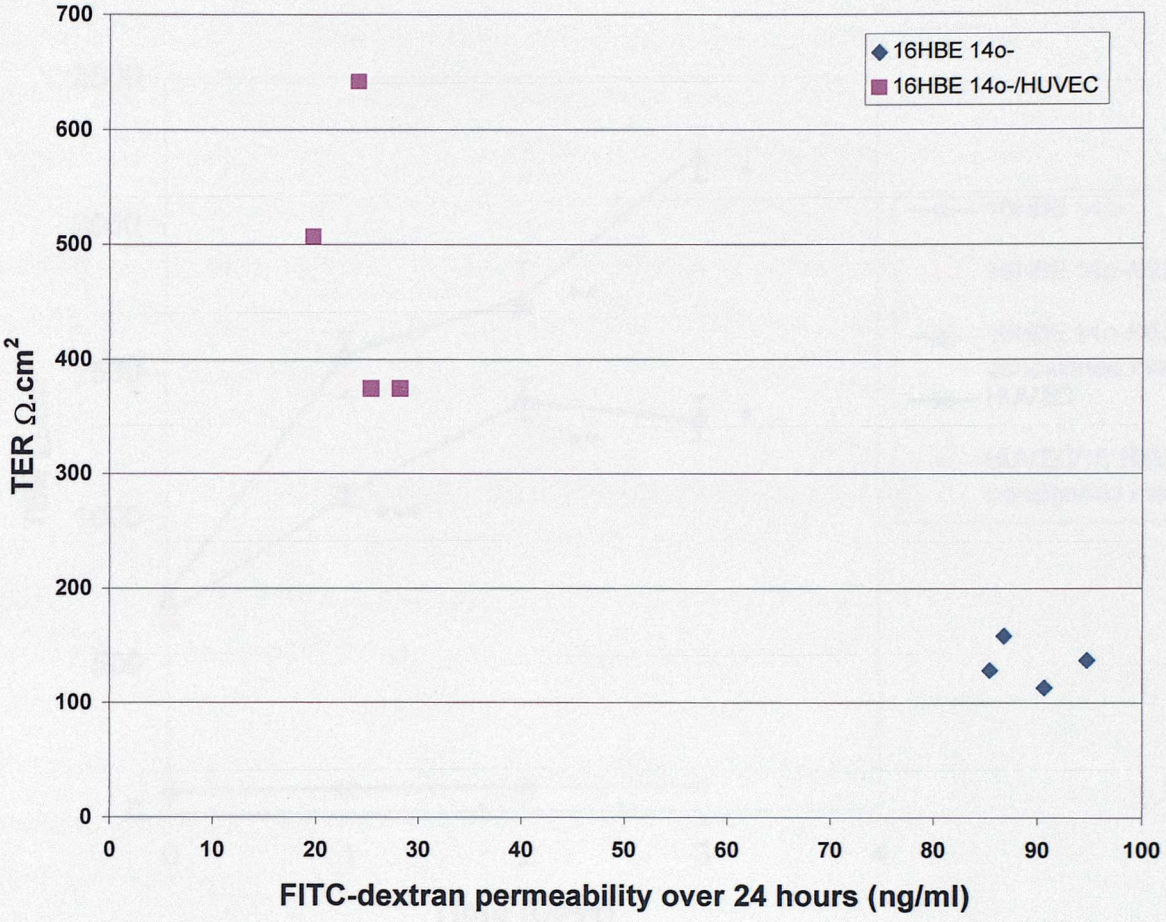

Fig.4.3 Comparison of TER with FITC-dextran permeability across 16HBE 14o- monolayer and 16HBE 14o-/HUVEC bilayer. There is an inverse relationship between TER and FITC dextran permeability (correlation coefficient=-0.917; p=0.001; n=4).

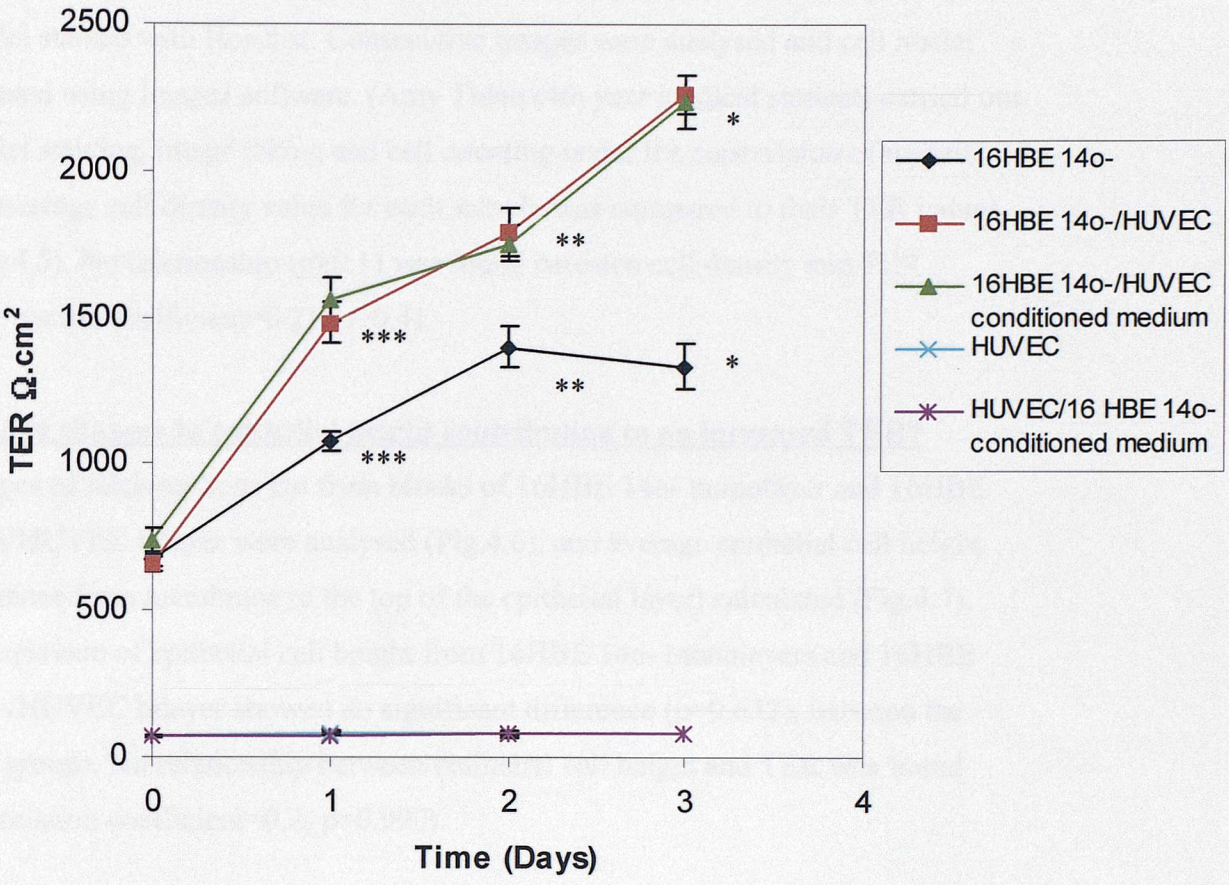

Fig. 4.4 Comparison of TER with time: 16HBE 14o- monolayer, 16HBE 14o-/HUVEC bilayer, 16HBE 14o- monolayer grown in HUVEC conditioned medium, and HUVEC monolayer grown in 16HBE 14o- conditioned medium. (n=8, * ** ***p<0.01).

4.5 Are changes in cell density contributing to an increased TER?

16HBE 14o- that had been grown on inserts as a monolayer, as a bilayer and in the presence of HUVEC conditioned medium, were fixed (after measuring TER) and nuclei stained with Hoechst. Consecutive images were analysed and cell nuclei counted using ImageJ software. (Amy Thien (4th year medical student) carried out nuclei staining, image taking and cell counting under the supervision of myself). An average cell density value for each sample was compared to their TER values (Fig.4.5). No relationship ($p>0.1$) was found between cell density and TER (correlation coefficient=0.21; $p=0.4$).

4.6 Are changes in epithelial height contributing to an increased TER?

Images of thick sections cut from blocks of 16HBE 14o- monolayer and 16HBE 14o-/HUVEC bilayer were analysed (Fig.4.6), and average epithelial cell height (distance from membrane to the top of the epithelial layer) calculated (Fig.4.7). Comparison of epithelial cell height from 16HBE 14o- monolayers and 16HBE 14o-/HUVEC bilayer showed no significant difference ($p=0.632$), between the two groups. No relationship between epithelial cell height and TER was found (correlation coefficient=0.2; $p=0.990$).

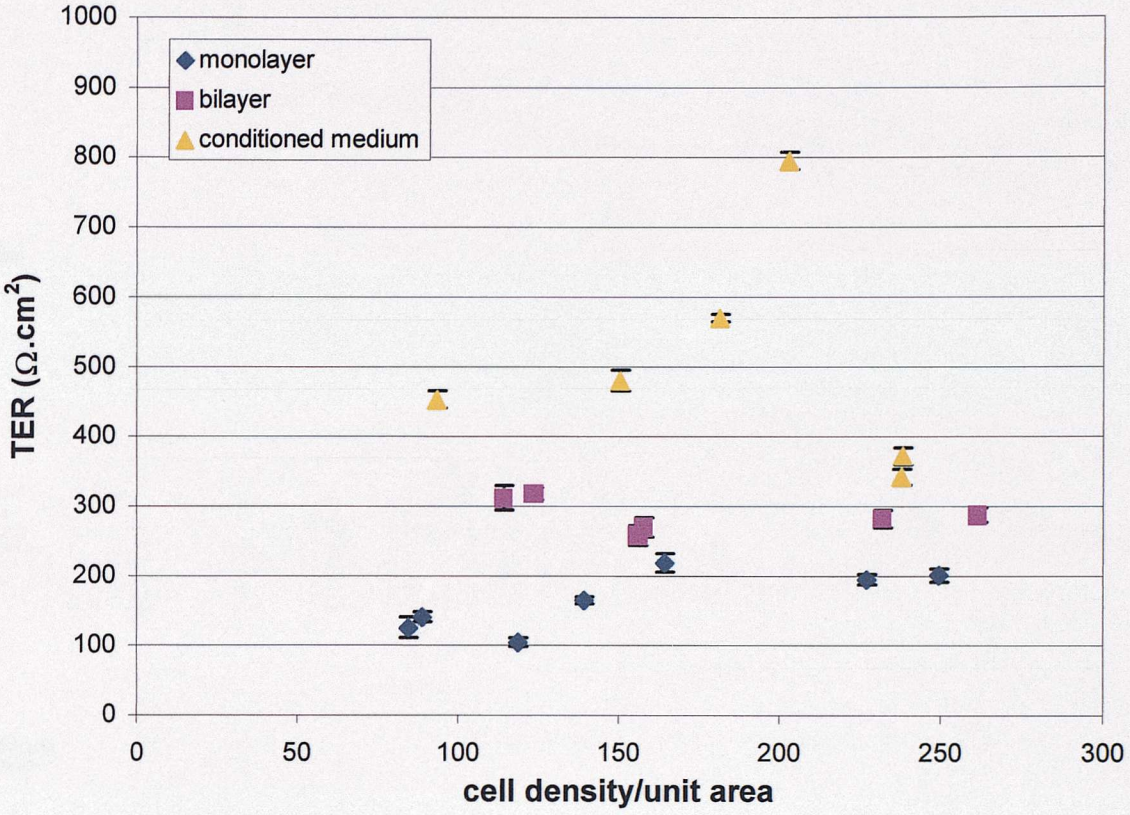

Fig.4.5 Comparison of TER and cell density show no correlation between the two values ie. an increase in TER does not relate to an increase in cell density (correlation coefficient=0.2; p=0.4).

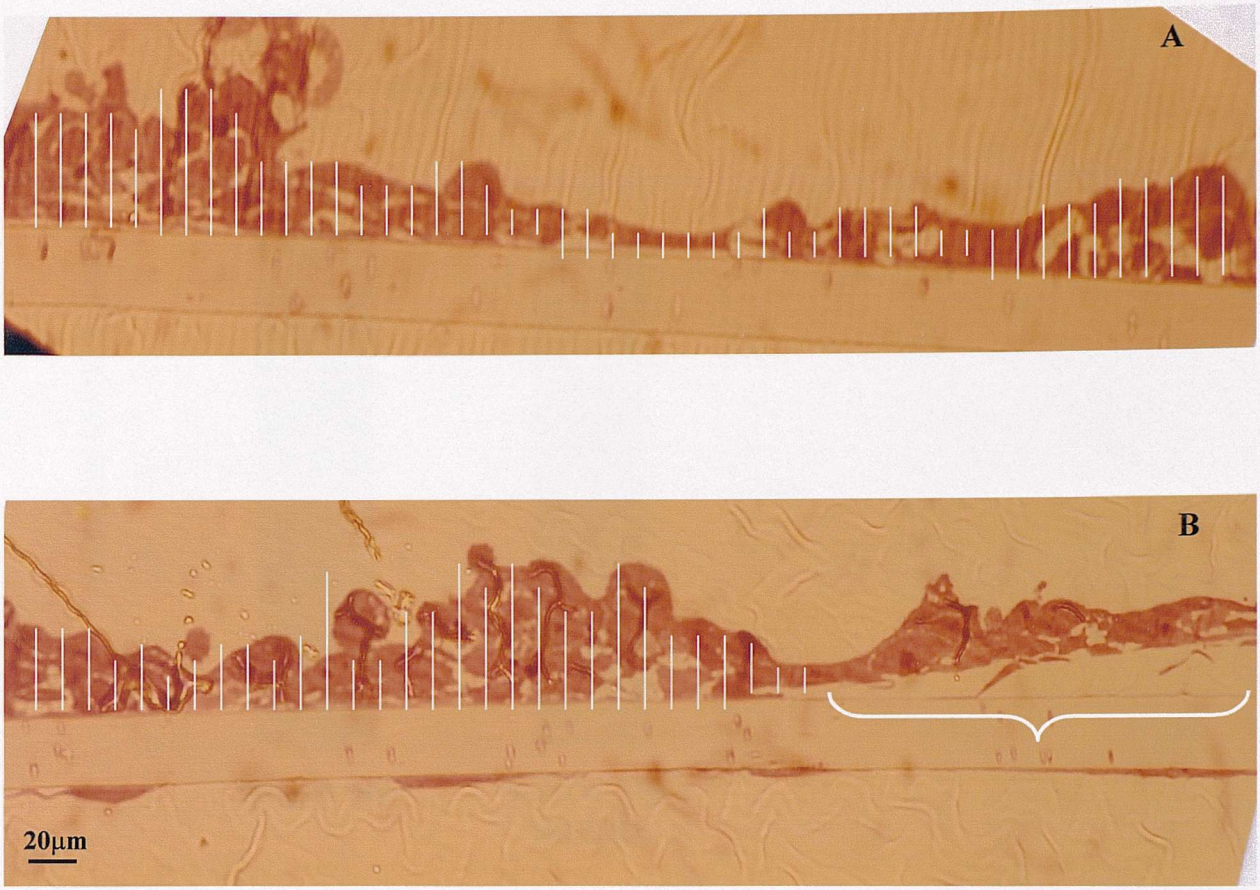

Fig.4.6 Images of thick sections from A) 16HBE 14o- monolayer and B) 16HBE 14o-/HUVEC on insert membrane. Epithelial cell height was measured at equal intervals (0.25cm) from the top of the insert membrane to the top of the epithelial cell (as shown by white lines). Areas of cell detachment from the membrane (as shown by white bracket) were not measured. Average epithelial cell height of images taken from two different blocks for each condition was calculated (Fig.4.7).

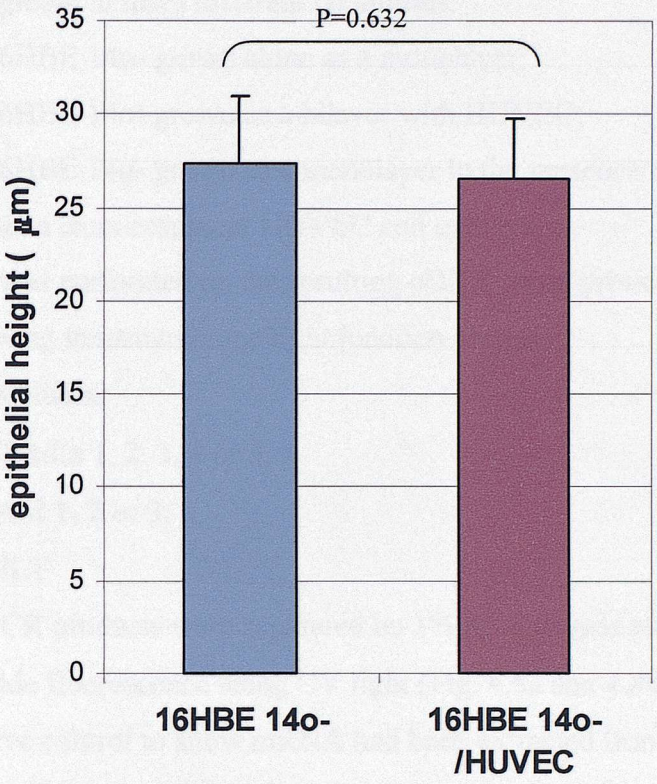

Fig.4.7 Comparison of epithelial cell height from 16HBE 14o- monolayers and 16HBE 14o-/HUVEC bilayer showed no significant difference between the two groups (p=0.632, n=45). No relationship between epithelial cell height and TER was found (correlation coefficient=0.2; p=0.990).

4.7 RT-PCR to identify tight junction protein mRNA expression

Reverse transcription was performed, using mRNA extracted from 16HBE 14o- cells grown in three different conditions:

1. 16HBE 14o- grown alone as a monolayer;
2. 16HBE 14o- grown as a bilayer with HUVEC;
3. 16HBE 14o- grown as a monolayer in the presence of conditioned medium taken from confluent HUVEC cell cultures.

PCR was performed on the resulting cDNA using primers designed to amplify the following transmembrane tight junction proteins:

- Occludin;
- Claudin 1, 2, 3, 4 or 5;
- JAM 1, 2 or 3;
- PILT

RT-PCR products were separated on 1% agarose gels and detected by ethidium bromide fluorescence using UV light (Fig. 4.8a and 4.8b). β-actin was used as a positive control to show mRNA had been extracted from all the samples with equal efficiency and that the RT-PCR had worked. The results show that gene expression could be detected for claudin-1, claudin-4, PILT, JAM-1, JAM-2 and occludin for all three 16HBE 14o- growth conditions, but not for claudin-2, claudin-3, claudin-5 or JAM-3.

RT-PCR was also performed on mRNA extracted from HUVEC, and it was found to express claudin-4, claudin-5, PILT, JAM-1, JAM-3 and occludin, but not claudin-1, claudin-2, claudin-3 or JAM-2 (fig. 4.8a and 4.8b).

To estimate the amount of mRNA present in relation to β-actin, the intensity of the bands were measured by densitometry using ImageJ software. The same size box to cover the area of each band was measured. Background intensity was measured using the same size box, as an area below each band and was subtracted from the band intensity to give a mean intensity value. The intensity value of the β-actin band was given 100 units, and the sample values calculated in relation to this (ie. sample value/β-actin value x 100).

Densitometry values showed insignificant differences in levels of mRNA expressed in the three 16HBE 14o- samples (ie. 16HBE 14o- monolayer, 16HBE 14o- from the bilayer and 16HBE 14o- grown in the presence of HUVEC

conditioned medium), except for occludin, which showed wider and more intense bands. Densitometry measurements showed that the density of the band for claudin-1 was greater in the bilayer, and for JAM-1 it was greater in the bilayer and condition medium treatments. However, the differences are not apparent visually, but the differences in occludin expression are visible, because the actual band size is wider as well as having a greater density. These results suggested that an increase in occludin expression was the major change occurring at the level of gene expression, which would now be investigated at the level of protein expression. These two conditions (bilayer and conditioned medium) also appear to produce a second mRNA species since a second band (approx.500bp) is detected just below the main band (approx.655bp). This second band is also detected in HUVEC mRNA, which has lower levels of the main product. The 16HBE 14o- monolayer however, only shows a faint band for this second product.
It should be noted however, that these PCR results are not quantitative and that the number of cell cycles used may have reached saturation levels. However, since the same cycle number was used for each transcript in different treatments, an increased signal for occludin and conditioned medium treatments, would be indicative of an increased mRNA level.

4.8 RT-PCR product sequence analysis

The cDNA of the PCR products were sequenced and analysed. The sequence was aligned with the relevant published sequence using the Blast program on the NCBI website (www.ncbi.nlm.nih.gov/), and a percentage match made. All the amplicons were found to have a 99-100% accuracy match with the published sequence confirming that the primers had amplified the correct product. The RT-PCR for occludin produced two amplicons (500 and 655bp). The larger amplicon matched the sequence for the published human occludin cDNA sequence (Fig.4.9). However, the smaller amplicon proved difficult to sequence, as there were technical difficulties in separating it from the larger product, and the resulting sequencing data was unclear. Since the larger product corresponded to the published occludin sequence, the smaller product is most likely to be a smaller isoform of occludin. To date, data on one such isoform, the TM4- has been published (Ghassemifar *et al.* 2002).

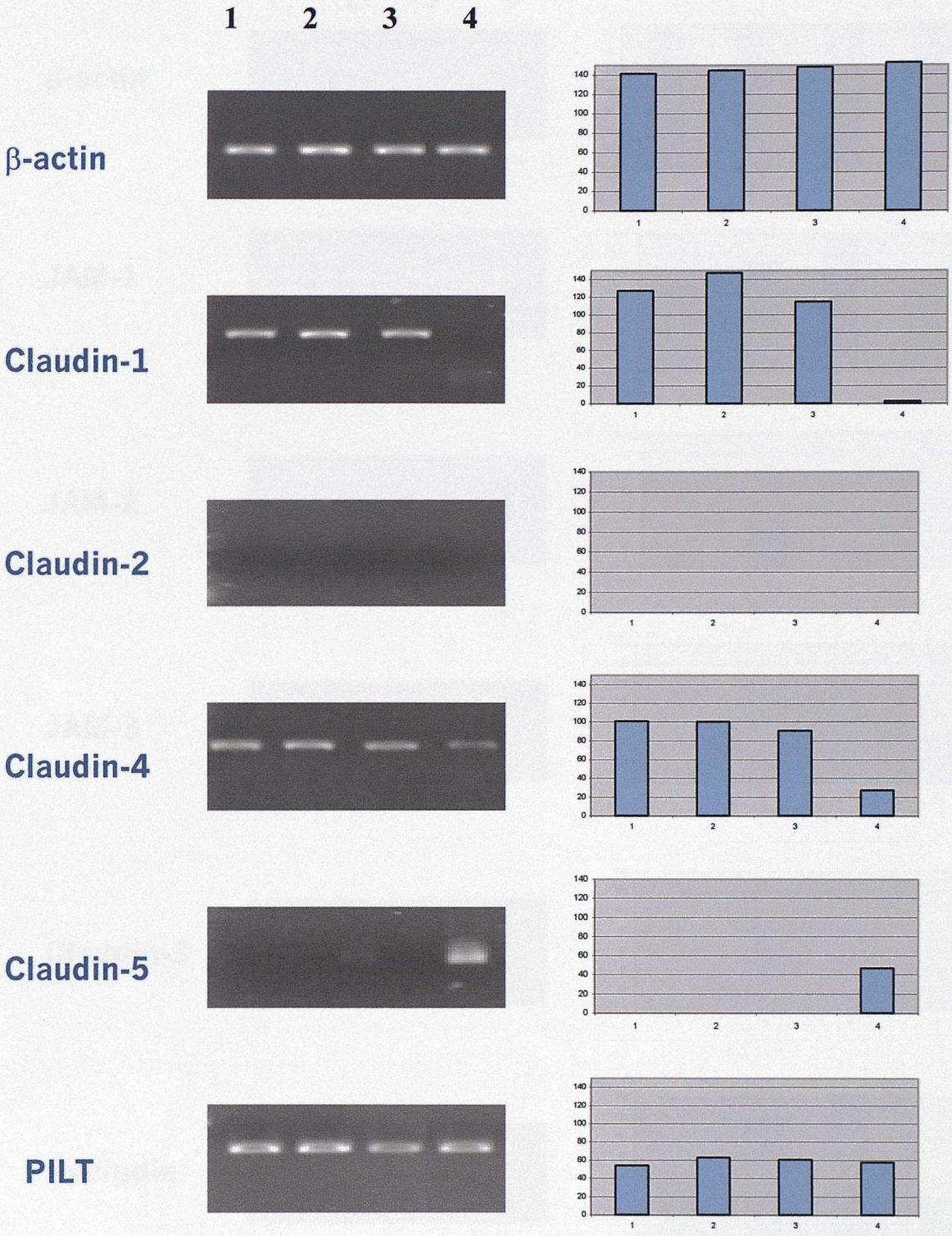

Fig. 4.8a RT-PCR performed on mRNA extracted from the following conditions:
1 = 16HBE 14o- grown as monolayer;
2 = 16HBE 14o- grown as bilayer with HUVEC;
3 = 16HBE 14o- grown in the presence of HUVEC supernatant;
4 = HUVEC grown as a monolayer.
Products were run on 1% agarose gels, stained with ethidium bromide and viewed by UV irradiation. Densitometry of bands shown as a percentage in comparison to β-actin (raw data normalised to 100%) shown in adjacent charts.

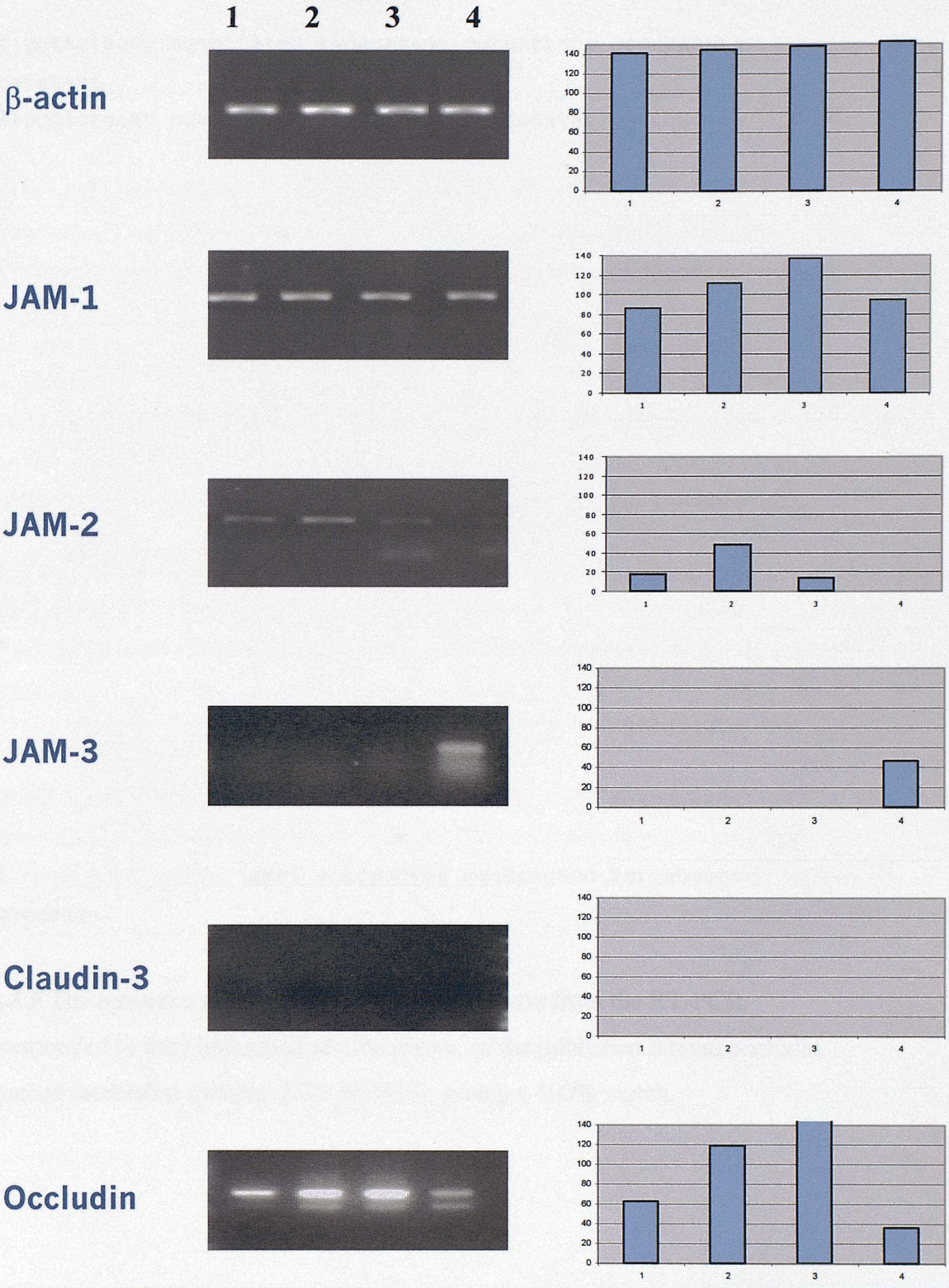

Fig. 4.8b RT-PCR performed on mRNA extracted from the following conditions:
1 = 16HBE 14o- grown as monolayer;
2 = 16HBE 14o- grown as bilayer with HUVEC;
3 = 16HBE 14o- grown in the presence of HUVEC supernatant;
4 = HUVEC grown as a monolayer.
Products were run on 1% agarose gels, stained with ethidium bromide and viewed by UV irradiation. Densitometry of bands as a percentage in comparison to β-actin (raw data normalised to 100%) shown in adjacent charts.

961 gataatagtg agtgctatcc tgggcatcat ggtgtttatt gccacaattg
tctatataat
1021gggagtgaac ccaactgctc agtcttctgg atctctatat ggttcacaaa
tatatgccct
1081ctgcaaccaa ttttatacac ctgcagctac tggactctac gtggatcagt
atttgtatca
1141ctactgtgtt gtggatcccc aggaggccat tgccattgta ctggggttca
tgattattgt
1201ggcttttgct ttaataattt tctttgctgt gaaaactcga agaaagatgg
acaggtatga
1261caagtccaat attttgtggg acaaggaaca catttatgat gagcagcccc
ccaatgtcga
1321ggagtgggtt aaaaatgtgt ctgcaggcac acaggacgtg ccttcacccc
catctgacta
1381tgtggaaaga gttgacagtc ccatggcata ctcttccaat ggcaaagtga
atgacaagcg
1441gttttatcca gagtcttcct ataaatccac gccggttcct gaagtggttc
aggagcttcc
1501attaacttcg cctgtggatg acttcaggca gcctcgttac agcagcggtg
gtaactttga
1561gacaccttca aaaagagcac ctgcaaaggg aagagcagga aggtcaaaga
gaacagagca
1621agatcactat gagacagact acacaactgg cggcgagtcc tgtgatgagc
tggaggagga

Fig.4.9 The sequence for the larger occludin amplicon from the RT-PCR corresponded to the highlighted section above, of the published human occludin sequence (accession number: NM_002538), giving a 100% match.

4.9 Tight junction protein- occludin expression

The RT-PCR results give information at the level of mRNA expression but may not be translated to the level of protein expression. Since there was an increase in occludin mRNA in the RT-PCR results, the possibility of increased protein expression was explored using western blotting and immunofluorescent labeling. Whole cell protein was extracted from 16HBE 14o- cells grown as a monolayer, bilayer or in the presence of conditioned medium (see 2.11.1). After SDS-PAGE, and semi-dry western blotting, the nitrocellulose membrane was incubated with the relevant antibodies and bands detected with the Bio-rad Opti-4CN detection kit.

Western blotting was performed using diluted amounts of protein (1, 0.75, 0.5, 0.25μg), to ensure the level of protein was not saturated, since any amount of protein above this saturated level would give the same result and so any differences would not be detected. The immunoblots showed that lowering protein concentration resulted in weaker band density (Fig. 4.10). It also shows that the detection level was not saturated, and is a linear response.

The density of bands for the 1μg dilution of total protein for the 16HBE 14o- bilayer and for the 16HBE 14o- grown in conditioned medium were compared with the corresponding band for the monolayer (fig.4.11). The band density for the 16HBE 14o- bilayer and 16HBE 14o- grown in conditioned medium was greater, suggesting there was an increase in total occludin expression. However, the results reflect the total amount of occludin expressed in the cells and will not reflect changes in expression of different isoforms. The results will also not give an indication of occludin distribution, which would be investigated using immunofluorescent staining.

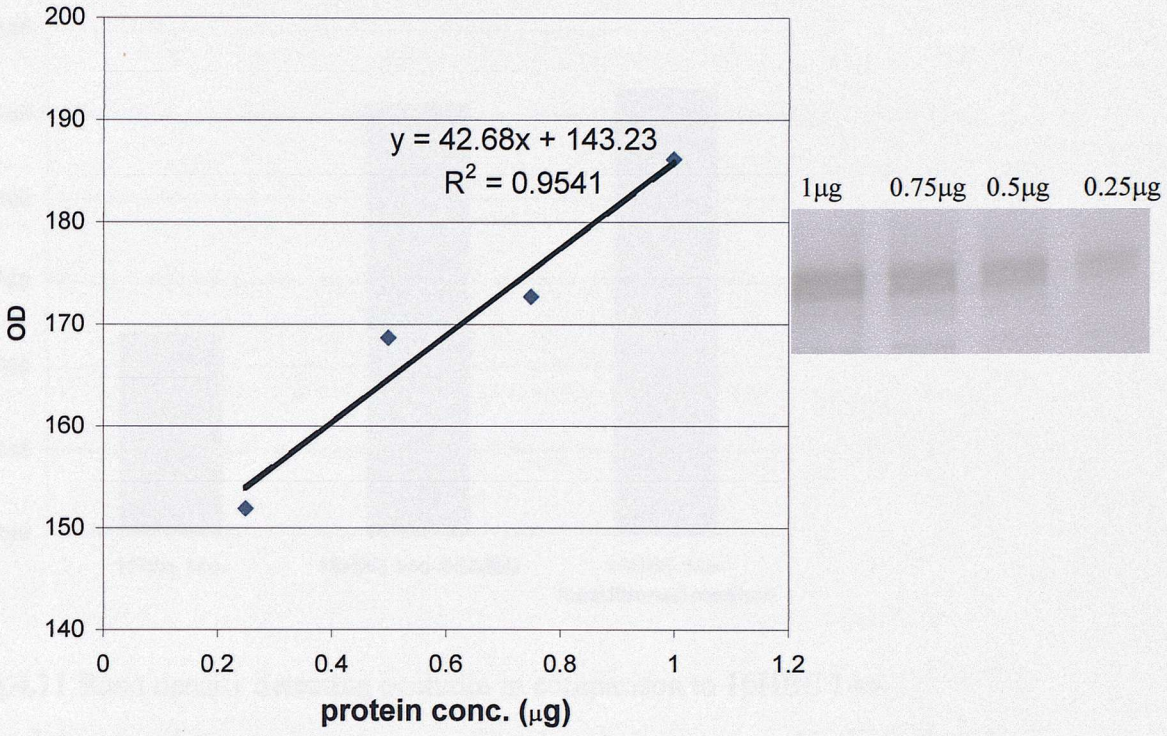

Fig.4.10 Titrated levels of protein from 16HBE 14o- sample showed corresponding sized bands on western blot, resulting in a near linear graph.

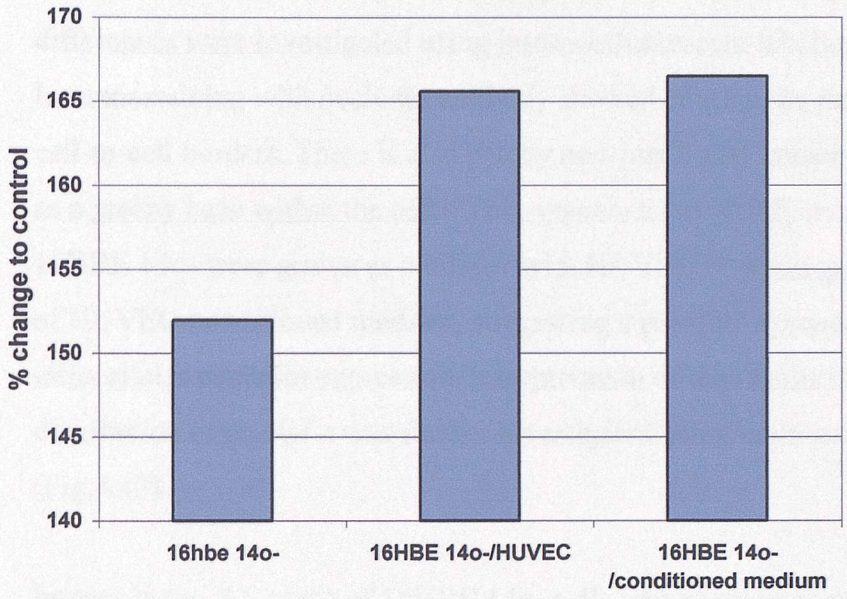

Fig.4.11 Band density detecting occludin in comparison to 16HBE 14o- monolayer, suggests a greater amount of total occludin expressed in 1μg of total protein in 16HBE 14o- grown as a bilayer or in the presence of conditioned medium (Single measurements of band density from one immunoblot representative of 3 immunoblots).

4.10 Distribution of occludin: using immunofluorescent labeling

The results from western blotting will not distinguish possible differences in the distribution of occludin since total cell protein was extracted (see 2.11.1), and such differences were investigated using immunofluorescent labeling (Fig. 4.12). Immunostaining with occludin antibody showed continuous ring-like staining at cell-to-cell borders. There is also patchy non-junctional intracellular staining, seen as a greeny haze within the cells. This appears to be visibly more intense when 16HBE 14o- were grown as a bilayer with HUVEC or when grown in the presence of HUVEC-conditioned medium, suggesting a possible upregulation in intracellular occludin expression. Interpretation of the results is subjective and distribution of occludin was further investigated using confocal microscopy (Fig.4.13).

Images in the XY plane of 16HBE 14o- cells immunostained with occludin antibody were taken in the apical to basolateral direction. Staining was stronger at the apical side of the cells where ring-like staining was visible at cell-to-cell borders (arrows in images). Comparison of 16HBE 14o- cells grown as a monolayer, bilayer and with conditioned medium showed no visible difference in their staining patterns or in the intensity of the ring-staining. The cells appear to have stained in different sections because the membrane the cells are sitting on has become detached and is not sitting flat on the slide, resulting in uneven cell layers. Therefore, a single image of the maximum intensity of the combined XY slices for each sample was used to compare possible differences (fig.4.14).

The maximum intensity images for 16HBE 14o- grown as a monolayer, bilayer and in conditioned medium, show no visible variability in occludin labelling (fig.4.14). It has proved difficult to measure the intensity and extent of staining, and conclusions have been made on what was visible. Uneven staining occurs within each sample, such that some cells are positively labelled whereas others are negative. Cells also show differences in occludin distribution; having either intracellular staining, ring staining at cell-to-cell borders, or both.

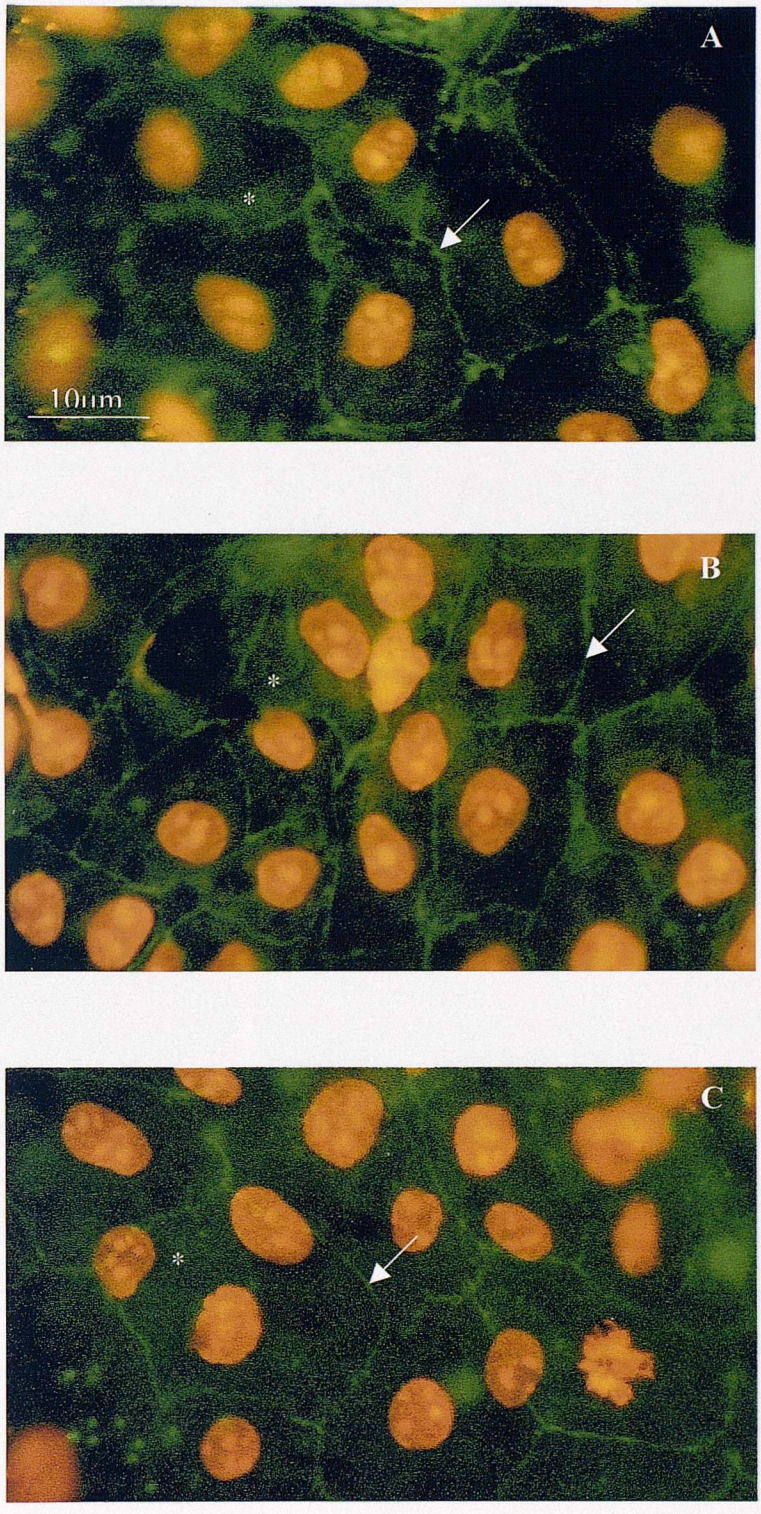

Fig. 4.12 Immunostaining with occludin primary antibody and FITC conjugated secondary antibody. Comparison of 16HBE 14o- monolayer (A); 16HBE 14o- from bilayer (B); 16HBE 14o- grown in HUVEC-conditioned medium (C). Arrows show continuous ring-like staining at cell-to-cell borders. * Areas of intracellular staining.

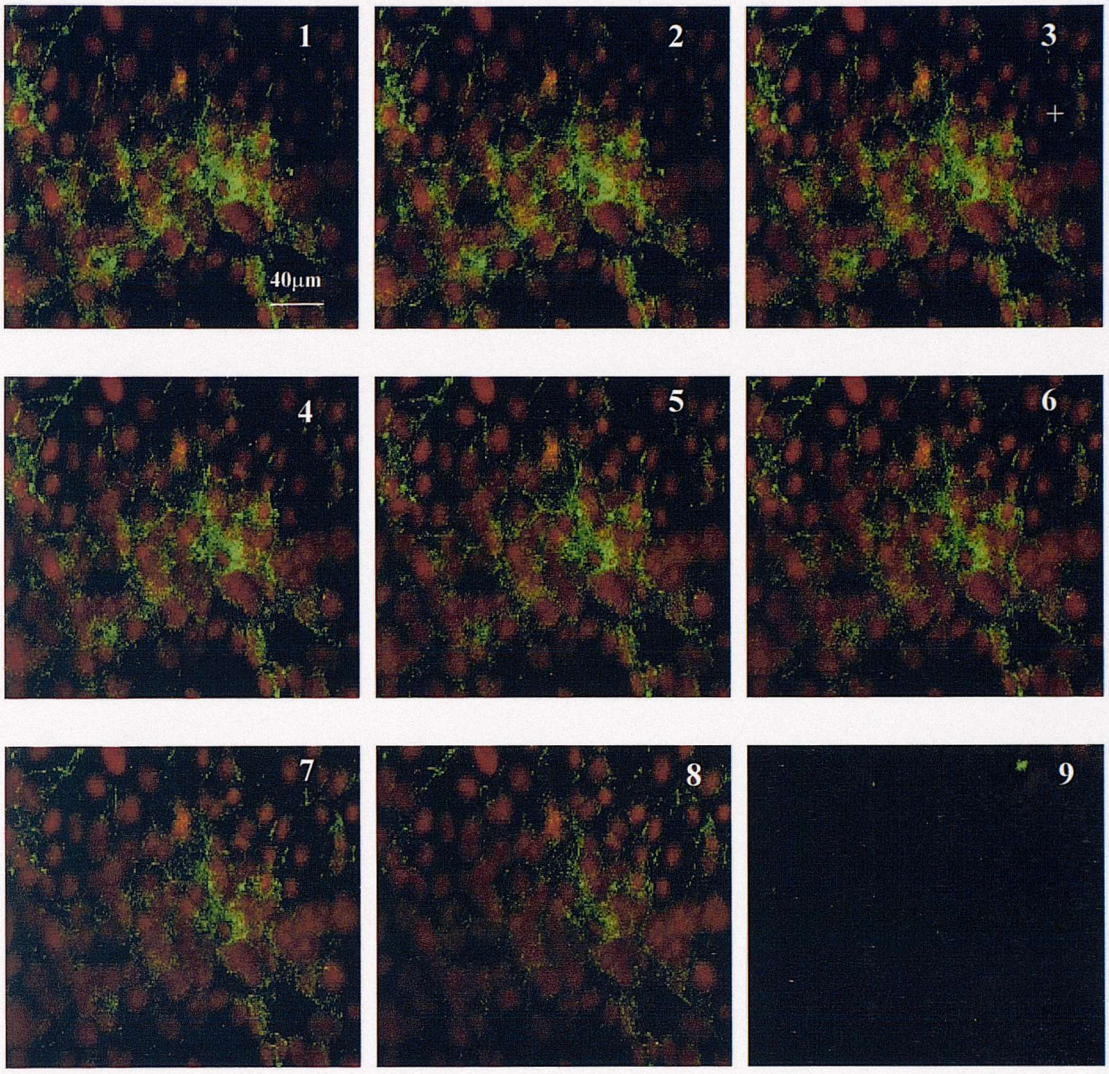

Fig.4.13A XY slices of 16HBE 14o- monolayer labelled with occludin primary antibody and FITC conjugated secondary antibody (green). Nuclei were counterstained with propidium iodide (red).

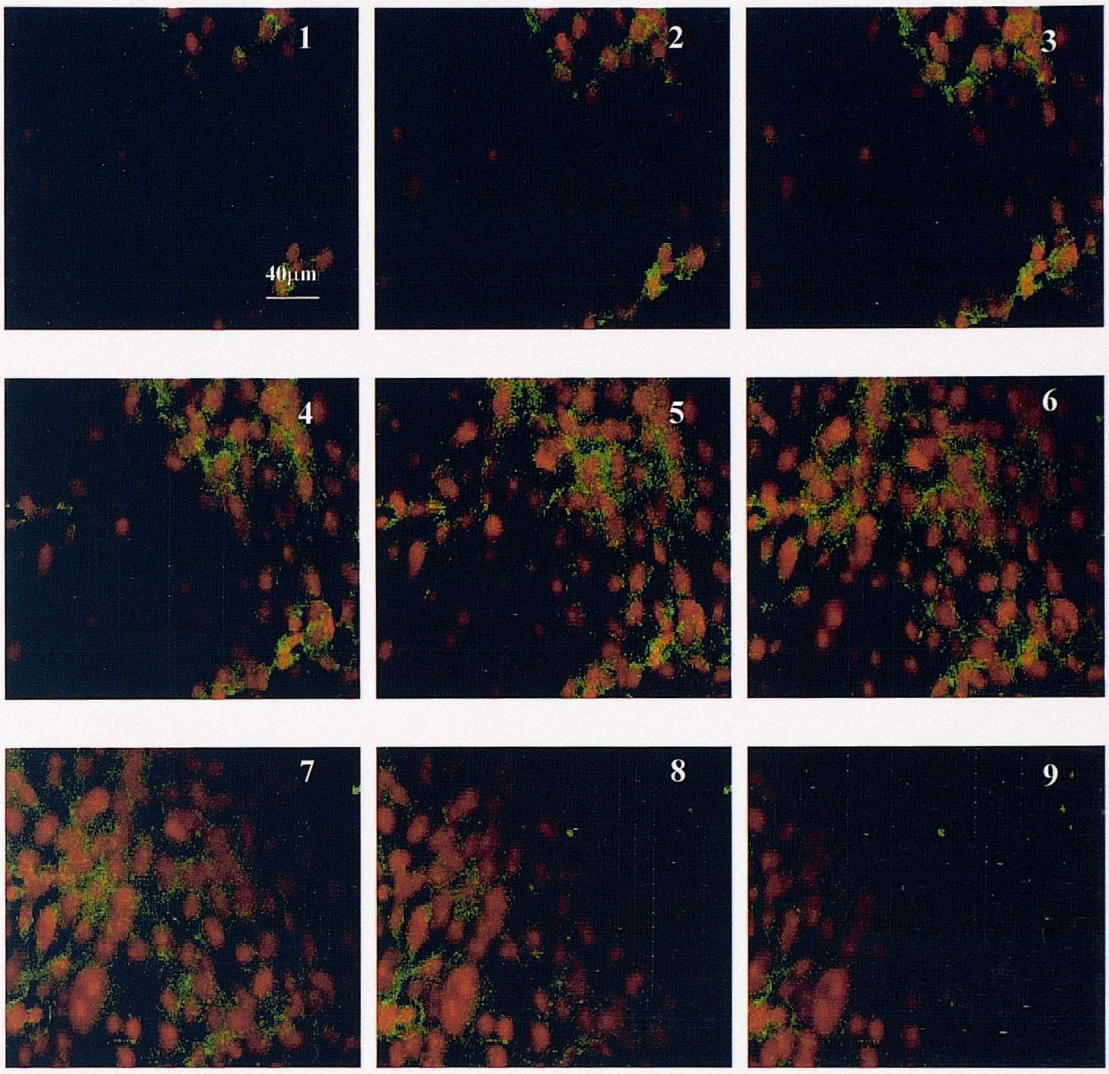

Fig.4.13B XY slices of 16HBE 14o- (grown as a bilayer with HUVEC), labelled with occludin primary antibody and FITC conjugated secondary antibody (green). Nuclei were counterstained with propidium iodide (red).

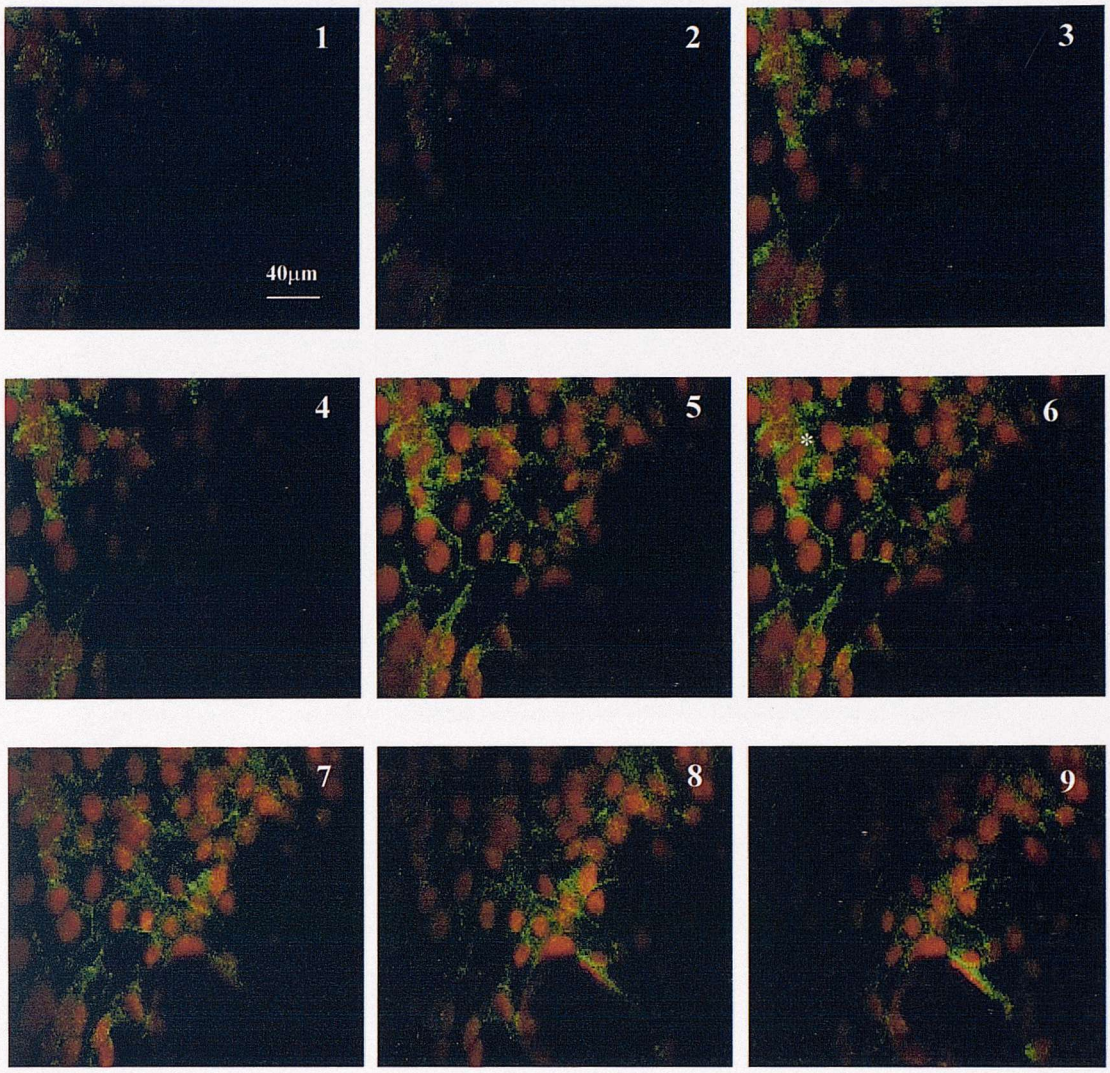

Fig.4.13C XY slices of 16HBE 14o- (grown in the presence of HUVEC-conditioned medium), labelled with occludin primary antibody and FITC conjugated secondary antibody (green). Nuclei were counterstained with propidium iodide (red).

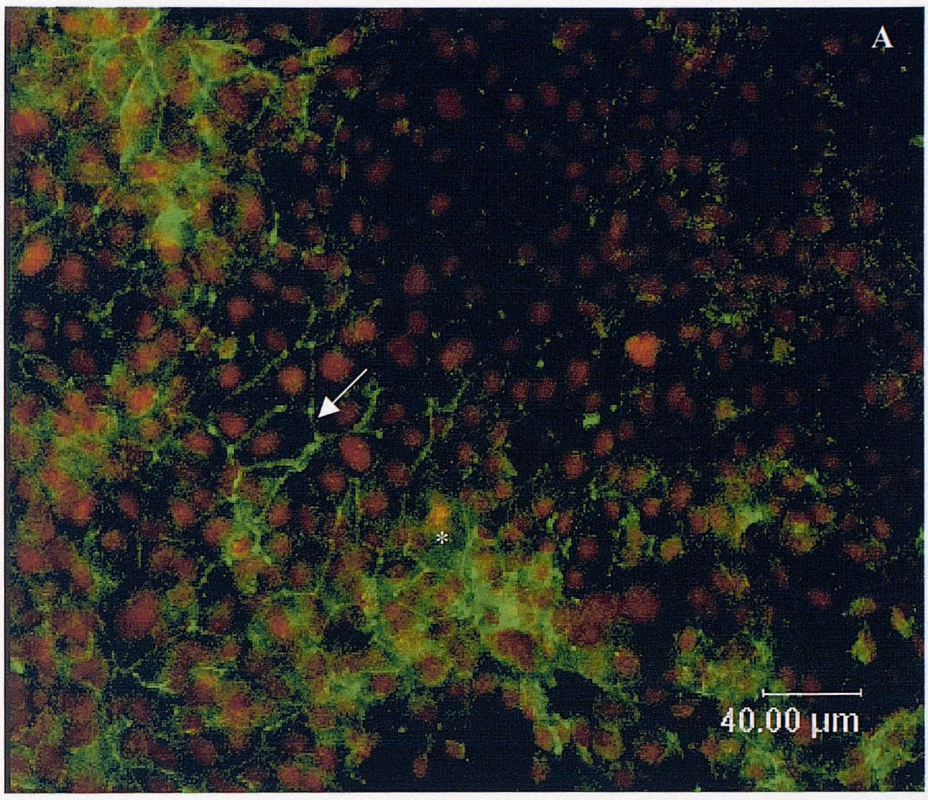

Fig. 4.14A Image showing maximum intensity of combined XY confocal slices in 4.13A, of 16HBE 14o- monolayer labelled with occludin primary antibody and FITC conjugated secondary antibody (green). Nuclei were counterstained with propidium iodide (red). Arrow indicates ring-like staining, * indicates intracellular staining.

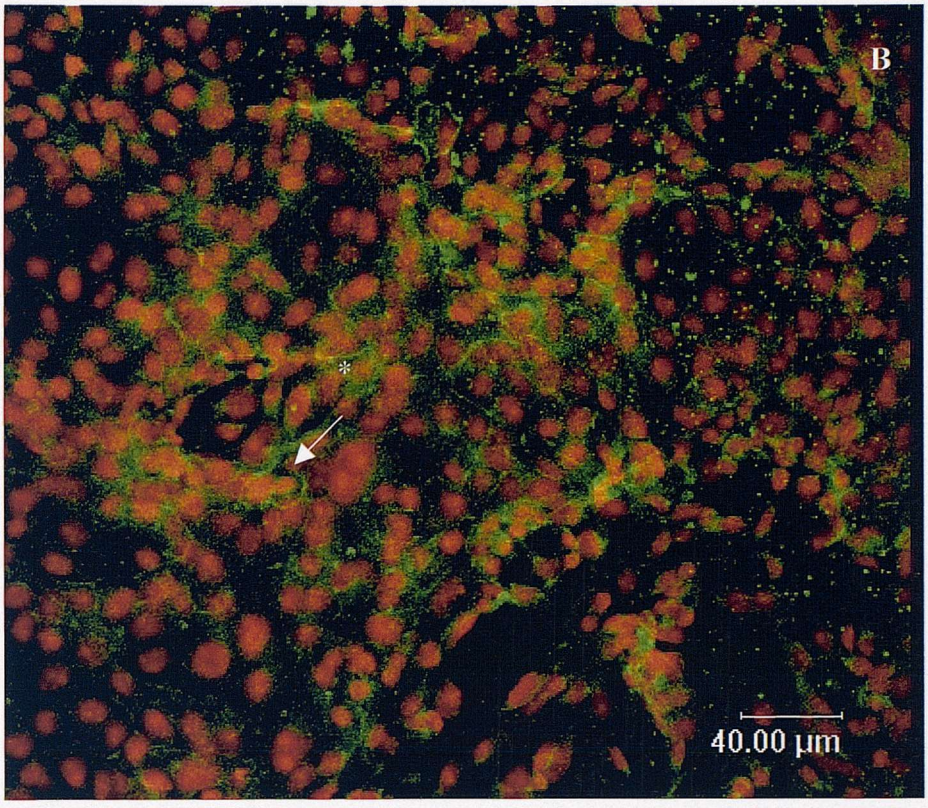

Fig. 4.14B Image showing maximum intensity of combined XY confocal slices in 4.13B, of 16HBE 14o- grown as a bilayer with HUVEC labelled with occludin primary antibody and FITC conjugated secondary antibody (green). Nuclei were counterstained with propidium iodide (red). Arrow indicates ring-like staining, * indicates intracellular staining.

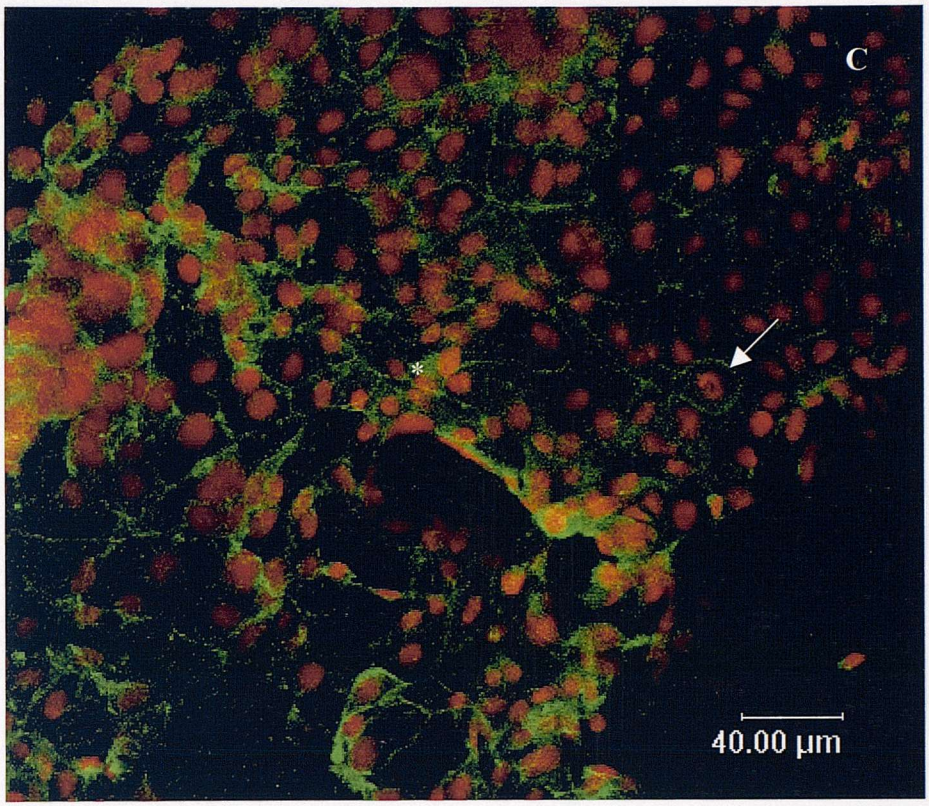

Fig. 4.14C Image showing maximum intensity of combined XY confocal slices in 4.13C, of 16HBE 14o- grown in HUVEC conditioned medium, labelled with occludin primary antibody and FITC conjugated secondary antibody (green). Nuclei were counterstained with propidium iodide (red). Arrow indicates ring-like staining, * indicates intracellular staining.

4.11 Discussion: what is changing to cause an increase in epithelial TER?

The bilayer model consisting of epithelial and endothelial cells grown in close proximity, reflecting the normal configuration in bronchial tissue, has shown that cell-to-cell interaction occurs. This interaction causes an increased TER in epithelial cells, induced by a diffusible mediator produced by the endothelial cells. This was shown by growing 16HBE 14o- cells in the presence of HUVEC conditioned medium, which resulted in the same increase in TER as that seen in the bilayer (4.4). There was no change in endothelial TER when grown in the presence of 16HBE 14o- conditioned medium.

There were various possibilities as to why TER was increasing. Firstly, a change in cell growth and proliferation may be induced, which would result in more tight junctions per unit area, or multi-layers of cells each layer forming tight junctions resulting in a combined series of resistance. Measuring cell density and cell layers of 16HBE 14o- grown as a monolayer, a bilayer or in HUVEC-conditioned medium would detect any such changes. There was found to be no significant difference in epithelial cell density or cell height between the three treatments, hence ruling out the possibility of changes in cell growth (4.5; 4.6). An increase in TER did however, correlate to a decrease in FITC-dextran permeability (4.3). It could be concluded that the increase in TER was not representing an increase in cell numbers or cell layers, but was related to a change in permeability, suggesting a change in the tight junctions.

The conditioned medium may be producing a change at the epithelial tight junction via different signaling molecules and signaling pathways, but the final outcome is most likely to be a change in the expression, phosphorylation or organisation of transmembrane proteins at the tight junction, as these compose the cell-to-cell contacts. Studies already show that expression of different transmembrane proteins result in different tight junction properties as will be discussed below. Possible changes at the level of tight junction proteins were therefore investigated.

Firstly, different structural domains of occludin, the first transmembrane tight junction protein identified, are thought to contribute different regulatory functions, for example the first extracellular loop is thought to mediate cell-to-cell adhesion and the second extracellular domain to control paracellular permeability (Lacaz-Vieira *et al.* 1999). The COOH-terminal may also have a role in regulating

permeability, since expression of a truncated COOH-terminal results in increased permeability (Chen *et al.* 1997), and occludin lacking the cytoplasmic amino terminal and both extracellular loops was also found to enhance permeability of markers and decrease TER, suggesting a relationship between TER and permeability (Bamforth *et al.* 1999). Furthermore, overexpression of occludin leads to an increase in transepithelial electrical resistance in MDCK cells, indicating a direct correlation between expression of occludin and electrical resistance (McCarthy *et al.* 1996). All these studies show a relationship between increasing permeability and decreasing TER, and emphasize the importance of occludin in regulating barrier function. Since the results in this thesis not only shows increasing TER in 16HBE 14o- cells but also suggests a correlation between increasing TER and decreasing permeability (4.3), occludin was a potential candidate in which changes could be contributing to the increase seen in the bilayer model.

The RT-PCR results from my studies show increased levels of occludin gene expression (655bp product) when the 16HBE 14o- epithelial cells are grown either as a bilayer with HUVEC or in the presence of HUVEC supernatant. Interestingly, a second smaller product (500bp) is also detected in my RT-PCR using occludin primers, which may be due to a variant of the occludin gene. Alternative splicing can lead to the production of occludin isoforms. Alternative spliced variants already discovered include occludin 1B in MDCK cells (Muresan *et al.* 2000), and more recently the TM4- isoform in which there is a deletion at the fourth transmembrane domain (Ghassemifar *et al.* 2002), and is shown to be present in various cells including 16HBE 14o- cells. The TM4- isoform was found to be 162bp smaller than the main occludin product. Sequencing of PCR amplicons in my study, show the larger occludin product to be that of the complete occludin mRNA gene (100% match) (4.9), but the lower product appears to be of a similar size to that of the TM4- isoform, although this could not be confirmed by sequencing as problems arose in isolating this product. However, there is no detectable level of this second product when the 16HBE 14o- cells are grown as a monolayer (4.8). It may be argued that since levels of the main occludin product are lower in the monolayer sample, the smaller isoform product may be expressed at lower levels and may therefore be difficult to detect. However, this is unlikely, since the HUVEC sample expresses even lower levels of the main occludin

product, but the smaller isoform is still detectable. The TM4- isoform has an altered structure, such that the cytoplasmic COOH-terminal is no longer extracellular but intracellular. Since, the COOH-terminal has been shown to be important in regulating paracellular permeability, it is thought that this regulation is no longer performed in the TM4- isoform, which would lead to increased permeability and tight junction integrity diminished. If this is the case, then our results are contradictory, showing 16HBE 14o- cells exhibiting higher TER and hence enhanced tight junction integrity, are also expressing this negative isoform. Occludin is not always necessary for tight junction formation, since disrupting the occluding gene still results in tight junction formation (Saitou *et al.* 1998). For this reason other tight junctions already shown to influence tight junction were investigated, to determine any possible contribution to the increased TER seen in the bilayer and conditioned medium treatments.

The two other families of transmembrane proteins found at the tight junction are the claudin family and JAM family of proteins, which seem to play a role in determining the extent of tight junction formation. Firstly, JAM-1, expressed in both epithelial and endothelial cells, colocalises with occludin and plays a role in paracellular permeability (Martin-Padura *et al.* 1998). The roles of JAM-2 and JAM-3 are less clear, but JAM-2 is thought to be important in forming cell-to-cell junctions in HEV's and lymphatic endothelial cells (Aurrand-Lions *et al.* 2000), and JAM-3 is found in most vascular endothelial cells and is thought to have a role in transendothelial leukocyte migration (Cunningham *et al.* 2000). These studies suggest JAM molecules are more important in endothelial cells rather than epithelial cells, and my RT-PCR results showed no differences in the mRNA level of JAM molecules in 16HBE 14o- cells grown in the three treatments. Therefore, it is perhaps more likely that the TER differences seen in the 16HBE 14o- cells are due to changes in the claudin molecules.

Claudins, a relatively newly described family with new members still being identified, copolymerise with occludin to form the backbone of the tight junctions (Furuse *et al.*1999). Different claudins are expressed in different tissues but claudins 1-5 have all been shown to be present in lung epithelium (Heiskala *et al.* 2001), hence these were investigated. In particular, upregulation of claudin-1 may be causing an increase in TER of 16HBE 14o- cells grown as a bilayer or with HUVEC conditioned medium, since over expression of claudin-1 in MDCK cells

leads to increased TER (Inai *et al.* 1999). On the otherhand, claudin-2 forms discontinuous tight junction strands (Furuse *et al.* 1998), leading to a reduced barrier integrity, so a downregulation of claudin-2 would result in enhanced barrier integrity and may be the cause of increased TER seen in 16HBE 14o- grown as a bilayer or in HUVEC conditioned medium.

However, RT-PCR results were unable to detect a difference between the three different 16HBE 14o- conditions, in mRNA expression for claudin-1, 2,3,4 and 5 (4.7).

One other novel tight junction protein that may be causing an increase in TER in cells that already have tight junctions, (such as the 16HBE 14o- cells in my study) is PILT, since this protein has been shown to be incorporated into tight junctions after tight junction strands have formed (Kawabe *et al.* 2001). However, RT-PCR showed no difference in the amount of PILT expression between the three 16HBE 14o- treatments.

There may be differences in the mRNA expression of other tight junction proteins, but based on my current results, there is no difference except in occludin mRNA expression; this then raises the question as to whether differences lie in the actual protein expression, activation or distribution of these tight junction proteins.

Western blotting was performed to determine whether the increase in occludin mRNA seen in 16HBE 14o- grown as a bilayer and in HUVEC conditioned medium was translated at the level of protein expression. Western blotting revealed some increase in the level of total occludin protein expression in 16HBE 14o- grown as a bilayer and conditioned medium (4.9). However, the antibody used for western blotting does not distinguish between the different isoforms (as only one antibody is available that recognizes all forms of occludin), and provides no information on distribution. Nevertheless, the results still indicate some increase in the level of occludin protein expression, which may be the cause of the increased TER seen in the bilayer and conditioned medium situations.

The distribution of the occludin was investigated using immunofluorescent confocal microscopy. Immunofluorescent labeling of 16HBE 14o- grown in the three treatments (as a monolayer, bilayer with HUVEC, or in HUVEC conditioned medium) with occludin antibody, have shown three staining patterns- ring-like staining at cell-to-cell borders, intracellular (cytoplasmic) staining, or negative staining. Areas of negative staining in all three 16HBE 14o- treatments, suggests

not all the cells have formed tight junctions. Increases in cytoplasmic staining may indicate upregulation of occludin production, and increases in ring-like staining may indicate more occludin forming tight junctions, however, it has proved to be difficult to analyse and measure the intensity of immunofluorescent staining. Cell-to-cell border and cytoplasmic staining may be reflecting occludin with different levels of phosphorylation. Studies with epithelial cells suggest an increase in occludin phosphorylation is related to an increase in tight junction assembly, as highly phosphorylated occludin is found to be concentrated at TJs but less phosphorylated occludin is found in the cytoplasm (Andreeva *et al.* 2001). This suggests the level of phosphorylation determines the location of occludin, and may be important in tight junction assembly. Even though the level of phosphorylation has not been studied here, the immunostaining with occludin shows occludin is present at both the cell-to-cell borders as well as in the cytoplasm, which may be due to different levels of occludin phosphorylation. Upregulation of occludin and changes in distribution such that more is concentrated at the cell-to-cell borders would account for an increased TER, which in turn would reflect better tight junction formation. However, my western blotting and immunofluorescent results do not distinguish between the different isoforms, and changes occurring at the level of mRNA of different isoforms, may be translated at the level of protein, which may contribute to changes in tight junction function. Another possibility is an increase in the actual number of tight junction strands being formed per cell, which could be investigated using freeze fracture techniques. There may also be changes in the phosphorylation state of tight junction proteins. Differences, not only in occludin expression but also in the expression of other tight junction proteins, in particular the claudins need to be further investigated.

CHAPTER 5

ENDOTHELIAL EFFECTS ON EPITHELIAL CELLS:

What is mediating the increase in TER?

Chapter 5: Endothelial effects on epithelial cells: What is mediating the increase in TER?

5.1 Introduction

The bilayer model established has shown that 16HBE 14o- grown as a bilayer with HUVEC has different functional properties to 16HBE 14o- grown as a monolayer. In particular, when 16HBE 14o- cells are grown with HUVEC an increase in TER is seen, reflecting a change in barrier function. The question that arises is 'what is mediating the increase in TER' which was addressed by growing the 16HBE 14o- cells in the presence of medium taken from confluent HUVEC cell cultures, which had been sterile-filtered through a 0.2μm filter. Results showed that this HUVEC conditioned medium induced the same TER increase in 16HBE 14o- cells as that seen in the bilayer (Fig.4.3). It was therefore concluded that a soluble endothelial factor was mediating this increase. The next step was to investigate this factor and perform a preliminary characterisation. This increase was attributed to a soluble factor secreted by the HUVEC cells, since 16HBE 14o- cells grown in HUVEC-conditioned medium replicated the same increase in TER as that seen in the bilayer.

Firstly, TER was measured over 24 hours to determine how soon after addition of conditioned medium, the factor was producing an effect. The results in the previous chapter (4.4), clearly show that the medium was acting via a pathway present on the basolateral cell surface, but it was important to determine whether the medium had the same effect when added to the apical side of the epithelial cells.

The factor in the medium is a soluble mediator being produced by the endothelial cells, but that does not necessarily imply that it is a protein or peptide, it may for example, be an ion such as Ca2+ which is implicated in the formation of tight junctions, since increasing the concentration of extracellular Ca2+ leads to the formation of well-formed tight junctions in MDCK cells (Nigam *et al.* 1992), or it may be a lipid mediated effect, for example cholesterol is required to maintain the TER of MDCK cells suggesting tight junction structure is susceptible to changes in the lipids of the cell environment (Francis *et al.* 1999).

To determine whether the factor was a heat-labile protein, the medium was heat-inactivated to see if the increase in TER was inhibited. If not, then this would indicate a heat-resistant factor, such as a small peptide or ion. Other possibilities that may be mediating this effect are growth factors or proteases.

In particular, it has been shown that treating MDCK cells with epidermal growth factor (EGF) causes phosphorylation of the epidermal growth factor receptor resulting in an increase in TER (Singh and Harris, 2003). Therefore, an EGF-receptor activating ligand is a possible candidate mediating the increase seen when 16HBE 14o- cells are treated with HUVEC conditioned medium. To investigate this HUVEC-conditioned medium was treated with an antibody against the EGF receptor, which selectively inhibits tyrosine kinase phosphorylation.

Proteases are also a potential mediator of the increase in TER, for example studies show that treating the basolateral side of MDCK cells with trypsin resulted in an increase in TER, which was reversed by the addition of trypsin inhibitor (Lynch *et al.* 1995). Therefore, the HUVEC-conditioned medium was treated with protease inhibitors to try and reverse the increase in TER seen when 16HBE 14o- cells are treated with this medium.

5.2 Is the change in TER of the bilayer an immediate effect?

The TER of 16HBE 14o- grown as a bilayer and as a monolayer was measured after 1,4,6 and 24 hours after addition of HUVEC (Fig.5.1).

Initially (1-4 hours after HUVEC/conditioned medium added) there was no significant difference in TER values between the groups ($p=1.00$). After 6 hours the TER of the bilayer ($p=0.0037$) and the conditioned medium ($p=0.0014$) was significantly higher than the monolayer. This shows that endothelial cells require at least 6 hours before exerting a significant effect on epithelial cells, and this effect is further enhanced after 24 hours (At 24 hours TER still significantly higher, $p=0.0024$ for bilayer, and $p=0.0009$ for conditioned medium in comparison to monolayer).

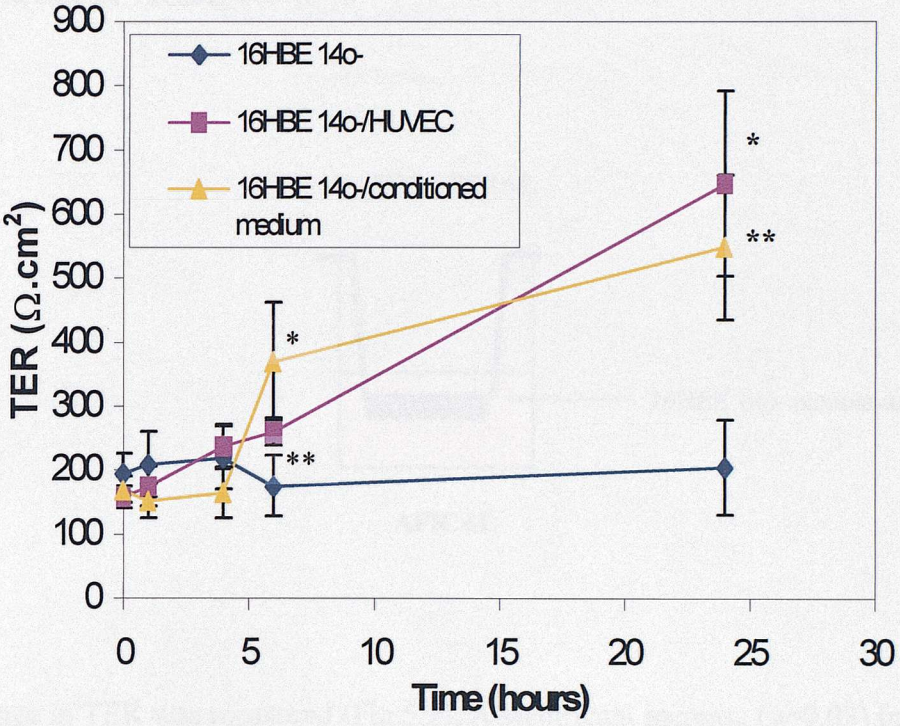

Fig.5.1 Comparison of TER: 16HBE 14o-, 16HBE 14o-/HUVEC and 16HBE 14o-/conditioned medium, at 1, 4, 6 and 24 hours after addition of HUVEC and conditioned medium. (*$p<0.05$; **$p<0.01$; n=8)

5.3 Endothelial conditioned medium acts from the basolateral direction.

16HBE 14o- cells were grown as a monolayer on the underside of inserts. Once confluent, sterile filtered HUVEC-conditioned medium was added to either the inside of the insert (basolateral side of 16HBE 14o-), or to the well of the plate (apical side of 16HBE 14o-).

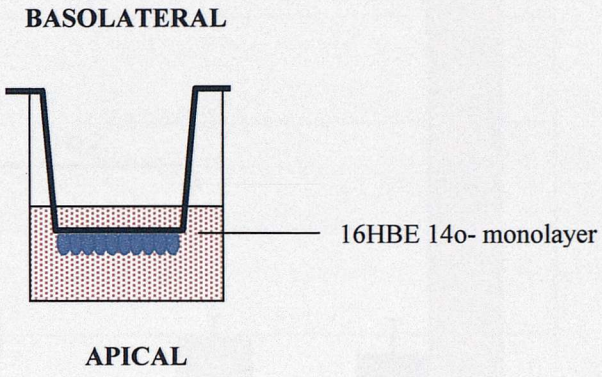

The change in TER was measured (Fig.5.2). A significant increase ($p=0.03$) in TER was seen when conditioned medium was added to the basolateral side of the epithelial monolayer, reaching a maximum of $324\Omega.cm^2$ on day 1. However, there was no increase in TER when HUVEC-conditioned-medium was added to the apical side of the 16HBE 14o- monolayer ($p=0.25$), reaching a maximum of $96\Omega.cm^2$ on day 1. This shows that the factor causing an increase in TER only acts when applied from the basolateral direction.

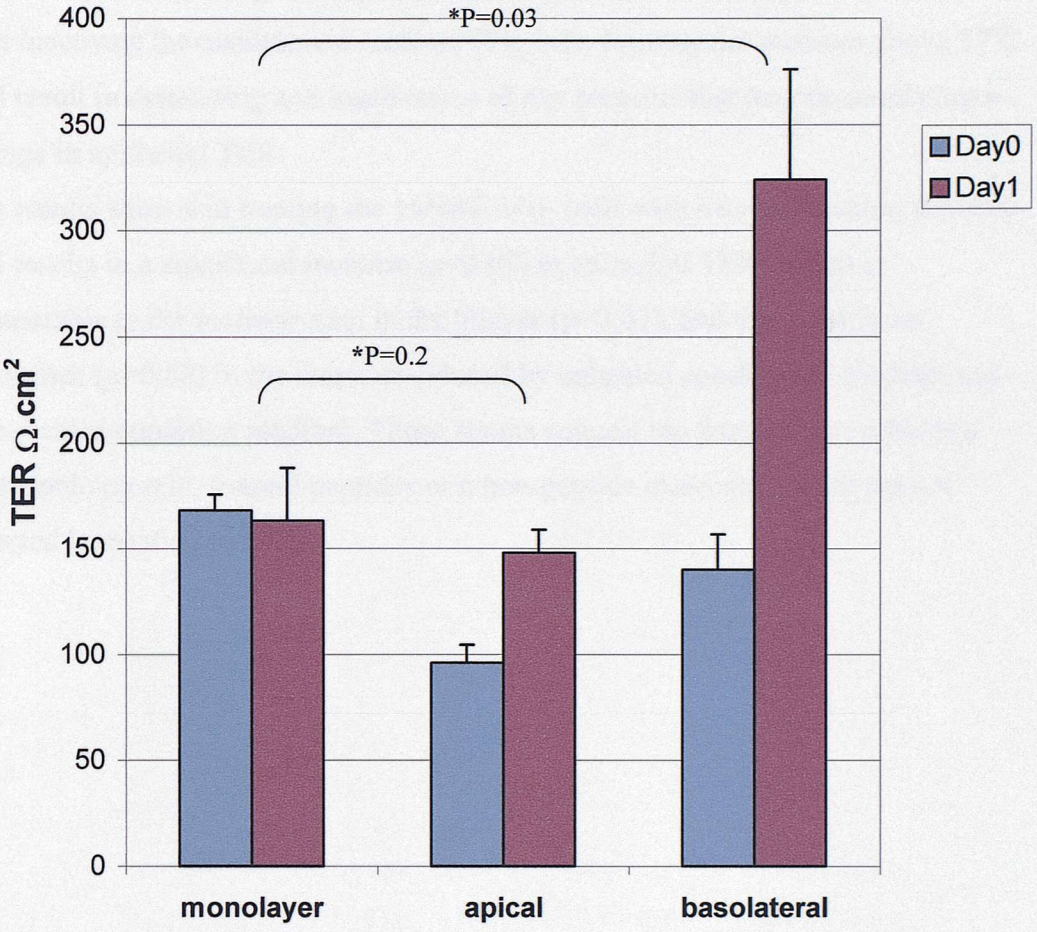

Fig.5.2 Comparison of 16HBE 14o- TER after addition of conditioned medium to either the apical or basolateral side of the epithelial monolayer. A significant increase in TER is only seen when conditioned medium is added to the basolateral side, but no difference is seen when added to the apical side (*p=0.03; *p=0.25; n=4 consisting of one experiment with four inserts).

5.4 Effect of heat inactivated conditioned medium

The task of trying to identify the endothelial factor being produced is an immense one- as there have been very few studies on increasing TER of epithelial cells, which may have given possible candidates to pursue. The first approach was to heat inactivate the conditioned medium (Fig.5.3). Heating the medium above 57°C will result in denaturing and inactivation of any proteins that may be mediating a change in epithelial TER.

The results show that treating the 16HBE 14o- cells with heat-inactivated medium still results in a significant increase ($p=0.03$) in epithelial TER, which is comparable to the increase seen in the bilayer ($p=0.03$), and that there is no difference ($p=0.88$) in the increase induced by unheated conditioned medium and heat-treated condition medium. These results suggest the factor responsible is a heat stable protein, a small peptides or a non-peptide molecule, which are not affected by heating to 57°C.

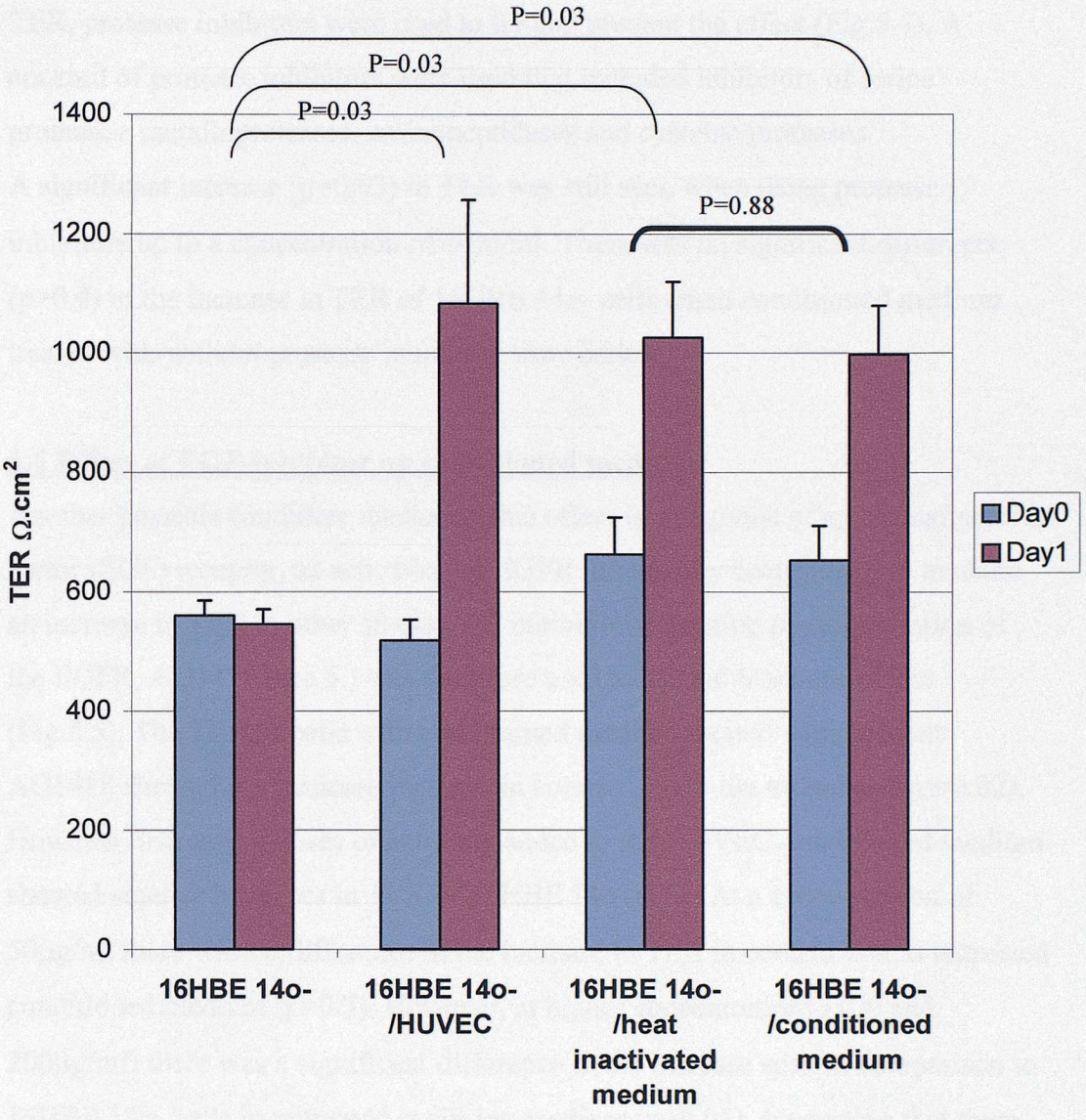

Fig.5.3 Effects of heat-inactivated HUVEC-conditioned medium on the TER of 16HBE 14o- cells. 16HBE 14o- bilayer, heat-inactivated medium and conditioned medium treatments all have a significantly higher (p=0.03) TER than 16HBE 14o- monolayer, but there is no significant difference (p=0.88) between the heat-inactivated medium and conditioned medium treatments. (n=4 consisting of one experiment with four inserts).

5.5 Effect of protease inhibitors on conditioned medium

To investigate whether a protease was responsible for the increase in epithelial TER, protease inhibitors were used to try and prevent the effect (Fig.5.4). A cocktail of protease inhibitors were used that included inhibitors of serine proteases, metalloproteases, aminopeptidases and cysteine proteases.
A significant increase ($p=0.03$) in TER was still seen when using protease inhibitors up to a concentration of 40µl/ml. There was no significant difference ($p>0.4$) in the increase in TER of 16HBE 14o- cells when conditioned medium treated with/without protease inhibitors were added.

5.6 Effect of EGF-inhibitor on conditioned medium

Another possible candidate mediating this effect is an agonist of epidermal growth factor (EGF) receptor, as activation of EGFR has already been shown to mediate an increase in TER in other studies. An inhibitor of tyrosine phosphorylation of the EGFR, AG1478 (see 5.) was therefore used to try and block the effect (Fig.5.5). The TER of cells with conditioned medium treated with/without AG1478 showed a significant increase in comparison to the monolayer ($p=0.02$). However, increasing doses of antibody added to the HUVEC-conditioned medium showed smaller increases in TER of 16HBE 14o- cells. At a concentration of 50µg/ml there was no difference in the increase in TER in comparison to untreated conditioned medium ($p=0.3$). However, at higher concentrations (100 and 200µg/ml) there was a significant difference in the increase seen in comparison to 16HBE 14o- cells in untreated condition medium ($p=0.04$), suggesting that there was an inhibiting effect on the conditioned medium.

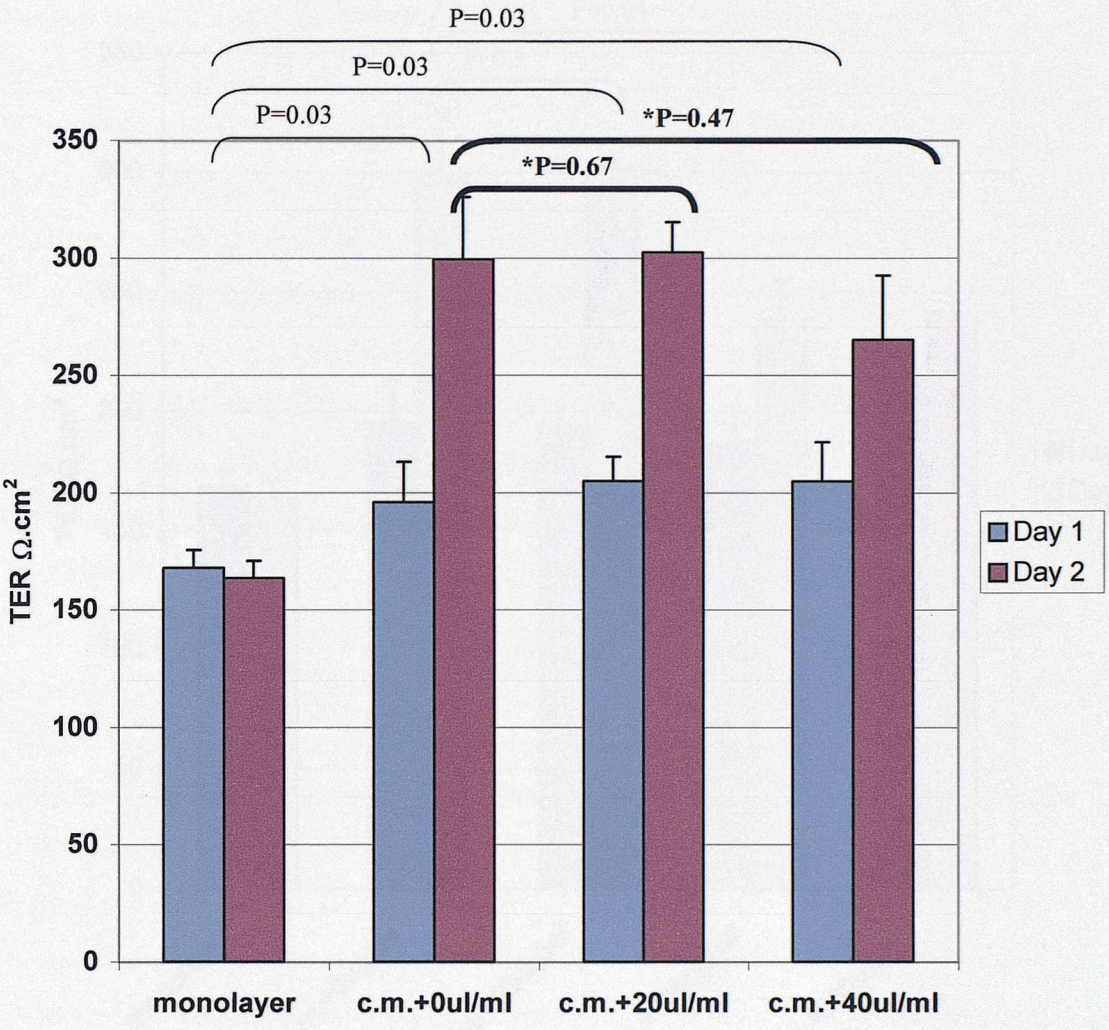

Fig.5.4 Effect of addition of protease inhibitor to HUVEC conditioned medium on TER of 16HBE 14o- cells. The TER of 16HBE 14o- cells grown in conditioned medium treated with/without protease inhibitors showed a significant increase in comparison to the monolayer (p=0.03). There is no significant difference between treating 16HBE 14o- cells with conditioned medium with or without protease inhibitors, (*p >0.4; n=4).

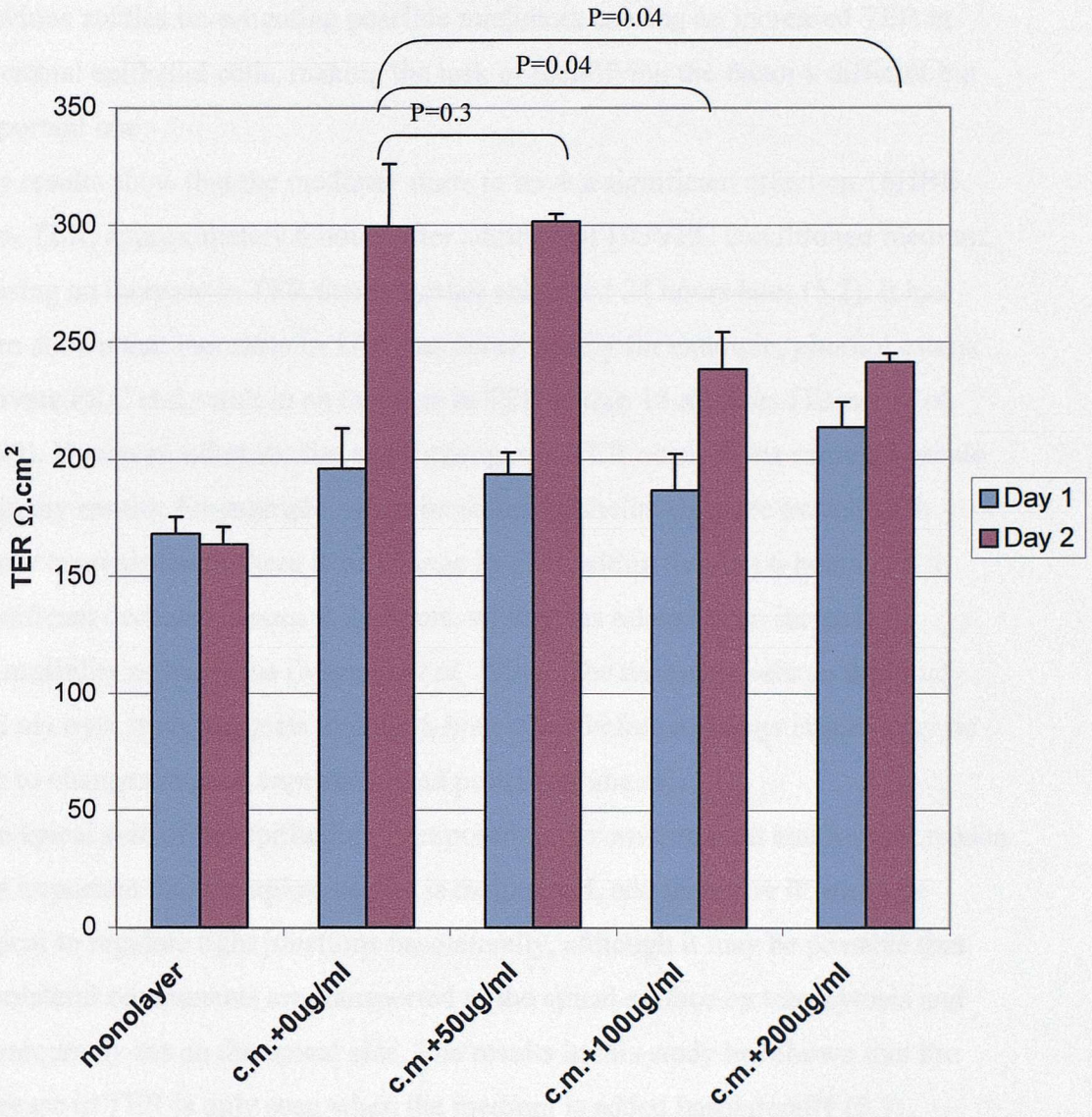

Fig.5.5 Effect of addition of EGF inhibitor, AG1478 to HUVEC conditioned medium on TER of 16HBE 14o- cells. The TER of 16HBE 14o- cells grown in conditioned medium treated with/without EGF receptor inhibitor showed a significant increase in comparison to the monolayer (p=0.02). A significant difference is seen in the increase in TER seen between conditioned medium and conditioned medium containing 100 and 200μg/ml (p=0.04; n=4).

5.7 Discussion

Endothelial cells (HUVEC) are producing a soluble factor that is mediating an increase in TER of respiratory epithelial cells (16HBE 14o-). There have been no previous studies investigating possible mediators causing an increased TER in bronchial epithelial cells, making the task of identifying the factor a difficult but important one.

The results show that the mediator starts to have a significant effect on 16HBE 14o- TER, approximately 6 hours after addition of HUVEC conditioned medium, causing an increase in TER that is further enhanced 24 hours later (5.2). It has been shown that increases in TER can occur rapidly for example, phorbol esters, activate PKC and result in an increase in TER within 15 minutes (Turner *et al.* 1999). However, other studies show changes in TER occur in the same timescale as in my results, for example, when intestinal epithelial cells are treated with tumor necrosis factor there is no change in TER within the first 6 hours, but a significant decrease is seen at 24 hours, which was related to an increase in permeability of Na+ ions (Marano *et al.* 1998). The timescale seen in this study and my own study suggests that the 6-hour delay before a change is seen may be due to changes in gene expression and protein synthesis.

The apical side of the epithelium is exposed to the environment and for that reason it is important that the apical barrier is maintained, and therefore it would be logical to regulate tight junctions basolaterally, although it may be possible that basolateral components are transported to the apical surface by transcytosis and subsequently act on the apical side. The results in this study has shown that the increase in TER is only seen when the medium is added basolaterally (5.3), suggesting that there is an interaction with a component on the basolateral side of the epithelial cells, this may be directly with tight junction components, or indirectly such as an effect on the actin cytoskeleton influencing tight junction function.

Studies linking the cytoskeleton to tight junctions have focussed on the perijunctional actinmyosin ring (PAMR), a band of actin filaments just below the apical junctional complex associated with myosin, which has contractile properties (Keller and Mooseker, 1982). For example, protein kinase C (PKC) agonists, such as phorbol esters, activate PKC and result in an increase in TER in intestinal epithelial cells, which is thought to be caused by inhibiting myosin light chain

kinase and a corresponding decrease in myosin light chain phosphorylation, reducing PAMR tension (Turner *et al.* 1999). However, this is unlikely to be the reason for increasing TER in my study as it takes at least 6 hours before an increase is seen. Other changes in the cytoskeleton can be induced by cytokines, such as interferon-γ (IFN-γ), which has been shown to decrease TER in intestinal epithelial cells, due to disruption and disorganisation of F-actin, which is associated with a decrease in ZO-1 and redistribution of ZO-2 and occludin (Madara and Stafford, 1989).

Heat inactivating the medium to 57°C has no effect (5.4), suggesting the protein may be small in size, that the factor is a peptide rather than a protein or a lipid or ion. It may also be possible that the active part of the protein may still be intact after denaturing the whole protein. A recent study showed that a 30-50KDa peptide, present in dog urine, upregulated TER of MDCK cells, and that this effect was suppressed with type 1 protease, but not by boiling (Gallardo *et al.* 2002). Other studies show proteases can enhance TER, such as addition of trypsin to the basolateral surface of MDCK cells, which incidentally does not have an effect when added to the apical surface (Lynch *et al.* 1995). However, the increased TER effect of the endothelial-secreted component in my study was not inhibited by protease inhibitors or by heating, suggesting the component is not enzymatically active. However, it is possible that a different protease is acting, which is not recognised by the protease inhibitors used.

Studies have investigated the effect of cytokines on tight junction function. One study showed that treating MDCK cells with epidermal growth factor (EGF) activates the EGF receptor, resulting in a three-fold increase in TER by selectively regulating claudin expression (Singh and Harris, 2003). EGF has been shown to be a regulator of migration, proliferation and differentiation of epithelial cells, indicating an involvement in epithelial wound healing, (Carpenter and Wahl, 1991). However, it is the activation of the EGF receptor, which appears central in epithelial repair (whose main priority will be restore barrier function), as elevated levels of EGF receptor are found in areas of epithelial damage in normal individuals (Polosa *et al.* 2000). The possibility that the active component in the endothelial medium, causing an increase in TER of 16HBE 14o- cells, was interacting with the EGF receptor was investigated, using the tyrosine kinase

inhibitor, tyrphostin AG1478. AG1478 has been shown to specifically block tyrosine kinase phosphorylation of the EGF receptor (Puddicombe *et al.* 2000). However, there was still a significant increase in TER after treating the endothelial medium with this inhibitor, but the increase was reduced at higher doses of 100-200μg/ml (5.6). This suggests that an EGFR agonist increasing EGFR phosphorylation may be causing the increase in TER. It should be noted that the HUVEC culture medium already contains EGF, and it may be that the antibody is inhibiting the effect of this EGF on activation of EGFR, resulting in an overall decrease in TER.

Other possibilities that may be causing the increase in TER are changes in ion or lipid concentration in the extracellular environment of the 16HBE 14o- cells. The involvement of Ca^{2+} in the formation of tight junctions has been shown in MDCK cells, such that in the absence or low Ca^{2+} the cells do not polarise and do not form tight junctions, but when extracellular Ca^{2+} levels are raised tight junctions form, the cells become polarised and increased TER can be measured (Nigam *et al.* 1992). Extracellular Ca^{2+} is important in the initial stages of cell-to-cell junction formation, as it is required for homotypic interactions of E-cadherin (Gumbiner, 1996), The exact signalling pathways involving Ca^{2+} during tight junction formation are not well defined, but it is thought to be important in triggering a signalling cascade (Denker and Nigam, 1998), by activating protein kinase C (PKC), which is translocated from the cytosol to the tight junction, phosphorylating ZO-1 and ZO-2 which are subsequently translocated to the tight junction and become tightly associated with the actin cytoskeleton (Stuart and Nigam, 1995), leading to the formation of tight junctions. In addition to intracellular Ca^{2+} and the activation of PKC, heterotrimeric G proteins are also thought to be part of the signalling pathway during tight junction formation (Denker *et al.* 1996).

Lipids have also been shown to modify tight junction, and any change in the lipid content of the extracellular environment can alter tight junction function, for example a decrease in the cholesterol level of MDCK medium results in a decrease in TER (Francis *et al.* 1999). Other fatty acids that have been shown to increase TER are gamma linoleic acid and eicosapentaenoic acid, which have been

shown to reduce paracellular permeability and increase TER in endothelial cells (Jiang *et al.* 1998).

Based on my results, the endothelial cells are producing a soluble factor, which increases TER of epithelial cells. This factor is heat-resistant to temperatures up to 57°C, and acts only when applied to the basolateral surface of epithelial cells. An effect is not seen until at least 6 hours after treatment, suggesting an event is being triggered that will take longer to have a detectable outcome, such as protein synthesis. The increased TER is not prevented by the addition of a cocktail of protease inhibitors to the HUVEC medium, suggesting the active factor is not a protease, which is also supported by the results of heat inactivation. However, addition of an EGF receptor inhibitor to the HUVEC medium does result in a reduction in the increase of TER seen with untreated medium, suggesting one possible factor is an EGF receptor agonist upregulating tyrosine phosphorylation of the receptor.

These results give a preliminary characterisation of the endothelial factor, and future work would need to include positive controls to demonstrate the biological effect of the protease and EGF-receptor inhibitors. One possible approach that could minimise ambiguous experiments would be to use proteomics on fractionated samples of endothelial-conditioned medium that cause an increase in TER.

CHAPTER 6
FINAL DISCUSSION

Chapter 6: Final Discussion

The key points established from this thesis are the development and characterisation of a co-culture model reflecting the bronchial epithelium and endothelium of the human conducting airways; the role of tight junctions in epithelial barrier function; the dynamic regulation of tight junction proteins in regulating epithelial barrier function and the influence of endothelial cells on epithelial barrier function.

6.1 The bilayer model

The aim of this project was to establish an *in vitro* system reflecting the human bronchial airways, which would allow potential epithelial and endothelial interactions, to reflect the *in vivo* situation. This model will help in the understanding of cell barrier interaction as a whole rather than as separate entities.

6.1.1 *Characterisation*

The final model established consists of 16HBE 14o- bronchial epithelial cells, and HUVEC endothelial cells grown on opposite sides of an insert membrane. The model has been fully characterised and conditions optimised such that the model gives consistent results. Each cell type was identified using specific immunofluorescent markers. 16HBE 14o- cells were identified with HEA-125, an antibody specifically designed to recognise an epithelial surface antigen. HUVEC were identified using an antibody against vWF, a fundamental component of endothelial cells, so even if other epithelial cells are used in the model, the endothelial cells can still be distinguished. This will allow results to be attributed to the correct cell type and there would be no confusion as to which cells were being studied. *In vivo*, the epithelium and endothelium of the bronchial airways are not in direct contact, but are separated by the submucosa, it was therefore important to have only one cell type on each side of the membrane, that were not in direct contact. This was confirmed by SEM and TEM, which showed that the final model had two specific cell layers separated by the insert membrane, (this will be discussed further in 6.1.3). The model was characterised functionally using TER as a measurement of tight junction function to ensure the same characteristics were exhibited repeatedly, and to set baseline measurements.

6.1.2 *Epithelial-endothelial interaction*

The bilayer system established has several advantages. It includes two components of the biological system, allowing cell-to-cell interaction between epithelial and endothelial cells, making a better *in vivo* equivalent than existing monolayer systems designed to study respiratory epithelium (Kidney and Proud 2000; Carolan *et al.* 1998). Functional differences are seen between my bilayer model and single epithelial monolayers, such that TER is enhanced in the bilayer model due to epithelial-endothelial interactions. Further evidence for epithelial-endothelial interaction influencing cell function comes from another respiratory epithelial-endothelial bilayer model showing increased neutrophil transmigration in the bilayer in comparison to single epithelial monolayers (Mul et al. 2000). These results emphasize the importance of considering the other biological components of the bronchial airways when studying respiratory epithelium. The epithelium is not an isolated component but part of an integrated unit, consisting of epithelium, endothelium and extracellular matrix components, and responses of the unit as a whole can differ in comparison to single cell studies.

6.1.3 *Cell species and characterisation in relation to the biological system*

The final model established improves on existing co-culture systems using non-human derived cells (Gueven *et al.* 1996), as my model uses human cell lines and primary human cell cultures, making a better human comparison, and moving away from the need for animal models. Furthermore, Guevens model was based on the alveolar system, ie. the respiratory portion of the airways rather than the conducting airways. Another similar bilayer model consisting of alveolar epithelial cells and endothelial cells on either side of an insert membrane has been established to study neutrophil migration (Casale and Carolan, 1999), but once again this is based on the alveolar system and not the conducting airways. The epithelium of the respiratory and conducting airways differ in their physiology and function. Respiratory epithelium is involved in gaseous exchange; whereas epithelium of the conducting airways are in protecting the underlying tissues as they are open to the environment. Therefore, models established to study respiratory epithelium would not be suitable for the study of conducting epithelium.

This is not to say that there are no existing models based on the bronchial system. In fact, two models have been established. The first (Mogel *et al.* 1998) consisted of growing bronchial epithelial cells in inserts and endothelial cells in the bottom of six-well plates, and then combining the two when the cells were confluent by placing the inserts into the wells. However, this has two drawbacks when comparing to the *in vivo* bronchial architecture- the distance between the cells would be greater than that seen in the physiological system, where bronchial epithelial cells and endothelial cells would be 20-200μm apart. The distance between the epithelial and endothelial cells of the model established in my thesis is approximately 25μm, which is the depth of the insert membrane. Also the endothelial cells are in the wrong orientation in relation to the epithelial cells, since in the model the apical side of the endothelial cells are facing the basolateral side of the epithelial cells, whereas *in vivo* the basolateral side of each cell should be facing each other.

The other existing model (Mul *et al.* 2000) consists of growing bronchial epithelial cells and endothelial cells on either side of an insert membrane, therefore having the correct orientation and distance between the two cell types, which is similar to mine. However, the main difference in the two models is that Mul's model has been set up to study neutrophil migration and mine has been set up to study TER and permeability in relation to tight junction function. It is for this reason that our characterisation differs. Mul used HUVEC with either primary bronchial epithelial cells or H292 epithelial cells, but has not functionally characterised them to ensure they are reflecting the barrier properties exhibited by bronchial respiratory epithelium. Although primary bronchial epithelial cells reach high electrical resistances, my own studies have shown that H292 only reach low electrical resistance measurements, which reflect low tight junction integrity and therefore low barrier properties, which is why they were not chosen for my model. Furthermore, the inserts Mul has used have a 3μm pore size, and my studies have shown that both epithelial cells and endothelial cells are able to migrate through pores of this size, and therefore it is not surprising that in Mul's model the cells have been shown to migrated through the pores. This means that the results of the study may not be physiologically valid since a mixture of cells will be present on each side of the insert, each capable of exerting an effect. To avoid this problem

my model uses inserts with a pore size of 0.4μm, which I have shown do not allow cell migration, ensuring the final model has two distinct cell layers, making it more physiologically valid. However, pores of this size would not allow neutrophil migration and therefore my model would not be suitable for leukocyte migration studies.

6.1.4 *Possible improvements to the model*

My model uses primary HUVEC cells as opposed to endothelial cells of the pulmonary capillaries. This is due to the availability and ease of culturing of HUVEC's, and has been extensively used for transendothelial migration studies (Casale and Carolan, 1999; Mul *et al.* 2000). HUVEC have also been shown to be similar in growth and appearance to human pulmonary artery endothelial cells (Mackarel *et al.* 1999), and are therefore useful in studying the endothelium system. However, as endothelial cells show heterogeneity, it would be ideal to use pulmonary endothelial cells to confirm the effects seen in my model reflect the bronchial system. The use of primary bronchial epithelial cells would also better reflect the *in vivo* system. The model could be manipulated further to give a closer biological representation of the bronchial airways, by exposing the epithelial cells to an air-liquid interface. Seeding endothelial cells to the underside of the insert, and epithelial cells to the upperside, and having medium only in the well could achieve this.

It should also be noted that epithelial cells and endothelial cells are not the only components of the bronchial airway, but other components, particularly those of the basement membrane, can also influence epithelial barrier function. Even though the cells are being grown on an insert membrane, this will not reflect the basement membrane. Introducing other components does have the drawback of making the model more complex, since any results could be due to a number of interactions and it would be too difficult to pinpoint the actual interaction(s) causing an effect.

In conclusion, the model in this thesis has been designed to allow epithelial-endothelial interactions, to study the subsequent tight junction function of the bronchial respiratory epithelium.

6.2 Tight junctions and epithelial barrier function

Tight junctions have three main roles; the regulation of the epithelial paracellular permeability barrier (Madara, 1998), maintenance of cell polarity (Cerijido *et al.* 1998) and a role in regulating cell growth and proliferation has been suggested (Balda *et al.* 2003).

6.2.1 *TER and paracellular permeability*

The integrity of tight junctions varies between different epithelium, and depends on the function of the tissue and the level of permeability required. For example, endothelial cells of the brain-blood-barrier need to have well-formed tight-junctions to prevent any solutes crossing the blood brain barrier (Bradbury 1993); whereas epithelium of the small intestine need to allow the transport of water and solutes and will have looser tight junctions (Thomson *et al.* 2001).

The paracellular flux of ions across epithelium will generate electrical-current flow or conductance, which will be related to ion permeability (Madara, 1998). Tight junctions regulate this permeability and block movement between cells generating a resistance (Claude, 1978). Resistance is the reciprocal of conductance, and for this reason TER measurements are used as an inverse of permeability (Madara *et al.* 1992). It is therefore logical that a high TER will reflect low paracellular permeability and tighter junction formation; and low TER will reflect high paracellular permeability and weaker junction formation. The TER results from my bilayer model reach significantly higher values than single epithelial monolayers (3.3.4), which suggested a lower permeability and were confirmed by measuring the permeability of FITC-dextran molecules across the bilayer and epithelial monolayer. The results supported the reciprocal relationship between TER and permeability, although non-linear, since lower levels of FITC-dextran migrated across the bilayer than in the epithelial monolayer. This emphasises the importance of using TER as a reflection of paracellular permeability.

6.2.2 *Cell polarity*

Membrane proteins, once synthesised in the rough endoplasmic reticulum, undergo intracellular sorting before being delivered to the cell membrane, and is thought to be mediated by signals contained within these proteins (Le Gall *et al.* 1995). Since tight junction proteins themselves must be sorted to the membrane in order to generate and maintain polarised membrane domains, it would be logical for them to contain such signals, although none have as yet been identified.
Tight junctions are important in preventing intramembrane diffusion of proteins in the apical and basolateral membranes of epithelial cells, resulting in cell polarity (Madara, 1998). Cells that are polarised do not necessarily show the same level of TER, for example 16HBE 14o- and HUVEC both form tight junctions (3.3.3) and display apical and basolateral domains, but they have different TER values (3.3.4).

6.2.3 *Cell growth and proliferation*

Tight junctions have been suggested to have a role in epithelial cell proliferation and differentiation, through the tight junction associated protein ZONAB (Balda and Matter, 2000). Low levels of ZO-1 are expressed in proliferating cells and as cell density increases levels of ZO-1 increases, but nuclear levels of ZONAB decreases (Balda and Matter, 2000).
Overexpression of ZONAB leads to its nuclear accumulation, which was associated with an increase in cell proliferation due to an increase in cell density. However, lower levels of ZONAB were found to associate with ZO-1 at the tight junction, and were linked to reduced proliferation due to a decrease in cell density (Balda *et al.* 2003). This study suggests that tight junctions are involved in cell proliferation due to tight junction associated proteins acting as regulators of transcription. The results of my study do not show any changes in cell density that may have contributed to an increase in TER.

6.3 Dynamic regulation of tight junction proteins

The dynamic regulation of tight junction proteins is essential in regulating tight junction function. Changes could occur in whole array of proteins involved in tight junction formation, including changes in the cytoskeleton, plaque proteins or transmembrane proteins of the tight junction. There are many possibilities that could be affecting tight junction function in my model, including a simple upregulation or downregulation of a protein, or different proteins being expressed or changes in phosphorylation. It would be too complex a task to consider all the proteins involved in tight junction formation and for this reason the study has focussed on changes occurring at the site of cell-to-cell adhesion ie. in the transmembrane proteins of the tight junction.

6.3.1 *The transmembrane proteins*

Tight junctions were first identified in 1963, seen as kissing points where adjacent cell membranes fuse together (Faruquar and Palade, 1963)). However, it was not until 1986 that the first TJ-associated protein, ZO-1 was identified (Stevenson *et al.* 1986), and it was later still when the first transmembrane protein, occludin, was identified (Furuse *et al.* 1993). Since its identification much work has been done to elucidate its molecular interactions and subsequent function, (which will be discussed below), as it was considered to be the only transmembrane tight junction protein for several years. It was experiments showing the formation of tight junctions in occludin-deficient epithelial cells that led researchers to consider other possible transmembrane proteins were involved and this led to the identification of claudins (Furuse *et al.* 1998).

A whole family of claudins have now emerged; with 24 claudins being identified so far (Tsukita *et al.* 2001). The molecular interactions and functions of the different claudins are still to be identified, but what is clear is that they are important components in regulating tight junction permeability. Different claudins are expressed in different tissues, and it is thought that tissue specific expression reflects different claudins possessing different functional properties, presumably due to tissue specific regulation (Rahner *et al.* 2001). My own results show differences in claudin expression between endothelial cells (HUVEC) and bronchial epithelial cells (16HBE 14o-). For example, claudin-5 is endothelial specific (Morita *et al.* 1999), and my own results show claudin-5 gene expression

only in HUVEC and not in 16HBE 14o-, and are therefore a possible candidate for giving HUVEC their low TER property. On the other hand, claudin-1 expression is only found in 16HBE 14o- cells and not in HUVEC, and since other studies show expression of claudin-1 is necessary for tight junction barrier function, it is possible that this contributes to the high electrical resistances seen in my 16HBE 14o- cells, and that its absence contributes to the low TER seen in my HUVEC. Differences in gene expression of claudins 1-5 in 16HBE 14o- cells grown in my three different conditions do not show any significant differences, suggesting that the increase in TER seen in my bilayer and conditioned medium treatments, are not due to changes in the amount of claudins 1-5 expressed. However, this does not rule out any changes in their molecular interactions. It has been shown that claudins have the ability to copolymerise both homophilically or heterophilically and with occludin, and this is central to sealing adjacent cell membranes (Furuse *et al.* 1999). However, not all claudins can interact with each other, and mismatches will reduce tight junction integrity (Heiskala *et al.* 2001). Therefore, even if no changes were occurring in the amount of claudins being expressed, changes may be occurring in the polymer of molecules forming the tight junction backbone, due to changes in claudin interactions with each other and with occludin itself.

The most recent family of transmembrane proteins identified, is the JAM family (Martin-Padura *et al.* 1998), and their molecular interactions and functions are still to be determined. To date, only three JAM molecules have been identified, and although they are unable to form tight junctions themselves (Itoh *et al.* 2001), they are thought to have regulatory roles in signalling tight junction formation, and establishing cell polarity (Ebnet *et al.* 2001; Ebnet *et al.* 2003). My RT-PCR results show JAM-1 is expressed in both 16HBE 14o- cells and HUVEC, with the highest levels being expressed in 16HBE 14o- cells grown in conditioned medium. This would support studies showing the highest levels of JAM-1 are expressed in cells with well-developed tight junctions, such as in brain endothelial cells (Kniesel and Wolburg, 2000), and is found to colocalise with ZO-1 during junction formation (Ebnet *et al.* 2001). JAM-2 has been shown to be expressed at high levels (and JAM-1 at low levels) in endothelial cells with high permeability (low barrier function) such as HEV's, (Aurrand-Lions *et al.* 2001). My results contradict these findings, since no JAM-2 gene expression is found in HUVEC,

but JAM-1 is expressed. JAM-3 is found in most vascular endothelial cells (Cunningham *et al.* 2000) and my results show it to be expressed in HUVEC but not in 16HBE 14o- cells. The expression of different JAM molecules in different tissues suggests they confer different functions relevant to the tissue in which they are expressed (Aurrand-Lions *et al.* 2001), however, the full extent of the role of JAM molecules is still to be determined. All the above-mentioned studies show that claudin and JAM molecules are important in regulating tight junction function and formation. Nevertheless, my work has focussed on occludin, as a key tight junction protein, as when comparing changes in tight junction protein gene expression in 16HBE 14o- cells grown in the three different conditions, the biggest change seen is an increase in occludin gene expression.

6.3.2 *Tight junction regulation by occludin*

The RT-PCR results in my work show an increase in occludin gene expression in 16HBE 14o- cells grown as a bilayer or in conditioned medium. There was also an increased expression of an occludin isoform, TM4-. An increase in occludin expression would give an explanation for the increase in TER since other studies have shown increased occludin expression leads to an increase in TER (McCarthy *et al.* 1996). However, the role of TM4- is not known but it has been suggested to have a negative effect on tight junction integrity since a deletion occurs at the cytoplasmic C-terminal resulting in the C-terminal becoming extracellular (Ghassemifar *et al.* 2002). This has negative implications on tight junction function, since the cytoplasmic C-terminal has been shown to be important in interacting with tight junction associated proteins, ZO-1, ZO-2 and ZO-3 as well as directly interacting with F-actin which is important in linking tight junctions to the cytoskeleton (Gonzalez-Mariscal *et al.* 2003). Truncating the C-terminal has also been shown to result in a reduced tight junction barrier seen as an increase in permeability (Chen *et al.* 1997). However, the function of TM4- has not yet been determined, and if it does have a negative regulatory effect it raises the dilemma as to why it is being expressed in 16HBE 14o- cells with an increased TER (ie. when grown in a bilayer with endothelial cells or in HUVEC conditioned medium). One explanation is that it is acting as a regulator of tight junction function, and is counter-actioning any possible over-expression of occludin, to maintain the tight junction barrier at a particular level.

There may also be differences in distribution of occludin, and although this was difficult to assess, it is clear from the immunofluorescent staining with occludin antibody, that occludin is expressed both at the cell-to-cell borders and within the cytoplasm in all three of my 16HBE 14o- treatments, (monolayer, bilayer and conditioned medium). The level of phosphorylation determines the location of the occludin, such that highly phosphorylated occludin is located at tight junctions and less phosphorylated occludin is found within the cytoplasm (Andreeva *et al.* 2001). It is possible that when 16HBE 14o- are grown as a bilayer or in HUVEC-conditioned medium there is an increase in occludin phosphorylation, which would be reflected in changes in distribution such that more occludin is located at the tight junctions, resulting in more tight junction strands being formed and a subsequent increase in tight junction integrity seen as an increase in TER.
In conclusion changes in TER seen in my bilayer model can be partly attributed to an increased in occludin expression, and may also be due to changes in distribution such that more is located at the tight junctions. However, it is important to realise that this may not be the only change occurring as tight junction proteins form complex interactions and a change in one protein will have influences on others.

6.4 Cell-to-cell interactions in regulating barrier function

The increase in TER seen in 16HBE 14o- cells when grown as a bilayer is attributable to a soluble endothelial factor. This has been shown by treating 16HBE 14o- cells grown as a monolayer with conditioned medium from confluent endothelial (HUVEC) cell cultures, which produced the same increase in TER as that seen in the bilayer model.
Studies have shown that some cytokines such as IFNγ, TNFα, IL-13 and IL-4 increase epithelial permeability in T84 intestinal epithelial cell monolayers, but TGFβ1 and EGF have the opposite effect and decrease permeability (Walsh *et al.* 2000). However, these cytokines may exert a different effect on bronchial epithelial cells, as it has been shown that IFN-γ can enhance epithelial lung barrier function (Ahdieh *et al.* 2001). These studies illustrate the potential of cytokines to induce different cell responses in different tissues. It is possible that the HUVEC cells are producing one or more of these cytokines, but there is also a possibility

that some unknown factor is being produced. One possible cytokine the HUVEC cells may be producing is EGF, (or an EGF agonist), which has been shown to cause phosphorylation of the EGF receptor resulting in an increase in TER (Singh and Harris, 2003). In my study, the addition of a specific inhibitor of tyrosine phosphorylation of the EGF receptor, to the HUVEC conditioned medium, still induced a significant increase in TER in comparison to the monolayer. However, this increase was lower than that seen in 16HBE 14o- cells grown in untreated medium, suggesting an EGF receptor ligand may be involved.

Proteases, such as trypsin, have also been shown to increase TER (Lynch *et al.* 1995), but the protease inhibitors used in this study were unable to inhibit the increased TER effect.

Initial characterisation of the factor producing the increased TER, show it to be heat-stable at 57°C, further supporting it not to be a protease, and that it only acts in the basolateral direction taking at least 6 hours before a significant change is seen. This suggests the factor is interacting with a molecule on the basolateral side of the tight junction, which would be logical, as the apical side needs to maintain its integrity as a protective barrier to the external environment.

These results are based on a preliminary characterisation, and other possible candidates may be mediating the change in TER. In particular, changes in ion concentration, such as Ca^{2+} (Nigam *et al.* 1992), or lipid concentrations, such as fatty acids (Jiang *et al.* 1998), have been shown to induce an increase in TER.

6.5 Importance of this study

The bilayer system established would be a useful tool in studying bronchial epithelial-endothelial cell interactions, and is a better reflection of the *in vivo* situation in comparison to existing models. Any system that can provide further insight into cell-to-cell interactions will be invaluable in broadening the knowledge of *in vivo* interactions in biological systems that are not well defined, in particular the regulation of mucosal tight junctions by non-epithelial cells. This would be of particular biological importance, for example, when the epithelium barrier function is damaged during disease, viral, bacterial or allergen challenge. An extreme example of epithelium damage occurs with influenza virus. The influenza virus possess hemagluttinins, which attach to sialyloligosaccharides, a

group of carbohydrates present on the epithelial surface, and release neuraminidases, which degrade mucus, enabling the virus to evade mucocilliary clearance, resulting in evasion of the host epithelial cells (Couceiro *et al.* 1993). Other viruses also evade mucocilliary clearance by attaching to the epithelium, such as rhinoviruses, which recognise ICAM-1 expressed on the surface of epithelial cells (Bella and Rossmann, 1999). Once attached, respiratory viral infections cause damage to the epithelium such as desquamation, oedema, excess mucus production and increased inflammatory cell infiltration, resulting in deficient mucocilliary clearance, obstructive airways and reduced macrophage killing, resulting in the airways becoming prone to bacterial infection (Hogg, 2000). Bacterial pathogens can also attach to the epithelial surface. An example is H.Influenzae, which has pili on its surface that attach to the respiratory epithelium, and produce a factor that disorganises ciliary beating and a protease that degrades IgA (Gilsdorf *et al.* 1997). Once attached the virus or bacteria can enter the epithelial cells directly or cross the epithelium via the paracellular route by disrupting epithelial tight junctions. One example of this is the coxsackievirus and adenovirus. The coxsackievirus and adenovirus receptor (CAR) has been colocalised with ZO-1 at tight junctions, and when expressed at the tight junction reduced paracellular permeability is seen but soluble CAR results in dysfunctional tight junctions being formed (Cohen *et al.* 2001). These examples demonstrate the importance of maintaining barrier function to prevent infection, but an inappropriate response such as that seen in asthma, results in chronic inflammation of the airways leading to epithelial damage and reduced barrier function (Holgate, 2000). Any knowledge that may help identify the mechanisms of maintaining barrier function will therefore be useful in trying to combat these clinical conditions.

The model has already shown that endothelial cells influence epithelial function in such a way, that epithelial tight junction integrity is increased. Tight junctions form an important barrier between the internal and external environments. A whole array of proteins has been identified that participate in tight junction assembly and function, but many of the protein interactions and functions are yet to be determined. This study has shown that endothelial cells can cause a change in tight junction proteins, such as upregulation of occludin gene expression, or changes in occludin distribution and phosphorylation.

Any study that can identify the role of tight junction proteins, or the consequence of changes in tight junction proteins, will not only expand our knowledge of tight junctions but may have important implications in the understanding of medical disorders. If a particular disorder can be related to the modification of a particular tight junction protein, then it will provide a target for treatment such as gene therapy. In particular, altered or defective claudin expression has been implicated in several disorders. For example, insufficient expression of claudin-3 and claudin-4 is found in the gut disorder William-Beuren syndrome (Paperna *et al.* 1998), in which developmental defects and constipation occurs. Altered claudin-5 expression has been found in brain capillary endothelial cells in DiGeorge's syndrome (Sirotkin *et al.* 1997). The studies clearly demonstrate that claudins are important in tight junction formation, and their correct expression, distribution and activation within the epithelium is important in maintaining the appropriate barrier function for the tissue environment. However, much more work still needs to be done, to elucidate the actual function of each claudin in different cell types, and the effects of different combinations and ratios of the claudins. Other studies have implicated occludin in disease, for example the downregulation of occludin in colonic epithelial cells is thought to play a role in increasing paracellular permeability and neutrophil transmigration seen in inflammatory bowel disease (Kucharzik *et al.* 2001).

Understanding tight junction protein modifications is important, but the cell-to-cell interactions mediating these modifications are also of importance, as has been shown in the blood-brain-barrier, where endothelial-astrocyte cell interactions enhance barrier function of endothelial cells (Isobe *et al.* 1996). It has been shown that this increase in barrier function (TER) is being induced by an astrocyte released soluble, heat-labile factor (Gardner *et al.* 1997). Therefore, the environment in which cells exist must be considered when studying epithelial barrier function of the bronchial airways. This thesis is the first study to show endothelial cells are producing a factor, which is increasing tight junction integrity of the epithelial cells. Any component that has the ability to tighten the integrity of tight junctions has important therapeutic implications in disorders where tight junction function is impaired.

CHAPTER 7
REFERENCE LIST

CHAPTER 7: Reference List

Adams, C.L., and Nelson, W.J., 1998, Cytomechanics of cadherin-mediated cell-cell adhesion: Curr Opin Cell Biol, 10(5):572-7. Review.

Ahdieh, M., Vandenbos, T., and Youakim, A., 2001, Lung epithelial barrier function and wound healing are decreased by IL- 4 and IL-13 and enhanced by IFN-gamma: Am.J.Physiol Cell Physiol, 281, C2029-C2038.

Alexander, J.S., Elrod, J.W., Park, J.H., 2001, Roles of leukocyte and immune cell junctional proteins: Microcirculation, 8(3):169-79. Review.

Allport, J.R., Ding, H., Collins, T., Gerritsen, M.E., and Luscinskas, F.W., 1997, Endothelial-dependent mechanisms regulate leukocyte transmigration: a process involving the proteasome and disruption of the vascular endothelial-cadherin complex at endothelial cell-to-cell junctions: J Exp Med, 18;186(4):517-27.

Allport, J.R., Ding, H., Collins, T., Gerritsen, M.E., and Luscinskas, F.W., 1997, Endothelial-dependent mechanisms regulate leukocyte transmigration: a process involving the proteasome and disruption of the vascular endothelial-cadherin complex at endothelial cell-to-cell junctions: J Exp Med, 18;186(4):517-27.

Anderson, J. M. and Van Itallie, C. M., 1995, Tight junctions and the molecular basis for regulation of paracellular permeability: Am.J.Physiol, 269, G467-G475.

Ando-Akatsuka, Y., Yonemura, S., Itoh, M., Furuse, M., and Tsukita, S., 1999, Differential behavior of E-cadherin and occludin in their colocalization with ZO-1 during the establishment of epithelial cell polarity: J Cell Physiol, 179(2):115-25.

Andreeva, A.Y., Krause, E., Muller, E.C., and Blasig, I.E., 2001, Utepbergenov DI.Protein kinase C regulates the phosphorylation and cellular localization of occludin: J Biol Chem, 276(42):38480-6.

Arrate, M. P., Rodriguez, J. M., Tran, T. M., Brock, T. A., and Cunningham, S. A., 2001, Cloning of human junctional adhesion molecule 3 (JAM3) and its identification as the JAM2 counter-receptor: J.Biol.Chem., 276, 45826-45832.

Asakura, T., Nakanishi, H., Sakisaka, T., Takahashi, K., Mandai, K., Nishimura, M., Sasaki, T., and Takai, Y., 1999, Similar and differential behaviour between the nectin-afadin-ponsin and cadherin-catenin systems during the formation and disruption of the polarized junctional alignment in epithelial cells: Genes Cells, 4(10):573-81.

Aurrand-Lions, M., Duncan, L., Ballestrem, C., and Imhof, B. A., 2001, JAM-2, a novel immunoglobulin superfamily molecule, expressed by endothelial and lymphatic cells: J.Biol.Chem., 276, 2733-2741.

Aurrand-Lions, M.A., Duncan, L., Du Pasquier, L., and Imhof, B.A., 2000, Cloning of JAM-2 and JAM-3: an emerging junctional adhesion molecular family?: Curr Top Microbiol Immunol, 251:91-8.

Ayers, M. M. and Jeffery, P. K., 1988, Proliferation and differentiation in mammalian airway epithelium: Eur.Respir.J., 1, 58-80.

Balbi, B., Aufiero, A., Pesci, A., Oddera, S., Zanon, P., Rossi, G.A., and Olivieri, D., 1994, Lower respiratory tract inflammation in chronic bronchitis. Evaluation by bronchoalveolar lavage and changes associated with treatment with Immucytal, a biological response modifier: Chest, 106(3):819-26.

Balda, M.S., Anderson, J.M., 1993, Two classes of tight junctions are revealed by ZO-1 isoforms: Am J Physiol, 264(4 Pt 1):C918-24.

Balda, M.S., Anderson, J.M., and Matter, K., 1996, The SH3 domain of the tight junction protein ZO-1 binds to a serine protein kinase that phosphorylates a region C-terminal to this domain: FEBS Lett. 16;399(3):326-32.

Balda, M. S. and Matter, K., 2000, Transmembrane proteins of tight junctions: Semin.Cell Dev.Biol., 11, 281-289.

Balda, M. S., Garrett, M.D., and Matter, K., 2003 The ZO-1-associated Y-box factor ZONAB regulates epithelial cell proliferation and cell density: J Cell Biol, 160(3):423-32.

Bamforth, S.D., Kniesel, U., Wolburg, H., Engelhardt, B., Risau, W., 1999, A dominant mutant of occludin disrupts tight junction structure and function: J Cell Sci, 112 (Pt 12):1879-88.

Bascom, R., Kesavanathan, J., Swift, D.L., 1995, Human susceptibility to indoor contaminants: Occup Med., 10(1):119-32. Review

Bazzoni, G., Martinez-Estrada, O. M., Orsenigo, F., Cordenonsi, M., Citi, S., and Dejana, E., 2000, Interaction of junctional adhesion molecule with the tight junction components ZO-1, cingulin, and occludin: J.Biol.Chem., 275, 20520-20526.

Beatch, M., Jesaitis, L. A., Gallin, W. J., Goodenough, D. A., and Stevenson, B. R., 1996, The tight junction protein ZO-2 contains three PDZ (PSD-95/Discs- Large/ZO-1) domains and an alternatively spliced region: J.Biol.Chem., 271, 25723-25726.

Bella, J., and Rossmann, M.G., 2000, ICAM-1 receptors and cold viruses. Pharm Acta Helv, 74(2-3):291-7. Review.

Bendayan, M., 2002, Vascular permeability in blood capillary: Microsc Res Tech, 57(5):263-8.

Bennett, V., and Gilligan, D.M., 1993, The spectrin-based membrane skeleton and micron-scale organization of the plasma membrane: Annu Rev Cell Biol, 9:27-66. Review

Borman, R. A., Jewell, R., and Hillier, K., 1998, Investigation of the effects of platelet-activating factor (PAF) on ion transport and prostaglandin synthesis in human colonic mucosa in vitro: Br.J.Pharmacol., 123, 231-236.

Boyton, R.J., and Openshaw, P.J., 2002, Pulmonary defences to acute respiratory infection: Br Med Bull., 61:1-12. Review.

Bradbury, M. W., 1993, The blood-brain barrier: Exp.Physiol, 78, 453-472.

Burkitt, H.G., Young, B., and Heath, J.W., 1993, In: Wheater's Functional Histology 3rd Edition. Churchill Livingstone.

Burns, A. R., Walker, D. C., Brown, E. S., Thurmon, L. T., Bowden, R. A., Keese, C. R., Simon, S. I., Entman, M. L., and Smith, C. W., 1997, Neutrophil transendothelial migration is independent of tight junctions and occurs preferentially at tricellular corners: J.Immunol., 159, 2893-2903.

Burns, A. R., Bowden, R. A., MacDonell, S. D., Walker, D. C., Odebunmi, T. O., Donnachie, E. M., Simon, S. I., Entman, M. L., and Smith, C. W., 2000, Analysis of tight junctions during neutrophil transendothelial migration: J.Cell Sci., 113 (Pt 1), 45-57.

Carden, D., Xiao, F., Moak, C., Willis, B.H., Robinson-Jackson, S., and Alexander, S., 1998, Neutrophil elastase promotes lung microvascular injury and proteolysis of endothelial cadherins: Am J Physiol, 275(2 Pt 2):H385-92.

Carpenter, G., and Wahl, M.I., 1991, The epidermal growth factor family. Sporn, M. B. Roberts, . B. eds. *Peptide Growth Factors and their Receptors* ,69-171 Springer-Verlag New York.

Casale, T.B., Mower, D.A., Carolan, E.J., 1998, The sequential migration of neutrophils through endothelium and epithelium: a new model system: Exp Lung Res, 24(6):709-19.

Casale, T. B. and Carolan, E. J., 1999, Cytokine-induced sequential migration of neutrophils through endothelium and epithelium: Inflamm.Res., 48, 22-27.

Cereijido, M., Valdes, J., Shoshani, L., and Contreras, R. G., 1998, Role of tight junctions in establishing and maintaining cell polarity: Annu.Rev.Physiol, 60, 161-177.

Cereijido, M., Shoshani, L., and Contreras, R. G., 2000, Molecular physiology and pathophysiology of tight junctions. I. Biogenesis of tight junctions and epithelial polarity: Am.J.Physiol Gastrointest.Liver Physiol, 279, G477-G482.

Chen, Y., Merzdorf, C., Paul, D. L., and Goodenough, D. A., 1997, COOH terminus of occludin is required for tight junction barrier function in early Xenopus embryos: J.Cell Biol., 138, 891-899.

Chen, Y., Lu, Q., Schneeberger, E. E., and Goodenough, D. A., 2000, Restoration of tight junction structure and barrier function by down- regulation of the mitogen-activated protein kinase pathway in ras- transformed Madin-Darby canine kidney cells: Mol.Biol.Cell, 11, 849-862.

Citi, S., D'Atri, F., and Parry, D.A., 2000, Human and Xenopus cingulin share a modular organization of the coiled-coil rod domain: predictions for intra- and intermolecular assembly: J Struct Biol, 131(2):135-45.

Claude, P., 1978, Morphological factors influencing transepithelial permeability: a model for the resistance of the zonula occludens: J.Membr.Biol., 39, 219-232.

Cohen, C.J., Shieh, J.T., Pickles, R.J., Okegawa, T., Hsieh, J.T., and Bergelson, J.M., 2001,The coxsackievirus and adenovirus receptor is a transmembrane component of the tight junction: Proc Natl Acad Sci U S A. 98(26):15191-6.

Colgan, S. P., Resnick, M. B., Parkos, C. A., Delp-Archer, C., McGuirk, D., Bacarra, A. E., Weller, P. F., and Madara, J. L., 1994, IL-4 directly modulates function of a model human intestinal epithelium: J.Immunol., 153, 2122-2129.

Collins, J.E., 2002, Adhesion between dendritic cells and epithelial cells maintains the gut barrier during bacterial sampling: Gut, 50(4):449-50.

Couceiro, J.N., Paulson, J.C., and Baum, L.G., 1993, Influenza virus strains selectively recognize sialyloligosaccharides on human respiratory epithelium; the role of the host cell in selection of hemagglutinin receptor specificity: Virus Res, 29(2):155-65.

Coyne, C. B., Kelly, M. M., Boucher, R. C., and Johnson, L. G., 2000, Enhanced epithelial gene transfer by modulation of tight junctions with sodium caprate: Am.J.Respir.Cell Mol.Biol., 23, 602-609.

Cromwell, O., Hamid, Q., Corrigan, C. J., Barkans, J., Meng, Q., Collins, P. D., and Kay, A. B., 1992, Expression and generation of interleukin-8, IL-6 and granulocyte-macrophage colony-stimulating factor by bronchial epithelial cells and enhancement by IL-1 beta and tumour necrosis factor-alpha: Immunology, 77, 330-337.

Cunningham, S.A., Arrate, M.P., Rodriguez, J.M., Bjercke, R.J., Vanderslice, P., Morris, A.P., and Brock, T.A., 2000, .A novel protein with homology to the junctional

adhesion molecule. Characterization of leukocyte interactions: J Biol Chem, 275(44):34750-6.

DeFouw, D. O., Brown, K. L., and Feinberg, R. N., 1993, Canine jugular vein endothelial cell monolayers in vitro: vasomediator- activated diffusive albumin pathway: J.Vasc.Res., 30, 154-160.

Dejana, E., Corada, M., and Lampugnani, M. G., 1995, Endothelial cell-to-cell junctions: FASEB J., 9, 910-918.

Dejana, E., Spagnuolo, R., and Bazzoni, G., 2001, Interendothelial junctions and their role in the control of angiogenesis, vascular permeability and leukocyte transmigration: Thromb Haemost, 86(1):308-15. Review.

Del Maschio, A., Zanetti, A., Corada, M., Rival, Y., Ruco, L., Lampugnani, M.G., and Dejana, E., 1996, Polymorphonuclear leukocyte adhesion triggers the disorganization of endothelial cell-to-cell adherens junctions: J Cell Biol, 135(2):497-510.

Denker, B.M., Saha, C., Khawaja, S., and Nigam, S.K., 1996, Involvement of a heterotrimeric G protein alpha subunit in tight junction biogenesis: J Biol Chem, 271(42):25750-3.

Denker, B.M., and Nigam, S.K., 1998, Molecular structure and assembly of the tight junction: Am J Physiol, 274(1 Pt 2):F1-9. Review.

Dodane, V., and Kachar, B., 1996, Identification of isoforms of G proteins and PKC that colocalize with tight junctions: J Membr Biol, 149(3):199-209.

Ebnet, K., Schulz, C.U., Meyer Zu Brickwedde, M.K., Pendl, G.G., and Vestweber, D., 2000, Junctional adhesion molecule interacts with the PDZ domain-containing proteins AF-6 and ZO-1: J Biol Chem, 275(36):27979-88.

Ebnet, K., Suzuki, A., Horikoshi, Y., Hirose, T., Meyer Zu Brickwedde, M.K., Ohno, S., and Vestweber, D., 2001, The cell polarity protein ASIP/PAR-3 directly associates with junctional adhesion molecule (JAM): EMBO J. 20(14):3738-48.

Ebnet, K., Aurrand-Lions, M., Kuhn, A., Kiefer, F., Butz, S., Zander, K., Meyer zu Brickwedde, M.K., Suzuki, A., Imhof, B.A., and Vestweber, D., 2003, The junctional adhesion molecule (JAM) family members JAM-2 and JAM-3 associate with the cell polarity protein PAR-3: a possible role for JAMs in endothelial cell polarity: J Cell Sci, 116(Pt 19):3879-91.

Edens, H. A. and Parkos, C. A., 2000, Modulation of epithelial and endothelial paracellular permeability by leukocytes: Adv.Drug Deliv.Rev., 41, 315-328.

Evans, M.J., Van Winkle, L.S., Fanucchi, M.V., and Plopper, C.G., 2001, Cellular and molecular characteristics of basal cells in airway epithelium: Exp Lung Res, 27(5):401-15. Review.

Fanning, A. S., Jameson, B. J., Jesaitis, L. A., and Anderson, J. M., 1998, The tight junction protein ZO-1 establishes a link between the transmembrane protein occludin and the actin cytoskeleton: J.Biol.Chem., 273, 29745-29753.

Farquhar, M.G., and Palade, G.E., 1963, Junctional complexes in various epithelia. J Cell Biol, 17:375-412.

Foster, W.M., 2002, Mucociliary transport and cough in humans: Pulm Pharmacol Ther. 15(3):277-82. Review.

Francis, S.A., Kelly, J.M., McCormack, J., Rogers, R.A., Lai, J., Schneeberger, E.E., and Lynch, R.D., 1999 Rapid reduction of MDCK cell cholesterol by methyl-beta-cyclodextrin alters steady state transepithelial electrical resistance: Eur J Cell Biol, 78(7):473-84.

Frew, A.J., 1998, Effects of anti-IgE in asthmatic subjects: Thorax, 53 Suppl 2:S52-7. Review.

Furuse, M., Hirase, T., Itoh, M., Nagafuchi, A., Yonemura, S., Tsukita, S., and Tsukita, S., 1993, Occludin: a novel integral membrane protein localizing at tight junctions: J.Cell Biol., 123, 1777-1788.

Furuse, M., Sasaki, H., Fujimoto, K., and Tsukita, S., 1998, A single gene product, claudin-1 or -2, reconstitutes tight junction strands and recruits occludin in fibroblasts: J.Cell Biol., 143, 391-401.

Furuse, M., Sasaki, H., and Tsukita, S., 1999, Manner of interaction of heterogeneous claudin species within and between tight junction strands: J.Cell Biol., 147, 891-903.

Furuse, M., Furuse, K., Sasaki, H., and Tsukita, S., 2001, Conversion of zonulae occludentes from tight to leaky strand type by introducing claudin-2 into Madin-Darby canine kidney I cells: J.Cell Biol., 153, 263-272.

Furuse, M., Hata, M., Furuse, K., Yoshida, Y., Haratake, A., Sugitani, Y., Noda, T., Kubo, A., and Tsukita, S., 2002, Claudin-based tight junctions are crucial for the mammalian epidermal barrier: a lesson from claudin-1-deficient mice: J Cell Biol, 156(6):1099-111.

Gaillard, P. J., Voorwinden, L. H., Nielsen, J. L., Ivanov, A., Atsumi, R., Engman, H., Ringbom, C., de Boer, A. G., and Breimer, D. D., 2001, Establishment and functional characterization of an in vitro model of the blood-brain barrier, comprising a co-culture of brain capillary endothelial cells and astrocytes: Eur.J.Pharm.Sci., 12, 215-222.

Gallardo, J.M., Hernandez, J.M., Contreras, R.G., Flores-Maldonado, C., Gonzalez-Mariscal, L., and Cereijido, M., 2002, Tight junctions are sensitive to peptides eliminated in the urine: J Membr Biol, 188(1):33-42.

Gallucci, S., and Matzinger, P., 2001, Danger signals: SOS to the immune system: Curr Opin Immunol, 13(1):114-9. Review.

Gardner, T.W., Lieth, E., Khin, S.A., Barber, A.J., Bonsall, D.J., Lesher, T., Rice, K., and Brennan, W.A. Jr., 1997, Astrocytes increase barrier properties and ZO-1 expression in retinal vascular endothelial cells: Invest Ophthalmol Vis Sci, 38(11):2423-7.

Gerritsen, M. E., 1987, Functional heterogeneity of vascular endothelial cells: Biochem.Pharmacol., 36, 2701-2711.

Ghassemifar, M. R., Sheth, B., Papenbrock, T., Leese, H. J., Houghton, F. D., and Fleming, T. P., 2002, Occludin TM4(-): an isoform of the tight junction protein present in primates lacking the fourth transmembrane domain: J.Cell Sci., 115, 3171-3180.

Gilsdorf, J.R., McCrea, K.W.,and Marrs, C.F., 1997, Role of pili in Haemophilus influenzae adherence and colonization: Infect Immun, 65(8):2997-3002.

Girard, J.P., and Springer, T.A., 1995, High endothelial venules (HEVs): specialized endothelium for lymphocyte migration: Immunol Today, 16(9):449-57. Review.

Godfrey, R. W., Severs, N. J., and Jeffery, P. K., 1994, A comparison between the epithelial tight junction morphology of human extrapulmonary bronchi and rat trachea: Eur.Respir.J., 7, 1409-1415.

Gonzalez-Mariscal, L., Islas, S., Contreras, R. G., Garcia-Villegas, M. R., Betanzos, A., Vega, J., Diaz-Quinonez, A., Martin-Orozco, N., Ortiz-Navarrete, V., Cereijido, M., and Valdes, J., 1999, Molecular characterization of the tight junction protein ZO-1 in MDCK cells: Exp.Cell Res., 248, 97-109.

Gonzalez-Mariscal, L., Betanzos, A., and Avila-Flores, A., 2000, MAGUK proteins: structure and role in the tight junction: Semin.Cell Dev.Biol., 11, 315-324.

Gonzalez-Mariscal, L., Betanzos, A., Nava, P., and Jaramillo, B.E., 2003, Tight junction proteins: Prog Biophys Mol Biol, 81(1):1-44. Review.

Gordon, S.B., and Read, R.C., 2002, Macrophage defences against respiratory tract infections: Br Med Bull. 61:45-61. Review.

Gotte, M., 2003, Syndecans in inflammation: FASEB J, 17(6):575-91. Review.

Gueven, N., Glatthaar, B., Manke, H. G., and Haemmerle, H., 1996, Co-cultivation of rat pneumocytes and bovine endothelial cells on a liquid-air interface: Eur.Respir.J., 9, 968-975.

Gumbiner, B., Lowenkopf, T., Apatira, D., 1991, Identification of a 160-kDa polypeptide that binds to the tight junction protein ZO-1: Proc Natl Acad Sci U S A, 15;88(8):3460-4.

Gumbiner, B.M., 1996, Cell adhesion: the molecular basis of tissue architecture and morphogenesis: Cell, 84(3):345-57. Review.

Hamazaki, Y., Itoh, M., Sasaki, H., Furuse, M., and Tsukita, S., 2002, Multi-PDZ domain protein 1 (MUPP1) is concentrated at tight junctions through its possible interaction with claudin-1 and junctional adhesion molecule: J.Biol.Chem., 277, 455-461.

Haskins, J., Gu, L., Wittchen, E.S., Hibbard, J., and Stevenson, B.R., 1998, ZO-3, a novel member of the MAGUK protein family found at the tight junction, interacts with ZO-1 and occludin: J Cell Biol, 141(1):199-208.

Heiskala, M., Peterson, P. A., and Yang, Y., 2001, The roles of claudin superfamily proteins in paracellular transport: Traffic., 2, 93-98.

Hixenbaugh, E.A., Goeckeler, Z.M., Papaiya, N.N., Wysolmerski, R.B., Silverstein, S.C., and Huang, A.J., 1997, Stimulated neutrophils induce myosin light chain phosphorylation and isometric tension in endothelial cells: Am J Physiol, 273(2 Pt 2):H981-8.

Hogg, J.C., 2000 Chronic bronchitis: the role of viruses: Semin Respir Infect, 15(1):32-40. Review.

Holgate, S.T., 2000, Epithelial damage and response: Clin Exp Allergy, 30 Suppl 1:37-41. Review.

Holt, P.G., 1996, Immunoregulation of the allergic reaction in the respiratory tract: Eur Respir J Suppl, 22:85s-89s. Review.

Hordijk, P.L., Anthony, E., Mul, F.P., Rientsma, R., Oomen, L.C., and Roos, D., 1999, Vascular-endothelial-cadherin modulates endothelial monolayer permeability: J Cell Sci, 112 (Pt 12):1915-23.

Huber, C.M., Saffrich, R., Ansorge, W., Just, W.W., 1999, Receptor-mediated regulation of peroxisomal motility in CHO and endothelial cells: EMBO J, 18(20):5476-85.

Huber, D., Balda, M. S., and Matter, K., 2000, Occludin modulates transepithelial migration of neutrophils: J.Biol.Chem., 275, 5773-5778.

Ide, N., Hata, Y., Nishioka, H., Hirao, K., Yao, I., Deguchi, M., Mizoguchi, A., Nishimori, H., Tokino, T., Nakamura, Y., and Takai, Y., 1999, Localization of membrane-associated guanylate kinase (MAGI)-1/BAI-associated protein (BAP) 1 at tight junctions of epithelial cells: Oncogene, 18(54):7810-5.

Inai, T., Kobayashi, J., and Shibata, Y., 1999, Claudin-1 contributes to the epithelial barrier function in MDCK cells: Eur.J.Cell Biol., 78, 849-855.

Isobe, I., Watanabe, T., Yotsuyanagi, T., Hazemoto, N., Yamagata, K., Ueki, T., Nakanishi, K., Asai, K., and Kato, T., 1996, .Astrocytic contributions to blood-brain barrier (BBB) formation by endothelial cells: a possible use of aortic endothelial cell for in vitro BBB model: Neurochem Int, 28(5-6):523-33.

Itoh, M., Furuse, M., Morita, K., Kubota, K., Saitou, M., and Tsukita, S., 1999, Direct binding of three tight junction-associated MAGUKs, ZO-1, ZO-2, and ZO-3, with the COOH termini of claudins: J.Cell Biol., 147, 1351-1363.

Itoh, M., Morita, K., and Tsukita, S., 1999, Characterization of ZO-2 as a MAGUK family member associated with tight as well as adherens junctions with a binding affinity to occludin and alpha catenin: J.Biol.Chem., 274, 5981-5986.

Itoh, M., Sasaki, H., Furuse, M., Ozaki, H., Kita, T., and Tsukita, S., 2001, Junctional adhesion molecule (JAM) binds to PAR-3: a possible mechanism for the recruitment of PAR-3 to tight junctions: J.Cell Biol., 154, 491-497.

Izumi, Y., Hirose, T., Tamai, Y., Hirai, S., Nagashima, Y., Fujimoto, T., Tabuse, Y., Kemphues, K.J., and Ohno, S., 1998, An atypical PKC directly associates and colocalizes at the epithelial tight junction with ASIP, a mammalian homologue of Caenorhabditis elegans polarity protein PAR-3: J Cell Biol, 143(1):95-106.

Jackson, D.E., 2003, The unfolding tale of PECAM-1:FEBS Lett, 540(1-3):7-14. Review.

Jeffery, P. K., 1983, Morphologic features of airway surface epithelial cells and glands: Am.Rev.Respir.Dis., 128, S14-S20.

Jeffery, P. K., 1995, Microscopic structure of Normal Lung, In: Brewis, R., Corrin, B., Geddes, D.M., and Gibson, G.J., (eds), Respiratory Medicine Vol. I 2nd Edition.

Jiang, W.G., Bryce, R.P., Horrobin, D.F., Mansel, R.E., 1998, Regulation of tight junction permeability and occludin expression by polyunsaturated fatty acids: Biochem Biophys Res Commun, 244(2):414-20.

Joberty, G., Petersen, C., Gao, L., and Macara, I.G., 2000,The cell-polarity protein Par6 links Par3 and atypical protein kinase C to Cdc42: Nat Cell Biol, 2(8):531-9.

Johansson, A., Driessens, M., Aspenstrom, P., 2000, The mammalian homologue of the Caenorhabditis elegans polarity protein PAR-6 is a binding partner for the Rho GTPases Cdc42 and Rac1: J Cell Sci, 113 (Pt 18):3267-75.

Kalb, T.H., Chuang, M.T., Marom, Z., and Mayer, L., 1991, Evidence for accessory cell function by class II MHC antigen-expressing airway epithelial cells: Am J Respir Cell Mol Biol, 4(4):320-9.

Kawabe, H., Nakanishi, H., Asada, M., Fukuhara, A., Morimoto, K., Takeuchi, M., and Takai, Y., 2001, Pilt, a novel peripheral membrane protein at tight junctions in epithelial cells: J.Biol.Chem., 276, 48350-48355.

Keller, T.C. 3rd, and Mooseker, M.S., 1982, Ca++-calmodulin-dependent phosphorylation of myosin, and its role in brush border contraction in vitro: J Cell Biol, 95(3):943-59.

Keon, B.H., Schafer, S., Kuhn, C., Grund, C., and Franke, W.W., 1996, Symplekin, a novel type of tight junction plaque protein: J Cell Biol, 134(4):1003-18.

Kidney, J. C. and Proud, D., 2000, Neutrophil transmigration across human airway epithelial monolayers: mechanisms and dependence on electrical resistance: Am.J.Respir.Cell Mol.Biol., 23, 389-395.

Kidney, J. C. and Proud, D., 2000, Neutrophil transmigration across human airway epithelial monolayers: mechanisms and dependence on electrical resistance: Am.J.Respir.Cell Mol.Biol., 23, 389-395.

Kostrewa, D., Brockhaus, M., D'Arcy, A., Dale, G.E., Nelboeck, P., Schmid, G., Mueller, F., Bazzoni, G., Dejana, E., Bartfai, T., Winkler, F.K., and Hennig, M., 2001, X-ray structure of junctional adhesion molecule: structural basis for homophilic adhesion via a novel dimerization motif: EMBO J, 20(16):4391-8.

Kucharzik, T., Walsh, S.V., Chen, J., Parkos, C.A., and Nusrat, A., 2001, Neutrophil transmigration in inflammatory bowel disease is associated with differential expression of epithelial intercellular junction proteins: Am J Pathol, 159(6):2001-9.

Lacaz-Vieira, F., Jaeger, M. M., Farshori, P., and Kachar, B., 1999, Small synthetic peptides homologous to segments of the first external loop of occludin impair tight junction resealing: J.Membr.Biol., 168, 289-297.

Lambrecht, B.N., 2001, Allergen uptake and presentation by dendritic cells: Curr Opin Allergy Clin Immunol, 1(1):51-9. Review.

Lampugnani, M.G., Resnati, M., Raiteri, M., Pigott, R., Pisacane, A., Houen, G., Ruco, L.P., and Dejana, E., 1992, A novel endothelial-specific membrane protein is a marker of cell-cell contacts: J Cell Biol, 118(6):1511-22.

Le Gall, A.H., Yeaman, C., Muesch, A., and Rodriguez-Boulan, E., 1995, Epithelial cell polarity: new perspectives: Semin Nephrol, 15(4):272-84. Review.

Lee, J. and Zhao, X., 2000, Recombinant human interleukin-8, but not human interleukin-1beta, induces bovine neutrophil migration in an in vitro co-culture system: Cell Biol.Int., 24, 889-895.

Liebner, S., Fischmann, A., Rascher, G., Duffner, F., Grote, E. H., Kalbacher, H., and Wolburg, H., 2000, Claudin-1 and claudin-5 expression and tight junction morphology are altered in blood vessels of human glioblastoma multiforme: Acta Neuropathol.(Berl), 100, 323-331.

Lillehoj, E.R., and Kim, K.C., 2002 Airway mucus: its components and function: Arch Pharm Res, 25(6):770-80. Review.

Liu, L., Mul, F.P., Kuijpers, T.W., Lutter, R., Roos, D., and Knol, E.F., 1996, Neutrophil transmigration across monolayers of endothelial cells and airway epithelial cells is regulated by different mechanisms: Ann N Y Acad Sci, 796:21-9. Review.

Liu, Y., Nusrat, A., Schnell, F. J., Reaves, T. A., Walsh, S., Pochet, M., and Parkos, C. A., 2000, Human junction adhesion molecule regulates tight junction resealing in epithelia: J.Cell Sci., 113 (Pt 13), 2363-2374.

Luu, N. T., Rainger, G. E., and Nash, G. B., 2000, Differential ability of exogenous chemotactic agents to disrupt transendothelial migration of flowing neutrophils: J.Immunol., 164, 5961-5969.

Lynch, R.D., Tkachuk-Ross, L.J., McCormack, J.M., McCarthy, K.M., Rogers, R.A., and Schneeberger, E.E., 1995, Basolateral but not apical application of protease results in a rapid rise of transepithelial electrical resistance and formation of aberrant tight junction strands in MDCK cells: Eur J Cell Biol, 66(3):257-67.

Mackarel, A. J., Cottell, D. C., FitzGerald, M. X., and O'Connor, C. M., 1999, Human endothelial cells cultured on microporous filters used for leukocyte transmigration studies form monolayers on both sides of the filter: In Vitro Cell Dev.Biol.Anim, 35, 346-351.

Mackarel, A. J., Cottell, D. C., Russell, K. J., FitzGerald, M. X., and O'Connor, C. M., 1999, Migration of neutrophils across human pulmonary endothelial cells is not blocked by matrix metalloproteinase or serine protease inhibitors: Am.J.Respir.Cell Mol.Biol., 20, 1209-1219.

Mackarel, A. J., Russell, K. J., Brady, C. S., FitzGerald, M. X., and O'Connor, C. M., 2000, Interleukin-8 and leukotriene-B(4), but not formylmethionyl leucylphenylalanine, stimulate CD18-independent migration of neutrophils across human pulmonary endothelial cells in vitro: Am.J.Respir.Cell Mol.Biol., 23, 154-161.

Madara, J. L. and Stafford, J., 1989, Interferon-gamma directly affects barrier function of cultured intestinal epithelial monolayers: J.Clin.Invest, 83, 724-727.

Madara, J.L., Parkos, C., Colgan, S., Nusrat, A., Atisook, K., and Kaoutzani, P., 1992, The movement of solutes and cells across tight junctions: Ann N Y Acad Sci, 664:47-60. Review

Madara, J. L., 1998, Regulation of the movement of solutes across tight junctions: Annu.Rev.Physiol, 60, 143-159.

Maddox, L., and Schwartz, D.A., 2002, The pathophysiology of asthma: Annu Rev Med, 53:477-98. Review.

Mandel, L. J., Bacallao, R., and Zampighi, G., 1993, Uncoupling of the molecular 'fence' and paracellular 'gate' functions in epithelial tight junctions: Nature, 361, 552-555.

Marano, C.W., Lewis, S.A., Garulacan, L.A., Soler, A.P., and Mullin, J.M., 1998, Tumor necrosis factor-alpha increases sodium and chloride conductance across the tight junction of CACO-2 BBE, a human intestinal epithelial cell line: J Membr Biol, 161(3):263-74.

Marcial, M.A., Carlson, S.L., and Madara, J.L., 1984, Partitioning of paracellular conductance along the ileal crypt-villus axis: a hypothesis based on structural analysis with detailed consideration of tight junction structure-function relationships: J Membr Biol, 80(1):59-70.

Marcus, B. C. and Gewertz, B. L., 1998, Measurement of endothelial permeability: Ann.Vasc.Surg., 12, 384-390.

Martin-Padura, I., Lostaglio, S., Schneemann, M., Williams, L., Romano, M., Fruscella, P., Panzeri, C., Stoppacciaro, A., Ruco, L., Villa, A., Simmons, D., and Dejana, E., 1998, Junctional adhesion molecule, a novel member of the immunoglobulin superfamily that distributes at intercellular junctions and modulates monocyte transmigration: J.Cell Biol., 142, 117-127.

Matter, K. and Balda, M. S., 1999, Occludin and the functions of tight junctions: Int.Rev.Cytol., 186, 117-146.

McCarthy, K. M., Skare, I. B., Stankewich, M. C., Furuse, M., Tsukita, S., Rogers, R. A., Lynch, R. D., and Schneeberger, E. E., 1996, Occludin is a functional component of the tight junction: J.Cell Sci., 109 (Pt 9), 2287-2298.

Mezzetti, M., Soloperto, M., Fasoli, A., and Mattoli, S., 1991, Human bronchial epithelial cells modulate CD3 and mitogen-induced DNA synthesis in T cells but function poorly as antigen-presenting cells compared to pulmonary macrophages: J Allergy Clin Immunol, 87(5):930-8.

Middleton, J., Patterson, A.M., Gardner, L., Schmutz, C., and Ashton, B.A., 2002, Leukocyte extravasation: chemokine transport and presentation by the endothelium: Blood, 1;100(12):3853-60. Review

Miller, L.A., and Butcher, E.C., 1998, Human airway epithelial monolayers promote selective transmigration of memory T cells: a transepithelial model of lymphocyte migration into the airways: Am J Respir Cell Mol Biol, 19(6):892-900.

Mitic, L. L., Van Itallie, C. M., and Anderson, J. M., 2000, Molecular physiology and pathophysiology of tight junctions I. Tight junction structure and function: lessons from mutant animals and proteins: Am.J.Physiol Gastrointest.Liver Physiol, 279, G250-G254.

Mogel, M., Kruger, E., Krug, H. F., and Seidel, A., 1998, A new coculture-system of bronchial epithelial and endothelial cells as a model for studying ozone effects on airway tissue: Toxicol.Lett., 96-97, 25-32.

Moll, T., Dejana, E., and Vestweber, D., 1998, In vitro degradation of endothelial catenins by a neutrophil protease: J.Cell Biol., 140, 403-407.

Moore, B.B., Moore, T.A., Toews, G.B., 2001, Role of T- and B-lymphocytes in pulmonary host defences: Eur Respir J, 18(5):846-56. Review.

Mori, L., Kleimberg, J., Mancini, C., Bellini, A., Marini, M., and Mattoli, S., 1995, Bronchial epithelial cells of atopic patients with asthma lack the ability to inactivate allergens: Biochem Biophys Res Commun, 26;217(3):817-24.

Morita, K., Furuse, M., Fujimoto, K., and Tsukita, S., 1999, Claudin multigene family encoding four-transmembrane domain protein components of tight junction strands: Proc.Natl.Acad.Sci.U.S.A, 96, 511-516.

Morita, K., Sasaki, H., Furuse, M., and Tsukita, S., 1999, Endothelial claudin: claudin-5/TMVCF constitutes tight junction strands in endothelial cells: J.Cell Biol., 147, 185-194.

Mul, F.P., Zuurbier, A.E., Janssen, H., Calafat, J., van Wetering, S., Hiemstra, P.S., Roos, D., and Hordijk, P.L., 2000, Sequential migration of neutrophils across monolayers of endothelial and epithelial cells: J Leukoc Biol, 2000 Oct;68(4):529-37.

Muresan, Z., Paul, D. L., and Goodenough, D. A., 2000, Occludin 1B, a variant of the tight junction protein occludin: Mol.Biol.Cell, 11, 627-634.

Naik, U. P., Naik, M. U., Eckfeld, K., Martin-DeLeon, P., and Spychala, J., 2001, Characterization and chromosomal localization of JAM-1, a platelet receptor for a stimulatory monoclonal antibody: J.Cell Sci., 114, 539-547.

Nakamura, T., Blechman, J., Tada, S., Rozovskaia, T., Itoyama, T., Bullrich, F., Mazo, A., Croce, C.M., Geiger, B., and Canaani, E., 2000, huASH1 protein, a

putative transcription factor encoded by a human homologue of the Drosophila ash1 gene, localizes to both nuclei and cell-cell tight junctions: Proc Natl Acad Sci U S A, 97(13):7284-9.

Mattagajasingh, S.N., Huang, S.C., Hartenstein, J.S., and Benz, E.J. Jr., 2000, Characterization of the interaction between protein 4.1R and ZO-2. A possible link between the tight junction and the actin cytoskeleton: J Biol Chem, 275(39):30573-85.

Nigam, S.K., Rodriguez-Boulan, E., and Silver, R.B., 1992, Changes in intracellular calcium during the development of epithelial polarity and junctions: Proc Natl Acad Sci U S A. 89(13):6162-6.

Nusrat, A., Parkos, C. A., Bacarra, A. E., Godowski, P. J., Delp-Archer, C., Rosen, E. M., and Madara, J. L., 1994, Hepatocyte growth factor/scatter factor effects on epithelia. Regulation of intercellular junctions in transformed and nontransformed cell lines, basolateral polarization of c-met receptor in transformed and natural intestinal epithelia, and induction of rapid wound repair in a transformed model epithelium: J.Clin.Invest, 93, 2056-2065.

Nusrat, A., Chen, J. A., Foley, C. S., Liang, T. W., Tom, J., Cromwell, M., Quan, C., and Mrsny, R. J., 2000, The coiled-coil domain of occludin can act to organize structural and functional elements of the epithelial tight junction: J.Biol.Chem, 275, 29816-29822.

Paperna, T., Peoples, R., Wang, Y. K., Kaplan, P., and Francke, U., 1998, Genes for the CPE receptor (CPETR1) and the human homolog of RVP1 (CPETR2) are localized within the Williams-Beuren syndrome deletion: Genomics, 54, 453-459.

Pettersen, C.A., and Adler, K.B., 2002, Airways inflammation and COPD: epithelial-neutrophil interactions: Chest, 121(5 Suppl):142S-150S. Review.

Pilette, C., Ouadrhiri, Y., Godding, V., Vaerman, J.P., and Sibille, Y., 2001, Lung mucosal immunity: immunoglobulin-A revisited.
Eur Respir J, 18(3):571-88. Review.

Planchon, S., Fiocchi, C., Takafuji, V., and Roche, J. K., 1999, Transforming growth factor-beta1 preserves epithelial barrier function: identification of receptors, biochemical intermediates, and cytokine antagonists: J.Cell Physiol, 181, 55-66.

Polosa, R., Prosperini, G., Tomaselli, V., Howarth, P.H., Holgate, S.T., Davies, D.E., 2000, Expression of c-erbB receptors and ligands in human nasal epithelium: J Allergy Clin Immunol, 106(6):1124-31.

Prasad, R., Gu, Y., Alder, H., Nakamura, T., Canaani, O., Saito, H., Huebner, K., Gale, R.P., Nowell, P.C., Kuriyama, K., et al., 1993, Cloning of the ALL-1 fusion partner, the AF-6 gene, involved in acute myeloid leukemias with the t(6;11) chromosome translocation: Cancer Res, 53(23):5624-8.

Prince, J.E., Kheradmand, F., Corry, D.B., 2003, 16. Immunologic lung disease. J Allergy Clin Immunol, 111(2 Suppl):S613-23. Review.

Puddicombe, S.M.,Polosa, R., Richter, A., Krishna, M.T., Howarth, P.H., Holgate, S.T., and Davies, D.E., 2000, Involvement of the epidermal growth factor receptor in epithelial repair in asthma: FASEB J, 14(10):1362-74.

Rahner, C., Mitic, L.L., and Anderson, J.M., 2001, .Heterogeneity in expression and subcellular localization of claudins 2, 3, 4, and 5 in the rat liver, pancreas, and gut: Gastroenterology, 120(2):411-22.

Reaves, T.A., Colgan, S.P., Selvaraj, P., Pochet, M.M., Walsh, S., Nusrat, A., Liang, T.W., Madara, J.L., and Parkos, C.A., 2001, Neutrophil transepithelial migration: regulation at the apical epithelial surface by Fc-mediated events: Am J Physiol Gastrointest Liver Physiol, 280(4):G746-54.

Rennard, S.I., and Romberger, D.J., 2000, Host defenses and pathogenesis: Semin Respir Infect. 15(1):7-13. Review

Rescigno, M., Rotta, G., Valzasina, B., and Ricciardi-Castagnoli, P., 2001, Dendritic cells shuttle microbes across gut epithelial monolayers: Immunobiology, 204(5):572-81.

Rogers, D.F., 2003, The airway goblet cell: Int J Biochem Cell Biol, 35(1):1-6. Review.

Roh, M.H., Liu, C.J., Laurinec, S., and Margolis, B., 2002, The carboxyl terminus of zona occludens-3 binds and recruits a mammalian homologue of discs lost to tight junctions: J Biol Chem, 26;277(30):27501-9

Rojas, R., and Apodaca, G., 2002, Immunoglobulin transport across polarized epithelial cells: Nat Rev Mol Cell Biol, 3(12):944-55. Review.

Ryeom, S. W., Paul, D., and Goodenough, D. A., 2000, Truncation mutants of the tight junction protein ZO-1 disrupt corneal epithelial cell morphology: Mol.Biol.Cell, 11, 1687-1696.

Rubin, L.L., and Staddon, J.M., 1999, The cell biology of the blood-brain barrier: Annu Rev Neurosci, 22:11-28. Review.

Rubin, B.K., 2002, Physiology of airway mucus clearance: Respir Care, 47(7):761-8. Review.

Saitou, M., Fujimoto, K., Doi, Y., Itoh, M., Fujimoto, T., Furuse, M., Takano, H., Noda, T., and Tsukita, S., 1998, Occludin-deficient embryonic stem cells can differentiate into polarized epithelial cells bearing tight junctions: J.Cell Biol., 141, 397-408.

Satir, P., 1992 Mechanisms of ciliary movement: contributions from electron microscopy: Scanning Microsc, 6(2):573-9. Review.

Salvi, S., and Holgate, S.T., 1999, Could the airway epithelium play an important role in mucosal immunoglobulin A production? Clin Exp Allergy, 29(12):1597-605. Review.

Schmitz, H., Fromm, M., Bentzel, C. J., Scholz, P., Detjen, K., Mankertz, J., Bode, H., Epple, H. J., Riecken, E. O., and Schulzke, J. D., 1999, Tumor necrosis factor-alpha (TNFalpha) regulates the epithelial barrier in the human intestinal cell line HT-29/B6: J.Cell Sci., 112 (Pt 1), 137-146.

Sheth, B., Fesenko, I., Collins, J. E., Moran, B., Wild, A. E., Anderson, J. M., and Fleming, T. P., 1997, Tight junction assembly during mouse blastocyst formation is regulated by late expression of ZO-1 alpha+ isoform: Development, 124, 2027-2037.

Simionescu, D., Alper, R., Kefalides, N.A., 1988, Partial characterization of a low molecular weight proteoglycan isolated from bovine parietal pericardium: Biochem Biophys Res Commun, 29;151(1):480-6.

Simionescu, M. and Simionescu, N., 1991, Endothelial transport of macromolecules: transcytosis and endocytosis. A look from cell biology: Cell Biol.Rev., 25, 5-78.

Singh, A.B., and Harris, R.C., 2003, EGF receptor activation differentially regulates Claudin expression and enhances trans-epithelial resistance in MDCK cells: J Biol Chem, [Epub ahead of print].

Sirotkin, H., Morrow, B., Saint-Jore, B., Puech, A., Das, Gupta R., Patanjali, S. R., Skoultchi, A., Weissman, S. M., and Kucherlapati, R., 1997, Identification, characterization, and precise mapping of a human gene encoding a novel membrane-spanning protein from the 22q11 region deleted in velo-cardio-facial syndrome: Genomics, 42, 245-251.

Sleigh, M.A., Blake, J.R., Liron, N., 1988, The propulsion of mucus by cilia: Am Rev Respir Dis, 137(3):726-41. Review

Soler, A. P., Laughlin, K. V., and Mullin, J. M., 1993, Effects of epidermal growth factor versus phorbol ester on kidney epithelial (LLC-PK1) tight junction permeability and cell division: Exp.Cell Res., 207, 398-406.

Sonoda, N., Furuse, M., Sasaki, H., Yonemura, S., Katahira, J., Horiguchi, Y., and Tsukita, S., 1999, Clostridium perfringens enterotoxin fragment removes specific claudins from tight junction strands: Evidence for direct involvement of claudins in tight junction barrier: J Cell Biol, 147(1):195-204.

Springer, T. A., 1995, Traffic signals on endothelium for lymphocyte recirculation and leukocyte emigration: Annu.Rev.Physiol, 57, 827-872.

Staddon, J. M., Herrenknecht, K., Smales, C., and Rubin, L. L., 1995, Evidence that tyrosine phosphorylation may increase tight junction permeability: J.Cell Sci., 108 (Pt 2), 609-619.

Staehelin, L. A., 1973, Further observations on the fine structure of freeze-cleaved tight junctions: J.Cell Sci., 13, 763-786.

Stevens, T., Rosenberg, R., Aird, W., Quertermous, T., Johnson, F. L., Garcia, J. G., Hebbel, R. P., Tuder, R. M., and Garfinkel, S., 2001, NHLBI workshop report: endothelial cell phenotypes in heart, lung, and blood diseases: Am.J.Physiol Cell Physiol, 281, C1422-C1433.

Stevenson, B. R., Siliciano, J. D., Mooseker, M. S., and Goodenough, D. A., 1986, Identification of ZO-1: a high molecular weight polypeptide associated with the tight junction (zonula occludens) in a variety of epithelia: J.Cell Biol., 103, 755-766.

Stevenson, B. R., Anderson, J. M., Goodenough, D. A., and Mooseker, M. S., 1988, Tight junction structure and ZO-1 content are identical in two strains of Madin-Darby canine kidney cells which differ in transepithelial resistance: J.Cell Biol., 107, 2401-2408.

Stuart, R.O., and Nigam, S.K., 1995, Regulated assembly of tight junctions by protein kinase C: Proc Natl Acad Sci U S A., 92(13):6072-6.

Stumbles, P.A., Upham, J.W., Holt, P.G., 2003, Airway dendritic cells: co-ordinators of immunological homeostasis and immunity in the respiratory tract: APMIS, 111(7-8):741-55. Review.

Sumpio, B.E., Riley, J.T., and Dardik, A., 2002, Cells in focus: endothelial cell: Int J Biochem Cell Biol, 34(12):1508-12. Review.

Szekanecz, Z, and Koch, A.E., 2000, Cell-cell interactions in synovitis. Endothelial cells and immune cell migration: Arthritis Res, 2(5):368-73. Review.

Thomson, A.B., Keelan, M., Thiesen, A., Clandinin, M.T., Ropeleski, M., and Wild, G.E., 2001, Small bowel review: normal physiology part 2: Dig Dis Sci, 46(12):2588-607. Review.

Tomee, J. F., Wierenga, A. T., Hiemstra, P. S., and Kauffman, H. K., 1997, Proteases from Aspergillus fumigatus induce release of proinflammatory cytokines and cell detachment in airway epithelial cell lines: J.Infect.Dis., 176, 300-303.

Tsukita, S. and Furuse, M., 2000, Pores in the wall: claudins constitute tight junction strands containing aqueous pores: J.Cell Biol., 149, 13-16.

Tsukita, S. and Furuse, M., 2000, The structure and function of claudins, cell adhesion molecules at tight junctions: Ann.N.Y.Acad.Sci., 915, 129-135.

Tsukita, S., Furuse, M., and Itoh, M., 2001, Multifunctional strands in tight junctions: Nat Rev Mol Cell Biol, 2(4):285-93. Review.

Tuma, P.L. and Hubbard, A.L., 2003, Transcytosis: crossing cellular barriers: Physiol Rev, 83(3):871-932. Review.

Turner, J.R., Angle, J.M., Black, E.D., Joyal, J.L., Sacks, D.B., and Madara, J.L., 1999, PKC-dependent regulation of transepithelial resistance: roles of MLC and MLC kinase: Am J Physiol, 277(3 Pt 1):C554-62.

Van Itallie, C. M., Balda, M. S., and Anderson, J. M., 1995, Epidermal growth factor induces tyrosine phosphorylation and reorganization of the tight junction protein ZO-1 in A431 cells: J.Cell Sci., 108 (Pt 4), 1735-1742.

Van Itallie, C. M. and Anderson, J. M., 1997, Occludin confers adhesiveness when expressed in fibroblasts: J.Cell Sci., 110 (Pt 9), 1113-1121.

Van Itallie, C., Rahner, C., and Anderson, J. M., 2001, Regulated expression of claudin-4 decreases paracellular conductance through a selective decrease in sodium permeability: J.Clin.Invest, 107, 1319-1327.

Vestweber, D., 2000, Molecular mechanisms that control endothelial cell contacts: J Pathol, 190(3):281-91. Review.

Walsh, S. V., Hopkins, A. M., and Nusrat, A., 2000, Modulation of tight junction structure and function by cytokines: Adv.Drug Deliv.Rev., 41, 303-313.

Wan, H., Winton, H. L., Soeller, C., Stewart, G. A., Thompson, P. J., Gruenert, D. C., Cannell, M. B., Garrod, D. R., and Robinson, C., 2000, Tight junction properties of the immortalized human bronchial epithelial cell lines Calu-3 and 16HBE14o-: Eur.Respir.J., 15, 1058-1068.

Wan, H., Winton, H. L., Soeller, C., Gruenert, D. C., Thompson, P. J., Stewart, G. A., Taylor, G.W., Garrod, D. R., Cannell, M.B. and Robinson, C., 1999, Der p 1 facilitates transepithelial allergen delivery by disruption of tight junctions: J Clin Invest, 104(1):123-33.

Wanner, A., Salathe, M., and O'Riordan, T.G., 1996, Mucociliary clearance in the airways:Am J Respir Crit Care Med, 154(6 Pt 1):1868-902. Review.

Weibel, E.M., 1991, Design of airways and blood vessels considered as branching trees, In: Crystal, R.G., and West, J.B., (eds.) The Lung, Scientific Foundations, New York, Raven Press.

Weidermann, U., 2003, Mucosal immunity--mucosal tolerance. A strategy for treatment of allergic diseases: Chem Immunol Allergy, 82:11-24. Review.

Willott, E., Balda, M. S., Fanning, A. S., Jameson, B., Van Itallie, C., and Anderson, J. M., 1993, The tight junction protein ZO-1 is homologous to the Drosophila discs-large tumor suppressor protein of septate junctions: Proc.Natl.Acad.Sci.U.S.A, 90, 7834-7838.

Wills-Karp M., 1999, Immunologic basis of antigen-induced airway hyperresponsiveness: Annu Rev Immunol, 17:255-81. Review.

Wittchen, E.S., Haskins, J., and Stevenson, B.R., 1999, Protein interactions at the tight junction. Actin has multiple binding partners, and ZO-1 forms independent complexes with ZO-2 and ZO-3: J Biol Chem, 274(49):35179-85.

Wodarz, A., Ramrath, A., Grimm, A., and Knust, E., 2000, Drosophila atypical protein kinase C associates with Bazooka and controls polarity of epithelia and neuroblasts: J Cell Biol, 150(6):1361-74.

Wolburg, H., Neuhaus, J., Kniesel, U., Krauss, B., Schmid, E.M., Ocalan, M., Farrell, C., and Risau, W., 1994, Modulation of tight junction structure in blood-brain barrier endothelial cells. Effects of tissue culture, second messengers and cocultured astrocytes: J Cell Sci, 107 (Pt 5):1347-57.

Wong, V., and Goodenough, D.A., 1999, Paracellular channels!: Science, 285(5424):62.

Yamamoto, H., Sedgwick, J.B., Vrtis, R.F., Busse, W.W., 2000, The effect of transendothelial migration on eosinophil function: Am J Respir Cell Mol Biol, 23(3):379-88.

Zahraoui, A., Joberty, G., Arpin, M., Fontaine, J.J., Hellio, R., Tavitian, A., and Louvard, D., 1994, A small rab GTPase is distributed in cytoplasmic vesicles in non polarized cells but colocalizes with the tight junction marker ZO-1 in polarized epithelial cells: J Cell Biol, 124(1-2):101-15.

Zanetta, L., Marcus, S.G., Vasile, J., Dobryansky, M., Cohen, H., Eng, K., Shamamian, P., and Mignatti, P., 2000, Expression of Von Willebrand factor, an endothelial cell marker, is up-regulated by angiogenesis factors: a potential method for objective assessment of tumor angiogenesis: Int J Cancer, 15;85(2):281-8.

Zhang, P., Summer, W.R., Bagby, G.J., and Nelson, S., 2000, Innate immunity and pulmonary host defense: Immunol Rev, 173:39-51. Review